Functional Analysis of the *Legionella pneumophila* Nitric Oxide Regulatory Network and its Link to Quorum Sensing

---

Dissertation

zur

Erlangung der naturwissenschaftlichen Doktorwürde
(Dr. sc. nat.)

vorgelegt der

Mathematisch-naturwissenschaftlichen Fakultät

der
Universität Zürich

von
Sarah Michaelis

aus
Deutschland

Promotionskommission

Prof. Dr. Hubert Hilbi (Vorsitz und Leitung der Dissertation)

Prof. Dr. Rolf Kümmerli

Prof. Dr. Urs Jenal

Zürich, 2024

Contents

Summary

Legionella pneumophila is a ubiquitous Gram-negative bacterium and the causative agent of Legionnaires' disease and Pontiac fever. The facultative intracellular bacterium colonizes natural and man-made water systems. In the environment, *Legionella* resides in complex biofilms, that comprise several bacterial species and eukaryotic cells. Moreover, the pathogen can infect free-living amoebae such as *Acanthamoeba castellanii* and replicate intracellularly. Human infection occurs via inhalation of contaminated aerosols. In the lungs, the opportunistic pathogen infects alveolar macrophages and translocates more than 300 effector proteins into the host cell through an Icm/Dot type IV secretion system (Icm/Dot T4SS). This allows the pathogen to multiply within a unique compartment called the *Legionella*-containing vacuole (LCV).

L. pneumophila employs the *Legionella* quorum sensing (Lqs) system to regulate various traits including the growth phase switch, virulence, and bacterial motility. The Lqs system is linked to the bacterial c-di-GMP metabolism through the pleiotropic transcription factor LvbR. The Lqs system comprises the autoinducer synthase LqsA, which produces the α-hydroxyketone LAI-1 (*Legionella* autoinducer-1, 3-hydroxypentadecan-4-one), the homologous sensor kinases LqsS and LqsT, and the response regulator LqsR. The interactions between *L. pneumophila* and its natural host cells in biofilms are poorly understood. In this study, we investigated the interactions of *Legionella* and the amoeba *A. castellanii* in mono-species *L. pneumophila* biofilms using confocal microscopy and flow cytometry. We found that the transcription factor LvbR, the response regulator LqsR, the bacterial flagellum (FlaA) and the Icm/Dot T4SS regulate the migration of *A. castellanii* through *L. pneumophila* biofilms. Furthermore, LvbR, LqsR and FlaA were found to govern the adherence and cluster formation of *L. pneumophila* on the surface of amoebae. The bacterial clusters were found to comprise motile (P_{flaA}-positive) and virulent (P_{sidC}-positive) bacteria.

Macrophages and amoeba hosts of *L. pneumophila* synthesize nitric oxide (NO), a highly reactive gaseous molecule, which freely diffuses across membranes. NO has a bactericidal effect at high (micromolar) concentrations, however at low (nanomolar) concentrations, NO has been shown to act as a signalling molecule in many bacterial species. *L. pneumophila* possesses three NO sensors, Hnox1, Hnox2 and NosP. To investigate the role of the NO receptors in *L. pneumophila* signaling, marker-less *L. pneumophila* mutant strains lacking individual (Hnox1, Hnox2, or NosP) or all three NO receptors (triple knockout, TKO) were generated. We found that in the Δ*nosP* mutant, the *lvbR* promoter was upregulated, indicating that NosP negatively regulates LvbR. Furthermore, the NO receptor mutants were impaired for growth in *A. castellanii* and macrophages. In addition, we found that phenotypic heterogeneity of non-growing/growing bacteria in amoeba was regulated by the NO receptors. Moreover, the NO receptor mutant strains revealed an altered biofilm architecture and no longer responded to NO in biofilms. In summary, the NO receptors Hnox1, Hnox2 and NosP were shown to be involved in NO detection, replication in host cells, intracellular phenotypic heterogeneity, as well as biofilm formation and dispersion. Our results provide a deeper understanding of NO signaling in *L. pneumophila* and form the basis for further studies on the molecular components and mechanisms involved in intra-species and inter-kingdom NO signaling.

1. Chapter one – General introduction

1.1 *Legionella pneumophila*

1.1.1 Discovery of a novel pathogen and epidemiology of Legionellosis

Legionella pneumophila was first described following an explosive, common-source outbreak of pneumonia among attendees of an American Legion convention in Philadelphia, in 1976. The typical illness began seven days after the Legionnaires arrived at the convention. At that time, the mode of spread had not yet been proven, but already appeared to be air borne. Out of 182 patients, 81% ultimately needed to be hospitalized and 16% died. Based on review of hospital records it was found that many of them had a history of pre-existing illnesses including emphysema or other pulmonary disease (Fraser et al., 1977).

Following the outbreak an extensive laboratory investigation was undertaken to identify the etiologic agent of the respiratory disease. A new Gram-negative bacterium was isolated from guinea pigs being infected with lung tissues from sick patients (McDade et al., 1977). In retrospect, earlier unexplained epidemics of acute respiratory disease were also attributed to the pathogen (Winn, 1988). Due to the historical association with the American Legion convention, the disease was called Legionnaires' disease and the causative bacterium was named *Legionella pneumophila* (Brenner et al., 1979).

In 1968, an outbreak of a non-pneumonic disease was found to be likewise caused by *Legionella*. The acute febrile illness was named Pontic fever, after Pontiac, Michigan, where the epidemic occurred in a health department. At least 144 people were affected, and typical symptoms of the illness included fever, headache, myalgia, and malaise. The illness was self-limited, lasted two to five days and secondary cases among contacts were not observed (Glick et al., 1978). In summary, Legionellosis classically occurs as Legionnaires' disease, a severe pneumonia with multisystem disease, or Pontic fever, a self-limited flu-like illness. While Pontiac fever only has an incubation period of 36 hours, the incubation period for Legionnaires' disease is two to ten days (Doebbeling and Wenzel, 1987).

Legionella are gamma-proteobacteria and belong to the the order of Legionellales, which comprises two families, Coxiellaceae and Legionellaceae (Duron et al., 2018). *Coxiella burnetti* is an obligate intracellular organsim and the causative agent of Q fever, a highly infectious zoonosis (Berman, 2019). The genus *Legionella* comprises more than 50 species, of which at least 24 have been associated with human disease. Causing approximately 90% of all Legionnaires' disease cases worldwide, *L. pneumophila* represents a clinically highly relevant species. Even though at least 15 serogroups were described, *L. pneumophila* serogroup 1 causes about 85% of cases. Interestingly, the clinical prevalence of *L. pneumophila* does not represent the environmental distribution of the genus, indicating that *L. pneumophila* is more pathogenic to humans than other *Legionella* species. In contrast, in Australia and New Zealand, only around 45% of cases of community acquired Legionellosis were caused by *L. pneumophila* serogroup 1, whereas *L. longbeachae* accounted for about 30% of cases (Newton et al., 2010; Yu et al., 2002).

Risk factors associated with Legionellosis include age (≥50 years), smoking, male gender, chronic obstructive pulmonary disease, alcoholism, diabetes, and immunosuppression (**Fig. 1.1**). However, many people who are exposed to *L. pneumophila* remain asymptomatic or suffer only from a mild course of disease (Newton et al., 2010; Yu et al., 2019).Interestingly, the risk for Legionnaires' disease has been shown to be weather-dependent. In fact, the risk of Legionnaires' disease increases when weather is warm and humid. Also, rainfall has been shown to be a significant risk factor for sporadic *Legionella* pneumonia. Seasonal changes in the incidence of Legionnaires' disease, with more reported cases during the summer, have been described in many countries (Garcia-Vidal et al., 2013; Simmering et al., 2017).

L. pneumophila is a common cause of community-acquired and nosocomial pneumonia (Vergis et al., 2000). Detection methods of *Legionella* are based on different samples (respiratory tract specimens, blood, urine) and in addition to classical cultural isolation include serological assays, urinary antigen tests, mass spectrometry, polymerase chain reaction, and metagenomic next-generation sequencing. Each pathogen detection technique has its advantages and limitations. However, despite long turnaround time and low sensitivity, traditional cultural isolation remains the gold standard for the diagnosis for *Legionella* pneumonia (Bai et al., 2023).Buffered charcoal yeast extract (BCYE) agar serves as the primary medium for cultural isolation. The isolation of *Legionella* from contaminated samples can be improved by acid pretreatment and by addition of antimicrobial agents to generate selective media (Roig et al., 1994).In the future, culture-independent molecular diagnostic methods promise to improve the laboratory diagnosis of legionellosis, but so far molecular diagnostic techniques have not yet proven to be sufficiently superior (Chahin and Opal, 2017). Rapid routine diagnosis combined with early adequate treatment can reduce the mortality rate of Legionnaires' disease (Gudiol et al., 2007). Since *Legionella* spp are primarily intracellular pathogens, Legionnaires' disease should be treated with antibiotics that are active inside eukaryotic cells (Cunha et al., 2016). Therapeutic options for adult patients with severe pneumonia caused by *L. pneumophila* include treatment with a fluoroquinolone and/or a macrolide (Chahin and Opal, 2017).

Switzerland has one of the highest incidences of Legionnaires' disease in Europe, and the number of cases has been increasing since 2001 (Wymann, 2023). In fact, the number of Legionnaires' disease cases in Switzerland has more than doubled since 2008. Also, in European countries and the US, case numbers have been increasing over the past years. The reason for the increase in incidences is not exactly known but could be due to an increased susceptibility of the population and physician awareness, climate change, efforts to save energy and changes in energy policy, or improvements in diagnosis and surveillance. In fact, the analysis of *Legionella* spp. testing data (2007-2016) showed that the number of positive tests increased proportionally to the number of diagnostic tests performed. Hence, the interpretation of the results is difficult, as it remains unclear, why the number of positive diagnostic tests has more than doubled over the study period. (Fischer et al., 2020).

1.1.2 Ecology of *Legionella pneumophila*

Legionella are Gram-negative, non-spore-forming, aerobic bacteria that are 0.3 to 0.9 µm wide and 2 to 20 µm long (Marrie et al., 2012). The size and shape of the bacteria depend on the culturing conditions and

vary from small and rod-shaped to long and filamentous (Moronta, 2022). *L. pneumophila* is ubiquitous in natural aquatic environments and can cope with a wide range of physical and chemical conditions (Fliermans et al., 1981). Naturally occurring *L. pneumophila* strains multiply at a pH value of 5.5 to 9.2 and at a temperature between 25 and 45 °C (Hochstrasser and Hilbi, 2022; Wadowsky et al., 1985). At temperatures above 50 °C, *L. pneumophila* does not grow and appears to lose viability (Hochstrasser and Hilbi, 2022; Katz and Hammel, 1987). Interestingly, temperature sensitivity seems to vary between *Legionella* spp and between isolates from different sites, when being grown in minimal defined medium (Hochstrasser and Hilbi, 2022). Under laboratory conditions, *L. pneumophila* is fastidious and does not grow on usual laboratory media. In order to multiply, the bacteria require supplementation of the growth medium with trace elements such as iron and a number of amino acids such as L-cysteine, which they cannot synthesize themselves (Taylor et al., 2009).

L. pneumophila has been found in natural water habitats such as lakes and rivers, but was also isolated from various man-made aquatic habitats including showers, air conditioning cooling towers, fountains and whirlpools (**Fig. 1.1**) (Dondero Jr et al., 1980; Haupt et al., 2015; Sethi and Brandis, 1983; Spitalny et al., 1984). However, *L. longbeachae* represents an exception, as it was mainly found in potting soil (Steele et al., 1990).

Like most bacteria, members of the family Legionellaceae prefer to live in multispecies communities in the environment, so-called biofilms, that consist of prokaryotic and eukaryotic organisms embedded in an extracellular matrix (Hilbi et al., 2011). *L. pneumophila* colonizes biofilms in natural environments as well as in human-made habitats such as plumbing systems (Hilbi et al., 2011; Rogers et al., 1994). There are several factors that influence the risk of biofilm formation. On one hand, biofilm formation and growth of *L. pneumophila* in potable water systems depends on the plumbing material. It was found that elastomeric surfaces are favorable for the formation of biofilms, as the material releases nutrients that promote bacterial growth (Rogers et al., 1994). In addition, the formation of biofilms and the growth of *L. pneumophila* in potable water systems depends on the temperature. It was found that *L. pneumophila* is most prevalent in biofilms on plastics at 40 °C. Moreover, the pathogen was able to survive in biofilms on the surface of plastics at 50 °C, but could not be detected at 60 °C (Rogers et al., 1994). Other factors that increase the risk of biofilm formation include scale deposits and corrosion as well as water stagnation or low flow rates. Biofilm prevention and maintenance of water systems are important to control *Legionella* proliferation (Cunha et al., 2016).

Legionella are frequently found as intracellular parasites of protozoa such as free-living amoeba including *Acanthameoba* spp., *Naegleria* spp., *Hartmanella* spp. and *Vahlkampfia* spp.. Amoeba are ubiquitous in aquatic environments and feed on bacteria by phagocytosis (Hsu et al., 2011). Protozoan host of *Legionella* spp. have also been detected in drinking water supplies (Valster et al., 2011). Protozoan predators such as *A. castellanii* “graze” on mixed communities and influence population dynamics within biofilms (Huws et al., 2005). *Legionella* uses this predatory behavior to its own advantage by replicating intracellularly in amoeba (Declerck et al., 2007; Rowbotham, 1980). The ability to replicate within many

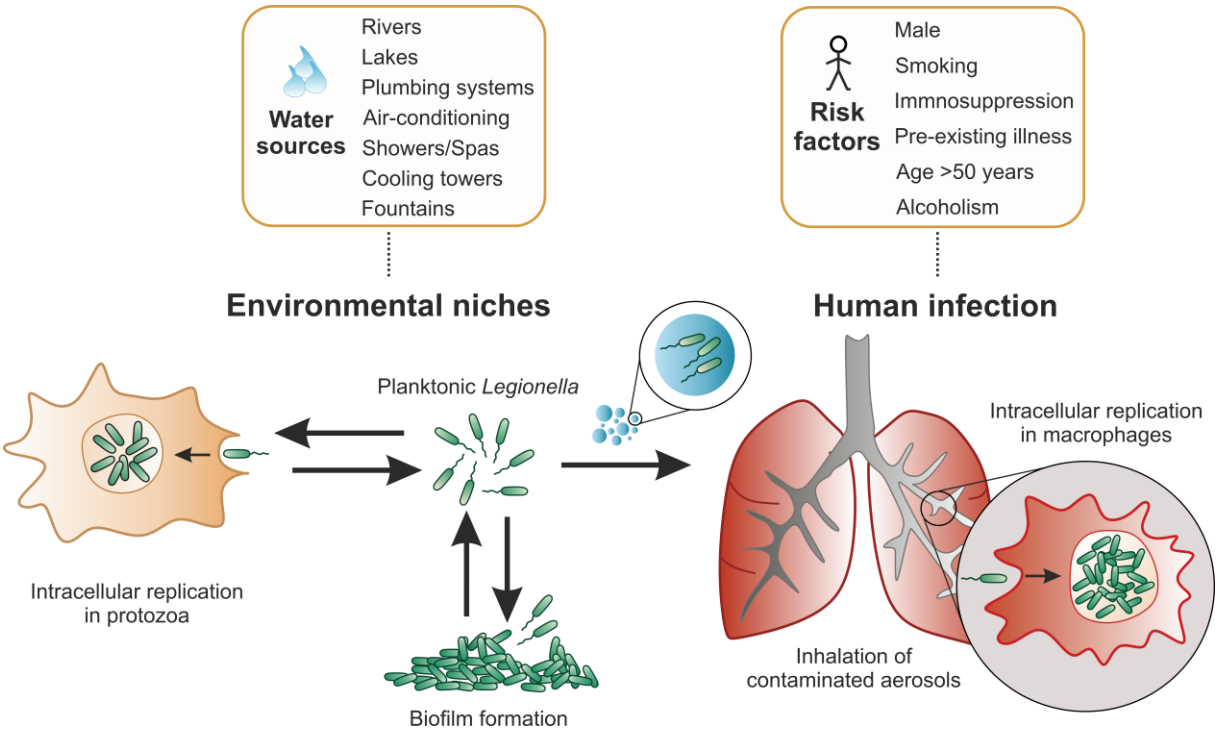

Figure 1.1. Environmental niches of *Legionella* and human infection.
In the environment, *Legionella* bacteria can persist as planktonic cells, colonize biofilms and replicate within protozoa. Within the host cells, the bacteria form a unique compartment, the so-called "*Legionella*-containing vacuole" (LCV), which allows them to replicate. *Legionella*-contaminated water sources can be of natural origin (e.g., rivers and lakes) or man-made, such as plumbing and air-conditioning systems, showers and spas, cooling towers, or fountains. Transmission to humans occurs via bacteria-containing aerosols. By inhaling contaminated water droplets, the bacteria enter the lungs, infect and destroy lung macrophages, and thus cause Legionnaires' disease. Risk factors for acquiring the disease include male gender, smoking, immunosuppression, certain pre-exiting illnesses, age over 50 years, and alcoholism.

types of protozoa is of central importance regarding the ecology of *Legionella*, as host cells not only provide a niche for replication, but also protect the bacteria from harsh environmental conditions such as biocides, antibiotics, acids, or thermal stress (Newton et al., 2010).

The ability to replicate within protozoa has enabled *Legionella* to also multiply within human alveolar macrophages (Newton et al., 2010). *L. pneumophila* enters the lung via inhalation of contaminated aerosols. After transmission, *L. pneumophila* can infect macrophages of the innate immune system (Hilbi et al., 2007). Human infection is a dead end for the replication of *Legionella*, as human-to-human transmission is not common (Newton et al., 2010) (**Fig. 1.1**).

1.1.3 Intracellular growth of *Legionella pneumophila*

The interaction of *L. pneumophila* with eukaryotic cells has been investigated in many protozoan and mammalian host models. To study the interactions of the pathogen with host cells in the environment, *Acanthamoeba castellanii*, *Hartmannella vermiformis*, *Naegleria* spp., and *Dictyostelium discoideum* were used. *D. discoideum* is a popular host model as it is genetically tractable, which allows the investigation of

host factors involved in the pathogenesis of *L. pneumophila*. To characterize the interaction of *L. pneumophila* with mammalian cells, macrophage-like tissue culture cells as well as mouse bone marrow-derived macrophages, human blood primary macrophages, HeLa cells, A459 cells and CHO-K1 epithelial cell derivates were used (Newton et al., 2010).Cell biological techniques helped to identify host pathways that are altered by *L. pneumophila* and enabled mechanistic studies on intracellular trafficking and survival strategies of the pathogen (Hubber and Roy, 2010).

The infection cycle of *L. pneumophila* begins with adhesion of the bacterium to a host cell, followed by cell entry involving the flagellum, pili, and surface proteins of the pathogen such as the major outer membrane protein, the heat shock protein and the mip protein (Cunha et al., 2016). The *mip* gene was the first virulence-associated gene of *L. pneumophila* shown to be involved in the infection of mammalian and protozoan hosts. This gene, called *mip* for macrophage infectivity potentiator, encodes at 24 kDa surface protein required for efficient infection of guinea pigs, phagocytic mammalian cells and protozoa (Fields et al., 2002).

L. pneumophila inhibits the bactericidal activity of phagocytes by preventing fusion of the phagosome with the lysosome, inhibiting the oxidative burst, reducing phagosome acidification, blocking phagosome maturation, and altering organelle trafficking, thus transforming the phagosome into a niche for intracellular replication (**Fig. 1.2**) (Cunha et al., 2016). Both *L. pneumophila* and *C. burnettii* utilize an Icm/Dot (intracellular multiplication/defective organelle trafficking) type IV secretion system (T4SS), which consists of approximately 27 components that form several subcomplexes (Ghosal et al., 2019). *L. pneumophila* secretes a remarkable number of around 300 effectors via the Icm/Dot T4SS, to modify various processes in the host cells. About 50 effectors have been studied so far and assigned a cellular function. Since *L. pneumophila* produces a total of around 3000 different proteins, the bacteria use around 10% of their genome to define the “interactome” with host cells (Finsel and Hilbi, 2015).The impressive number of effectors could be the result of co-evolution of *Legionella* spp. in a wide range of protozoan hosts (Hubber and Roy, 2010).

Several studies indicate that effector proteins are translocated into the host cells via the Icm/Dot system already at early stages of the infection cycle, e.g., to inhibit endocytic maturation and to promote vacuole modification. Mutants carrying a deletion of the *dotA* gene were studied in detail to analyze the contribution of the Icm/Dot system to the intracellular transport of *L. pneumophila* (Hubber and Roy, 2010). DotA is an integral inner membrane protein that is essential for the Icsm/Dot T4SS to regulate early phagosome trafficking. Phagosomes of *dotA* mutants showed accumulation of the lysosomal glycoprotein LAMP-1 within minutes after bacterial uptake. The data suggest that DotA plays an important role in regulating early phagosome trafficking decisions either at or immediately after uptake by the host cell (Roy et al., 1998).

The LCV matures into a replication-permissive organelle in a bi-phasic two-step process (Kagan and Roy, 2002). Initially, ER-derived host vesicles associate and fuse with the LCV (**Fig. 1.2**). *L. pneumophila* utilizes a variety of host factors to facilitate the recruitment and fusion of ER-derived vesicles with the LCV (Hubber and Roy, 2010). Two examples are Rab1, a small guanosine triphosphatase (GTPase) and

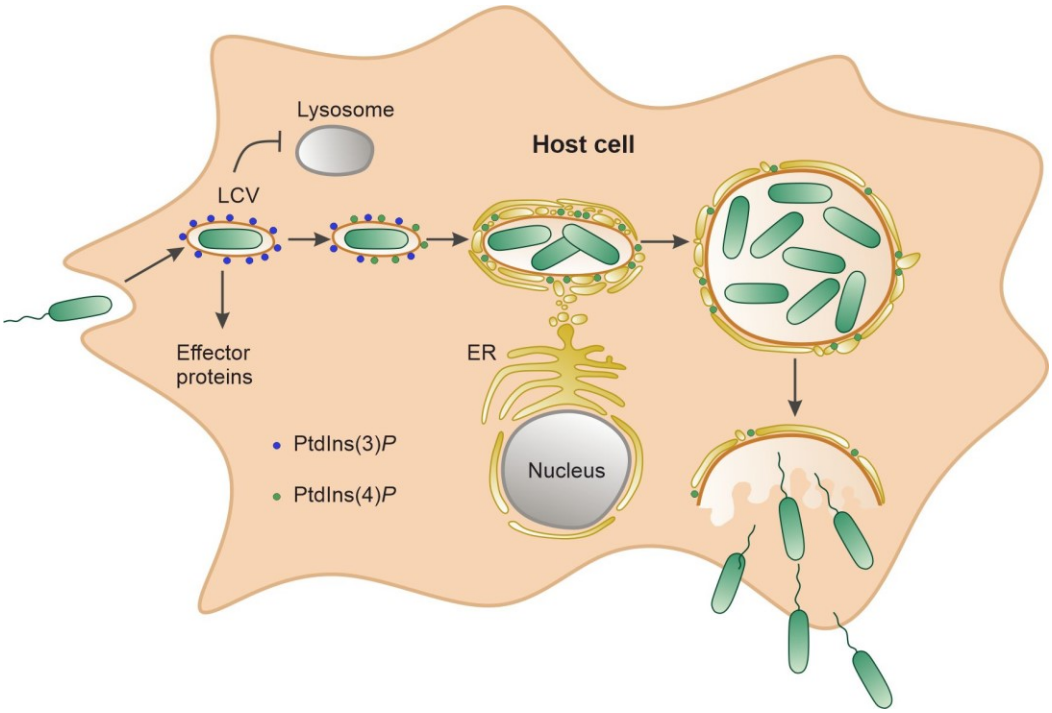

Figure 1.2. Formation of a *Legionella* containing vacuole within a host cell.
Following uptake into the host cell, *L. pneumophila* prevents fusion with the lysosome and employs the Icm/Dot type IV secretion system (T4SS) to translocate more than 300 effector proteins into the host cell. The formation and maturation of the LCV is accompanied by a phosphoinositide (PI) lipid conversion from the endosomal PI phosphatidylinositol 3-phosphate (PtdIns(3)P) to the secretory PI PtdIns(4)P. The effector proteins target many cellular pathways and manipulate important host processes. This enables *L. pneumophila* to recruit ER-derived vesicles and to form a unique compartment, the *Legionella* containing vacuole (LCV). This allows the pathogen to replicate intracellularly and to finally exit the cell again and to initiate a new round of infection.

Sec22b, a soluble *N*-ethylmaleimide-sensitive factor attachment protein receptor (SNARE). *L. pneumophila* subverts the function of the host proteins Rab1 and Sec 22b to facilitate the transport and fusion of ER-derived vesicles with the LCV to create a replicative organelle (Kagan et al., 2004). LepB, is an effector protein of *L. pneumophila* that acts as a GTPase activating protein (GAP), which inactivates Rab1 by stimulating GTP hydrolysis. This could potentially facilitate the removal of the GTPase from the early LCV after maturation mediated by association and fusion of secretory vesicles (Ingmundson et al., 2007).

The host GTPase ARF1 is involved in the second phase of vacuole maturation (Hubber and Roy, 2010). Proteins of the ADP-ribosylation factor (ARF) family are important regulators of membrane dynamics (Donaldson and Jackson, 2000). The effector protein RalF functions as a guanine nucleotide exchange factor (GEF) for the ARF family and is required for the localization of ARF on *L. pneumophila* phagosomes (Nagai et al., 2002).

Phosphoinositides (PIs) are lipids that occur in various forms and contribute to the identity of organelles. Their functions include signal transduction at the cell surface, as well as the regulation of membrane traffic and cytoskeleton dynamics (Di Paolo and De Camilli, 2006). PI lipids are derivates of

phosphatidylinositol (PtdIns), which have a head group that can be phosphorylated and dephosphorylated at positions 3'', 4'', and/or 5''. *L. pneumophila* uses PI-subverting effectors that either anchor to PIs, directly modify the lipids, or recruit PI-metabolizing enzymes to the LCV membrane to promote LCV formation (Haneburger and Hilbi, 2013). Following internalization of *L. pneumophila*, the PI lipid pattern on the LCV is converted from the endocytotic PI PtdIns(3)*P* to the secretory PI PtdIns(4)*P* (**Fig. 1.2**). The PI lipid PtdIns(4)*P* is a hallmark of the host cell secretory pathway, and the LCV steadily acquires PtdIns(4)P-positive Golgi-derived vesicles. Throughout the infection, the LCV remains PtdIns(4)*P*-positive (Weber et al., 2018). PtdIns(4)*P* is bound by a number of *L. pneumophila* effectors, including SidC and SidM. The Icm/Dot substrate SidC anchors to the LCV via PtdIns(4)*P* and recruits ER vesicles to the LCV (Ragaz et al., 2008). Purified SidM specifically and directly binds to PtdIns(4)*P* (Brombacher et al., 2009). SidM functions as a GEF as well as a guanine nucleotide dissociation inhibitor displacement factor (GDF) for Rab1, a GTPase that regulates the transport of ER derived vesicles (Ingmundson et al., 2007).

In summary, *L. pneumophila* employs a variety of effectors to modulate several crucial host processes in its favor to create a unique compartment that enables intracellular survival and replication of the pathogen. Until now, much remains unknown regarding the effectors involved and how they interfere with host processes. The characterization of these effectors will continue to be an important focus of research in this field and could possibly reveal new regulatory mechanisms of eukaryotic pathways.

1.1.4 The bi-phasic life cycle of *L. pneumophila*

As a pathogen that survives in water as a free-living microbe, resides in biofilms, but also replicates in phagocytes, and therefore, the pathogen is exposed to various environmental conditions. The adaption of the pathogen to distinct environments correlates with a bi-phasic life cycle that includes a replicative phase and a transmissive phase (Molofsky and Swanson, 2004). The bi-phasic lifestyle of *L. pneumophila* is accompanied by a number of phenotypic changes. Throughout the replicative phase, *L. pneumophila* grows exponentially, is non-motile, and represses transmissive traits. In contrast, the post-exponential transmissive phase is associated with an increased virulence of *L. pneumophila*, and the bacteria become cytotoxic, motile and osmotically resistant (Best and Kwaik, 2019). Interestingly, growth and virulence are reciprocally linked in the *L. pneumophila* life cycle, as growing/exponential bacteria are non-virulent and non-growing/post-exponential bacteria are virulent and motile (Byrne and Swanson, 1998; Hochstrasser and Hilbi, 2022).

The bi-phasic life cycle of *L. pneumophila* is controlled by the availability of nutrients such as amino acids (Byrne and Swanson, 1998). In addition, *L. pneumophila* SpoT, a guanosine 3'-5'-bispyrophosphate (ppGpp) synthetase, monitors fatty acid biosynthesis to alternate between replication and transmission in macrophages (Best and Kwaik, 2019; Dalebroux et al., 2009).

Transcription profiles of *L. pneumophila* in the replicative and the transmissive phase both during infection of *A. castellanii* and in broth, highlighted the many changes that distinguish the two phases from each other. During the replicative phase, metabolic genes involved in carbohydrate utilization and amino acid catabolism were preferentially expressed. The transmissive phase of *L. pneumophila* was

characterized by an upregulated expression of many genese encoding proteins secreted by the Icm/Dot T4SS such as proteins involved in flagellar biosynthesis and other virulence factors. In addition, 18 of 24 GGDEF/EAL genes present in the *L. pneumophila* genome were found to be upregulated in the transmissive phase, suggesting that GGDEF/EAL domain proteins are important for *L. pneumophila* life cycle regulation (Brüggemann et al., 2006; Newton et al., 2010).

CsrA (carbon storage regulator A) is an RNA-binding regulator of the bi-phasic life cycle in *L. pneumophila*. CsrA functions as a global repressor of transmission traits and as an activator of intracellular replication (Forsbach-Birk et al., 2004; Molofsky and Swanson, 2003). In addition, *L. pneumophila* employs the Lqs (*Legionella* quorum sensing) system as a regulator of the growth phase switch. The Lqs system consists of the autoinducer synthase LqsA, the sensor kinases LqsS and LqsT and the response regulator LqsR. The Lqs system produces and reacts to the small signaling molecule LAI-1 (*Legionella* autoinducer-1, 3-hydroxypentadecan-4-one) (**Fig. 1.3**). Together, the Lqs system and the LAI-1 circuit regulate a number of transmissive traits such as pathogen-host cell interactions, virulence, motility, and expression of a 133 kb chromosomal "fitness island" (Hochstrasser and Hilbi, 2017). Interestingly, the production of LqsR is regulated by the alternative sigma factor RpoS and by CsrA, suggesting a direct link between the production of LqsR and the growth phase switch (Hochstrasser and Hilbi, 2017, 2022; Sahr et al., 2017). When nutrients are abundant, CsrA represses transmission traits and promotes replication. When nutrients become scarce (onset of stationary phase), RpoS and the two component system (TCS) LetA/LetS upregulate transmission traits (**Fig. 1.3**) (Personnic et al., 2018).

1.1.5 *Legionella* quorum sensing and LAI-1 mediated signaling

Bacteria employ small signaling molecules to communicate among each other and with their host cells. They produce, release, and detect signaling molecules to measure the density of their population and to control their behavior in response to fluctuating cell numbers. This process of intercellular communication is very common in the bacterial world and is referred to as quorum sensing. As a bacterial population grows, the concentration of an extracellular signaling molecule increases proportionally. Once a threshold concentration is reached, a population-wide change in gene expression is initiated. Quorum sensing usually controls processes that would be unproductive if carried out by an individual but become effective when undertaken by a community, such as the induction of bioluminescence, the secretion of virulence factors or biofilm formation (Bassler and Losick, 2006).

The small signaling molecules executing for quorum sensing are called autoinducers. The predominant type of autoinducers used by Gram-negative bacteria are acyl homoserine lactones (AHLs). AHL autoinducers of different bacterial species share a homoserine lactone moiety as a core molecule, but contain different acyl side chains (Camilli and Bassler, 2006). Additional signaling molecules employed by Gram-negative bacteria include autoinducer-2 (AI-2) and its precursor 4,5-dihydroxy-2,3-pentanedione (DPD), diffusible signal factor (DSF), 2-heptyl-3-hydroxy-4-quinolone (PQS), as well as dialkylresorcinol (DAR) and α-hydroxyketone (AHK) molecules. AI-2, DSF and AHKs are detected by membrane-bound sensor kinases of TCS (Personnic et al., 2018). *Vibrio cholerae*, the causative agent of the disease cholera,

controls the production of virulence factors and biofilm formation in response to two extracellular autoinducers, one of which is called CAI-1 (*cholera* autoinducer-1, (*S*)-3-hydroxytridecon-4-one). The enzyme CqsA is required for the biosynthesis of amino-CAI-1, which is then further converted to CAI-1 (Kelly et al., 2009). CAI-1 is detected by the receptor CqsS (*cholerae* quorum sensing sensor), a membrane-bound sensor histidine kinase (Miller et al., 2002).

Most bacteria release membrane vesicles with a diameter of 20 to 400 nm, that contain specific cargo molecules with diverse functions. They are often referred to as outer membrane vesicles (OMVs), as they were first found to be produced by blebbing of the outer membrane of Gram-negative bacteria (Toyofuku et al., 2019). Such vesicles are also employed for the transport of autoinducers, as shown in *Vibrio harveyi*, which packages the hydrophobic quorum sensing molecule CAI-1 into OMVs. This could stabilize CAI-1 in an aqueous environment and enable the unhindered passage of the molecule through the lipopolysaccharide layers of the producing and target cells. (Brameyer et al., 2018). The opportunistic human pathogen *Pseudomonas aeruginosa* also packages the hydrophobic quorum sensing signaling molecule PQS (pseudomonas quinolone signal) in extracellular OMVs in order to traffic the molecule within the population (Mashburn and Whiteley, 2005).

L. pneumophila apparently does not employ the commonly used AHLs and instead uses the AHK compound LAI-1 for interspecies and interkingdom signaling. Recent studies have shown that LAI-1 is secreted via OMVs to promote interbacterial communication and interactions with eukaryotic host cells. For example, *L. pneumophila* OMVs containing LAI-1 were shown to inhibit the migration of amoeba and overexpression of *lqsA* promoted the intracellular growth of *L. pneumophila* in macrophages (Fan et al., 2023).Previous investigations have shown that LAI-1 modulates cell migration via a pathway comprising the scaffold protein IQGAP1, the small GTPase CdC42 as well as the Cdc42-specific GEF ARHGEF9 (Simon et al., 2015). However, the eukaryotic LAI-1 receptor(s) remain unknown.

The Lgs (*lqsA-lqsR-hdeD-lqsS*) encodes the LAI-1 autoinducer synthase LqsA, the response regulator LqsR, a homologue of *Escherichia coli* HdeD and the cognate sensor kinase LqsS (**Fig. 1.3**). The function of *hdeD* is unknown. All four genes are expressed from individual promoters (Sahr et al., 2017). Interestingly, the Lqs system includes an orphan sensor kinase termed LqsT (*lpg2506*), which is expressed from its own promoter and does not appear to be linked to other genes (Kessler et al., 2013). A bioinformatic analysis revealed, that the *L. pneumophila lgsAS* genesare homologous to the *cqsAS* (*cholerae* quorum sensing) genes from *V. cholerae*, as the autoinducer synthase CqsA and the sensor kinase CqsS share 45% or 29% identity with the corresponding *L. pneumophila* proteins LqsA and LqsS, respectively (Tiaden et al., 2007).

LqsS and LqsT are putative six trans-membrane helix histidine sensor kinases and share 31% identity (Schell et al., 2014; Tiaden and Hilbi, 2012). The LAI-1 responsive sensor kinases function partially antagonistic and are differentially expressed in the post-exponential growth phase. In fact, transcriptome studies indicated that 90% of the genes that are downregulated in the absence of *lqsT* are upregulated in *L. pneumophila* lacking *lqsS*. (Kessler et al., 2013). LqsS and LqsT are autophosphorylated at a conserved

histidine residue (H_{200} or H_{204}) located in their cytoplasmic histidine kinase domain (Schell et al., 2014). At low cell density (exponential growth phase) and low concentrations of LAI-1, LqsS and LqsT are autophosphorylated and transfer the phosphoryl moiety to the response regulator LqsR, which forms dimers upon phosphorylation at the conserved aspartate residue Asp108 (**Fig. 1.3**). This promotes bacterial replication and negatively regulates motility, virulence, natural competence for DNA uptake, formation of extracellular filaments and the expression of the 133 kb fitness island. At high cell density (stationary growth phase) and high LAI-1 concentrations, the autophosphorylation of LqsS and LqsT is inhibited, and the phosphate flow is reversed, leading to dephosphorylation of LqsR. This represses replication and positively regulates motility, virulence, competence, extracellular filaments, and the expression of a fitness island. Taken together, the results suggest that the *lqs* genes and LAI-1 regulate the transition from the replicative to the transmissive growth phase of *L. pneumophila* (Schell et al., 2014; Schell et al., 2016b).Moreover, *L. pneumophila* LAI-1 signaling involves two sensor kinases and complex cross-talk among the two sensor kinase pathways is likely to occur (Kessler et al., 2013).

Individual cells in genetically homogenous cultures exhibit phenotypic heterogeneity, which is considered to increase the fitness at the population level. The heterogeneity is reflected in a broad range of phenotypes, for instance, individual cells may exhibit different degrees of virulence or antibiotic resistance (Avery, 2006). Phenotypic heterogeneity arises in response to extrinsic or intrinsic signals or due to stochastic switching of gene expression (Striednig and Hilbi, 2022).

Recent studies have shown that the Lqs system regulates the phenotypic heterogeneity of *L. pneumophila* in amoebae and macrophages as well as in biofilms and microcolonies. Specifically, quorum has been shown to modulate the formation of virulent persisters within infected cells and to control the persistence, resuscitation, and virulence of *L. pneumophila* subpopulations in biofilms (Personnic et al., 2021; Personnic et al., 2019). Persisters are a clinically important manifestation of phenotypic heterogeneity and comprise individuals in a clonal, antibiotic-tolerant population that survive exposure to high concentrations of antibiotics for a longer period of time. They pose a serious threat in clinical practice and are thought to be responsible for recurrent and recalcitrant infections (Striednig and Hilbi, 2022). Furthermore, quorum sensing was found to elicit a transmissive subpopulation at the LCV periphery towards the end of an infection cycle, which predominantly escapes the pathogen vacuole and spreads from the bursting cell, while non-motile bacteria remain behind (Striednig et al., 2021).Taken together the results suggest, that quorum sensing increases the overall fitness of a bacterial population by controlling group behavior as well as individual traits (Striednig and Hilbi, 2022).

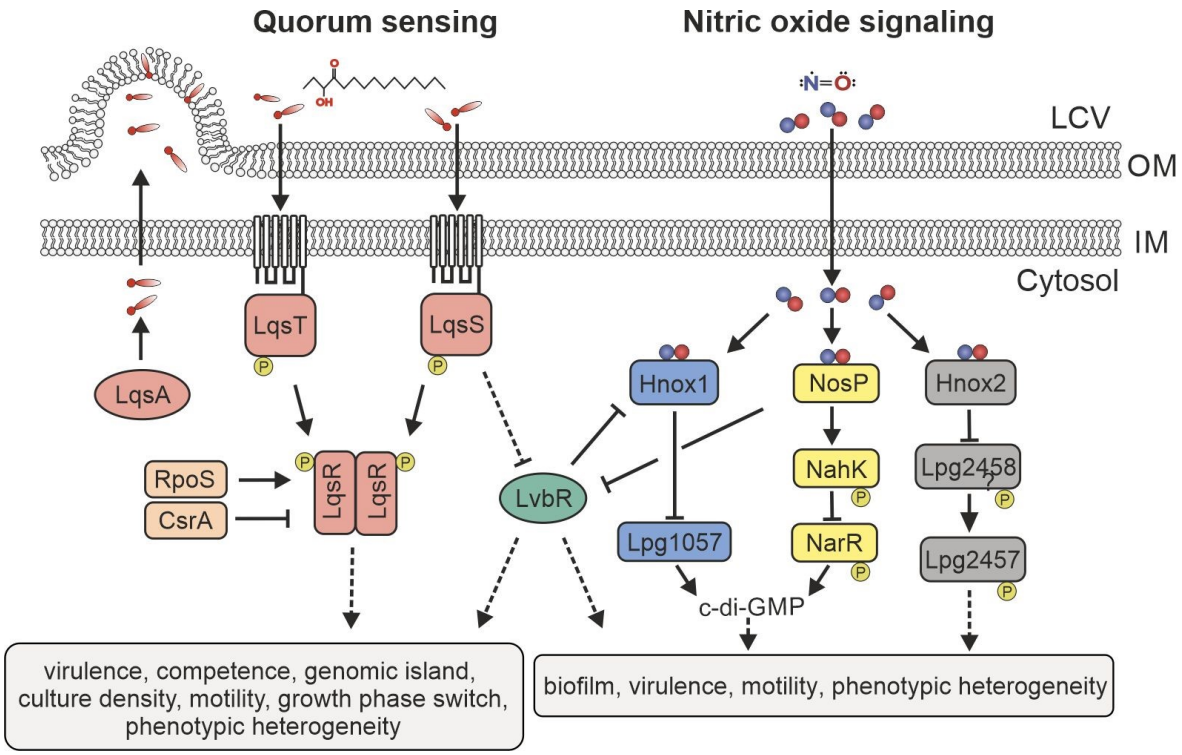

Figure 1.3. *Legionella* quorum sensing and nitric oxide signaling.
The *Legionella* quorum sensing (Lqs) system comprises the autoinducer synthase LqsA, the homologous sensor kinases LqsS and LqsT, and the response regulator LqsR. The autoinducer synthase LqsA produces the α-hydroxyketone LAI-1 (*Legionella* autoinducer-1, 3-hydroxypentadecan-4-one), which partitions into outer membrane vesicles (OMVs), to promote interbacterial and interkingdom signaling. The sensor kinases LqsS and LqsT detect LAI-1 and transmit the phosphorylation signal to the response regulator LqsR. The production of LqsR is regulated by carbon storage regulator A (CsrA) and the stationary sigma factor RpoS. The Lqs system and the LAI-1 signaling circuit regulate several traits of the pathogen including the growth phase switch, virulence, bacterial motility, natural competence for DNA uptake, culture density, expression of a "fitness island" and phenotypic heterogeneity. The Lqs system is linked to the c-di-GMP regulatory network by the LqsS-regulated, pleiotropic transcription factor LvbR (*Legionella* virulence and biofilm regulator). LvbR directly regulates the transcription of *hnox1* (encoding an inhibitor of the diguanylate cyclase Lpg1057) by binding to its promoter, and thus, regulates proteins involved in c-di-GMP metabolism. In addition, LvbR regulates different traits in *Legionella*, including biofilm architecture and pathogen-host interactions. *L. pneumophila* has two genes that code for H-NOX proteins and bind nitric oxide (NO), *lpg1056* (*hnox1*) and *lpg2459* (*hnox2*). One of them, *lpg1056* (*hnox1*), localizes adjacent to a gene encoding a GGDEF-EAL protein, *lpg1057*. Hnox1 inhibits the DGC activity of Lpg1057 in response to NO, resulting in lower levels of the second messenger bis-(3'-5')-cyclic dimeric guanosime monophosphate (c-di-GMP). The other H-NOX gene, *hnox2*, localizes adjacent to a sensor histidine kinase gene (*lpg2458*), and a CheY-like response regulator gene (*lpg2457*). Another NO sensor of *L. pneumophila* is called NosP (NO sensing protein). Through binding of NO to NosP, NahK autophosphorylation is activated. Following phosphate transfer from NahK (sensor histidine kinase) to the bifunctional enzyme NarR (response regulator), NarR shows decreased DGC and increased PDE activity, which results in lower levels of c-di-GMP. Together, the NO-responsive systems Hnox1-Lpg1057 and NosP-NahK-NarR regulate the intracellular level of c-di-GMP. The second messenger c-di-GMP is synthesized by diguanylate cyclases (DGCs) from two molecules of GTP and degraded by phosphodiesterases (PDEs) to 5'-phosphoguanylyl-(3'-5')-guanosine (pGpG) or GMP. Through binding to effector molecules c-di-GMP regulates numerous complex traits in bacteria, including biofilm formation, virulence, and motility.

1.1.6 C-di-GMP and nitric oxide signaling in *L. pneumophila*

L. pneumophila gene regulation integrates a broad spectrum of distinct endogenous and exogenous signals Endogenous signals produced and detected by the pathogen include the previously discussed quorum sensing molecule LAI-1 as well as the intracellular signaling molecule bis-3'-5'-cyclic dimeric guanosine monosphosphate (c-di-GMP) (Hochstrasser et al., 2019). The conserved second messenger c-di-GMP is synthesized by diguanylate cyclases (DCGs) and the cooperative action of their two GGDEF domains. The catalytic domains are named after their conserved signature motif Gly-Gly-Asp-Glu-Phe and are responsible for positioning two GTP molecules in an antiparallel manner to allow their condensation into c-di-GMP. The degradation of c-di-GMP is catalyzed by the mechanistically distinct c-di-GMP specific phosphodiesterases (PDEs) that contain an EAL domain or an HD-GYP domain. EAL-domain-containing PDEs hydrolyze c-di-GMP to yield the linear product 5'-phosphoguanylyl-(3'-5')-guanosine (pGpG). Specific phosphodiesterases containing an HD-GYP domain hydrolyze c-di-GMP in a one-step reaction, generating two molecules of GMP. By binding to effector molecules such as mRNA riboswitches, transcriptional regulators or proteins that contain PilZ domains, c-di-GMP regulates numerous cellular processes, including motility, adherence, biofilm formation, virulence, and cell cycle progression (Jenal et al., 2017).

The Lqs system is linked to the c-di-GMP regulatory network via the pleiotropic transcription factor LvbR (*Legionella* virulence and biofilm regulator) (**Fig. 1.3**). LvbR is a conserved transcription factor, which is negatively regulated by the sensor histidine kinase LqsS. In the genome of *L. pneumophila* Philadelphia-1, the *lvbR* gene is located between the genes *lpg1055* (hypothetical protein) and *lpg1056* (Hnox1). Interestingly, LvbR binds to the intergenic region between *lvbR* and *lpg1056*, not to autoregulate its own expression, but to negatively regulate the expression of *lpg1056*. Hnox1 (lpg1056) is a negative regulator of the adjacently encoded diguanylate cyclase Lpg1057. Since LvbR negatively regulates the inhibitor Lpg1056, it positively regulates Lpg1057 (and the production of c-di-GMP). LvbR determines biofilm architecture, as Δ*lvbR* forms homogeneous "mat"-like biofilms, while the parental strain develops "clustered" or "patchy" biofilms with more compact aggregates comprising bacterial clusters. Furthermore, *L. pneumophila* lacking *lvbR* is defective for infecting phagocytes, outcompeted by the parental strain in amoebae co-infections, and impaired for inhibiting cell migration. Overall, LvbR is a pleiotropic transcription factor that regulates proteins involved in c-di-GMP metabolism and controls biofilm architecture as well as pathogen-host cell interactions (Hochstrasser et al., 2019).

Nitric oxide (NO) is a gaseous, diatomic radical that can rapidly diffuse across cell membranes (Boon and Marletta, 2005). NO is used by eukaryotes in low concentrations as a cardiovascular signaling molecule and neurotransmitter. Furthermore, the molecule is produced by macrophages in much higher, cytotoxic concentrations, where it serves as a defense against pathogens (Plate and Marletta, 2013). However, bacteria are not only exposed to host-derived NO during infection, but also encounter NO derived from bacterial denitrification processes or from inorganic sources (Nisbett and Boon, 2016; Stern and Zhu, 2014). In addition, amoeba hosts of *Legionella* such as *Dictyostelium discoideum* were found to produce nitric oxide (Tao et al., 1997). Since high concentrations of NO cause nitrosative stress and can lead to cell

death, bacteria have developed several mechanisms to detect and detoxify NO. These include NO-responsive transcriptional regulators that detect NO, e.g., NorR (regulator of NO reductase) and detoxifying NO-binding enzymes such as flavohaemoglobins, which convert NO into less toxic molecules. While NO detoxification is associated with micromolar concentrations of NO, bacteria (as well as eukaryotes) can also detect NO as signaling molecule at low concentrations to regulate various processes such as biofilm formation (Bacon et al., 2017).

In mammalian cells, NO is produced from the amino acid L-arginine by a family of three different nitric oxide synthases (NOS). The NOS isoforms comprise the endothelial nitric oxide synthase (eNOS), the neuronal nitric oxide synthase (nNOS) and the inducible nitric oxide synthase (iNOS), reflecting the tissues of origin of the original enzyme isolates (Michel and Feron, 1997). NO can rapidly diffuse across cell membranes and bind to the heme protein soluble guanylate cyclase (sGC). Other diatomic gases such as dioxygen or carbon monoxide either do not bind to sGC, or do not significantly activate the heme protein, thereby providing selectivity and efficiency for NO even in aerobic environments (Derbyshire and Marletta, 2009). sGC consists of two homologous subunits (α1 and β1), each comprising a heme-nitric oxide and oxygen (H-NOX) domain, a central PAS domain, an amphipathic helix, and a catalytic domain. Heme binds to the N-terminal H-NOX domain on the β1 subunit. As NO binds to the heme iron, the ferrous-NO [Fe(II)-NO] complex is formed and the conversion of GTP to the second messenger cyclic GMP (cGMP) is activated. cGMP regulates various physiological functions such as vasodilation and neurotransmission (Bacon et al., 2017; Derbyshire and Marletta, 2009). While it was previously thought that the sGC heme binding domain was only associated with mammalian NO-activated guanylate cyclases, it is now known that the sGC heme domain belongs to the conserved large family of H-NOX proteins found in eukaryotes as well as in prokaryotes (Derbyshire and Marletta, 2009; Iyer et al., 2003).

Prokaryotic H-NOX proteins are found in operons together with histidine kinases, c-di-GMP synthases/phosphodiesterases or methyl-accepting chemotaxis proteins (Bacon et al., 2017; Iyer et al., 2003). Operon predictions revealed that the genome of *L. pneumophila* Philadelphia comprises two H-NOX operons (**Fig. 1.4**) (Price et al., 2007). The *L. pneumophila* H-NOX proteins, termed Hnox1 and Hnox2 were both found bind to NO, but not to O_2. The gene encoding Hnox1 (*lpg1056*), is adjacent to a GGDEF-EAL protein (encoded by *lpg1057*). The *hnox2* gene (*lpg2459*) is adjacent to a histidine kinase (*lpg2458*), and a CheY-like response regulator (encoded by *lpg2457*), to which no function has yet been assigned. Experimental studies on the *L. pneumophila* Hnox1 protein revealed that the deletion of the *hnox1* gene results in a hyper-biofilm phenotype. Furthermore, overexpression of Lpg1057 in *L. pneumophila* also resulted in a hyper-biofilm phenotype. The additional deletion of *lpg1057* in the Δ*hnox1* background reversed the hyper-biofilm phenotype of the Δ*hnox1* mutant, demonstrating that Lpg1057 is part of the Hnox1 signaling pathway. Moreover, Lpg1057 was shown to be an active diguanylate cyclase, which is inhibited by the Hnox1 protein in the Fe(II)-NO ligated state. However, phosphodiesterase activity of Lpg1057 could not be measured, which could be due to mutations in the EAL domain of the protein that

may render this domain catalytically inactive. In summary, the results suggest that Hnox1 regulates c-di-GMP production by Lpg1057 in response to NO (**Fig. 1.4**) (Carlson et al., 2010).

All bacterial H-NOX proteins described so far bind heme and were termed H-NOX proteins to describe the ability of some of these proteins to bind O_2 in addition to NO and CO (Derbyshire and Marletta, 2009). Biochemical studies on bacterial wild-type and mutant H-NOX proteins provided further insights into ligand binding characteristics and selectivity against O_2 (Boon et al., 2005). Structural studies on the oxygen-binding H-NOX domain of the obligate anaerobe *Thermoanaerobacter tengcongensis* (later renamed *Caldanaerobacter subterraneus* (Fardeau et al., 2004)) suggested that a tyrosine (Tyr140) in the distal pocket is involved in O_2 binding. Interestingly, sequence alignment of H-NOX domains revealed that a tyrosine at this position was only found in H-NOX domains that are part of chemotaxis receptors in anerobic organisms, whereas residues at this position in the H-NOX domains of facultative aerobes and in animal sGC are mostly hydrophobic (Pellicena et al., 2004).

Both *L. pneumophila* H-NOX proteins *L1* H-NOX (*lpg1056*) and *L2* H-NOX (*lpg2459*) were shown to form Fe^{II}-NO complexes and share 19 and 16% identity with sGC (**Fig. 1.4**). *L1* H-NOX1 was shown to form a 5-coordinate, temperature-independent Fe^{II}-NO complex, whereas *L2* H-NOX forms a temperature-dependent mixture of 5- and 6-coordinate Fe^{II}-NO complexes (Boon et al., 2006). The *L. pneumophila* H-NOX domain L2 H-NOX (*lpg2459*) does not bind O_2 and has a phenylalanine at position 142 (homologous position to Tyr140 in *T. tengcongensis* H-NOX). Interestingly, the mutated protein *L2* H-NOX F142Y was capable of binding O_2 and was purified as a Fe^{II}-O_2 complex, indicating that the replacement only of a single hydrogen (-H) with a hydroxyl group (-OH) allows to modulate binding properties of the protein (Boon et al., 2005).

To date, bacterial H-NOX domains from many different species have been characterized and are thought to have nanomolar to picomolar affinity for NO, highlighting the importance of H-NOX domains in bacterial NO signaling. In addition to the relatively well-studied H-NOX family, there is another heme-based bacterial NO sensor, termed nitric oxide sensing protein (NosP), which in contrast to H-NOX proteins, is almost exclusively encoded in bacterial genomes (Bacon et al., 2017).

The *L. pneumophila* Philadelphia NosP protein (Lpg0279) is encoded in a putative operon together with the histidine kinase NahK (Lpg0278) and the c-di-GMP synthase/phosphodiesterase NarR (Lpg0277) (Fischer et al., 2019). The c-di-GMP metabolizing response regulator NarR contains a diguanylate cyclase, a phosphodiesterase as well as a receiver domain and has been previously shown to regulate biofilm formation and c-di-GMP levels in the *L. pneumophila* Lens strain (Fischer et al., 2019; Pecastaings et al., 2016). Moreover, it has been shown in the *L. pneumophila* Lens strain that Lpl0330 (NahK homolog) and LpL0329 (NarR homolog) form a two-component signaling system, and that Lpl0330 modulates the activity of Lpl0329 by phosphorylation to regulate c-di-GMP levels (Fischer et al., 2019; Levet-Paulo et al., 2011). Further biochemical studies revealed that NahK is an active kinase that transfers phosphate to NarR and that phosphorylation of the NarR receiver domain affects both diguanylate cyclase and phosphodiesterase activity. In addition, it was shown that NosP is a hemoprotein that binds NO and

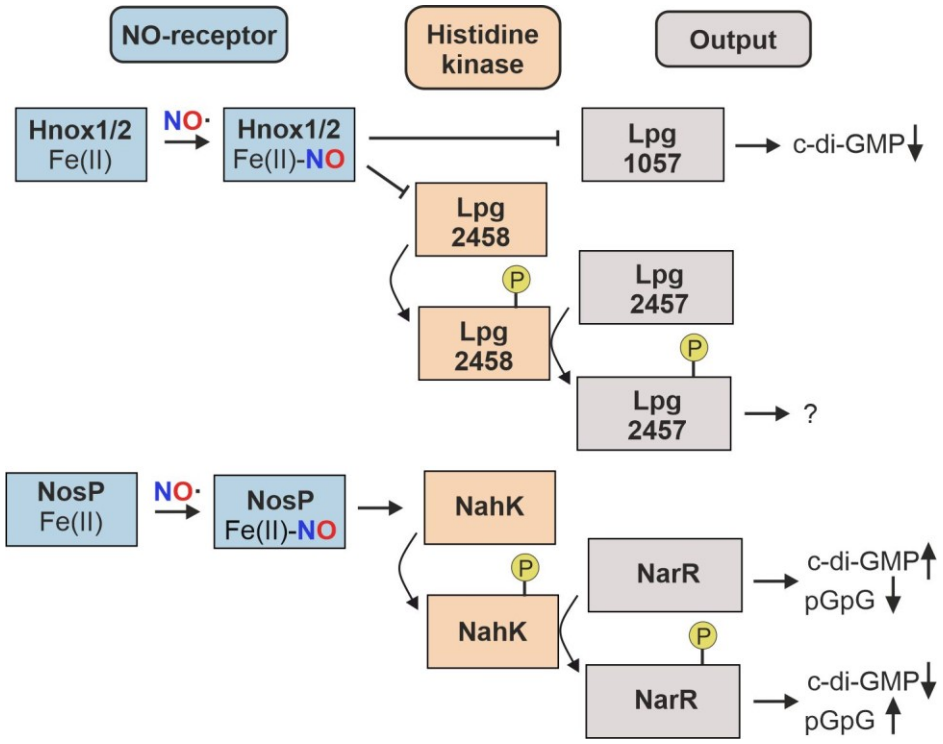

Figure 1.4. Nitric oxide signaling pathways in *L. pneumophila*.
To date, three NO receptors of *L. pneumophila* have been identified and termed Hnox1, Hnox2 and NosP. Hnox1 forms a 5-coordinate, Fe^{II}-NO complex, whereas Hnox2 forms a temperature-dependent mixture of 5- and 6-coordinate Fe^{II}-NO complexes. The gene coding for Hnox1 (*lpg1056*) is found adjacent to a gene encding a GGDEF-EAL protein (*lpg1057*). The other H-NOX gene, *hnox2* (*lpg2459*) is adjacent to genes encoding a histidine kinase, (*lpg2458*), and a CheY-like response regulator (*lpg2457*). Upon binding of NO, Hnox1 inhibits the diguanylate cyclase activity of Lpg1057, which results in lower c-di-GMP levels. The *L. pneumophila* NosP protein (Lpg0279) is encoded in an operon adjacent to genes encoding the histidine kinase NahK and the cylic-di-GMP metabolizing response regulator NarR, which is predicted to have both diguanylate cyclase and phosphodiesterase activity. Fe(II)-NO NosP likely functions to activate NahK autophosphorylation. NahK is a histidine kinase that transfers phosphate to NarR. The phosphorylation of NarR modulates its activity and causes a decrease in its diguanylate cyclase activity and an increase in its phosphodiesterase activity, which ultimately leads to a decrease of the c-di-GMP level. Overall, NO binds to three distinct NO receptors and thus exogenously controls the c-di-GMP regulatory network of *L. pneumophila*.

modulates NahK activity. In particular, Fe(II)-NO NosP likely activates the autophosphorylation of NahK, causing an overall decrease in c-di-GMP levels. In summary, the NO-sensor NosP binds NO and is involved in the regulation of c-di-GMP production by the two component system proteins NahK and NarR (**Fig. 1.4**) (Fischer et al., 2019).

Taken together, the results of numerous studies suggest that *L. pneumophila* possesses two H-NOX proteins (Hnox1 and Hnox2) and one NosP protein, that bind low concentration of NO with high affinity and are involved in the modulation of *L. pneumophila* signaling pathways that, at least in the case of Hnox1 and NosP, involve the second messenger molecule c-di-GMP.

1.2 The ins and outs of Legionella autoinducer and nitric oxide signaling

The ins and outs of Legionella autoinducer and nitric oxide signaling

Sarah Michaelis[1], Laura Gomez-Valero[2], Tong Chen[1], Camille Schmid[1], Carmen Buchrieser[2] and Hubert Hilbi[1*]

[1]Institute of Medical Microbiology, University of Zürich, Gloriastrasse 30, 8006 Zürich, Switzerland.

[2]Institut Pasteur, Université de Paris, Unité Biologie des Bactéries Intracellulaires, 75015 Paris, France

RUNNING TITLE: *Legionella* small molecule signaling

KEYWORDS: α-hydroxyketone, amoeba, autoinducer, cell-cell communication, c-di-GMP, *Dictyostelium*, inter-kingdom signaling, *Legionella*, macrophage, motility, nitric oxide, signal transduction, phospho-transfer, response regulator, sensor kinase, quorum sensing, virulence.

ABBREVIATIONS: CAI-1, cholerae autoinducer-1; c-di-GMP; cyclic-di-guanylate mono phosphate; *cqs*, cholerae quorum sensing; DPTA (dipropylenetriamine) NONOate, (Z)-1-[N-(3-aminopropyl)-N-(3-ammoniopropyl)amino]diazen-1-ium-1,2-diolate; Icm/Dot, intracellular multiplication/defective organelle trafficking; LAI-1, *Legionella* autoinducer-1; LCV, *Legionella*-containing vacuole; Lqs, *Legionella* quorum sensing; NO, nitric oxide, SNP, sodium nitroprusside; T4SS, type IV secretion system.

*Correspondence: E-mail hilbi@imm.uzh.ch

Article submitted to: *MMBR*

1.2.1 Summary

Legionella pneumophila is a Gram-negative environmental bacterium, which survives in planktonic form, colonizes biofilms, and infects protozoa. Upon inhalation of *Legionella*-contaminated aerosols, the opportunistic pathogen replicates within and destroys alveolar macrophages, thereby causing a severe pneumonia termed Legionnaires' disease. Gram-negative bacteria employ low molecular weight organic compounds as well as the inorganic gas nitric oxide (NO) for cell-cell communication. *L. pneumophila* produces, secretes, and detects the α-hydroxyketone compound *Legionella* autoinducer-1 (LAI-1, 3-hydroxypentadecane-4-one). LAI-1 is secreted by *L. pneumophila* in outer membrane vesicles and not only promotes communication among bacteria but also triggers responses from eukaryotic cells. *L. pneumophila* detects NO through three different receptors, and signaling through the volatile molecule translates into fluctuations of the intracellular second messenger cyclic-di-guanylate monophosphate (c-di-GMP). The LAI-1 and NO signaling pathways are linked *via* the pleiotropic transcription factor LvbR. In this review, we summarize current knowledge about intra-bacterial and inter-kingdom signaling through LAI-1 and NO by *Legionella* species.

1.2.2 Ecology and pathogenesis of the amoeba-resistant genus *Legionella*

The genus *Legionella* comprises ubiquitous environmental bacteria, which inhabit natural and technical water systems (Mondino et al., 2020; Newton et al., 2010; Whiley and Bentham, 2011). The obligate aerobic bacteria survive in planktonic form and colonize biofilms (Abdel-Nour et al., 2013; Declerck, 2010) (**Fig. 1.5**), complex microbial communities consisting of bacteria, fungi, and predatory protozoa, which feed ("graze") on prey cells (Hall-Stoodley et al., 2004; Sauer et al., 2022; Taylor et al., 2009). Upon uptake by free-living protozoa, *Legionella* species resist degradation and instead grow and ultimately destroy the host cells (Boamah et al., 2017; Hoffmann et al., 2014; Swart et al., 2018) (**Fig. 1.5**). *Legionella pneumophila* replicates intracellularly in numerous protozoa, including amoeba such as *Acanthamoeba*, *Echinamoeba*, *Naegleria*, *Vahlkampfia*, *Vermamoeba* (*Hartmannella*), and *Rhogostoma*, ciliates like *Tetrahymena*, or the haploid social amoeba *Dictyostelium discoideum* (Boamah et al., 2017; Fields, 1996; Greub and Raoult, 2004; Hilbi et al., 2011; Pohl et al., 2021; Steinert and Heuner, 2005).

Legionella spp. are the causative agents of a life-threatening pneumonia called Legionnaires' disease. *L. pneumophila* is the clinically predominant species in most parts of the world, followed by *Legionella longbeachae*, which is most prevalent in, e.g., Australia and New Zealand (Mondino et al., 2020; Newton et al., 2010; Whiley and Bentham, 2011). *Legionella* spp. are opportunistic pathogens, which reach the human lung through the inhalation of contaminated aerosols. In the lung, the bacteria grow within and destroy alveolar macrophages, consequently triggering a fulminant pneumonia. While an infection with *Legionella* spp. usually occurs through environmental sources, such as cooling towers, fountains, whirl pools, or showers (Benin et al., 2002; Newton et al., 2010; Wuthrich et al., 2019), the transmission of a highly virulent *L. pneumophila* strain from one person to another was reported on one instance (Correia et al., 2016).

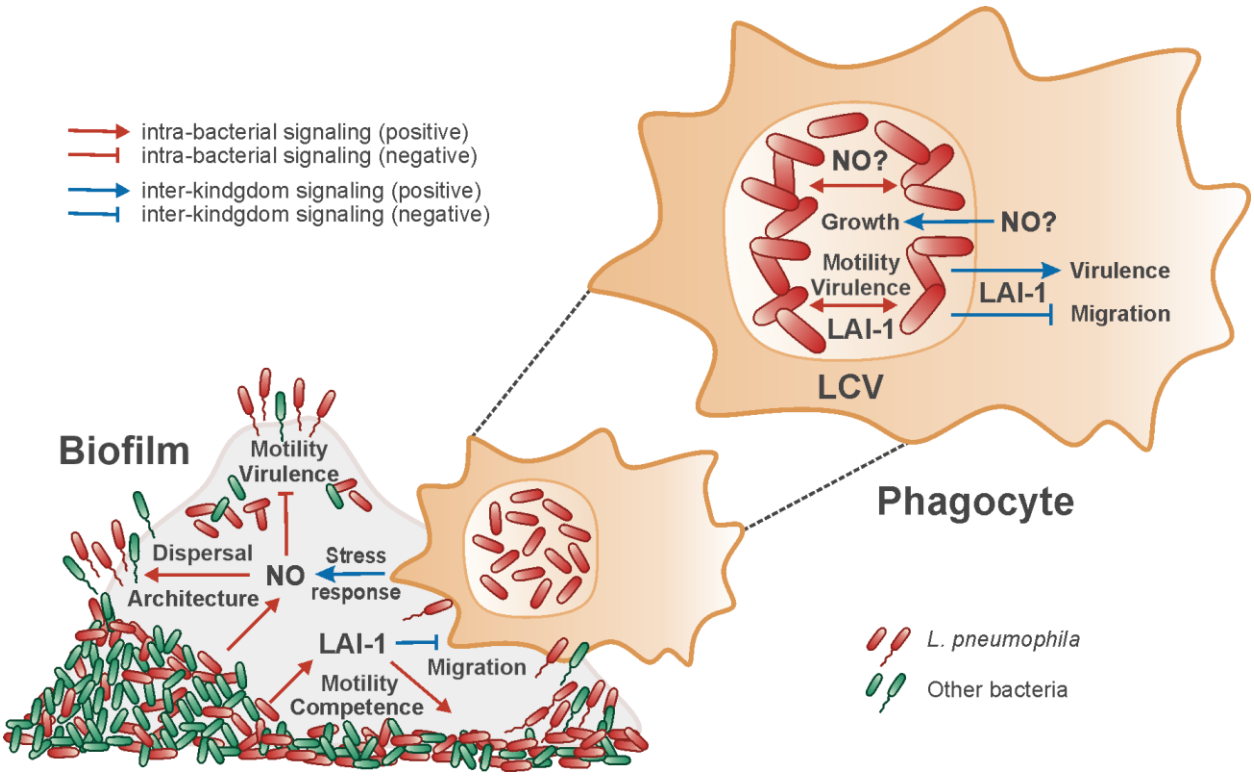

Figure 1.5. Intra-bacterial and inter-kingdom signaling of *L. pneumophila* by LAI-1 and NO in biofilms and phagocytes.
The opportunistic bacterial pathogen *L. pneumophila* colonizes and forms biofilms and replicates within environmental (amoeba) and lung (macrophages) phagocytes. The *Legionella* quorum sensing (Lqs) system and the small organic signaling molecule *Legionella* autoinducer-1 (LAI-1, 3-hydroxypentadecane-4-one) as well as the inorganic radical gas nitric oxide (NO) jointly promote intra-bacterial and inter-kingdom signaling. LAI-1 regulates the virulence, motility, phenotypic heterogeneity, natural competence, and physiology of *L. pneumophila*, as well as the inhibition of host cell migration and intracellular bacterial replication. NO regulates *L. pneumophila* virulence and motility, as well as biofilm architecture and dispersal.

1.2.3 Virulence of the opportunistic pathogen *Legionella pneumophila*

Within amoeba and macrophages, *L. pneumophila* forms in a mechanistically similar manner a distinct membrane-bound compartment, the *Legionella*-containing vacuole (LCV) (Asrat et al., 2014; Hubber and Roy, 2010; Personnic et al., 2016; Steiner et al., 2018; Swart and Hilbi, 2020). LCVs avoid acidification and fusion with lysosomes, and instead, communicate with different vesicle trafficking routes, including the endosomal, secretory and retrograde pathways. LCVs also interact with different organelles (Escoll et al., 2016), such as the ER (Abu Kwaik, 1996; Hüsler et al., 2021; Lu and Clarke, 2005; Robinson and Roy, 2006; Solomon and Isberg, 2000; Steiner et al., 2017; Swanson and Isberg, 1995), the nucleus (Rolando et al., 2013; Schator et al., 2023), mitochondria (Escoll et al., 2021; Escoll et al., 2017; Fu et al., 2022; Garcia-Rodriguez et al., 2023; Kubori et al., 2022), and lipid droplets (Hüsler et al., 2023a; Hüsler et al., 2023b). Accordingly, in addition to intercepting vesicle trafficking, LCVs also form intimate membrane

contact sites (MCSs) with the ER and possibly other cellular organelles (Vormittag et al., 2023a; Vormittag et al., 2023b).

L. pneumophila employs a type IV secretion system (T4SS) termed Icm/Dot (intracellular multiplication/defective organelle trafficking) to govern interactions with eukaryotic host cells and promote LCV formation (Böck et al., 2021; Ghosal et al., 2019; Kubori and Nagai, 2016). The Icm/Dot T4SS injects more than 300 different “effector proteins” into host cells; some of these effectors have been shown to target conserved eukaryotic components and thus subvert cellular processes in favor of the pathogen (Finsel and Hilbi, 2015; Hilbi and Buchrieser, 2022; Lockwood et al., 2022; Qiu and Luo, 2017). The processes modulated by *L. pneumophila* effector proteins include host signal transduction, vesicle trafficking, membrane and cytoskeleton dynamics, transcription, and translation, as well as metabolism.

In addition to cell-cell interactions governed by effector proteins, *L. pneumophila* also interacts with bacteria and eukaryotic cells through small organic and inorganic signaling molecules. In this review, we will discuss recent insights into the structures, functions, and release mode of small signaling molecules of Gram-negative bacteria in general and of *L. pneumophila* in particular.

1.2.4 Small organic signaling molecules of Gram-negative bacteria

Bacteria synthesize, secrete, and respond to low molecular weight organic molecules of different chemical classes (Papenfort and Bassler, 2016; Shank and Kolter, 2009; Whiteley et al., 2017). Some of these signaling molecules, called “autoinducers”, trigger processes above a certain threshold concentration (termed “quorum”), and therefore, this population- or density-dependent signaling process has been dubbed quorum sensing (Fuqua and Greenberg, 2002; Papenfort and Bassler, 2016). The diffusible autoinducer molecules regulate bacterial gene expression by either directly binding to cytosolic transcription factors (Fuqua and Greenberg, 2002), or by binding to distinct membrane-bound sensor kinases, which transmit the signal by phospho-relay to a cognate two component system (TCS) response regulator protein (Ng and Bassler, 2009; Tiaden and Hilbi, 2012). Quorum sensing can be incredibly complex, as distinct receptors detect specific low molecular weight compounds, which trigger convergent or separate signal transduction pathways. These pathways can act synergistically or antagonistically in each species, between different bacterial genera, or even in an inter-kingdom-dependent manner.

Well-studied examples of autoinducers are the boron-containing autoinducer-2 (AI-2) produced by the vast majority of bacteria (Pereira et al., 2013) and N-acyl-homoserine lactones (AHLs) produced primarily by Gram-negative bacteria (Fuqua and Greenberg, 2002; Ng and Bassler, 2009). Other small signaling molecules synthesized by Gram-negative bacteria include 2-heptyl-3-hydroxy-4-quinolone (PQS) and cis-2-decenoic acid from *Pseudomonas aeruginosa*, cis-11-methyl-2-dodecenoic acid (diffusible signal factor, DSF) or cis-2-dodecenoic acid (BDSF) from *P. aeruginosa* or *Burkholderia cenocepacia*, 3-hydroxypalmitic acid methyl ester (3-OH-PAME) from *Ralstonia solanacearum*, as well as α-hydroxyketone (AHK) compounds from *Vibrio cholerae* (cholera autoinducer-1, CAI-1) or *L. pneumophila* (*Legionella* autoinducer-1, LAI-1) (Papenfort and Bassler, 2016; Papenfort et al., 2017; Shank and Kolter, 2009; Striednig and Hilbi, 2022; Tiaden and Hilbi, 2012; Tiaden et al., 2010a).

Independently of LAI-1 and the underlying quorum sensing system (see below), *L. pneumophila* also shows a density-dependent resistance towards its own antimicrobial metabolite homogentisic acid (HGA) (Levin et al., 2019). HGA antagonizes the growth of *Legionella* species and is produced and secreted only by conditionally HGA-resistant *L. pneumophila*. This strategy allows the production of a potentially self-toxic molecule while avoiding self-harm. The mechanism and/or signaling molecules mediating HGA resistance are unknown.

1.2.5 Signaling by the inorganic volatile compound nitric oxide

Nitric oxide (NO) represents another small molecule implicated in bacterial signaling (Cary et al., 2006; Nisbett and Boon, 2016; Williams et al., 2018). NO is a membrane-permeable diatomic radical and a highly reactive inorganic gas, which is produced by bacteria and eukaryotes to promote short-range and transient signaling within and between neighboring cells. The volatile NO serves as a chemical cue for bacteria and eukaryotic cells at low (nanomolar) concentrations and is toxic at high (micromolar) concentrations (Bogdan et al., 2000). In many bacteria, NO is sensed by heme-nitric oxide/oxygen binding (H-NOX) domain proteins, which interact with TCSs and modulate c-di-GMP metabolism to regulate complex processes such as motility, quorum sensing, biofilm formation and dispersal, and symbiosis (Arora et al., 2015; Plate and Marletta, 2013; Stern and Zhu, 2014; Wang and Ruby, 2011). In fact, NO is involved in the regulation of biofilms of many bacteria, including *P. aeruginosa*, *V. cholerae*, *V. harveyi*, and *E. coli* (Arora et al., 2015). Intriguingly, NO signaling also regulates quorum sensing in various bacterial genera, including *Pseudomonas* and *Vibrio* (Heckler and Boon, 2019). Accordingly, NO controls *Vibrio* bioluminescence, motility, as well as biofilm formation and dispersal (Barraud et al., 2009b; Henares et al., 2012; Henares et al., 2013; Hossain et al., 2018; Thompson et al., 2019; Ueno et al., 2019).

NO signaling is also intimately linked to the intracellular bacterial second messenger cyclic-di-guanylate monophosphate (c-di-GMP). The production of c-di-GMP is catalyzed by GGDEF domain-containing diguanylate cyclases (DGCs), and the compound is hydrolyzed to the linear molecule 5'-phosphoguanylyl-(3'-5') guanosine (pGpG) and/or to GMP by EAL or HD-GYP domain-containing phosphodiesterases (PDEs) (Hengge, 2009; Jenal et al., 2017; Romling et al., 2013; Valentini and Filloux, 2019). *L. pneumophila* harbors 22 genes predicted to encode proteins with domains implicated in c-di-GMP synthesis, hydrolysis, or recognition (Allombert et al., 2014; Levi et al., 2011). Some of these NO-responsive, c-di-GMP-modulating pathways, e.g., the Hnox1-Lpg1057 and NosP-NahK-NarR systems, regulate biofilm formation of *L. pneumophila* (Carlson et al., 2010; Pecastaings et al., 2016) (**Fig. 1.6**, see below), while others are implicated in virulence and the Icm/Dot-dependent secretion of effector proteins (Allombert et al., 2021; Allombert et al., 2014; Levi et al., 2011).

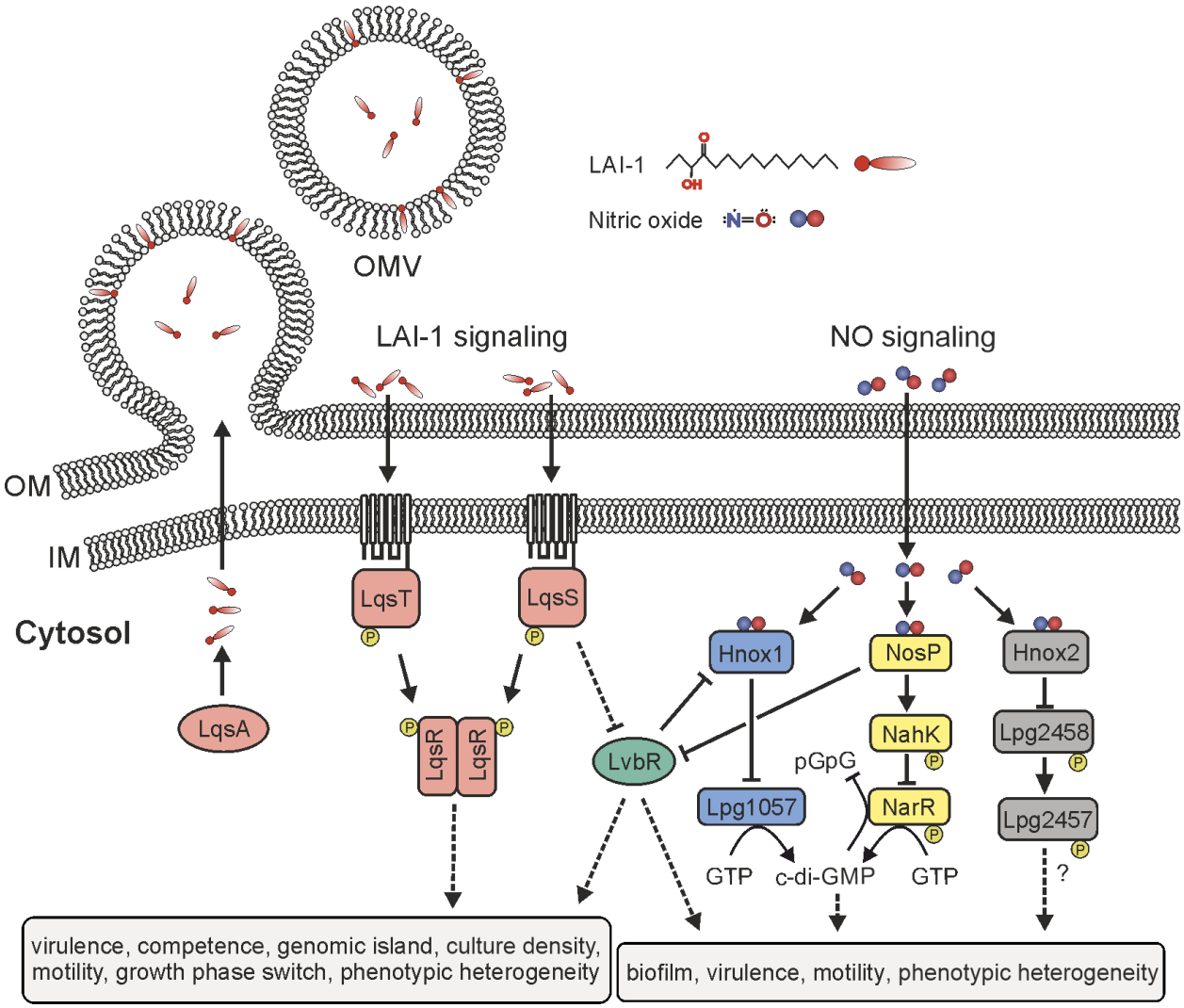

Figure 1.6. The *L. pneumophila* Lqs-LvbR-NO regulatory network.
L. pneumophila integrates intra- and extracellular cues by employing endogenous signals (LAI-1 and cyclic di-guanosine monophosphate, c-di-GMP) and exogenous signals (nitric oxide, NO). The Lqs (*Legionella* quorum sensing) system produces, secretes, detects, and responds to the α-hydroxyketone compound LAI-1 (*Legionella* autoinducer-1), which is released from the bacteria by outer membrane vesicles (OMVs). The Lqs system comprises the autoinducer synthase LqsA, the cognate membrane-bound sensor histidine kinases LqsS and LqsT, and the aspartate receiver domain response regulator LqsR. The transcription factor LvbR (*Legionella* virulence and biofilm regulator) is regulated by LqsS, regulates the NO sensor Hnox1 and, through the diguanylate cyclase Lpg1057, c-di-GMP signaling. The NO sensor NosP regulates LvbR and signals through the two-component system (TCS) NahK-NarR to regulate c-di-GMP levels. The NO sensor Hnox2 is upstream of a TCS comprising the histidine kinase Lpg2458 and the CheY-like single domain response regulator Lpg2457, the downstream signal of which is not known. The Lqs-LvbR-NO network regulates various traits of *L. pneumophila*, such as virulence, motility, natural competence, phenotypic heterogeneity, a 133 kb genomic “fitness island”, biofilm architecture and dispersal, culture density and growth phase switch.

1.2.6 Cell-cell communication trough bacterial outer membrane vesicles

Many of the small organic signaling molecules produced by Gram-negative bacteria are rather hydrophobic. Accordingly, the compounds partition into and might cross the bacterial membrane(s). Alternatively, or additionally, a number of autoinducers is released by outer membrane vesicles (OMVs) (Toyofuku et al., 2017), multi-functional vesicles of 10-300 nm diameter enclosed by a membrane bilayer containing lipopolysaccharide in the outer leaflet (Schwechheimer and Kuehn, 2015; Toyofuku et al., 2023). Indeed, PQS promotes OMV formation of *P. aeruginosa*, is packaged into OMVs and mediates quorum sensing-dependent bacterial activities (Mashburn and Whiteley, 2005), and *Burkholderia thailandensis* hydroxyalkyl quinolone HMNQ is also released through OMVs (Wang et al., 2020). Moreover, the marine coral pathogen *Vibrio shilonii* (Li et al., 2016) as well as *Paracoccus denitrificans* (Toyofuku et al., 2017) produce OMVs that contain AHL autoinducers. Finally, *Vibrio harveyi* CAI-1 (Brameyer et al., 2018) and *L. pneumophila* LAI-1 (Fan et al., 2023) are packaged into OMVs and promote inter-bacterial as well as inter-kingdom signaling (**Fig. 1.6**; see below). Overall, OMVs solubilize hydrophobic signaling molecules in aqueous environments and promote their distribution over rather large distances at biologically active concentrations (Toyofuku et al., 2023).

L. pneumophila produces OMVs, which contain virulence-relevant proteins such as lipolytic and proteolytic enzymes, the macrophage infectivity potentiator (Mip) protein, Icm/Dot components and substrates, the major flagellum component flagellin, as well as small regulatory RNAs (Galka et al., 2008; Sahr et al., 2022; Shevchuk et al., 2011). These OMVs fuse with eukaryotic membranes and promote amoeba growth, and they activate mammalian cells and modulate their cytokine response (Galka et al., 2008; Jager et al., 2015; Jung et al., 2017; Jung et al., 2016).

1.2.7 Components of the *L. pneumophila* LAI signaling circuit

Small molecule communication of *L. pneumophila* involves the organic signaling molecule LAI-1, which is produced and detected by the *Legionella* quorum sensing (Lqs) system (Tiaden et al., 2010a). The Lqs system was first described in 2007 (Tiaden et al., 2007) and comprises the autoinducer synthase LqsA, the homologous sensor kinases LqsS and LqsT, and the cognate response regulator LqsR (Hochstrasser and Hilbi, 2017; Tiaden et al., 2010a) (**Fig. 1.6**). The corresponding genes *lqsA*, *lqsS*, *lqsT*, and *lqsR* are all expressed from individual promoters (Sahr et al., 2012) and are organized in a cluster (*lqsA–lqsR–hdeD–lqsS*; *lpg2731–2734*) (Tiaden and Hilbi, 2012; Tiaden et al., 2008; Tiaden et al., 2007) or localize at a distant site in the *L. pneumophila* genome (*lqsT*; *lpg2506*), respectively (Kessler et al., 2013). The expression of *lqsR* is positively regulated by the alternative (stationary phase) sigma factor RpoS (Tiaden et al., 2007), by LAI-1 (Schell et al., 2016b), and by the carbon storage regulator A (CsrA), a global repressor of transmission traits, which is sequestered by small non-coding RNAs (Sahr et al., 2009; Sahr et al., 2017). The *lqsS* and *lqsT* genes are reciprocally expressed upon growth of *L. pneumophila* in AYE broth, mirroring their partly antagonistic functions (Kessler et al., 2013).

LqsA is a pyridoxal-5′-phosphate (PLP)-dependent enzyme that produces the small signaling molecule LAI-1 (Spirig et al., 2008) (**Fig. 1.6**. LAI-1 was identified by mass spectrometry as 3-hydroxypentadecane-

4-one upon expression of *lqsA* in *E. coli* (Spirig et al., 2008) or in *L. pneumophila* (Fan et al., 2023). The biosynthesis of LAI-1 has not been elucidated but might occur analogously to *V. cholerae* CAI-1 (3-hydroxytridecane-4-one) (Jahan et al., 2009; Kelly et al., 2009). CAI-1 is produced by the *V. cholerae* autoinducer synthase CqsA, which is 41% identical to LqsA (Higgins et al., 2007; Miller et al., 2002; Spirig et al., 2008). CqsA uses decanoyl-CoA and (*S*)-2-aminobutyric acid as the substrates to catalyze the formation of (*S*)-3-aminotridecan-4-one (amino-CAI-1), which is further converted to CAI-1 by *V. cholerae* (Jahan et al., 2009; Kelly et al., 2009). CqsA also couples decanoyl-CoA and (*S*)-adenosylmethionine (SAM) to yield the enamine CAI-1 precursor 3-aminotridec-2-en-4-one (Ea-CAI-1) (Wei et al., 2011). Analogously, LqsA likely uses dodecanoyl-CoA and (*S*)-2-aminobutyric acid or SAM as substrates to synthesize amino-LAI-1 or Ea-LAI-1, respectively.

LqsS (Tiaden et al., 2010b) and LqsT (Kessler et al., 2013) share 31% identity and are members of the six-transmembrane helix sensor histidine kinase family (Tiaden and Hilbi, 2012). The membrane-bound sensor kinases LqsS and LqsT are autophosphorylated by ATP at the conserved histidine residue His_{200} or His_{204}, respectively, which is embedded in the cytosolic kinase domain (Schell et al., 2014). Autophosphorylation is inhibited in a dose-dependent manner by synthetic LAI-1 or amino-LAI-1, indicating that the sensor kinases indeed respond to the signaling molecule (Schell et al., 2016b). Moreover, the autophosphorylation of LqsS or LqsT is inhibited and dephosphorylation of the corresponding phospho-enzymes is promoted by purified LqsR, in agreement with the notion that the sensor kinases directly interact with the response regulator (Schell et al., 2014) (**Fig. 1.6**).

LqsR is a TCS response regulator that harbors a canonical receiver domain in the N-terminal part including the conserved aspartate residue Asp_{108} (Tiaden et al., 2007). LqsR is bound by both LqsS and LqsT, and the response regulator dimerizes upon chemical phosphorylation by acetyl phosphate or phosphorylation by phospho-LqsT (Schell et al., 2014) (**Fig. 1.6**). The crystal structure of LqsR revealed a receiver domain adopting a canonical $(\beta\alpha)_5$ fold, which is connected through an additional sixth helix and an extended α5-helix to a novel output domain with a five-stranded antiparallel β-sheet fold reminiscent of (di-)nucleotide binding proteins (Hochstrasser et al., 2020). Structure-based mutagenesis identified amino acids critical for aspartate phosphorylation and dimerization of LqsR; however, the function of the output domain is still unknown. Taken together, LAI-1-dependent phosphorylation signaling through the membrane-bound sensor histidine kinases LqsS and LqsT converges on the prototypic aspartate response regulator LqsR (**Fig. 1.6**).

1.2.8 Components of the *L. pneumophila* NO signaling network

L. pneumophila harbors three putative NO receptor proteins, which have been experimentally shown to bind NO *in vitro*: Hnox1 (heme-nitric oxide/oxygen binding domain; Lpg1056) and Hnox2 (Lpg2459) (Carlson et al., 2010), as well as NosP (NO sensing protein; Lpg0279) (Fischer et al., 2019) (**Fig. 1.6**). Upon treatment of *L. pneumophila* with the chemical NO donors dipropylenetriamine (DPTA) NONOate or sodium nitroprusside (SNP), the expression of the promoters for the 6S small regulatory RNA (P_{6SRNA}) and flagellin (P_{flaA}) was delayed (Michaelis et al., 2024). The reduction of P_{flaA} expression by DPTA NONOate

was less pronounced in a mutant strain lacking all three NO receptors (triple knockout, TKO), indicating that the NO receptors are indeed implicated in NO signaling *in vivo* (Michaelis et al., 2024).

The Hnox1-Lpg1057 pathway comprises the NO-binding regulator Hnox1 and a GGDEF/EAL domain enzyme (Carlson et al., 2010; Pecastaings et al., 2016) (**Fig. 1.6**). Binding of NO to Hnox1 leads to an inhibition of the DGC activity of Lpg1057 and thus reduces c-di-GMP production (Carlson et al., 2010). The NosP-NahK-NarR pathway comprises the NO-binding regulator NosP (Lpg0279) and a TCS with the sensor kinase NahK (NosP-associated histidine kinase, Lpg0278) and the GGDEF/EAL domain-containing response regulator NarR (Lpg0277) (Fischer et al., 2019; Hughes et al., 2019; Levet-Paulo et al., 2011; Pecastaings et al., 2016) (**Fig. 1.6**). Binding of NO to NosP leads to an activation of NahK autophosphorylation and phospho-transfer to NarR, thus decreasing its DGC activity and increasing its PDE activity, which also results in lower levels of c-di-GMP (Fischer et al., 2019; Hughes et al., 2019). The NO-binding regulator Hnox2 is encoded in a putative operon with genes predicted to encode a TCS comprising the sensor kinase Lpg2458 and the response regulator Lpg2457 (Carlson et al., 2010) (**Fig. 1.6**). The downstream signal(s) of this pathway are unknown.

1.2.9 *L. pneumophila* LAI-1 and NO signaling are linked *via* the transcription factor LvbR

L. pneumophila harbors a 133 kb genomic "fitness island" (Tiaden et al., 2010b), which has an overall higher G+C content (40.3%) than the average *L. pneumophila* genome (38%), localizes adjacent to the predicted $tRNA^{Thr}$ gene *lpg0972* and is flanked by predicted DNA-mobilizing elements, such as a putative integrase in the 5' region, and the phage-like gene *abiD*, phage-related integrases, as well as transposases and a reverse transcriptase in the 3' region. The genomic island is divided into two regions, which are separated by *lvrB1-lvrA1* (*lpg1004-1005*). Region I (26 kb) harbors many (conserved) unknown genes, some of which possibly encoding pili components, and region II encodes the subunits of a putative F_oF_1 ATP synthase and various putative metal ion resistance transport proteins.

Transcriptome analysis revealed that in the Δ*lqsS* mutant strain 52 of the 125 genes in the 133 kb genomic island are upregulated at least two-fold. Among them is a transcription factor gene annotated as *lpp2326* in the *L. pneumophila* strain Paris and located between *lpg1055* and *lpg1056* in strain Philadelphia-1 (Hochstrasser et al., 2019). The transcription factor, termed LvbR (*Legionella* virulence and biofilm regulator), binds to the promoter of *hnox1*/*lpg1056*, which is divergently transcribed from *lvbR*. Accordingly, LvbR negatively regulates the NO-binding inhibitor of the DGC Lpg1057 (**Fig. 1.6**), likely leading to increased c-di-GMP levels. Moreover, in an *L. pneumophila* Δ*nosP* mutant, the *lvbR* promoter is upregulated, indicating that NosP negatively regulates LvbR (Michaelis et al., 2024) (**Fig. 1.6**). Thus, LvbR links the Lqs system to NO signaling as well as to the c-di-GMP regulatory network (Hochstrasser and Hilbi, 2020). In summary, the *L. pneumophila* LAI-1-NO signaling network comprises the components of the Lqs system and three NO receptors, two of which are linked to the quorum sensing system by the transcription factor LvbR.

1.2.10 Distribution of the Lqs system and NO receptors among *Legionella* species

The *lqs* genes are present in all *L. pneumophila* strains investigated to date (Hochstrasser and Hilbi, 2022; Spirig et al., 2008). In contrast, among 58 *Legionella* genomes analysed, only 19 harbor a complete *lqs* cluster comprising *lqsA-lqsR-hdeD-lqsS*, 20 do not possess the autoinducer synthase gene *lqsA* but maintain *lqsR* and/or *lqsS*, and 19 do not carry any *lqs* genes (Herran et al., 2021). Moreover, 28 *Legionella* spp., including *L. longbeachae*, possess a homologue of *lqsT*, but lack *lqsA* or the entire *lqs* gene cluster (Herran et al., 2021; Hochstrasser and Hilbi, 2022; Spirig et al., 2008). Since the Lqs system is not strictly conserved among *Legionella* spp., the quorum sensing system is not essential for pathogenicity of the genus.

Beyond *Legionella* spp., the Lqs system is rather broadly distributed among environmental bacterial genera, including the families Legionellaceae, Vibrionaceae, Burkholderiaceae, and Chlorobiaceae (Tiaden et al., 2010a), or Oxalobacteraceae (Hornung et al., 2013). While some of the bacterial species harbor the entire *lqs* gene cluster, others lack the *hdeD* gene of unknown function (e.g. *Burkholderia xenovorans*), or possess only homologues of *lqsA* and *lqsS*, e.g., *cqsA* and *cqsS* of *Vibrio* spp. (Henke and Bassler, 2004; Miller et al., 2002).

Based on the finding that *L. pneumophila* harbors three different NO receptors, we performed a comprehensive analysis of the distribution of NO receptor proteins in 80 *Legionella* strains representing 58 different species/subspecies. The gene *hnox1* (*lpp2325*) is present in only ca. 60% of the *L. pneumophila* strains analysed and seven other *Legionella* species (*L. taurinensis*, *L. gratiana*, *L. dumoffii*, *L. gormanii*, *L. quateirensis*, *L. waltersii*, *L. norrlandica*). In contrast, the gene *hnox2* (*lpp2525*) is present in all *L. pneumophila* strains as well as in five other *Legionella* species (*L. yabuuchiae*, *L. impletisoli*, *L. gresilensis*, *L. busanensis*, *L. norrlandica*).

The gene *nosP* (*lpp0354*) encoding a FIST (F-box and intracellular signal transduction) domain protein is widely distributed among the genus *Legionella*, as it is present in all *L. pneumophila* strains analysed, as well as in 43 other *Legionella* species (**Fig. 1.7**). In the remaining species the gene is either absent (21 strains) or has become a pseudogene (*L. likebrunensis*, *L. israelensis*, *L. cincinnatiensis*). In the strains carrying one or several copies of *nosP* (50 strains), one copy always localizes upstream of genes encoding a predicted sensor histidine kinase and a predicted diguanylate kinase, as described for the corresponding operon in *L. pneumophila* (Fischer et al., 2019).

In the six strains carrying 2-3 *nosP* copies (in-paralogs), the genes do not localize in the same operon but are identical amongst each other, despite being present in species/strains that are not closely related (**Fig. 1.7**). Moreover, some of the additional *nosP* copies are found in plasmids. These findings suggest recent horizontal transfer of the *nosP* copies among the strains. The three species carrying pseudogenes also belong to different clusters in the species tree, indicating that the pseudogenization of *nosP* has occurred through independent inactivation events several times during evolution.

Comparing the *Legionella* species tree with the NosP protein tree revealed that most of the protein clusters are congruent with phylogenetically close strain clusters. However, there are several exceptions,

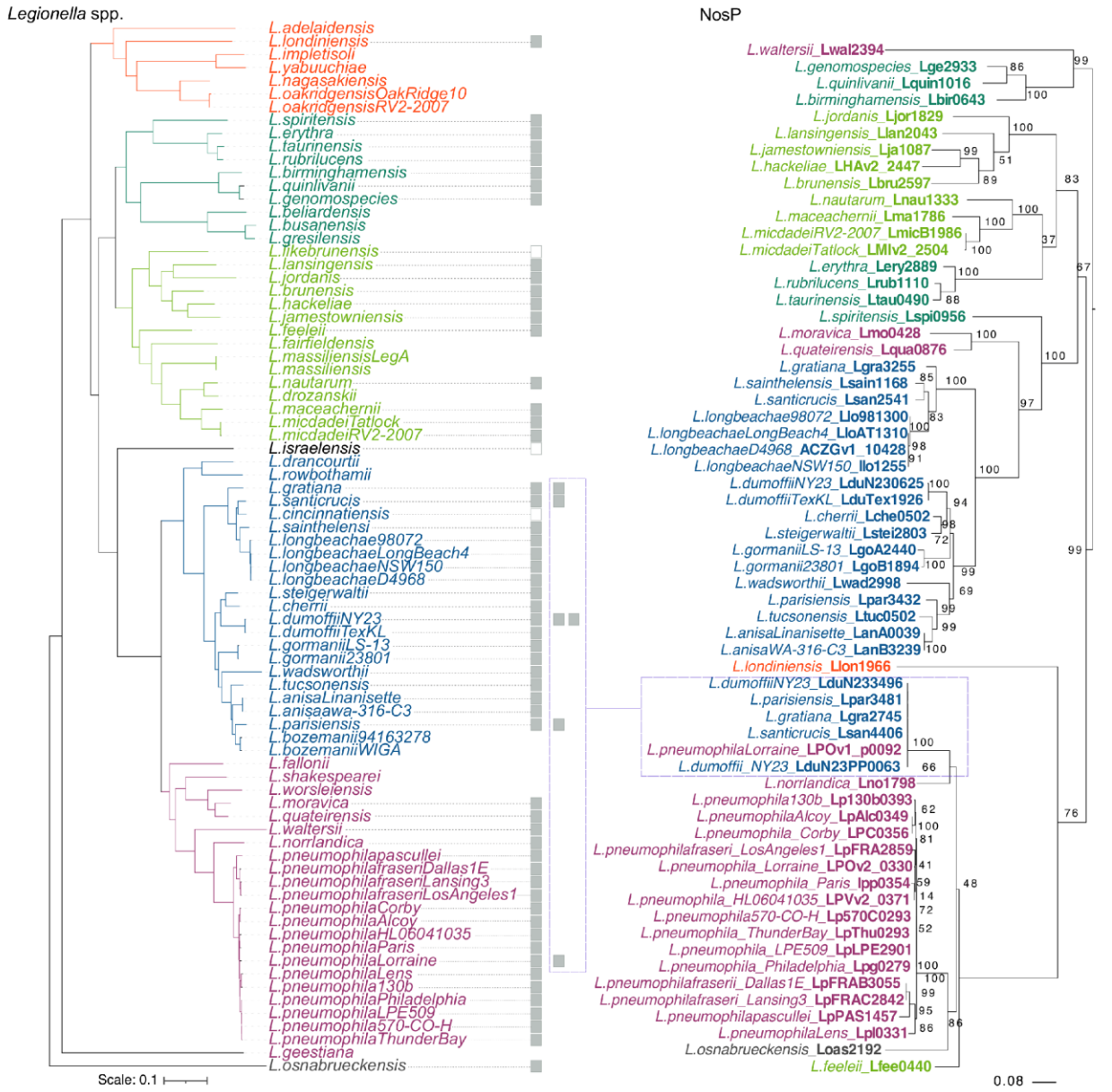

Figure 1.7. Evolutionary history of NosP in the genus *Legionella*.
The phylogenetic tree shown on the left represents the evolutionary relationship of 58 species of the genus *Legionella* based on the core genome (Gomez-Valero et al., 2019), and the phylogenetic tree shown on the right represents the NosP protein tree, with the name of each protein on the corresponding branch. The NosP protein tree has been reconstructed by maximum likelihood using the IQ-TREE software (Minh et al., 2020) with model LG+I+G+F. The distribution of NosP proteins was analyzed at the genus level by using OrthoMCL software (Li et al., 2003) and is represented on the tree by using the iTOL software (Letunic and Bork, 2007). NosP proteins and pseudogenes are represented as grey or empty grey squares, respectively. NosP in-paralogs from different non-related species, showing 100% nucleotide sequence identity, are inside a purple square with a dashed border. Numbers besides nodes represent UFBoot support values. Scale bar on the bottom of each tree indicates the tree scale. The distribution of *nosP* genes among *Legionella* spp. indicates a complex evolutionary history characterized by vertical evolution together with gene duplications, gene loss, and horizontal gene transfer.

suggesting horizontal movement of *nosP* copies among different species/strains rather than vertical strain evolution. For example, the *L. londinensis nosP* gene shows higher identity to *L. pneumophila nosP* than to phylogenetically closer species (**Fig. 1.7**). Other putative cases of horizontal gene transfer are found in *L. waltersii, L. moravica, L. quateirensis, L. erythra, L. osnabrueckensis*, and *L. feelei*. In summary, the analysis of the distribution of the *nosP* gene among *Legionella* spp. indicates a complex evolutionary history characterized by vertical evolution together with gene duplications, gene loss, and horizontal gene transfer.

1.2.11 Implications of the Lqs-LvbR system for competence and physiology of *L. pneumophila*

Horizontal gene transfer frequently occurs through “natural competence”, i.e., the uptake of free DNA by transformation of bacteria (in stationary growth phase). Indeed, upon growth of *L. pneumophila* in liquid culture at 30°C for 24 h, linear DNA encoding an antibiotic resistance cassette flanked by fragments homologous to genomic regions, is taken up by the bacteria and stably integrated into the genome by double homologous recombination (Kessler et al., 2013). Compared to the *L. pneumophila* parental strain JR32, four orders of magnitude more colonies of the Δ*lqsA*, Δ*lqsR*, Δ*lqsS*, Δ*lqsT*, or Δ*lvbR* mutant strains grew in natural competence assays (Hochstrasser et al., 2019; Kessler et al., 2013). Analogously, the P_{comEA} promoter regulating a small periplasmic DNA-binding protein, which is essential for competence of *L. pneumophila* (Charpentier et al., 2011), was strongly induced in absence of *lqsA*, *lqsR*, *lqsS*, or *lqsT* (Kessler et al., 2013). Accordingly, the Lqs components as well as LvbR negatively regulate the natural competence for DNA uptake of *L. pneumophila* (**Fig. 1.5**).

L. pneumophila adopts a bi-phasic lifestyle and alternates between a replicative, non-virulent form and a stationary, virulent and motile form (Manske and Hilbi, 2014; Molofsky and Swanson, 2004; Oliva et al., 2018). In addition to CsrA and the LetA/LetS TCS (Manske and Hilbi, 2014; Oliva et al., 2018), the Lqs system and in particular LqsR control the switch from the replicative to the transmissive form (Tiaden et al., 2007). The Lqs components and LvbR also regulate the lag phase, growth rate and cell density of *L. pneumophila* in minimal and complex media in a temperature-dependent manner (Hochstrasser and Hilbi, 2022; Tiaden et al., 2007). Compared to the parental *L. pneumophila* strain, ∆*lqsR* mutant bacteria exhibited a reduced lag phase at 30°C and reached a higher cell density at 45°C, while the ∆*lqsA*, ∆*lqsS* and ∆*lqsT* mutants showed a longer lag phase and reached only a lower cell density. ∆*lvbR* mutant bacteria resumed growth like the parental strain at 30°C, but reached only a substantially reduced cell density at 45°C. Thus, the Lqs-LvbR network and in particular LqsR and LvbR, regulate the temperature-dependent growth onset and cell density of *L. pneumophila*.

1.2.12 Promotion of *L. pneumophila* virulence by the Lqs-LvbR system and NO receptors

L. pneumophila strains lacking a functional Icm/Dot T4SS (Hilbi et al., 2001; Weber et al., 2006), *lqsR* (Tiaden et al., 2007), *lqsS* (Tiaden et al., 2010b), *lqsT* (Kessler et al., 2013), Δ*lqsS*-Δ*lqsT* (Kessler et al., 2013), the entire *lqs* cluster (Δ*lqs*) (Tiaden et al., 2008), or *lvbR* (Hochstrasser et al., 2019) are defective for efficient uptake by phagocytes (**Fig. 1.5**), in particular by *A. castellanii* and *D. discoideum* amoeba but also by macrophages. In contrast, the uptake defect of *L. pneumophila* lacking *lqsA* was only minor (Kessler

et al., 2013; Tiaden et al., 2010b), and addition of up to 20 µM synthetic LAI-1 did not affect the uptake or the virulence of *L. pneumophila* (Schell et al., 2016b). Noteworthy, synthetic LAI-1 dramatically up-regulated the expression of the regulatory 6S RNA (Schell et al., 2016b), which is implicated in stress response and virulence in the post-exponential growth phase (Faucher et al., 2010).

The Δ*lqsR* (Kessler et al., 2013; Tiaden et al., 2007), Δ*lqsS* and Δ*lqsS*-Δ*lqsT* (Kessler et al., 2013), Δ*lqs* (Tiaden et al., 2008) and Δ*lvbR* mutant strains (Hochstrasser et al., 2019) are impaired for intracellular replication in *A. castellanii*, *D. discoideum* and macrophages (**Fig. 1.5**). On the other hand, the Δ*lqsA* and Δ*lqsT* mutant strains did not show an intracellular growth defect in *A. castellanii* (Kessler et al., 2013). However, upon co-infection of the parental *L. pneumophila* strain JR32 with the Δ*lqsA*, Δ*lqsR*, Δ*lqsS*, Δ*lqsT*, Δ*lqsS*-Δ*lqsT* or the Δ*lvbR* mutant strains in *A. castellanii*, the mutant strains were outcompeted by the parental strain, and in most cases were no longer detectable after 2-3 weeks (Hochstrasser et al., 2019; Kessler et al., 2013). In contrast, the Δ*hdeD* mutant strain did not show any phenotype regarding pathogen-host cell interactions, not even in the amoeba competition assay (Kessler et al., 2013).

To assess a role for the *L. pneumophila* NO receptors for pathogen-host cell interactions, we generated marker-less mutant strains lacking individual (Hnox1, Hnox2, or NosP) or all three NO receptors (triple knockout, TKO) (Michaelis et al., 2024). The mutant strains grew like the parental strain in media but were impaired for intracellular replication in macrophages and *A. castellanii* (**Fig. 1.5**). While the growth defect of the single mutants was complemented by re-introducing the corresponding gene into the mutant genome, the TKO mutant could not be complemented by single NO receptor genes. These results indicate that the three different *L. pneumophila* NO receptors have non-redundant functions.

1.2.13 Regulation of *L. pneumophila* motility by the Lqs system, LAI-1, and NO

L. pneumophila not only upregulates virulence in the stationary growth phase but also motility (Molofsky and Swanson, 2004). Single cell tracking revealed that the Δ*lqsA,* Δ*lqsR,* Δ*lqsS,* Δ*lqsT*, or Δ*lqsS*-Δ*lqsT* mutant strains are impaired for motility, such that the migration distance and the velocity of individual bacteria was significantly reduced compared to the parental strain (Schell et al., 2016b) (**Fig. 1.5**). Conversely, the addition of 10 µM synthetic LAI-1 increased the migration distance and the velocity of the parental *L. pneumophila* strain JR32 but not the mutants, indicating that the promotion of motility requires functional *lqs* genes. In parallel, expression of the flagellin promoter, P_{flaA}, was significantly reduced in the Δ*lqsA,* Δ*lqsR,* or Δ*lqsS*-Δ*lqsT* mutant strains and to a lesser extent in the Δ*lqsS* and Δ*lqsT* mutants, while synthetic LAI-1 increased P_{flaA} expression in the parental strain and in mutants lacking *lqsA* or either *lqsS* or *lqsT,* but not in the Δ*lqsR* or Δ*lqsS*-Δ*lqsT* strains (Schell et al., 2016b).

Contrarily, NO seems to negatively regulate P_{flaA} (**Fig. 1.5**). Upon treatment of *L. pneumophila* with the chemical NO donors DPTA NONOate or SNP, the expression of P_{flaA} and P_{6SRNA} was delayed, indicating that NO negatively regulates bacterial motility and stress response (Michaelis et al., 2024). Taken together, while LAI-1 positively regulates P_{flaA} and the motility of *L. pneumophila*, NO is a negative regulator of P_{flaA} and, consequently, motility.

1.2.14 Determination of phenotypic heterogeneity by the Lqs system and NO receptors

Phenotypic heterogeneity describes the phenomenon of dynamic variations of traits among individual cells in a clonal bacterial population (Ackermann, 2015; Schroter and Dersch, 2019; Striednig and Hilbi, 2022). In the context of phenotypic heterogeneity, the terms “bet-hedging” (Grimbergen et al., 2015; Veening et al., 2008) or “division of labor” (Ackermann, 2013; West and Cooper, 2016) describe distinct survival strategies. Clonal bacterial populations adopt bet-hedging to adapt to consecutive fluctuations in environmental conditions, and division of labor occurs when interacting individuals concomitantly express distinct and often complementary traits.

The Lqs system regulates phenotypic heterogeneity of intracellular *L. pneumophila* in phagocytes (Personnic et al., 2019; Striednig et al., 2021), as well as in biofilms and microcolonies (Personnic et al., 2021). Within *A. castellanii*, *L. pneumophila* reversibly forms growing and non-growing subpopulations of similar size (Personnic et al., 2019). The non-growing bacteria are metabolically active, show increased antibiotic tolerance, and thus, are “persisters”. Within macrophages, the non-growing subpopulation is smaller but reaches 50% upon activation of the cells with interferon-γ. The Lqs system and in particular LqsA determine the portion of non-growing bacteria within amoeba, and thus, quorum sensing determines intracellular persistence of *L. pneumophila* (Personnic et al., 2019). At late stages of infection, virulent and motile *L. pneumophila* emerge at the periphery of the LCV in a bistable manner (Striednig et al., 2021). These motile bacteria spearhead LCV escape, host cell exit and environmental spread, thereby likely adopting a bet-hedging strategy. Thus, the Lqs system not only regulates motility of *L. pneumophila* on a population level (Schell et al., 2016a; Schell et al., 2016b), but also controls intracellular phenotypic heterogeneity and the emergence of motile individual bacteria (**Fig. 1.5**).

Furthermore, the Lqs system regulates phenotypic heterogeneity of *L. pneumophila* in biofilms and microcolonies (Personnic et al., 2021). Under sessile conditions, *L. pneumophila* exhibits growing and non-growing states, the ratio of which is controlled by the temperature, LvbR, and the Lqs system. The non-growing bacteria are metabolically active, virulent and antibiotic tolerant, and thus, are persisters. Finally, the Lqs system also determines the frequency of growth resumption ("resuscitation") and microcolony formation of individual bacteria.

In addition to the Lqs system, NO signaling also regulates phenotypic heterogeneity of *L. pneumophila* (Michaelis et al., 2024). Using the timer fluorescent reporter system as a growth rate proxy (Claudi et al., 2014; Personnic et al., 2019), *A. castellanii* amoeba were infected with timer-producing *L. pneumophila* JR32 or TKO mutant strains, and the ratio of growing (green) versus non-growing (red) intracellular bacteria was assessed by confocal fluorescence microscopy and flow cytometry. This approach revealed that a smaller portion of the intracellular TKO mutant bacteria was non-growing, compared to the parental strain, indicating that NO signaling regulates intracellular phenotypic heterogeneity of *L. pneumophila* and promotes the emergence of non-growing intracellular bacteria (Michaelis et al., 2024).

1.2.15 Control of biofilm architecture and dispersal by LvbR, NO receptors and NO

L. pneumophila colonizes and forms biofilms (Declerck, 2010; Taylor et al., 2009), which in complex medium under laboratory conditions appear as rather compact aggregates comprising “patchy” bacterial clusters (Hochstrasser et al., 2019). Components of the Lqs system do not regulate the formation and architecture of *L. pneumophila* biofilms, since the Δ*lqsA,* Δ*lqsR,* Δ*lqsS,* Δ*lqsT*, or Δ*lqsS*-Δ*lqsT* mutant strains form structures with similar morphology, biomass, and adherence characteristics as the parental strain JR32 (Hochstrasser and Hilbi, 2019). In contrast, LvbR is indeed a regulator of *L. pneumophila* biofilm formation, since biofilms formed by Δ*lvbR* mutant bacteria show a more homogeneous and “mat-like” architecture compared to the parental strain, while the sessile biomass is similar (Hochstrasser et al., 2019).

Analogously to biofilms formed by Δ*lvbR* mutant bacteria, biofilms formed by single NO receptor mutants (∆*hnox1*, ∆*hnox2*, ∆*nosP*) or the TKO mutant strain showed a “mat-like” architecture morphologically distinct from the “patchy” biofilms of the parental strain, while the biomass of the NO receptor mutant strains was larger and the attachment of the strains to the abiotic dish surface was undistinguishable (Michaelis et al., 2024) (**Fig. 1.5**). Interestingly, treatment of the biofilms with 10 µM of the chemical NO donor SNP led to the dispersal of one day old biofilms formed by GFP-producing *L. pneumophila* JR32, but not by single NO receptor or TKO mutant strains. These results implicate Hnox1, Hnox2, and NosP in the process of biofilm dispersal and confirm a non-redundant function of the three NO receptors (Michaelis et al., 2024).

Finally, the architecture of *L. pneumophila* biofilms does not correlate with the formation of extracellular filaments observed for the Δ*lqsR* and Δ*lqsS* mutants (Kessler et al., 2013; Tiaden et al., 2010b) or the TKO mutant strain (Michaelis et al., 2024), since the Δ*lvbR* mutant strain adopts a different biofilm architecture but does not produce these filaments (Hochstrasser et al., 2019).

1.2.16 Promotion of interkingdom communication by the Lqs system and LAI-1

The Lqs system and LAI-1 not only promote intra-bacterial signaling but also inter-kingdom communication between the bacterial pathogen and eukaryotic host cells (Hochstrasser and Hilbi, 2017; Personnic et al., 2018) (**Fig. 1.5**). Initial observations indicated that the inhibition of chemotactic migration of *D. discoideum* by *L. pneumophila* was not only dependent on the Icm/Dot T4SS but also on LqsA (Simon et al., 2015). *L. pneumophila* lacking *lqsA* no longer inhibited *D. discoideum* migration, but an avirulent *L. pneumophila* ∆*icmT* mutant strain overproducing LqsA interfered with migration of the amoeba (obviously in an Icm/Dot-independent manner). Similar to the Δ*lqsA* mutant strain, the migration of *D. discoideum* was also less strongly affected upon infection of the amoeba with Δ*lvbR* than upon infection with the parental strain (Hochstrasser et al., 2019). Accordingly, LqsA as well as LvbR are implicated in the inhibition of cell migration and chemotaxis by *L. pneumophila*.

In agreement with the role of LqsA for cell migration inhibition, synthetic LAI-1 in the micromolar range also inhibited the migration of *D. discoideum* and RAW 264.7 macrophages (Simon et al., 2015) (**Fig. 1.5**). To analyze host factors required for LAI-1 signaling, gene silencing by RNA interference was used in an epithelial cell scratch (“wound closure”) assay. This approach revealed that LAI-1 signaling requires the

scaffold protein IQGAP1, the small GTPase Cdc42 as well as the Cdc42-specific guanine nucleotide exchange factor (GEF) ARHGEF9, but not other modulators of Cdc42, RhoA, Rac1 or Ran GTPase.

While the overexpression of *lqsA* or synthetic LAI-1 inhibits cell migration, *L. pneumophila* expressing *lqsA* from a strong promoter, e.g., P_{flaA} or P_{6SRNA} (but not P_{lqsA}), showed enhanced intracellular replication in macrophages (Fan et al., 2023) (**Fig. 1.5**). This phenotype was dependent on the catalytic activity of LqsA, since the catalytically inactive mutant $LqsA^{K258A}$ did not show the effect. In this case, inter-kingdom signaling was mediated by OMVs, which under the conditions used accumulate LAI-1 (Fan et al., 2023). Taken together, LAI-1 either produced in the LCV by the overexpression of *lqsA* or synthetic LAI-1 added exogenously promotes inter-kingdom signaling between *L. pneumophila* and eukaryotic host cells (**Fig. 1.5**).

An intriguing aspect of inter-kingdom signaling was revealed by studies analyzing the migration of *A. castellanii* through *L. pneumophila* biofilms (Hochstrasser and Hilbi, 2019; Hochstrasser et al., 2022). The amoeba migrated more slowly through biofilms of *L. pneumophila* lacking *lqsR*, *lvbR*, *flaA*, or a functional Icm/Dot T4SS (Δ*icmT*). Furthermore, bacterial clusters decorated the amoeba migrating in biofilms of the parental strain, Δ*lvbR* or Δ*icmT* but not in Δ*lqsR* or Δ*flaA* biofilms. Thus, the Lqs-LvbR network regulates migration of *A. castellanii* through *L. pneumophila* biofilms and governs bacterial cluster formation on the amoeba.

Finally, given the fact that single NO receptor mutants and the TKO mutant strain show growth defects in macrophages and amoeba (Michaelis et al., 2024), one might speculate that host-derived NO at low concentrations promotes inter-kingdom signaling, which results in enhanced or more robust intracellular growth of *L. pneumophila* (**Fig. 1.5**). Indeed, NO is produced by free-living amoeba such as *Naegleria fowleri* (Rojas-Hernandez et al., 2007) and *D. discoideum* (Tao et al., 1997) as well as by phagocytes of the innate immune system (Bogdan, 2001; MacMicking et al., 1997). *L. pneumophila* replicates intracellularly in *Naegleria* spp. (Boamah et al., 2017; Dupuy et al., 2016; Tyson et al., 2013) and *D. discoideum* (Swart et al., 2018) and thus is likely exposed to NO produced by these host cells.

1.2.17 Concluding remarks and future perspectives

The ubiquitous environmental bacterium *L. pneumophila* employs the Lqs system and the organic compound LAI-1 as well as the inorganic gaseous molecule NO for intra-bacterial and inter-kingdom cell-cell communication. LAI-1 is released by *L. pneumophila* through OMVs, which bacteria and eukaryotic cells respond to. The LAI-1- and NO-dependent signaling pathways are linked by the transcription factor LvbR, and some of these pathways converge on the intracellular second messenger c-di-GMP. The small signaling molecules LAI-1 and NO regulate several different traits of *L. pneumophila*, including virulence, motility, phenotypic heterogeneity, natural competence, physiology, biofilm architecture and dispersal, as well as the inhibition of host cell migration and intracellular bacterial replication.

Future studies in the field of small molecule communication of *Legionella* species will address the spatio-temporal control of the LAI-1-, NO- and c-di-GMP-dependent signaling network. In particular, the hierarchy and crosstalk between the LAI-1 and the NO system is presently not understood, and the

molecular mechanism(s) underlying the non-redundancy of the three *L. pneumophila* NO receptors needs to be deciphered. Also, presently unknown quorum sensing systems other than the Lqs system might operate in *L. pneumophila*. Finally, almost nothing is known about small molecule signaling in clinical isolates of *L. pneumophila* and in *Legionella* spp. other than *L. pneumophila*. These intriguing topics will be experimentally addressed in the future.

1.2.18 Acknowledgements

The work in the group of H.H. was supported by the Swiss National Science Foundation (SNF; 31003A_175557, 310030_200706). Work in the group of C.B. was supported by the Institut Pasteur and the Agence National de Recherche (grant number ANR-10-LABX-62-IBEID). The authors declare no conflict of interest.

1.2.19 Own contributions

SM prepared figures (Fig. 1.5 and Fig. 1.6) and edited the manuscript.

1.3 Aims of the thesis

The aerobic, opportunistic pathogen *L. pneumophila* employs the Lqs (*Legionella* quorum sensing) system to regulate several traits, including the growth phase switch, motility, virulence, natural competence, expression of a “fitness island”, and phenotypic heterogeneity (Chapter 1.1.5).

The first aim of this PhD project was to characterize the interactions of *L. pneumophila* biofilms with their natural host *A. castellanii*. Specifically, I sought to investigate if *Legionella*-amoeba interactions within biofilms are regulated by the pleiotropic transcription factor LvbR, the Lqs system, effector proteins or the flagellum. For this purpose, mono species *L. pneumophila* biofilms were to be prepared and possible interactions with *A. castellanii* were to be investigated by confocal microscopy and flow cytometry. Moreover, the *Legionella*-ameoba interactions were to be further analyzed using *L. pneumophila* mutants lacking LvbR (Δ*lvbR*, components of the Lqs system (Δ*lgsA*, Δ*lgsS*, Δ*lgsT*, Δ*lgsR*), flagellar components (Δ*flaA*) or a functional Icm/Dot T4SS (Δ*icmT*). In addition, amoeba-interacting *L. pneumophila* strains were to be investigated for their expression of different promoters, reflecting motility (P_{flaA}) or virulence (P_{sidC}, P_{ralF}) traits.

The Lqs system is linked with the c-di-GMP regulatory network by the pleiotropic transcription factor LvbR. *L. pneumophila* possesses three nitric oxide (NO) receptors, at least two of which were found to be upstream of the c-di-GMP regulatory network. The second messenger molecule c-di-GMP regulates numerous complex traits in bacteria, including biofilm formation, virulence, and motility (Chapter 1.1.6).

The second aim of this PhD project was to investigate the physiological responses of *L. pneumophila* to NO. To this end, marker-less *L. pneumophila* deletion mutants lacking one of the three individual NO receptors Hnox1, Hnox2 and NosP or all three NO receptors at once were to be generated. The single and triple knockout mutants were to be further characterized and assessed for different traits including virulence, biofilm formation and phenotypic heterogeneity. Moreover, it was to be investigated whether the genomic deletions of the NO receptors as well as the exposure of the bacteria to nitric oxide affect the expression of different promoters in *L. pneumophila*.

Overall, the aims of this PhD thesis were to characterize the role of *L. pneumophila* genotypes for biofilm-amoeba interactions and the role of NO receptors for *L. pneumophila* traits such the interactions with host cells, or biofilm formation and dispersal.

2. Chapter two – Migration of *Acanthamoeba* through *Legionella* biofilms is regulated by the bacterial Lqs-LvbR network, effector proteins and the flagellum

Migration of *Acanthamoeba* through *Legionella* biofilms is regulated by the bacterial Lqs-LvbR network, effector proteins and the flagellum

Ramon Hochstrasser[1], Sarah Michaelis[1#], Sabrina Brülisauer[1#], Thomas Sura[2], Mingzhen Fan[1], Sandra Maaß[2], Dörte Becher[2], and Hubert Hilbi[1*]

[1]Institute of Medical Microbiology, University of Zurich, Gloriastrasse 30, 8006 Zürich, Switzerland.
[2]Institute of Microbiology, University of Greifswald, Felix-Hausdorff-Strasse 8, 17489 Greifswald, Germany.
[#]These authors contributed equally to this work.

Keywords: Amoeba, *Acanthamoeba*, cell migration, bacterial adherence, biofilm, cell-cell communication, flagellum, *Legionella*, response regulator, sensor kinase, transcription factor, quorum sensing.

Abbreviations: Icm/Dot, Intracellular multiplication / Defective organelle trafficking; LAI-1, *Legionella* autoinducer-1; LCV, *Legionella*-containing vacuole; Lqs, *Legionella* quorum sensing; LvbR, *Legionella* virulence and biofilm regulator; c-di-GMP, cyclic di-guanosine monophosphate; GFP, green fluorescent protein; T4SS, type IV secretion system.

* Correspondence: hilbi@imm.uzh.ch

Article published in: Environmental Microbiology. 2022; 24.8, p. 3672-3692.

2.1 Summary

The environmental bacterium *Legionella pneumophila* causes the pneumonia Legionnaires' disease. The opportunistic pathogen forms biofilms and employs the Icm/Dot type IV secretion system (T4SS) to replicate in amoebae and macrophages. A regulatory network comprising the *Legionella* quorum sensing (Lqs) system and the transcription factor LvbR controls bacterial motility, virulence and biofilm architecture. Here we show by comparative proteomics that in biofilms formed by the *L. pneumophila* Δ*lqsR* or Δ*lvbR* regulatory mutants the abundance of proteins encoded by a genomic 'fitness island', metabolic enzymes, effector proteins and flagellar components (e.g., FlaA) varies. Δ*lqsR* or Δ*flaA* mutants form 'patchy' biofilms like the parental strain JR32, while Δ*lvbR* forms a 'mat-like' biofilm. *Acanthamoeba castellanii* amoebae migrated more slowly through biofilms of *L. pneumophila* lacking *lqsR*, *lvbR*, *flaA*, a functional Icm/Dot T4SS (Δ*icmT*), or secreted effector proteins. Clusters of bacteria decorated amoebae in JR32, Δ*lvbR* or Δ*icmT* biofilms but not in Δ*lqsR* or Δ*flaA* biofilms. The amoeba-adherent bacteria induced promoters implicated in motility (P_{flaA}) or virulence (P_{sidC}, P_{ralF}). Taken together, the Lqs-LvbR network (quorum sensing), FlaA (motility) and the Icm/Dot T4SS (virulence) regulate migration of *A. castellanii* through *L. pneumophila* biofilms, and – apart from the T4SS – govern bacterial cluster formation on the amoebae.

2.2 Introduction

Legionella pneumophila is a Gram-negative environmental bacterium that resides in freshwater niches. Through inhalation of *L. pneumophila*-laden aerosols the opportunistic pathogen reaches the lung and infects alveolar macrophages, which can cause the life-threatening Legionnaires' disease (Fields et al., 2002; Hilbi et al., 2011; Newton et al., 2010). *Legionella pneumophila* replicates intracellularly within free-living protozoa, which appear to represent the preferential niche in the environment (Fields, 1996; Kuiper et al., 2004; Murga et al., 2001). The pathogen governs the interactions with host cells through the Icm/Dot type IV secretion system (T4SS) (Böck et al., 2021; Ghosal et al., 2019; Kubori and Nagai, 2016), which transports the impressive number of >300 different 'effector' proteins implicated in the formation of a unique, ER-associated compartment, the *Legionella*-containing vacuole (LCV) (Finsel and Hilbi, 2015; Hubber and Roy, 2010; Isberg et al., 2009; Personnic et al., 2016; Qiu and Luo, 2017; Steiner et al., 2018).

Legionella pneumophila is a facultative intracellular bacterium, which also colonizes and persists in complex biofilms composed of various microorganisms, including bacteria and protozoa (Abdel-Nour et al., 2013; Declerck, 2010; Hoffmann et al., 2014; Lau and Ashbolt, 2009; Swart et al., 2018). Predatory protozoa, such as the amoeba *Acanthamoeba castellanii*, migrate and 'graze' on the bacterial biofilm communities (Huws et al., 2005). Intriguingly, amoeba migration and endocytic processes such as micropinocytosis are antagonistically correlated, presumably, since they largely require the same cellular machinery implicated in cytoskeleton and membrane dynamics (Delgado et al., 2022; Veltman, 2015). Intracellular replication within amoebae seems to promote bacterial features that facilitate biofilm formation

by *L. pneumophila* (Bigot et al., 2013) and is likely important for *L. pneumophila* to grow within multispecies biofilms (Declerck et al., 2009; Declerck et al., 2007).

Under laboratory conditions, *L. pneumophila* forms mono-species biofilms that allow the investigation of bacterial determinants potentially implicated in biofilm development (Hindre et al., 2008; Hochstrasser et al., 2019; Mampel et al., 2006; Pecastaings et al., 2010). *Legionella pneumophila* biofilm formation is not well understood, and only a few bacterial determinants affecting biofilm formation have been described (Abu Khweek and Amer, 2018). The Tat transporter (De Buck et al., 2005), the *Legionella* collagen-like (Lcl) adhesin (Duncan et al., 2011; Mallegol et al., 2012) and to a limited extent the type IV pili (Lucas et al., 2006) have been found to be involved in biofilm development.

The flagellum assists biofilm development of various bacteria (Davey and O'Toole G, 2000; Petrova and Sauer, 2012). The *L. pneumophila* flagellum filament protein (flagellin) is encoded by the *flaA* gene, and its transcription is controlled by the alternative sigma factor FliA (Albert-Weissenberger et al., 2010). The production of sessile *L. pneumophila* biomass is regulated by FliA and seems to be independent of FlaA (Mampel et al., 2006; Stewart et al., 2012), but it remains unclear to which extent FlaA mediates the *L. pneumophila* biofilm architecture.

The pleiotropic transcription factor LvbR (*Legionella* virulence and biofilm regulator) controls *L. pneumophila* virulence and biofilm architecture, and its transcription is negatively regulated by the *Legionella* quorum sensing (Lqs) kinase LqsS (Hochstrasser and Hilbi, 2020; Hochstrasser et al., 2019) (**Fig. 2.1**). LvbR negatively regulates the nitric oxide (NO) sensor and di-guanylate cyclase inhibitor Hnox1, and thus, positively regulates the production of the second messenger cyclic di-guanosine monophosphate (c-di-GMP). Several c-di-GMP metabolizing enzymes are implicated in the regulation of *L. pneumophila* biofilm formation (Carlson et al., 2010; Pecastaings et al., 2016).

The Lqs system comprises the autoinducer synthase LqsA (Spirig et al., 2008), the sensor histidine kinases LqsS (Tiaden et al., 2010b) and LqsT (Kessler et al., 2013), and the response regulator LqsR (Tiaden et al., 2008; Tiaden et al., 2007), which dimerizes upon phosphorylation (Hochstrasser et al., 2020; Schell et al., 2014). The Lqs system produces, detects and responds to the signalling molecule LAI-1 (*Legionella* autoinducer-1, 3-hydroxypentadecane-4-one) (Tiaden and Hilbi, 2012; Tiaden et al., 2010a). The system regulates various traits in *L. pneumophila* (**Fig. 2.1**), such as motility and production of flagellin (Schell et al., 2016b), virulence (Hochstrasser and Hilbi, 2017; Personnic et al., 2018), the bacterial growth phase switch (Hochstrasser and Hilbi, 2022; Tiaden et al., 2007), expression of a genomic ‘fitness island’ and natural competence for DNA uptake (Hochstrasser and Hilbi, 2017; Personnic et al., 2018), as well as host cell motility (Simon et al., 2015). However, it is not known to what extent the Lqs system controls biofilm formation or architecture.

The interactions between biofilm/sessile bacterial pathogens and amoebae represent crucial ecological processes, which are not well understood on a molecular level. It is currently not known to which extent bacterial factors, such as regulatory systems, virulence factors, the flagellum, or the architecture of biofilms Cdetermine the encounter with amoebae. In this study, we visualized and quantified by confocal microscopy

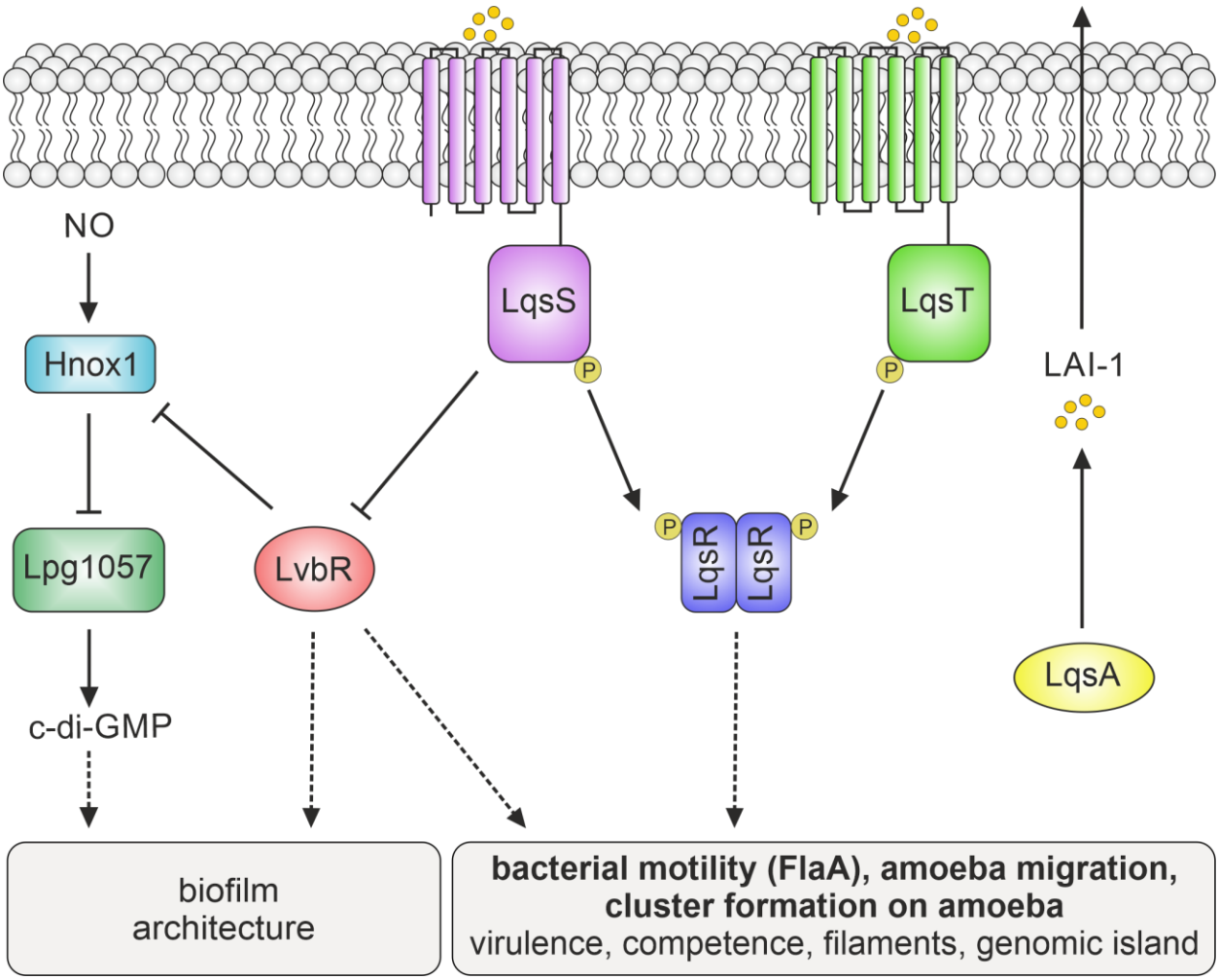

Figure 2.1. The *L. pneumophila* Lqs-LvbR regulatory network.
The Lqs (*Legionella* quorum sensing) system produces, detects and responds to the small signalling molecule LAI-1 (*Legionella* autoinducer-1, 3-hydroxypentadecane-4-one). The system comprises the autoinducer synthase LqsA, the cognate membrane-bound sensor kinases LqsS and LqsT, and the prototypic response regulator LqsR. LqsS negatively regulates the expression of *lvbR*, encoding the transcription factor LvbR (*Legionella* virulence and biofilm regulator). In turn, LvbR negatively regulates the expression of *hnox1*, encoding the NO sensor Hnox1, to control the diguanylate cyclase Lpg1057, c-di-GMP levels and biofilm architecture. The Lqs-LvbR network regulates bacterial growth phase switch and motility (flagellin, FlaA), amoeba migration in biofilms and bacterial cluster formation on amoebae, virulence, competence and extracellular filaments, as well as the expression of genes on a 133 kb genomic island, including *lvbR*.

the interactions of amoebae with genetically distinct *L. pneumophila* biofilms. We found that the Lqs regulator LqsR, the transcription factor LvbR, the flagellum and the Icm/Dot T4SS control the migration of *A. castellanii* through *L. pneumophila* biofilms, and – with the exception of the T4SS – also regulate bacterial adherence and cluster formation on the amoeba surface.

2.3 Results

2.3.1 Comparative proteomics and differential regulation of flagellum production in *L. pneumophila* Δ*lvbR* or Δ*lqsR* biofilms

The *L. pneumophila* transcription factor LvbR regulates biofilm architecture: biofilms formed by a Δ*lvbR* mutant are homogenous and 'mat-like', while biofilms formed by the parental strain JR32 appear aggregated and 'patchy' respectively (Hochstrasser et al., 2019). To further identify components relevant for *L. pneumophila* biofilm formation, we compared the proteomes of biofilms formed by JR32, Δ*lvbR* or Δ*lqsR* mutant strains. To this end, the strains were left to form biofilms in AYE medium for 6 days, bacteria-associated and secreted proteins were collected, and the proteomes of the mutant strains were compared to the parental strain JR32 (**Fig. 2.2A, Fig. S2.1**). In biofilms formed by the Δ*lvbR* strain, there were ca. 1.7 times more proteins produced than that in biofilms formed by the Δ*lqsR* strain (**Fig. 2.2A**). Among a total of 1241 proteins identified, 662 or 237 were uniquely produced in Δ*lvbR* or Δ*lqsR* biofilms respectively, while 342 were produced in concert in biofilms from both strains, the abundance of which changed synergistically (326 proteins) or reciprocally (16 proteins). Hence, in biofilms formed by the Δ*lvbR* or Δ*lqsR* mutants significantly more protein abundances changed jointly rather than reciprocally (**Fig. 2.2A, Fig. S2.1**). These results suggest that the regulators LvbR and LqsR share many common targets in biofilms.

A number of proteins with substantially changed abundances were identified in biofilms formed by the Δ*lvbR* or Δ*lqsR* mutant strains (**Fig. S2.1**). Specifically, proteins produced by the 133 kb genomic fitness island region I (*lpg0973*-*lpg1005*; e.g., Lpg0987, Lpg0995) and region II (*lpg1006*-*lpg1096*; e.g., Lpg1055) were less (region I) or more (region II) abundant in biofilms formed by the mutant strains (**Fig. S2.1, box 1–2**). Moreover, the *Legionella* collagen-like (Lcl) adhesin (Lpg2644; SclB tail fibre protein) (Duncan et al., 2011; Mallegol et al., 2012) was found in lower amounts in the Δ*lvbR* mutants compared to the wild-type strain (**Fig. S2.1**). Components of the Lvh T4SS (LvhB5/Lpg1253, LvhB10/Lpg1247, LvrE/Lpg1244) (Segal et al., 1999) (**Fig. S2.1, box 3**) and Icm/Dot-translocated effector proteins, such as the astacin protease LegP (Lpg2999) (de Felipe et al., 2008), the deAMPylase SidD (Lpg2465) (Neunuebel et al., 2011; Tan and Luo, 2011), the ubiquitin ligase SdeA (Lpg2157) (Qiu et al., 2016), the Rab1 GEF RalF (Lpg1950) (Nagai et al., 2002) and the protein kinase Lpg2603 (Sreelatha et al., 2020) were found in lower amounts in the Δ*lvbR* and/or Δ*lqsR* mutants compared to the parental strain JR32 (**Fig. S2.1**). In contrast, enzymes implicated in *myo*-inositol catabolism, such as IolG (Lpg1652), IolCB (Lpg1651), IolD (Lpg1650) and IolE (Lpg1649) (Manske et al., 2016) were more abundant in biofilms formed by the Δ*lvbR* or Δ*lqsR* mutant strains (**Fig. S2.1, box 4**), indicating that inositol catabolism in *L. pneumophila* biofilms might be negatively regulated by LvbR and LqsR.

Intriguingly, in biofilms formed by the Δ*lvbR* or Δ*lqsR* mutant strains components of the flagellum were differentially produced, in particular the major flagellar subunit flagellin (FlaA/FliC, Lpg1340) was depleted, while the flagellar hook-associated protein FliD (Lpg1338), some Flg proteins (Lpg1218-Lpg1222), the flagellar motor switch protein FliN (Lpg1791) and other Fli proteins (Lpg1758, Lpg1762), as well as the flagellar biosynthesis sigma factor FliA (Lpg1782) were enriched (**Fig. S2.1, box 5–8**).

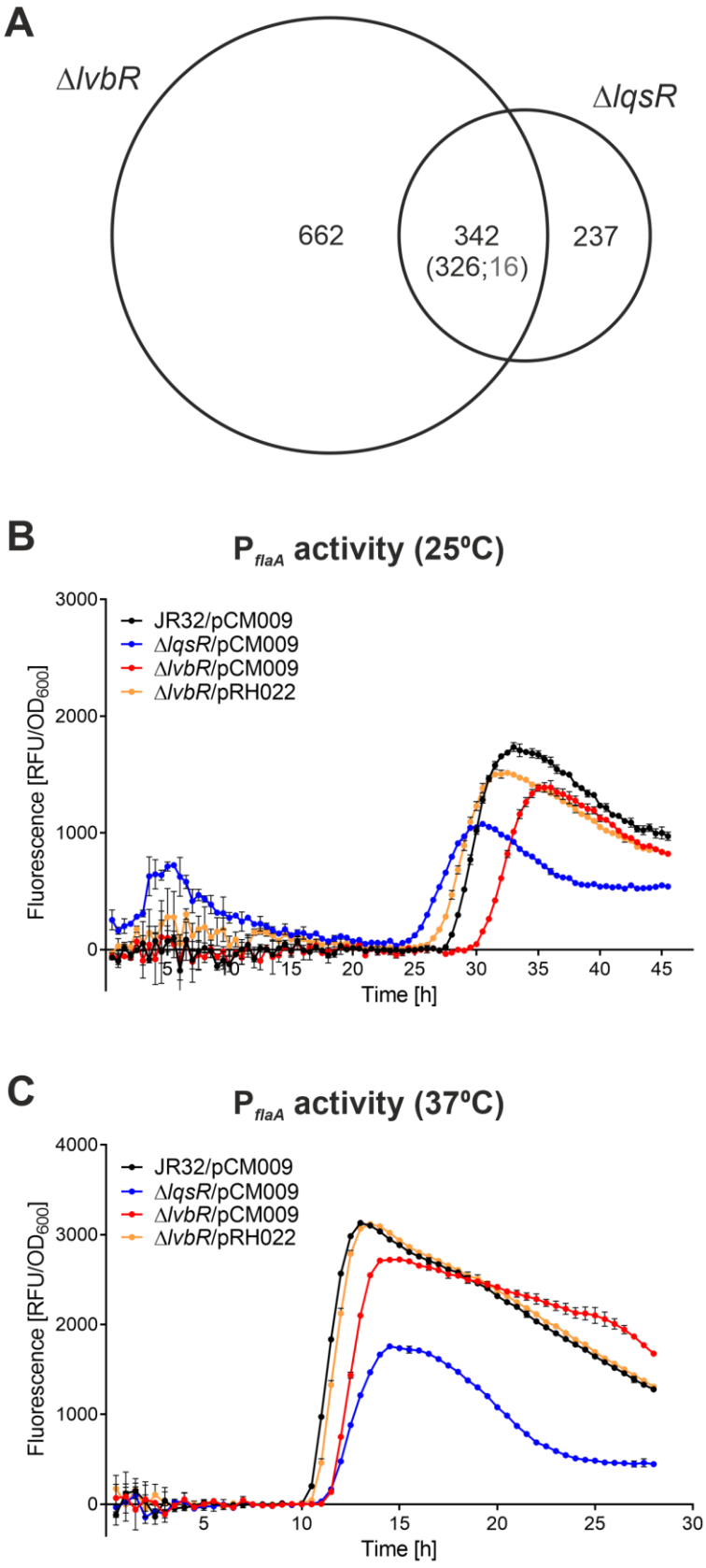
A
ΔlvbR
ΔlqsR
662
342
(326;16)
237
B
P flaA activity (25ºC)
Fluorescence [RFU/OD600]
Time [h]
JR32/pCM009
ΔlqsR/pCM009
ΔlvbR/pCM009
ΔlvbR/pRH022
C
P flaA activity (37ºC)
Fluorescence [RFU/OD600]
Time [h]
JR32/pCM009
ΔlqsR/pCM009
ΔlvbR/pCM009
ΔlvbR/pRH022

Figure 2.2. Comparative proteomics of *L. pneumophila* JR32, Δ*lvbR* and Δ*lqsR* biofilms and validation of differential P_{flaA} expression.
(A) Proteomics was performed with biofilms formed by Δ*lvbR* or Δ*lqsR* mutant strains and compared to the biofilms formed by the parental strain JR32. In the Venn diagrams all proteins are shown that are depleted or enriched in mutant biofilms (for details see Materials and Methods). Among the total of 1241 proteins identified, 342 were produced in concert depending on the presence of LvbR and LqsR (overlapping area; brackets: number of LvbR/LqsR-dependent proteins, which accumulate in parallel (326, black) or reciprocally (16, grey). (B, C) P_{flaA}-*gfp* expression in Δ*lvbR* and Δ*lqsR* mutant strains. *Legionella pneumophila* JR32, Δ*lvbR* or Δ*lqsR* strains harbouring the promoter-reporter constructs P_{flaA}-*gfp* (pCM009) or P_{flaA}-*gfp* and P_{lvbR}-*lvbR* (pRH022) were grown at (B) 25 °C or (C) 37 °C in AYE medium within microplates while orbitally shaking. GFP fluorescence (relative fluorescence units, RFU) at a gain of 50 and optical density at 600 nm (OD_{600}) were measured over time using a microplate reader. The kinetics of the GFP fluorescence/OD_{600} values are shown. The data are means and standard deviations of a technical triplicate and representative of two (B) or three (C) independent measurements.

In agreement with these findings, in the Δ*lvbR* and Δ*lqsR* mutant strains the expression of a P_{flaA}-*gfp* reporter construct lagged behind and was downregulated at 25 °C (**Fig. 2.2B**) as well as at 37 °C (**Fig. 2.2C**), confirming previous results for Δ*lqsR* (Schell et al., 2016b). Complementation of the Δ*lvbR* mutant phenotype was achieved with a plasmid producing LvbR under control of its natural promoter (P_{lvbR}-*lvbR*) in addition to GFP under control of P_{flaA} (**Fig. 2.2BC**). In agreement with the finding that components of the flagellum are downregulated in the Δ*lvbR* and Δ*lqsR* strains, the mutants showed reduced motility upon growth in AYE medium (**Movies S2.1–S2.3**). Taken together, these results suggest that LqsR and LvbR control the production of the flagellum, and in particular, act as positive regulators of FlaA production and *flaA* transcription.

Based on the finding that the flagellum is regulated by LqsR and LvbR in *L. pneumophila* biofilms, we assessed whether FlaA is a determinant of biofilm formation and architecture. To this end, GFP-producing *L. pneumophila* JR32 or Δ*flaA* were left to form biofilms in AYE medium for 1, 2, 3 and 6 days at 25 °C without disturbance, and biofilm formation, including architecture and adherence to an abiotic surface, was analysed by confocal microscopy (**Fig. 2.3**). Under these conditions, the Δ*flaA* mutant strain showed the same ‘clustered’ and ‘patchy’ biofilm architecture as the parental JR32 strain. In contrast, the Δ*lvbR* strain formed a ‘mat-like’ biofilm, as reported previously (Hochstrasser et al., 2019).

Analogously, we assessed the *L. pneumophila* Δ*lqsR*, Δ*lqsA*, Δ*lqsS*, Δ*lqsT* and Δ*lqsS*-Δ*lqsT* mutant strains for biofilm formation. The *lqs* mutant strains formed biofilms with the same morphology as the parental strain JR32 (**Fig. 2.3, Fig. S2.2A**), produced comparable biomass, i.e. the same number of bacteria per ml (**Fig. S2.2BC**), and adhered similarly to the abiotic surface of the microscopy dish (**Fig. S2.3**). In summary, biofilms formed by *L. pneumophila* lacking the major flagellum component FlaA or components of the Lqs system adopt a ‘patchy’ architecture morphologically similar to the parental strain JR32, produce a comparable biomass, and adhere indistinguishably to an abiotic surface. Therefore, under the conditions tested the flagellum is not required to establish *L. pneumophila* biofilms, and quorum sensing does not control biofilm formation and architecture. However, since the biofilms formed by the Δ*lvbR* or

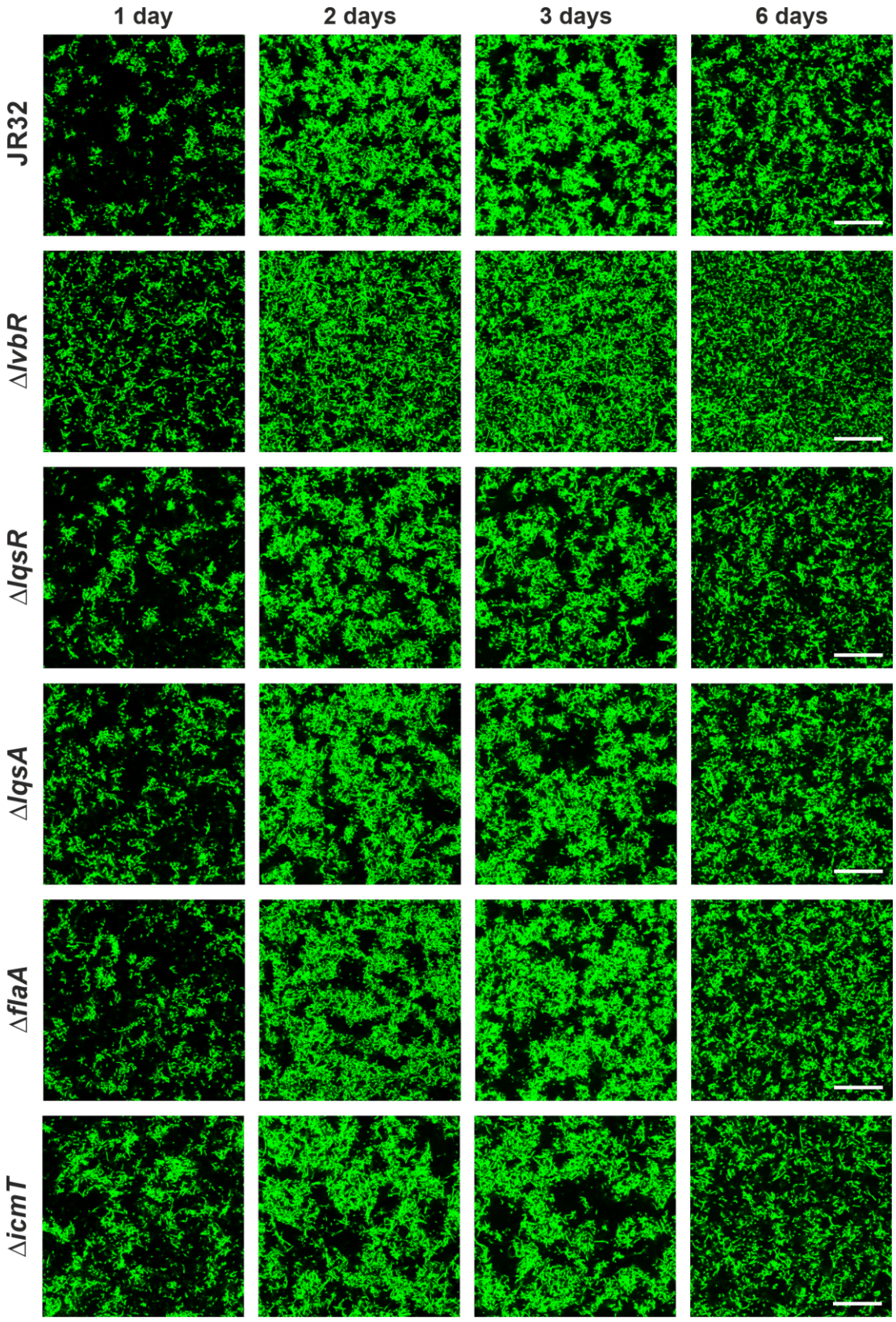
1 day
2 days
3 days
6 days
JR32
ΔlvbR
ΔlqsR
ΔlqsA
ΔflaA
ΔicmT

Figure 2.3. Biofilm formation of *L. pneumophila* Δ*lqs*, Δ*flaA* and Δ*icmT* mutant strains.
Biofilms were initiated with exponential phase *L. pneumophila* JR32, Δ*lvbR*, Δ*lqsR*, Δ*lqsA*, Δ*flaA* or Δ*icmT* mutant strains harbouring pNT28 (constitutive production of GFP) in AYE medium within ibiTreat microscopy dishes. Biofilms were grown at 25 °C without mechanical disturbance, and confocal microscopy images of biofilm architecture were acquired at 4 µm above the dish bottom after 1, 2, 3 and 6 days of growth. The images shown are representative of three independent experiments. Scale bars, 30 µm.

Δ*lqsR* mutants regulate flagellum production and differ in their protein pattern compared to JR32 (**Fig. S2.1**), a distinct protein composition underlies these morphologically similar biofilms.

2.3.2 LvbR, LqsR and FlaA promote *A. castellanii* migration through *L. pneumophila* biofilms

To further investigate the characteristics of genetically different *L. pneumophila* biofilms, we assessed their interactions with amoebae. The different protein composition profiles of biofilms formed by *L. pneumophila* JR32 or mutant strains might affect the migration of amoebae through a biofilm. To test this hypothesis, we quantified the migration of *A. castellanii* through biofilms formed by GFP-producing *L. pneumophila* JR32 or the Δ*lvbR*, Δ*lqsR*, Δ*lqsA* or Δ*flaA* mutant strains (**Fig. 2.4**). The biofilms were grown in AYE medium for 6 days at 25 °C, and after adding the amoebae, the migration of single cells through the biofilms was tracked by confocal microscopy in the bright field channel (**Movies S2.4–S2.8**).

Under these conditions, the amoebae within JR32 or Δ*lqsA* biofilms showed a more vigorous migration compared to Δ*lvbR*, Δ*lqsR* or Δ*flaA* biofilms (**Fig. 2.4A**). The amoebae velocity was highest in biofilms formed by JR32 (on average ca. 0.22 µm s^{-1}), lower in biofilms generated by Δ*lvbR* or Δ*flaA* (ca. 0.15 µm s^{-1}, not significant for Δ*lqsA*) and lowest in Δ*lqsR* biofilms (ca. 0.09 µm s^{-1}) (**Fig. 2.4B**). The migration distance (Euclidean distance) was ca. 75 µm for amoebae in biofilms formed by JR32, Δ*lqsA* or Δ*flaA* and less (but not significantly) for amoebae in biofilms formed by the Δ*lvbR* or Δ*lqsR* mutant strains (ca. 40 µm) (**Fig. 2.4C**). These observations were rather unexpected, since the JR32 and Δ*lqsA* strains are more virulent (and thus potentially more toxic) than the Δ*lvbR*, Δ*lqsR* or Δ*flaA* mutant strains. Taken together, *A. castellanii* amoebae migrate fastest in biofilms established by *L. pneumophila* JR32, with intermediate speed in Δ*lqsA*, Δ*flaA* or Δ*lvbR* biofilms and slowest in biofilms formed by Δ*lqsR*. Thus, amoeba migration in *L. pneumophila* biofilms is positively correlated to the virulence of a strain and promoted by LqsR and LvbR as well as by FlaA.

2.3.3 The Icm/Dot T4SS and the effector LegG1 promote *A. castellanii* migration through *L. pneumophila* biofilms

Given the positive correlation between amoeba migration and the *L. pneumophila* virulence regulators LqsR and LvbR (**Fig. 2.4**), we next tested the role of the Icm/Dot T4SS and secreted effector proteins for amoeba migration in *L. pneumophila* biofilms. To this end, we used the Δ*icmT* mutant strain, which lacks a functional Icm/Dot T4SS (Böck et al., 2021), is defective for intracellular growth (Segal and Shuman, 1998), and in contrast to the wild-type strain JR32, does not inhibit cell migration upon infection (Simon et al., 2014). Moreover, we used the Δ*legG1* (*lpg1976*), Δ*ppgA* (*lpg2224*) or Δ*legG1*-Δ*ppgA* mutant strains, lacking one or two RCC1 repeat effectors, which promote microtubule stabilization, LCV motility and host

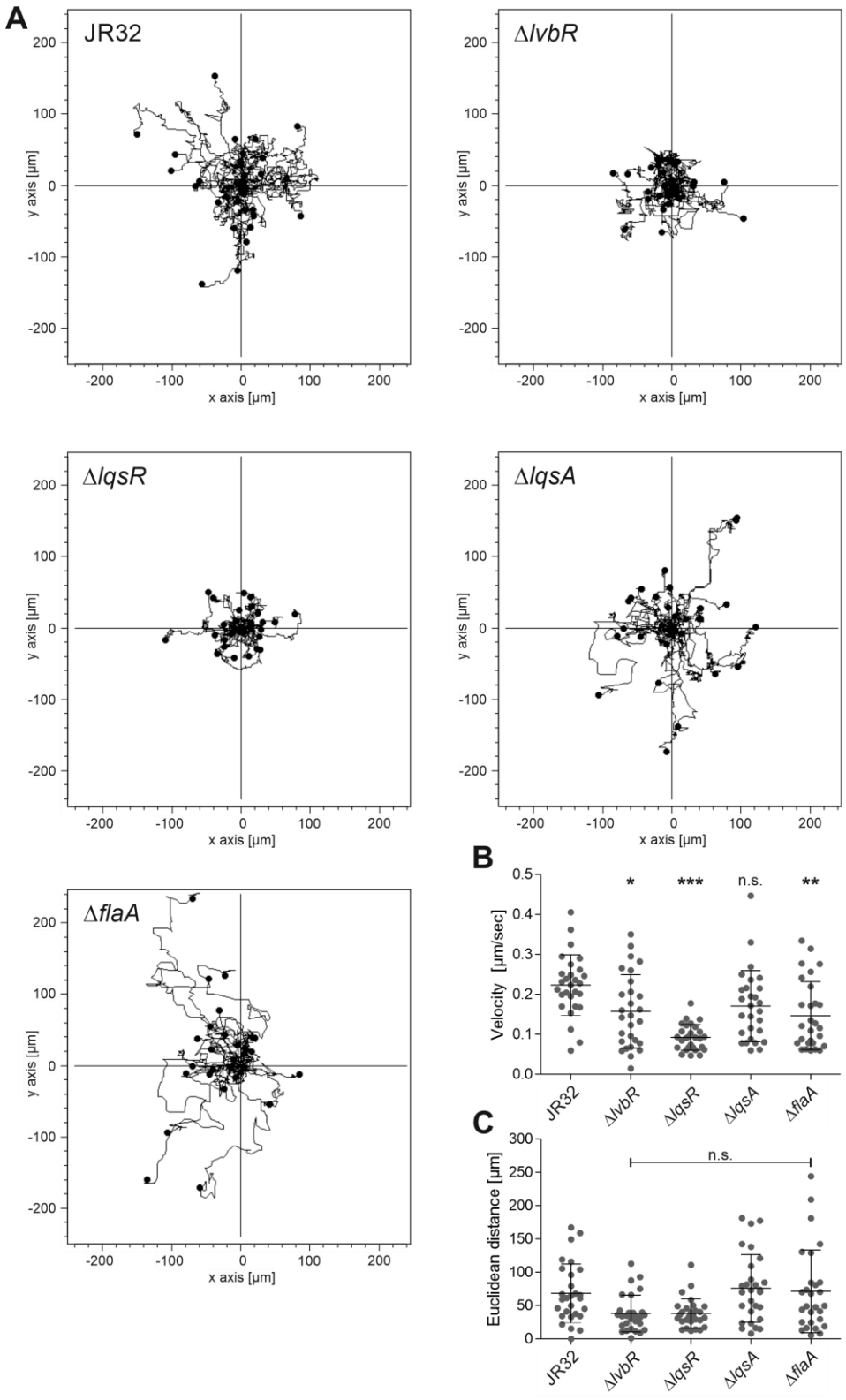
A
JR32
ΔlvbR
ΔlqsR
ΔlqsA
ΔflaA
y axis [µm]
x axis [µm]
B
Velocity [µm/sec]
*
***
n.s.
**
C
Euclidean distance [µm]
n.s.
JR32
ΔlvbR
ΔlqsR
ΔlqsA
ΔflaA

Figure 2.4. LvbR, LqsR and FlaA promote *A. castellanii* migration through *L. pneumophila* biofilms. Biofilms of *L. pneumophila* JR32, Δ*lvbR*, Δ*lqsR*, Δ*lqsA* or Δ*flaA* mutant strains harbouring pNT28 (constitutive production of GFP) were grown in AYE medium at 25 °C, *A. castellanii* was added to preformed biofilms after 6 days, and amoeba migration was followed by confocal microscopy. A. Single amoeba migrating through biofilms were tracked and individually shown as a line in migration plots. B. The velocities and (C) Euclidean distances of migrating amoebae tracked in (A) were quantified. The data (B, C) are means and standard deviations of the mean derived from all tracked amoebae (n.s., not significant; *$p \leq 0.05$; **$p \leq 0.01$; ***$p \leq 0.001$; one-way ANOVA with Tukey post-test; JR32 vs. mutant strains). Single amoebae were tracked in three biologically independent experiments with a total of $n = 28$ amoebae for each bacterial strain.

cell migration (Rothmeier et al., 2013; Swart et al., 2020b). Biofilms formed by the Δ*icmT* mutant strain in AYE medium for 1, 2, 3 and 6 days at 25 °C without disturbance were morphologically similar to the parental strain JR32 (**Fig. 2.3**), and the mutant adhered similarly (but due to faster growth more densely) to an abiotic surface (**Fig. S2.3**). Therefore, a functional Icm/Dot T4SS is not required for normal *L. pneumophila* biofilm formation.

We compared the migration of *A. castellanii* through biofilms formed by *L. pneumophila* JR32, or the Δ*icmT*, Δ*legG1*, Δ*ppgA* or Δ*legG1*-Δ*ppgA* mutant strains (**Fig. 2.5**). To this end, the biofilms were grown in AYE medium for 6 days at 25 °C, and after adding the amoebae, the migration of single cells through the biofilms was tracked by confocal microscopy in the bright field channel (**Movies S2.4 and S2.9**). In JR32 biofilms the amoebae showed a more vigorous migration compared to biofilms established either by the Δ*icmT*, Δ*legG1*, Δ*ppgA* or the Δ*legG1*-Δ*ppgA* double mutant strain (**Fig. 2.5A**). The amoeba velocity was highest in biofilms formed by JR32 (on average ca. 0.3 µm s^{-1}), followed by Δ*ppgA* (ca. 0.28 µm s^{-1}), and significantly lower in Δ*legG1* or Δ*legG1*-Δ*ppgA* biofilms (ca. 0.15–0.16 µm s^{-1}). Interestingly, amoeba movement was most strongly impaired in Δ*icmT* biofilms (ca. 0.09 µm s^{-1}) (**Fig. 2.5B**). The migration distance (Euclidean distance) was highest for amoebae in biofilms formed by JR32 (ca. 90 µm), lowest in biofilms formed by Δ*icmT* (ca. 40 µm) and intermediate for amoebae in biofilms formed by the Δ*legG1*, Δ*ppgA* or Δ*legG1*-Δ*ppgA* mutant strains (ca. 60–70 µm) (**Fig. 2.5C**).

In summary, compared to biofilms formed by the parental strain JR32, *A. castellanii* amoebae migrate less vigorously in biofilms formed by mutant strains lacking a functional Icm/Dot T4SS or RCC1 repeat effectors. Amoeba movement was most strongly impaired in Δ*icmT* biofilms, suggesting that in addition to the RCC1 repeat effectors other Icm/Dot substrates might also contribute to promoting protozoan motility. Hence, amoeba migration in *L. pneumophila* biofilms is positively correlated to the Icm/Dot-dependent virulence, similar to what was observed for biofilms formed by regulatory (and *flaA*) mutant strains (**Fig. 2.4**).

2.3.4 LvbR, LqsR and FlaA determine *L. pneumophila* cluster formation on *A. castellanii*

To further investigate the processes underlying the migration of *A. castellanii* through biofilms, we analysed by confocal microscopy the features of different *L. pneumophila* strains interacting with the amoebae. To this end, GFP-producing *L. pneumophila* JR32 or the Δ*lvbR*, Δ*lqsR*, Δ*lqsA*, Δ*flaA* or Δ*icmT* mutant strains

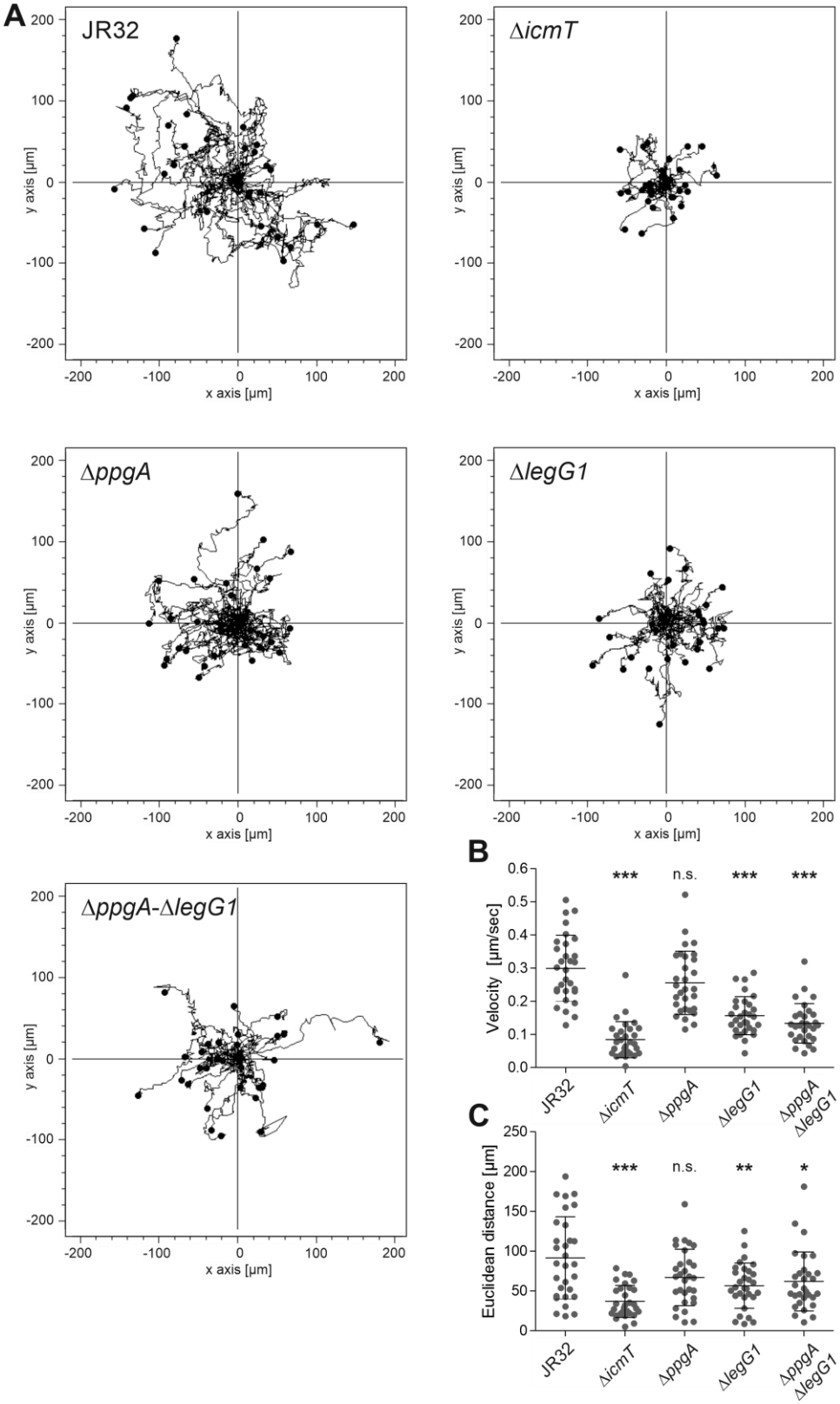
A
JR32
ΔicmT
ΔppgA
ΔlegG1
ΔppgA-ΔlegG1
y axis [µm]
x axis [µm]
B
Velocity [µm/sec]
C
Euclidean distance [µm]
***
n.s.
**
*
JR32
ΔicmT
ΔppgA
ΔlegG1
ΔppgA ΔlegG1

Figure 2.5. The Icm/Dot T4SS and the effector LegG1 promote *A. castellanii* migration through *L. pneumophila* biofilms.
Biofilms of *L. pneumophila* JR32, Δ*icmT*, Δ*ppgA*, Δ*legG1* or Δ*ppgA*-Δ*legG1* mutant strains harbouring pNT28 (constitutive production of GFP) were grown in AYE medium at 25 °C, *A. castellanii* was added to preformed biofilms after 6 days and amoeba migration was followed by confocal microscopy. A. Single amoeba migrating through biofilms were tracked and individually shown as a line in migration plots. B. The velocities and (C) Euclidean distances of migrating amoebae tracked in (A) were quantified. The data (B, C) are means and standard deviations of the mean derived from all tracked amoebae (n.s., not significant; *$p \leq 0.05$; **$p \leq 0.01$; ***$p \leq 0.001$; one-way ANOVA with Tukey post-test; JR32 vs. mutant strains). Single amoebae were tracked in three biologically independent experiments with a total of $n = 30$ amoebae for each bacterial strain.

were left to form biofilms in AYE medium for 6 days at 25 °C, and bacteria–amoeba interactions were assessed by confocal microscopy in the GFP or bright field channel respectively (**Fig. 2.6**).

Strikingly, amoebae placed onto biofilms generated by JR32, Δ*lqsA* or Δ*icmT* were decorated with bacteria that formed large aggregates or clusters adhering to the amoebae (**Fig. 2.6A**). Close-up inspection (**Fig. S2.4A**) and 3D-rendering (**Fig. S2.4B**) of these bacterial aggregates revealed multi-layered clusters decorating the polar or lateral side of amoebae, and preferentially the lagging end of moving amoebae (**Movies S2.4 and S2.7**). Furthermore, 'trails' of migrating amoebae were apparent in the surface-attached layer of JR32 biofilms, suggesting that the migrating amoebae 'grazed' through biofilms leaving behind a track devoid of bacteria (**Fig. S2.4C**, **Movies S2.4 and S2.7**).

The quantitative assessment of the clusters by confocal microscopy revealed that almost 100% of the amoebae in biofilms formed by the JR32, Δ*lqsA*, or Δ*icmT* strains were decorated by bacterial clusters (**Fig. 2.6B**). In contrast, ca. 75% of the amoebae were decorated with bacterial clusters in biofilms formed by the Δ*lvbR* strain, and only ca. 10% of the amoebae were decorated with bacterial clusters in biofilms formed by the Δ*lqsR* or Δ*flaA* mutant strains. Moreover, the size of the bacterial clusters was similar for strain JR32, Δ*lqsA* or Δ*icmT* (ca. 30 µm^2), and significantly smaller for the Δ*lvbR*, Δ*lqsR* or Δ*flaA* mutant strains (ca. 10–20 µm^2) (**Fig. 2.6C**). The quantification of the clusters by flow cytometry indicated very similar results: the amoeba-associated fluorescence intensity of GFP-producing *L. pneumophila* was highest for the JR32, Δ*lqsA*, or Δ*icmT* strains, followed by Δ*lvbR*, and lowest for the Δ*lqsR* or Δ*flaA* mutant strains (**Fig. 2.6D, Fig. S2.5AB**). In summary, these observations indicate that *L. pneumophila* forms large aggregates or clusters adhering to amoebae within biofilms, and neither the LqsA-produced quorum-sensing signalling molecule LAI-1 nor the Icm/Dot T4SS are required for cluster formation.

In contrast to the bacterial clusters on amoebae migrating in biofilms generated by JR32, Δ*lqsA*, or Δ*icmT*, these clusters were barely present and much smaller on amoebae in biofilms formed by Δ*lvbR* and entirely absent in biofilms formed by Δ*lqsR* or Δ*flaA* (**Fig. 2.6**). The bacterial clusters on amoebae in Δ*flaA* biofilms were partially restored by the expression of plasmid-borne *flaA* in the mutant strain (**Fig. S2.4DE**). Finally, the mCherry-producing parental strain JR32 clustered to *A. castellanii* also in presence of and upon competition with GFP-producing mutant strains (**Fig. S2.6**), indicating that the cluster phenotype is dominant. In summary, these results indicate that the regulatory proteins LvbR and LqsR as

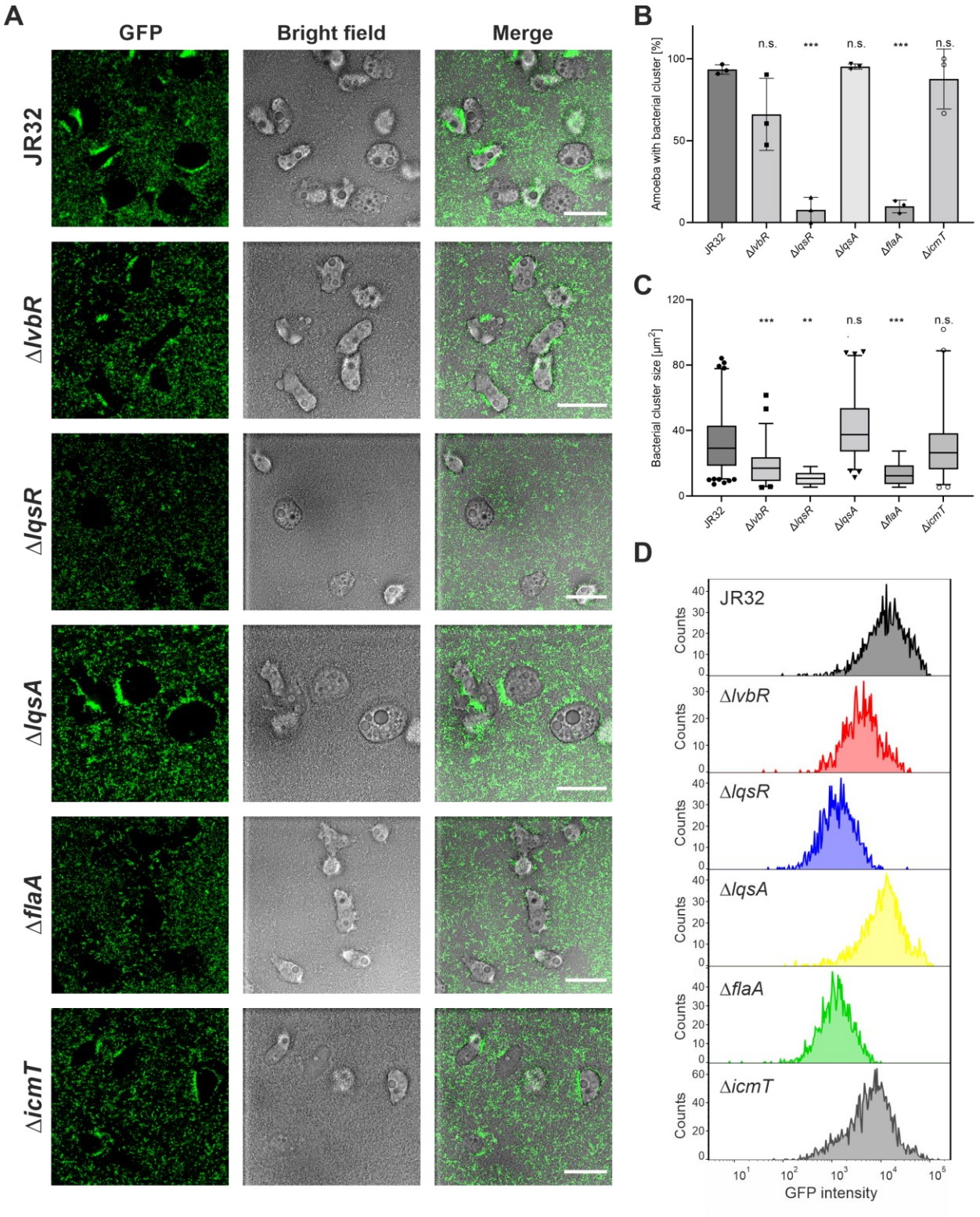

Figure 2.6. LvbR, LqsR and FlaA determine *L. pneumophila* cluster formation on *A. castellanii*. Biofilms of *L. pneumophila* JR32, Δ*lvbR*, Δ*lqsR*, Δ*lqsA,* Δ*flaA* or Δ*icmT* mutant strains harbouring pNT28 (constitutive production of GFP) were grown for 6 days in AYE medium at 25 °C, and *A. castellanii* was added to preformed biofilms. A. Bacterial adherence and cluster formation were monitored in biofilms

containing amoebae by confocal microscopy above the dish bottom. The images shown are representative of three independent experiments. Scale bars, 30 µm. B. Percentage of amoebae with bacterial cluster (or cluster-positive amoebae) in the total amoebae population. The columns display the mean value of three biological replicates (in dots) with standard deviations. C. Quantification by fluorescence microscopy of cluster size on cluster-positive amoebae. The box-and-whisker plots display 5th to 95th percentiles (whiskers), median and quartiles (box) of the pooled results from three biologically independent experiments with a total analysed number of amoebae $n = 124$ (JR32), $n = 60$ (Δ*lvbR*), $n = 9$ (Δ*lqsR*), $n = 66$ (Δ*lqsA*), $n = 8$ (Δ*flaA*), or $n = 48$ (Δ*icmT*). For (B) and (C): n.s., not significant; $*p \leq 0.05$; $**p \leq 0.01$; $***p \leq 0.001$; one-way ANOVA with Tukey post-test; JR32 vs. mutant strains. D. Quantification by flow cytometry (counts vs. fluorescence intensity) of amoeba-associated, GFP-positive *L. pneumophila* (JR32, Δ*lvbR*, Δ*lqsR*, Δ*lqsA*, Δ*flaA* or Δ*icmT* harbouring pNT28) using FlowJo software (protocol #1, see Materials and Methods).

well as flagellin (FlaA) not only promote the migration of amoebae in *L. pneumophila* biofilms but are also implicated in the formation of bacterial clusters on the migrating amoebae, while the autoinducer synthase LqsA and the Icm/Dot T4SS are dispensable for the phenotype.

2.3.5 Amoeba-adherent *L. pneumophila* clusters express motility and virulence genes

To further characterize the features of the *L. pneumophila* clusters on *A. castellanii* migrating in biofilms, we analysed the activity of promoters serving as prototypic proxies for motility (P_{flaA}), virulence (P_{sidC}, P_{ralF}), stress response (P_{6SRNA}) and replication (P_{csrA}). To this end, we constructed single GFP reporters, which produced the fluorescent protein under control of these promoters in AYE broth (**Fig. S2.7A–E**). The parental strain JR32 was transformed with transcriptional *gfp* fusions of the above promoters, and biofilms were grown in AYE medium for 6 days at 25 °C. After addition of *A. castellanii* for ca. 3 h, the promoter activity was analysed by fluorescence microscopy (**Fig. 2.7A**). This approach revealed that the P_{flaA}, P_{sidC} and P_{ralF} promoters showed strong activity in the amoeba-adherent *L. pneumophila* clusters, while P_{6SRNA} and P_{csrA} were less or not active. Quantitative assessment of promoter activity by flow cytometry confirmed that P_{flaA}, P_{sidC} and P_{ralF} were strongly induced in amoeba-associated *L. pneumophila*, while P_{6SRNA} and P_{csrA} were less or not active (**Fig. 2.7BC, Fig. S2.5C**).

We also tested dual GFP reporter constructs of P_{flaA} P_{sidC}, P_{ralF}, P_{6SRNA} and P_{csrA}, which in parallel also constitutively produce mCherry. Of these constructs, only P_{flaA} and P_{6SRNA} produced a robust GFP signal, which was observed in *L. pneumophila* in broth (**Fig. S2.8AB, data not shown**). Similar to the single reporter constructs, the P_{flaA} promoter was induced in the amoeba-adherent *L. pneumophila* clusters in biofilms, while P_{6SRNA} was not (**Fig. S2.8C**). Moreover, usage of the P_{flaA} dual reporter construct confirmed that amoeba-adherent *L. pneumophila* clusters were most robustly formed in biofilms formed by strain JR32, less in Δ*lvbR* biofilms and barely in biofilms formed by the Δ*lqsR* mutant strain (**Fig. S2.8D**). Taken together, these findings are in agreement with the notion that the bacteria in the clusters are in stationary growth phase and motile. In summary, the individual bacteria in the *L. pneumophila* clusters

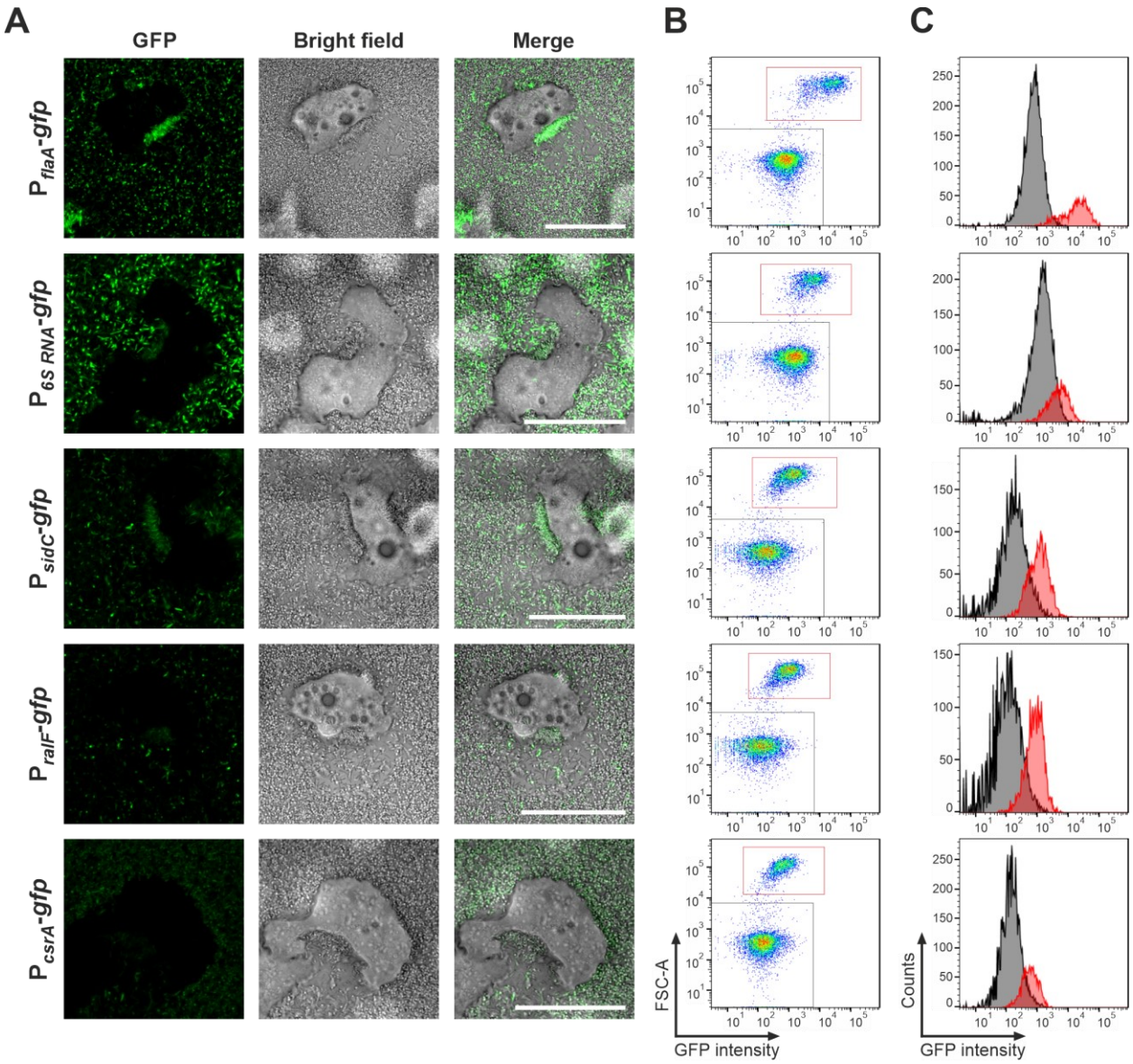

Figure 2.7. Amoeba-adherent *L. pneumophila* clusters express motility and virulence genes.
A. Biofilms of *L. pneumophila* JR32 harbouring promoter-reporter plasmids P_{flaA}-*gfp* (pCM009), P_{6SRNA}-*gfp* (pRH049), P_{sidC}-*gfp* (pRH035), P_{ralF}-*gfp* (pRH032) or P_{csrA}-*gfp* (pRH031) were grown in AYE medium for 6 days. *Acanthamoeba castellanii* was added to preformed biofilms and confocal microscopy images of amoebae with adherent bacterial clusters were acquired close to the bottom of microscopy dishes. The images shown are representative of at least two independent experiments. Scale bars, 30 µm. Quantification by flow cytometry of GFP-positive *L. pneumophila* JR32 harbouring promoter reporters (P_{flaA}, P_{6SRNA}, P_{sidC}, P_{ralF}, or P_{csrA}) using FlowJo software: (B) forward scatter area (FCS-A) versus fluorescence intensity, or (C) counts versus fluorescence intensity [amoebae-associated (red) and non-associated (black)] (protocol #2, see Materials and Methods).

on *A. castellanii* migrating in biofilms express the P_{flaA}, P_{sidC} and P_{ralF} promoters, and therefore, are likely in the non-growing, transmissive and virulent phase.

2.4 Discussion

In this study, we investigated the role of the *L. pneumophila* genotype on biofilm formation and morphology, the migration of amoebae within biofilms and the occurrence of amoeba-associated bacterial clusters (Table 2.1). We found that the transcription factor LvbR, the quorum-sensing response regulator LqsR, the bacterial flagellum (FlaA) and the Icm/Dot T4SS regulate the speed and (except for FlaA) the migration distance of *A. castellanii* moving through *L. pneumophila* biofilms (**Fig 2.4 and 2.5**). Furthermore, LvbR, LqsR and FlaA also regulate the adherence and cluster formation of *L. pneumophila* on the amoeba surface, and the clusters comprise P_{flaA}- and P_{sidC}-positive, i.e. motile and virulent bacteria (**Fig 2.6 and 2.7**).

Table 2.1. Summary of biofilm-amoeba interaction and virulence phenotypes.

Phenotypes	JR32	Δ*lvbR*	Δ*lqsR*	Δ*lqsA*	Δ*flaA*	Δ*icmT*
Biofilm architecture [a]	P	m	p	p	p	p
Amoeba migration	+ +	+	+	+ +	+	+
Cluster formation	+ +	+	-	+ +	-	+ +
Bacterial virulence	++	+	+	++	+	-

[a] Abbreviations: p, 'patchy'; m, 'mat'-like.

Intriguingly, the migration of amoebae through *L. pneumophila* biofilms was positively correlated to the virulence of the bacterial strains (Table 2.1). *Acanthamoeba castellanii* moved slower and less vigorously through biofilms formed by the Δ*lvbR* and Δ*lqsR* regulatory mutants (**Fig. 2.4**), which are impaired for virulence (Hochstrasser et al., 2019; Tiaden et al., 2007), and also through biofilms formed by the avirulent Δ*icmT* T4SS mutant strain, or biofilms formed by strains lacking the Icm/Dot-translocated effectors LegG1 or LegG1 and PpgA (**Fig. 2.5**). LegG1 and PpgA are RCC1 repeat effectors, which localize to LCVs or the plasma membrane, target the activation cycle of the small GTPase Ran and activate Ran either at the LCV or the plasma membrane respectively (Rothmeier et al., 2013; Swart et al., 2020b). The activation of Ran GTPase by the *L. pneumophila* RCC1 repeat effectors promotes microtubule stabilization, LCV motility and cell migration (Rothmeier et al., 2013; Simon et al., 2014; Swart et al., 2020a). Given the cell migration phenotypes of the Δ*legG1*, Δ*ppgA* and Δ*legG1*-Δ*ppgA* mutant strains, presumably the effectors also positively regulate the microtubule cytoskeleton and cell migration of *A. castellanii* moving through biofilms. The amoeba speed was also impaired in biofilms formed by *L. pneumophila* lacking *flaA* encoding bacterial flagellin (FlaA), and thus, was positively correlated to the presence of FlaA (**Fig. 2.4**). Moreover, the amoebae moved with a lower speed through biofilms formed by the Δ*lqsR* strain compared to Δ*lvbR* (**Fig. 2.4B**), in agreement with the decreasingly pronounced role of LqsR and LvbR in regulating P_{flaA} (**Fig. 2.2BC**). However, the amoebae moved with an even lower speed through Δ*lqsR* biofilms

compared to Δ*flaA*. Thus, FlaA is not essential for amoeba migration through *L. pneumophila* biofilms and LqsR likely regulates other factors implicated in the process.

The mechanism, by which FlaA and the flagellum promote amoeba migration through biofilms is unclear. Perhaps, the amoebae detect and respond to the 'pathogen-associated molecular pattern' flagellin. Overall, the enhanced migration of *A. castellanii* in biofilms formed by virulent *L. pneumophila* might be a 'flight' reaction. Such a reaction would expand the behavioural repertoire of biofilm-interacting amoebae, beyond 'grazing' on these bacterial communities (Huws et al., 2005; Matz and Kjelleberg, 2005; Ronn et al., 2002).

An obvious explanation for the biofilm genotype-dependent differences in the migration of amoebae might be distinct biofilm architectures and structures. The homogenous 'mat'-like biofilm architecture of Δ*lvbR* biofilms (Hochstrasser et al., 2019) could cause slower amoeba migration, while amoebae migrate faster through 'patchy' biofilms with interspersed clusters formed by wild-type JR32 bacteria and some mutant strains. However, this seems not to be the case, since the patchy biofilms formed by the Δ*lqsR*, Δ*flaA* and Δ*icmT* mutant strains (**Fig. 2.3**) also sustained only slow amoeba migration. Thus, the biofilm morphology and structure do not seem to correlate with the features of amoeba migration. However, we did not label any matrix components, e.g., exopolysaccharides, protein or eDNA, which might account for the differential migration of the amoebae. Hence, the mechanism(s), by which the lack of the regulatory factors (LvbR, LqsR) impede amoeba migration is unclear.

As a general mechanistic concept, LvbR- or LqsR-regulated bacterial factor(s) or feature(s) might trigger and affect the amoeba migration dynamics in *L. pneumophila* biofilms. *Legionella pneumophila* strains lacking *lvbR* (Hochstrasser et al., 2019) or *lqsR* (Tiaden et al., 2007) are impaired for virulence, and both regulatory factors control the production of Icm/Dot-translocated effector proteins. In sessile *L. pneumophila*, some Icm/Dot-translocated effectors are less abundantly produced by the Δ*lvbR* or Δ*lqsR* mutant strains compared to the parental strain (**Fig. S2.1**). These include the astacin protease LegP (de Felipe et al., 2008), the deAMPylase SidD (Neunuebel et al., 2011; Tan and Luo, 2011), the ubiquitin ligase SdeA (Qiu et al., 2016), the Rab1 GEF RalF (Nagai et al., 2002) and the protein kinase Lpg2603 (Sreelatha et al., 2020). SdeA and RalF are *L. pneumophila* effector proteins typically produced in the post exponential growth phase, while LegP and SidD are non-differentially produced (Aurass et al., 2016). The lack (or lower abundance) of specific effectors might account for the lower migration speed of *A. castellanii* through biofilms formed by the Δ*lvbR* or Δ*lqsR* mutants, analogously to what has been observed for the Δ*icmT*, Δ*legG1*, Δ*ppgA* and Δ*legG1*-Δ*ppgA* mutant strains (**Fig. 2.5**). Alternatively or additionally, the Δ*lvbR* or Δ*lqsR* mutants might be defective for the production of adhesins or components of the extracellular biofilm matrix. As the amoebae were added to *L. pneumophila* biofilms formed over 6 days, such bacterial structures might indeed play a role in determining amoeba migration.

In previous studies, the inhibition of migration and chemotaxis of *D. discoideum*, macrophages and neutrophils was positively correlated with the virulence of *L. pneumophila* (Hochstrasser et al., 2019; Simon et al., 2014). While the parental strain JR32 dose-dependently inhibited phagocyte migration in under-agar

and transwell assays, the Δ*icmT* mutant did not. Compared to JR32, the less virulent Δ*lvbR* mutant strain inhibited *D. discoideum* migration less efficiently, but more efficiently than Δ*icmT* (Hochstrasser et al., 2019). *Legionella pneumophila* Δ*legG1* even hyper-inhibited phagocyte migration, indicating that microtubule stabilization by the RCC1 repeat effector promotes cell motility (Simon et al., 2014). As outlined above, presumably the RCC1 repeat effectors also positively regulate the microtubule cytoskeleton and cell migration of *A. castellanii* moving through biofilms (**Fig. 2.5**).

In the previous migration and chemotaxis studies, the phagocytes were infected with *L. pneumophila* strains for 1 h prior a 4 h migration/chemotaxis assay, and therefore, had already taken up bacteria (Hochstrasser et al., 2019; Simon et al., 2014). Accordingly, the effect of *L. pneumophila* on eukaryotic cell migration seems to depend on whether planktonic bacteria are being taken up or cluster extracellularly. In agreement with this notion, the efficient uptake of *L. pneumophila* by amoebae and macrophages is promoted by LvbR (Hochstrasser et al., 2019), LqsR (Tiaden et al., 2008; Tiaden et al., 2007), the flagellum (FlaA) (Dietrich et al., 2001) and the Icm/Dot T4SS (Hilbi et al., 2001; Weber et al., 2006).

Another intriguing observation was the adherence and cluster formation of *L. pneumophila* on amoebae migrating in biofilms. Cluster formation was controlled by LvbR, LqsR and FlaA, but not by LqsA or the Icm/Dot T4SS, since the Δ*lvbR*, Δ*lqsR* and Δ*flaA* mutants were defective for cluster formation, while Δ*lqsA* or Δ*icmT* formed clusters like the parental strain JR32 (**Fig. 2.6**). *Legionella pneumophila* lacking *flaA* was severely impaired for cluster formation, and thus, FlaA might act as an adhesin and promote binding to the amoebae. While the bacterial flagellum is known to act as an adhesion factor (Haiko and Westerlund-Wikstrom, 2013), it is unclear whether the flagellum *per se* or flagella-based motility is required for cluster formation of *L. pneumophila*. LvbR and LqsR regulate the production of the *L. pneumophila* flagellum filament protein FlaA (Lpg1340) and the transcription of *flaA* (**Fig. S2.1, Fig. 2.2BC**), and thus, possibly contribute to cluster formation on amoebae. Finally, in agreement with a role of LqsR for the regulation of bacterial adherence and cluster formation, LqsR (but not LqsA) was previously found to be a regulator of 'extracellular filaments', which form a network and prevent the sedimentation of the bacteria (Tiaden et al., 2007).

In addition to the flagellum, other *L. pneumophila* factors possibly promote bacterial cluster formation on the amoeba surface in the biofilms. LvbR as well as LqsR are positive regulators of Tfp pili (pilus retraction ATPase PilT, Lpg0987) (**Fig. S2.1**), which might function as adhesins. Lcl (Lpg2644) is another candidate, since this adhesin mediates the adherence to host cells (Vandersmissen et al., 2010) and is implicated in bacterial adhesion during biofilm formation (Duncan et al., 2011; Mallegol et al., 2012). Intriguingly, Lcl is less abundant in biofilms formed by the Δ*lvbR* mutant strain (**Fig. S2.1**), which might contribute to the reduced adherence and cluster formation of the mutant on amoebae (**Fig. 2.6**). In general, bacterial factors contribute individually or in concert to the extracellular biofilm matrix, which might promote adherence and clustering of *L. pneumophila* on the surface of amoebae.

The function of the *L. pneumophila* clusters on amoebae in biofilms is unclear. Successful and efficient intracellular replication of *L. pneumophila* depends on adherence to host cells (Chang et al., 2005; Cirillo et al., 2001; Duncan et al., 2011), and thus, cluster formation might facilitate *L. pneumophila* uptake by host cells within biofilms. Alternatively or additionally, bacterial adherence to amoebae and subsequent cell migration possibly helps *L. pneumophila* to disseminate in the environment. A similar clustering phenomenon was recently reported for planktonic *Listeria monocytogenes*, a food-borne, extracellular Gram-positive bacterium. *Listeria monocytogenes* formed densely packed aggregates on *A. castellanii* and *A. polyphaga* called 'backpacks', and the formation was dependent on flagella-based motility (Doyscher et al., 2013). However, *L. monocytogenes* does not persist in *Acanthamoeba* spp. and simply serves as food for the amoebae. In contrast, *L. pneumophila* does not serve as food but rather consumes and destroys the amoebae. Hence, *L. pneumophila* might subvert a mechanism employed by *A. castellanii* to trap and feed on bacteria, in order to efficiently infect protozoan host cells.

Comparative proteomics of biofilms formed by JR32, Δ*lvbR* or Δ*lqsR* mutant strains revealed that LvbR and LqsR are implicated in the regulation of the flagellum, the Lvh T4SS, Icm/Dot-translocated effectors and proteins encoded by the 133 kb genomic island regions I and II (**Fig. S2.1**). Comparative transcriptomics of sessile and planktonic JR32, Δ*lvbR* or Δ*lqsR* mutant strains indicated similar target genes of the regulators, including the 133 kb genomic island region I (*lpg0973-1005*) and region II (*lpg1006-1096*), the *lvh* region (*lpg1244-1259*) and various genes involved in flagellar biosynthesis (*lpg1216-1226*, *lpg1337-1340*, *lpg1759-1763*, *lpg1780-1789* and *lpg1791-1792*) (Hochstrasser et al., 2019). Taken together, these studies provide insights on the components of *L. pneumophila* biofilms and their interactions with amoebae. Further studies will address the functions and mechanisms underlying the migration of amoebae in *L. pneumophila* biofilms and bacterial cluster formation on the amoebae.

2.5 Experimental procedures

2.5.1 Growth and motility of bacteria, cultivation of amoebae

Legionella pneumophila strains (Table 2.2) were grown on CYE agar plates for 3 days (Feeley et al., 1979), or were grown to exponential phase in liquid cultures with *N*-(2-acetamido)-2-aminoethanesulfonic acid-buffered yeast extract (AYE) medium (Horwitz, 1983) at 37 °C on a wheel (80 rpm) for approximately 18 h. AYE medium was supplemented with chloramphenicol (Cm; 5 µg ml^{-1}) to maintain plasmids if required.

Table 2. 2. Bacterial strains and plasmids used in this study.

Strain or plasmid	Relevant properties [a]	Reference
E. coli		
TOP10		Invitrogen

L. pneumophila

AK01 (Δ*lqsT*)	JR32 *lqsT*::Km	Kessler et al. (2013)
AK02 (Δ*lqsS*-Δ*lqsT*)	JR32 *lqsS*::Km *lqsT*::Gm	Kessler et al. (2013)
AK03 (Δ*lvbR*)	JR32 *lvbR*::Km	Hochstrasser et al. (2019)
ER01 (Δ*legG1*)	JR32 *legG1*::Km	Rothmeier et al. (2013)
GS3011 (Δ*icmT*)	JR32 *icmT3011*::Km	Segal and Shuman (1998)
JR32	*L. pneumophila* Philadelphia-1, serogroup 1, salt-sensitive isolate of AM511	Sadosky et al. (1993)
LS01 (Δ*ppgA*-Δ*legG1*)	JR32 *ppgA*::Gm *legG1*::Km	Swart et al. (2020b)
LS03 (Δ*ppgA*)	JR32 *ppgA*::Km	Swart et al. (2020b)
NT02 (Δ*lqsA*)	JR32 *lqsA*::Km	Tiaden et al. (2010b)
NT03 (Δ*lqsR*)	JR32 *lqsR*::Km	Tiaden et al. (2007)
NT05 (Δ*lqsS*)	JR32 *lqsS*::Km	Tiaden et al. (2010b)
Δ*flaA*	JR32 *flaA*::Km	Weber et al. (2012)

Plasmids

pAK18	pMMB207C-P_{lvbR}-*lvbR*, *gfp* (constitutive)	Hochstrasser et al. (2019)
pCM009	pMMB207C-P_{flaA}-*gfp* (ASV)	Schell et al. (2016b)
pNP102	pMMB207C, Δ*lacI*^{q}, *mcherry* (constitutive)	Steiner et al. (2017)
pNT28	pMMB207C, *gfp* (constitutive)	Tiaden et al. (2007)
pNT31	pMMB207C-P_{lqsS}-*lqsS*, *gfp* (constitutive)	Tiaden et al. (2010b)

pRH022	pMMB207C-P_{lvbR}-*lvbR*-P_{flaA}-*gfp* (ASV)	This study
pRH031	pMMB207C-P_{csrA}-*gfp* (ASV), Cm	This study
pRH032	pMMB207C-P_{ralF}-*gfp* (ASV), Cm	Striednig et al. (2021)
pRH035	pMMB207C-P_{sidC}-*gfp* (ASV), Cm	Striednig et al. (2021)
pRH046	pMMB207C-P_{csrA}-*gfp* (AAV), *mcherry* (constitutive), Cm	This study
pRH047	pMMB207C-P_{ralF}-*gfp* (AAV), *mcherry* (constitutive), Cm	This study
pRH049	pMMB207C-P_{6SRNA}-*gfp* (ASV), Cm	This study
pRH050	pMMB207C-P_{sidC}-*gfp* (AAV), *mcherry* (constitutive), Cm	This study
pSB001	pMMB207C-P_{flaA}-*flaA*, *gfp* (constitutive)	This study
pSN7	pMMB207C-P_{flaA}-*gfp* (AAV), *mcherry* (constitutive), Cm	Personnic et al. (2019)
pSN25	pMMB207C-$P_{6S\ RNA}$-*gfp* (AAV), *mcherry* (constitutive), Cm	Personnic et al. (2021)

[a] Abbreviations: Cm, chloramphenicol resistance; Km, kanamycin resistance; Gm, gentamicin resistance.

Bacterial motility was assessed basically as described (Schell et al., 2016b). Briefly, *L. pneumophila* JR32 or the Δ*lvbR* or Δ*lqsR* mutant strains were grown for 3 days on CYE/Cm agar plates. Liquid cultures were inoculated in AYE medium at an OD_{600} of 0.1 and grown for 21 h at 37 °C. After 21 h, bacterial cultures were diluted to an OD_{600} of 0.15, and 700 µl were filled into ibidi-microscopy dishes. Bacteria were tracked for 90 with 1.298 s intervals using a Leica SP8 confocal microscope (63× oil objective). Bacterial motility was visualized using the ImageJ software. The movies S1–S3 are representative of two independent experiments.

Acanthamoeba castellanii (ATCC 30234, lab collection) was cultured in PYG medium (Moffat and Tompkins, 1992; Segal and Shuman, 1999) at 23 °C using proteose from Becton Dickinson Biosciences and yeast extract from Difco.

2.5.2 Molecular cloning

Plasmids used in this study are listed in Table 2.2. DNA cloning was carried out according to standard protocols, plasmids were isolated using commercially available kits (Qiagen, Macherey-Nagel), and DNA fragments were amplified using the primers listed in Table S2.1. All the constructs were verified by DNA sequencing. The complementation plasmids pRH022 (P_{lvbR}-*lvbR*) and pSB001 (P_{flaA}-*flaA*) were generated

by amplifying the corresponding gene with its putative natural promoter region using the primer pair oRH040/oRH041 or oRH174/oRH175 and pAK18 or genomic JR32 DNA as template. The NEBuilder HiFi DNA Assembly reaction was used to clone the PCR product into BspQI-digested pCM009 (Schell et al., 2016b) resulting in pRH022 or into BamHI-digested pNT31 (Tiaden et al., 2010b) thereby replacing P_{lqsS}-*lqsS* and resulting in pSB001.

Single reporter constructs pRH031, and pRH049 containing a transcriptional fusion P_{csrA}-*gfp*(ASV), or P_{6SRNA}-*gfp*(ASV) were generated by PCR amplification of the putative promoter regions from genomic JR32 DNA using the primer pair oRH128/oRH129, or oRH215/oRH216. The putative promoter regions were defined as the upstream region of the corresponding genes with the following sizes: P_{csrA} (515 bp, *lpg0781*) and P_{6SRNA} (534 bp, *ssrS*, between *lpg0877* and *lpg0876*). The PCR products were cloned into SacI- and XbaI-digested pCM009 (Schell et al., 2016b) using the NEBuilder HiFi DNA Assembly reaction, thereby replacing P_{flaA}.

For construction of the dual reporter constructs pRH046, pRH047 and pRH050 harbouring P_{csrA}-*gfp*(AAV), P_{ralF}-*gfp*(AAV) or P_{sidC}-*gfp*(AAV), the putative promoter regions were amplified by PCR with the primer pairs oRH182/oRH210, oRH180/oRH211 or oRH217/oRH218 and pRH031, pRH032 or pRH035 as template. The putative promoter regions were defined as the upstream region of the corresponding genes with the following sizes: P_{ralF} (515 bp, *lpg1950*) and P_{sidC} (507 bp, *lpg2511*). The resulting PCR products were inserted into BamHI- and BglII-digested pSN7 (Personnic et al., 2019) using the NEBuilder HiFi DNA Assembly reaction, thereby exchanging P_{flaA}.

2.5.3 Kinetics of GFP reporter constructs

Legionella pneumophila strains (Table 2.2) harbouring GFP reporter constructs (single reporters: pCM009, pRH022, pRH031, pRH032, pRH035, pRH049, or dual reporters: pRH046, pRH047, pSN7, pSN25) were grown on CYE/Cm agar plates for 3 days, followed by cultivation in AYE/Cm medium at 37 °C on a rotating wheel (80 rpm) for approximately 18 h. The strains were diluted in AYE/Cm medium to an initial OD_{600} of 0.2, and 100 µl was distributed in triplicates into wells of a black clear bottom 96-well plate (polystyrene, 353219, Falcon). The plate was incubated at 25 °C or 37 °C while orbitally shaking, and GFP fluorescence (excitation, 485 nm; emission, 528 nm; gain, 50 or 100) as well as OD_{600} (bacterial growth) were measured over time using a microplate reader (Synergy H1 or Cytation5 Hybrid Multi-Mode Reader, BioTek). A blank value (AYE medium) was subtracted from all values, and numbers are expressed as relative fluorescence units (RFU), OD_{600} or RFU/OD_{600} quotient.

2.5.4 *Legionella pneumophila* biofilm formation

For analysis of biofilm architecture or *Legionella*–amoeba interactions, *L. pneumophila* biofilms were prepared, monitored and analysed as described (Hochstrasser and Hilbi, 2019). Briefly, *L. pneumophila* strains harbouring pNT28, pNP102 or single/dual reporter constructs (Table 2.2) were grown for 3 days at 37 °C on CYE agar plates supplemented with Cm (5 µg ml^{-1}) and subsequently cultivated in AYE/Cm medium on a rotating wheel (80 rpm) at 37 °C for approximately 17–18 h. The

exponential phase bacteria were inoculated at an optical density (OD_{600}) of 0.3 in 2 ml AYE/Cm medium placed into ibiTreat microscopy dishes (ibidi), incubated at 25 °C for the time indicated while avoiding any mechanical disturbance, and optionally stained with DAPI (1 µg ml^{-1}). The biofilm architecture was monitored by confocal fluorescence microscopy (Leica TCS SP5, 63× oil objective) by acquiring images at the dish bottom (0 µm, attachment layer) or at a level of 4 µm above the dish bottom. For competition assays, biofilms were generated analogously with an inoculation OD_{600} of 0.15 for each strain (start ratio of 1:1) using *L. pneumophila* JR32 harbouring pNP102 (mCherry) and mutant strains harbouring pNT28 (GFP).

To quantify biofilm formation, *L. pneumophila* strains harbouring pNT28 were left to form biofilms at 25 °C for 6 days as described above. The biofilms were re-suspended by excessive pipetting until the bottom of the dish appeared clear. The suspension was transferred into a falcon tube, excessively vortexed (to avoid that the bacteria stick together), and the OD_{600} was determined (usually 3.3–4.1). Subsequently, the suspension was diluted 1:100 (beads: bacteria) with a microsphere standards suspension (Bacteria counting kit, Invitrogen). The biofilm mass (bacteria ml^{-1}) was quantified using a Fortessa II flow cytometer and Diva software. Bacteria and microsphere standard were determined by employing a forward (FSC, 650 V) and sideward scatter (SSC, 230 V), with a threshold of 200 each. Additionally, GFP production (Blue 530_30, 350 V) was examined to identify *L. pneumophila*. 100000 events of each resuspended biofilm were recorded. Immediately before measuring, samples were strongly vortexed for 8 s. The data were analysed with the software FlowJo. The gating protocol was as follows: The beads were identified using a control sample (AYE/Cm without bacteria) that was supplemented with beads as a reference (gate 1, FSC vs. SSC). The number of events counted in the microsphere gate provides an accurate estimate of the volume analysed. The *L. pneumophila* populations were determined in pseudocolour graphs (gate 2, GFP vs. FSC) using a resuspended biofilm sample (of parental strain JR32) without beads as a reference. Bacterial density in the biofilm was determined from the ratio of *L. pneumophila* (gate 2) to beads (gate 1).

2.5.5 *Legionella*-amoeba interactions

For confocal fluorescence microscopy, *A. castellanii* amoebae were detached after 2–3 days of growth and diluted in fresh PYG medium to a density of 1.5×10^5 cells ml^{-1}. 1 ml of amoebae suspension was carefully added to preformed *L. pneumophila* biofilms grown for 6 days (as described above) resulting in a final amoebae concentration of 5×10^4 cells ml^{-1} in the dish. The dish was incubated for approximately 3 h (images) or 15 min (time-lapse stacks) at 25 °C to allow the amoebae to settle toward the bottom of the dish. *Legionella*–amoeba interactions were visualized by confocal fluorescence microscopy (Leica TCS SP5, 63× oil objective) by acquiring images or time-lapse stacks and 3D images or movies were generated using the program ImageJ. For further analysis of amoeba migration, single-cell tracking was manually performed in the bright field channel using time-lapse stacks and the program ImageJ. Time series of ca. 10 amoebae localizing above the dish bottom were recorded for the same time (25 or 30 min). Only viable, irregularly shaped amoebae were considered (rounded and clustered amoebae were ignored, except in the case of the Δ*icmT* mutant strain, which caused a larger portion of the amoebae to round up). The ibidi

program ‘Chemotaxis and Migration Tool’ was used to generate migration plots and to quantify the amoeba velocity (Hochstrasser and Hilbi, 2019).

The total number of amoebae and the number of amoebae with a bacterial cluster (or cluster-positive amoebae) were counted manually from the microscopy images of *L. pneumophila* strains harbouring pNT28 (constitutive production of GFP). The percentage of cluster-positive amoebae was assessed for each of three independent biological experiments. Subsequently, for each cluster-positive amoebae, the cluster size was quantified with ImageJ (Version 1.53f51). In brief, a detection mask was created for each microscopy image with its GFP channel (‘Image’ > ‘Adjust’ > ‘Threshold: 100–255’). Then the size of all clusters in the image was analysed using ‘Analyse particle’ function (‘Analyse’ > ‘Analyse particle’ > ‘Size 10 micron – Infinity’). The size of clusters was quantified for *L. pneumophila* strains harbouring pNT28 (constitutive production of GFP) in three independent biological experiments.

For flow cytometry, *A. castellanii* amoebae were added to preformed biofilms grown for 6 days at 25 °C as described above, optionally stained with DAPI (1 µg ml^{-1}) and incubated for approximately 2–3 h at 25 °C. Biofilms were harvested by resuspending the bacteria and amoebae, followed by centrifugation for 10 min at 100 *g* (biofilms including amoebae), or for 5 min at 4400 rpm (control biofilms without amoebae). Samples were fixed with 300 µl 4% PFA in PBS for approximately 30 min at RT, washed once in 300 µl PBS and resuspended in 150 µl PBS for flow cytometry analysis.

The size of GFP-positive *L. pneumophila* clusters on *A. castellanii* in bacterial biofilms was quantified by flow cytometry as amoeba-associated fluorescence using a Fortessa II flow cytometer (BD LSR II Fortessa) and Diva software. Different populations were identified employing a forward (FSC, 430 V) and sideward scatter (SSC, 270 V) gating, with a threshold of 200 each, and 10000 events per sample were recorded. Furthermore, the populations were examined for GFP production [Blue 530_30, 350 V (gating protocol #1) or 400 V (gating protocol #2)]. The data were analysed with the software FlowJo. The gating protocol #1 for strains containing plasmid pNT28 was as follows: amoebae populations were identified using an amoeba only sample as a reference (gate 1). Cluster formation was visualized by a GFP-shift of the amoebae population visible in pseudocolour graphs (including the *L. pneumophila* population) and histograms (not including the *L. pneumophila* population, gate 1). The gating protocol #2 for strains containing promoter expression constructs was as follows: amoebae/*L. pneumophila* populations were identified using amoebae/*L. pneumophila* only samples as a reference (gates 1 and 2). The GFP signal of the two populations was visualized together in a histogram (gate 1 and 2) and in pseudocolour graphs (no gating).

2.5.6 Comparative proteomics

Biofilms of *L. pneumophila* JR32, Δ*lvbR* and Δ*lqsR* were initiated as described above and incubated for 6 days at 25 °C. The biofilms were harvested by resuspending the bacteria, followed by centrifugation (5 min, 12850 *g*, 4 °C) and resulting supernatants (designated ‘s’, extracellular) and cell pellets (designated ‘p’, intracellular) were analysed separately.

For extracellular sample preparation, proteins in 1 ml of supernatant were enriched using StrataClean beads and eluted by the use of a 1D-SDS gel according to the established protocol for GeLC-MS samples (Bonn et al., 2014). Cell pellets (intracellular samples) were resuspended in TE-buffer pH 7.4 (50 mM Tris, 10 mM EDTA) and disrupted by bead beating. After centrifugation the protein concentration was determined using the Bradford assay and 20 µg protein was in solution digested (Maass et al., 2011) and purified using C_{18}-Stage tips (Thermo Fisher Scientific). Extracellular proteins (with three biological replicates for every sample) and intracellular proteins (with three biological replicates and three technical replicates each for every sample) were analysed with a QExactive-Mass spectrometer. Peptide samples were injected with the same volume to allow label-free relative protein quantification between biological samples.

To process the data, *.raw files were searched against the database using MaxQuant (1.6.0.16). The database for *L. pneumophila* Philadelphia-1 was downloaded from Uniprot on March 17th, 2017 and supplemented with the LvbR sequence and common laboratory contaminations resulting in 2973 entries. The results were filtered using 1% FDR in MaxQuant and at least two unique peptides were necessary for protein identification (filtered in Perseus vs. 1.5.3.0). For quantification the protein had to be detected in at least two replicates of one sample. Log2-transformed LFQ-values as proxy for protein abundance were exported and used for statistical analysis in TMEV. Only proteins with a minimal $\log_2$-fold change of −0.8 or 0.8 compared to JR32 were considered. In cases, where proteins were detected in Δ*lvbR* or Δ*lqsR* but not in JR32 biofilms (‘on’), or where proteins were detected in JR32 but not in Δ*lvbR* or Δ*lqsR* biofilms (‘off’), the maximum values of $2^{7.4}$ and 2^{-5} were used as ratios and coloured dark blue or dark red in the heat map (**Fig. S2.1**) respectively.

2.6 Acknowledgments

The work in the group of H.H. was supported by the Swiss National Science Foundation (SNF; 31003A_175557, 310030_200706), the Novartis Foundation for Medical-Biological Research (21C165). The work in the group of D.B. was supported by the Federal Ministry of Education and Research (BMBF; grant 031A410B). Open Access Funding provided by Universitat Zurich.

2.7 Supporting Information

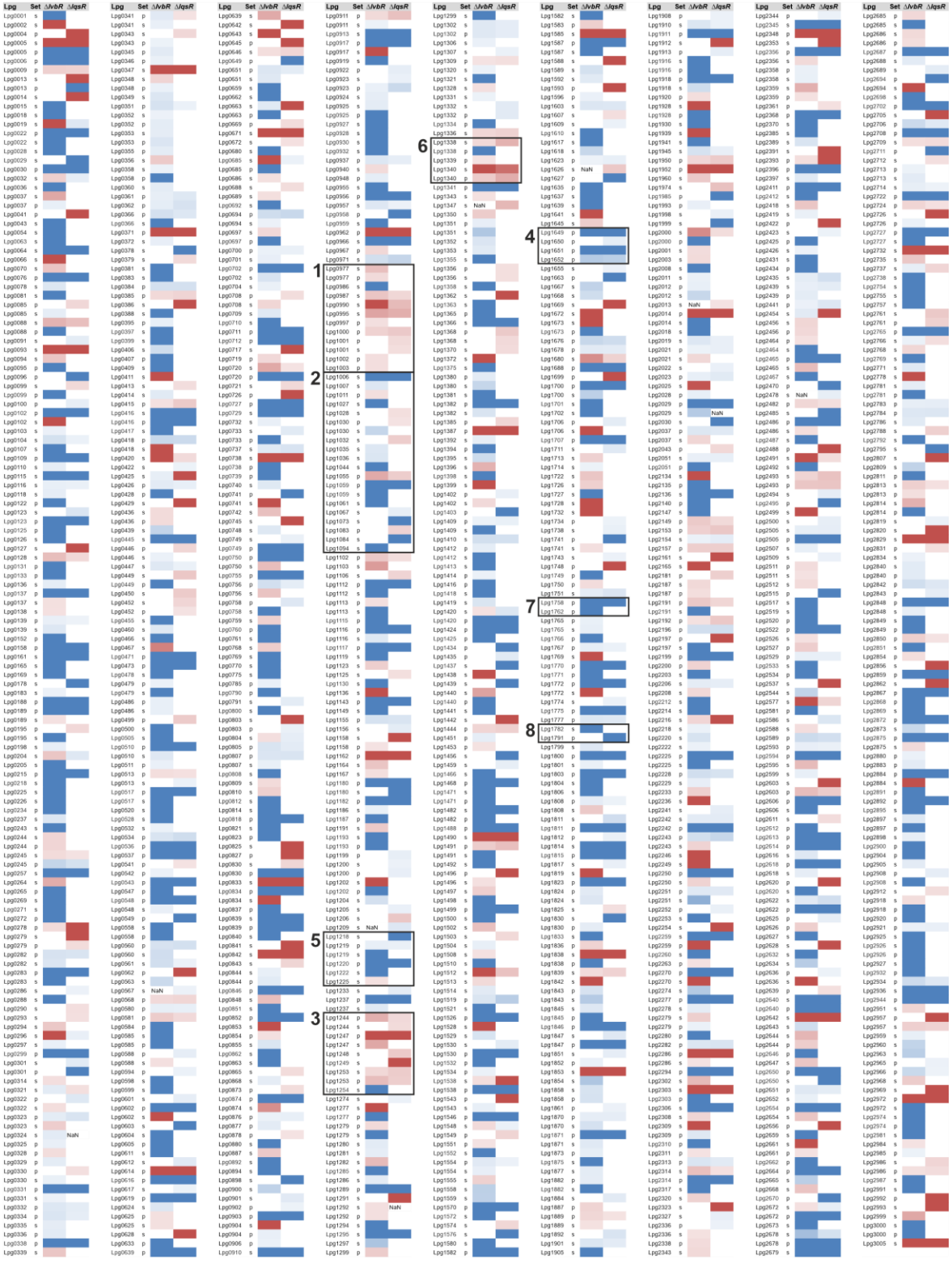

Patterns (boxes):

1 - 133kb genomic region I (Lpg0973-Lpg1005)

2 - 133kb genomic region II (Lpg1006-Lpg1096)

3 - Lvh T4SS/Lvr proteins

4 - Inositol catabolism

5-8 - Flagellum/motility

Figure S2.1 (overleaf). Heat map of proteins depleted or enriched in Δ*lvbR* and Δ*lqsR* biofilms compared to JR32.

Comparative proteomics was performed with biofilms formed by *L. pneumophila* JR32, Δ*lvbR* or Δ*lqsR*. In the heat map all proteins are shown that are depleted or enriched in mutant biofilms (for details see Materials and Methods). Biofilm bacteria were harvested by centrifugation and supernatants (designated 's', extracellular) and cell pellets (designated 'p', intracellular) were analysed separately. The proteins are listed by ascending Lpg numbers. The colour code indicates the level of regulation: the darker the colour the stronger the corresponding gene is regulated (red: depleted proteins, max. 2^{-5}; blue: accumulated proteins, max. $2^{7.4}$). Boxes highlight regions of interest, which are further discussed. 'NaN': not a number.

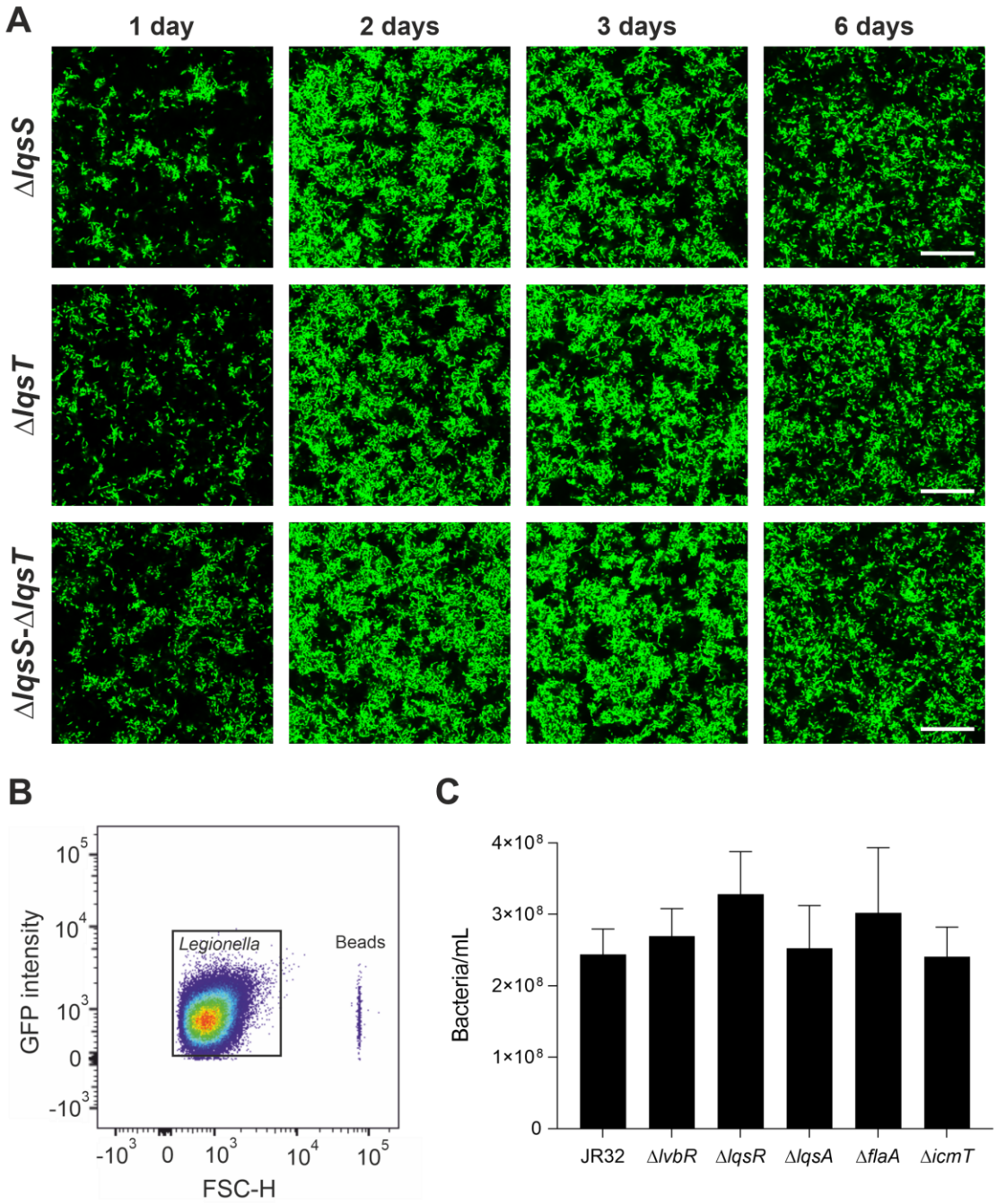

Figure S2.2 (overleaf). Biofilm formation and quantification of *L. pneumophila* strains.
(**A**) Biofilms were initiated with exponential phase *L. pneumophila* Δ*lqsS*, Δ*lqsT* or Δ*lqsS*-Δ*lqsT* mutant strains harbouring pNT28 (constitutive production of GFP) in AYE medium within ibiTreat microscopy dishes. Biofilms were grown at 25 °C without mechanical disturbance and confocal microscopy images of biofilm architecture were acquired at 4 µm above dish bottom after 1, 2, 3 and 6 days of growth. The images shown are representative of at least two independent experiments. Scale bars, 30 µm. (**B**, **C**) Quantification of *L. pneumophila* biofilms grown for 6 days. (**B**) Pseudocolour graph (GFP intensity vs. FSC) depicting the gate for GFP-producing *L. pneumophila* (identified by fluorescence) and the beads population (identified by SSC vs. FSC). (**C**) Means and standard deviation (bacteria/ml) of biological triplicates from 100′000 events of each biofilm suspension (differences between wild-type and mutant *L. pneumophila* are statistically not significant).

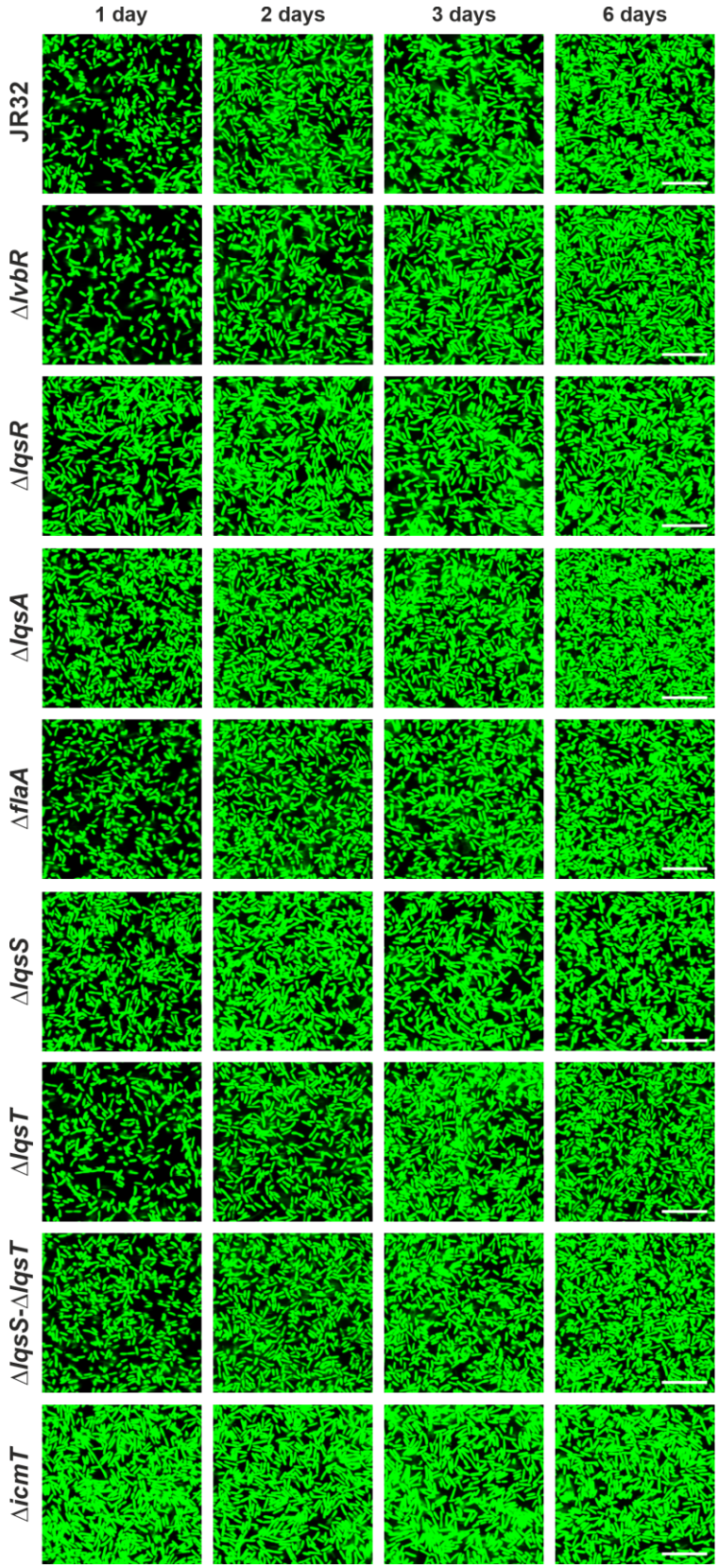
1 day
2 days
3 days
6 days
JR32
ΔlvbR
ΔlqsR
ΔlqsA
ΔflaA
ΔlqsS
ΔlqsT
ΔlqsS-ΔlqsT
ΔicmT

Figure S2.3 (overleaf). Surface adherence of biofilms formed by *L. pneumophila* JR32 and mutant strains.

Biofilms were initiated with exponential phase *L. pneumophila* JR32, Δ*lvbR*, Δ*lqsR*, Δ*lqsA*, Δ*lqsS*, Δ*lqsT*, Δ*lqsS*-Δ*lqsT*, Δ*flaA* or Δ*icmT* mutant strains harbouring pNT28 (constitutive production of GFP) in AYE medium within ibiTreat microscopy dishes. Biofilms were grown at 25 °C without mechanical disturbance and confocal microcopy images of biofilm attachments were acquired at the dish bottom (0 µm) after 1, 2, 3 and 6 days of growth. The images shown are representative of at least two independent experiments. Scale bars, 10 µm.

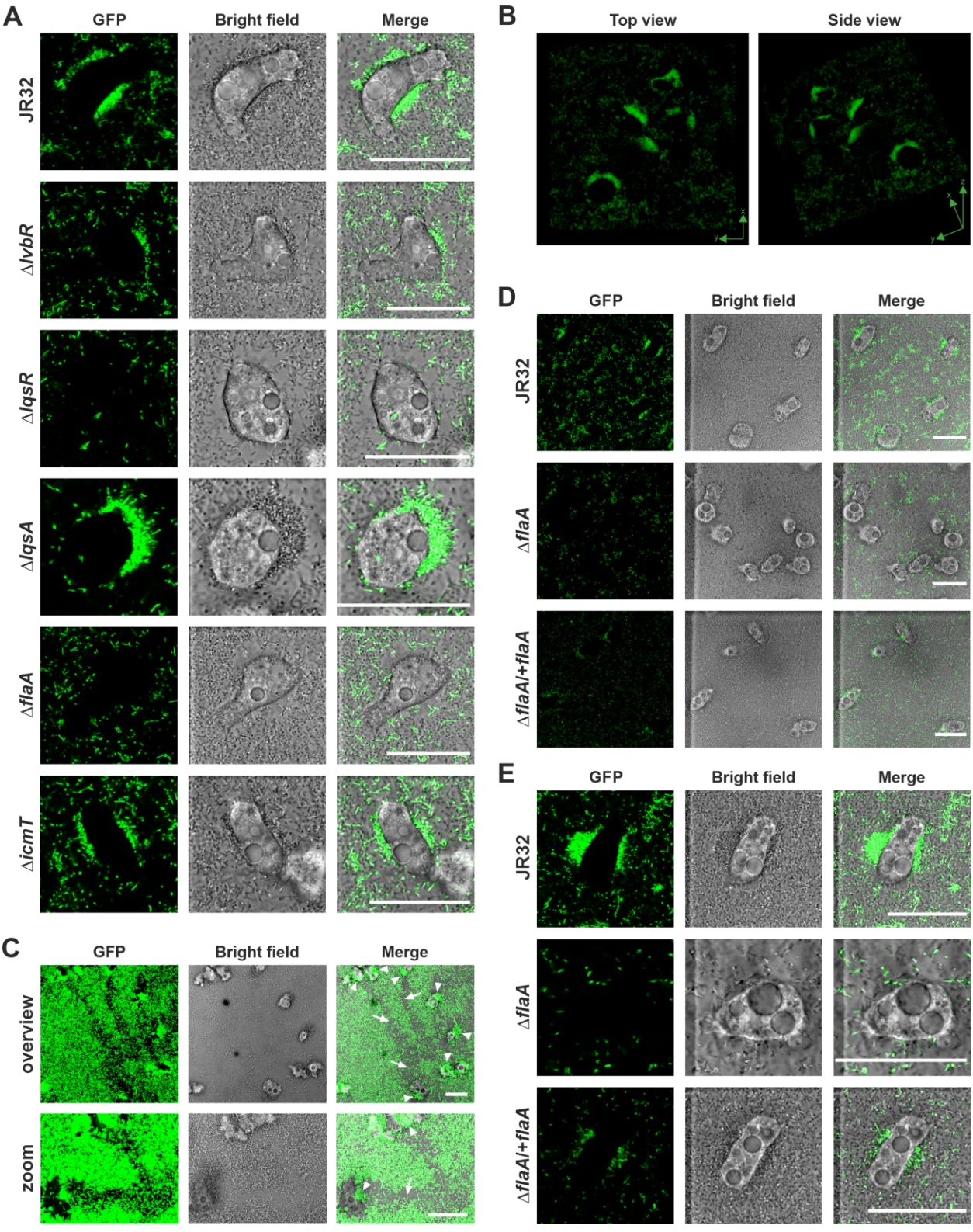
A
GFP
Bright field
Merge
JR32
ΔlvbR
ΔlqsR
ΔlqsA
ΔflaA
ΔicmT
B
Top view
Side view
C
GFP
Bright field
Merge
overview
zoom
D
GFP
Bright field
Merge
JR32
ΔflaA
ΔflaA/+flaA
E
GFP
Bright field
Merge
JR32
ΔflaA
ΔflaA/+flaA

Figure S2.4 (overleaf). *L. pneumophila* cluster formation on *A. castellanii* in JR32 or mutant strain biofilms.

Biofilms of (**A**) *L. pneumophila* JR32, Δ*lvbR*, Δ*lqsR*, Δ*lqsA*, Δ*flaA* or Δ*icmT* mutant strains harbouring pNT28 (constitutive production of GFP), or (**B**, **C**) strain JR32 harbouring pNT28 were grown for 6 days in AYE medium at 25 °C, and *A. castellanii* was added to preformed biofilms. Bacterial adherence and cluster formation were monitored by confocal microscopy (**A, B**) ca. 4 µm above or (**C**) at the dish bottom ("clusters": arrow heads, "trails": arrows). (**D**, **E**) Biofilms of *L. pneumophila* JR32 or Δ*flaA* mutant strains constitutively producing GFP (pNT28) or GFP and FlaA under control of its promoter (Δ*flaA*/+*flaA*, pSB001) were grown for 6 days in AYE medium at 25 °C, and *A. castellanii* was added to preformed biofilms. Confocal microscopy images of (**D**) overview and (**E**) zoom-in of *L. pneumophila* adherence and cluster formation on amoebae. The images shown are representative of three independent experiments. Scale bars, 30 µm.

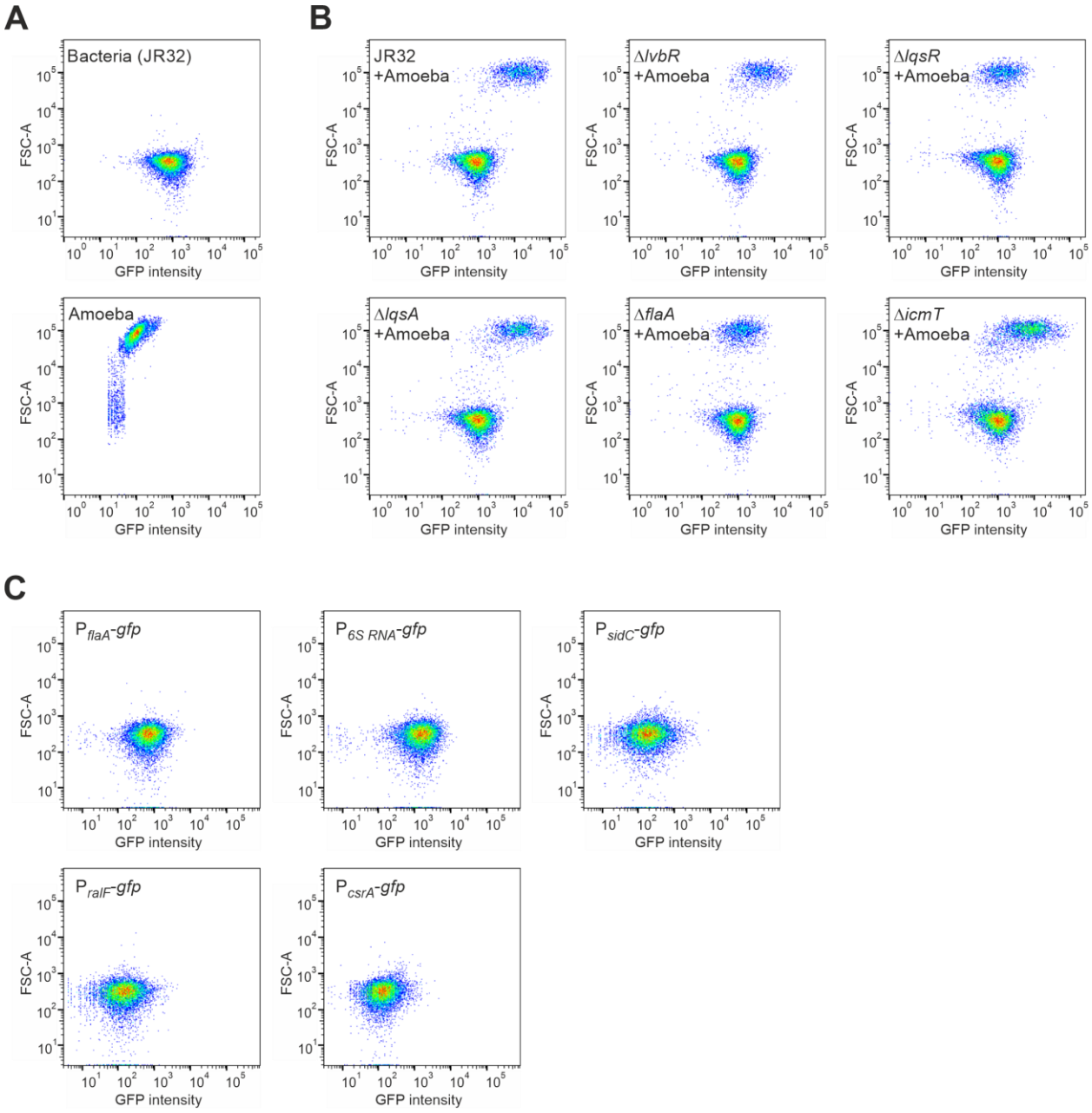

Figure S2.5. Quantification of amoeba-associated *L. pneumophila* clusters by flow cytometry. Quantification by flow cytometry (forward scatter area, FSC-A, vs. fluorescence intensity) using FlowJo software of (**A**) *L. pneumophila* strain JR32 or *A. castellanii*, (**B**) amoebae-associated or non-associated, GFP-positive *L. pneumophila* JR32, Δ*lvbR*, Δ*lqsR*, Δ*lqsA*, Δ*flaA* or Δ*icmT* harbouring pNT28 (protocol #1, see Material and Methods), or (**C**) non-associated, GFP-positive *L. pneumophila* JR32 harbouring promoter expression reporters (P_{flaA}, P_{6SRNA}, P_{sidC}, P_{ralF}, or P_{csrA}) (protocol #2, see Material and Methods).

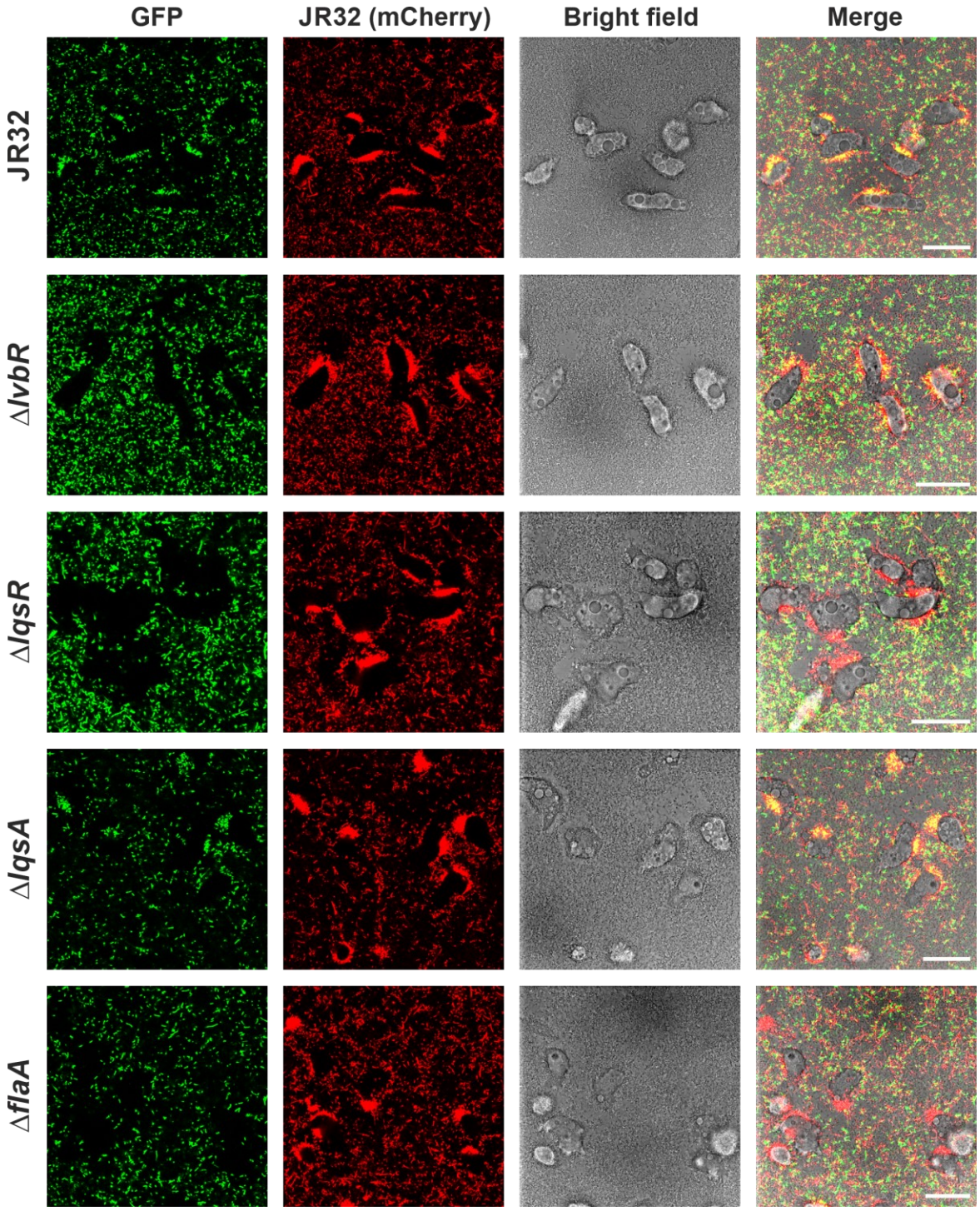

Figure S2.6. Competition of mCherry-producing *L. pneumophila* JR32 and GFP-producing mutants for cluster formation on amoebae.

Biofilm formation was initiated with a 1:1 ratio of exponential phase mCherry-producing L. pneumophila JR32 (pNP102) and GFP-producing JR32 or mutant strains (pNT28). Biofilms were grown in AYE medium within ibiTreat microscopy dishes at 25 °C for 6 days. A. castellanii were added to preformed biofilms, and amoebae with adherent bacterial clusters were monitored by confocal microcopy above dish bottom. The images shown are representative of at least two independent experiments. Scale bars, 30 µm.

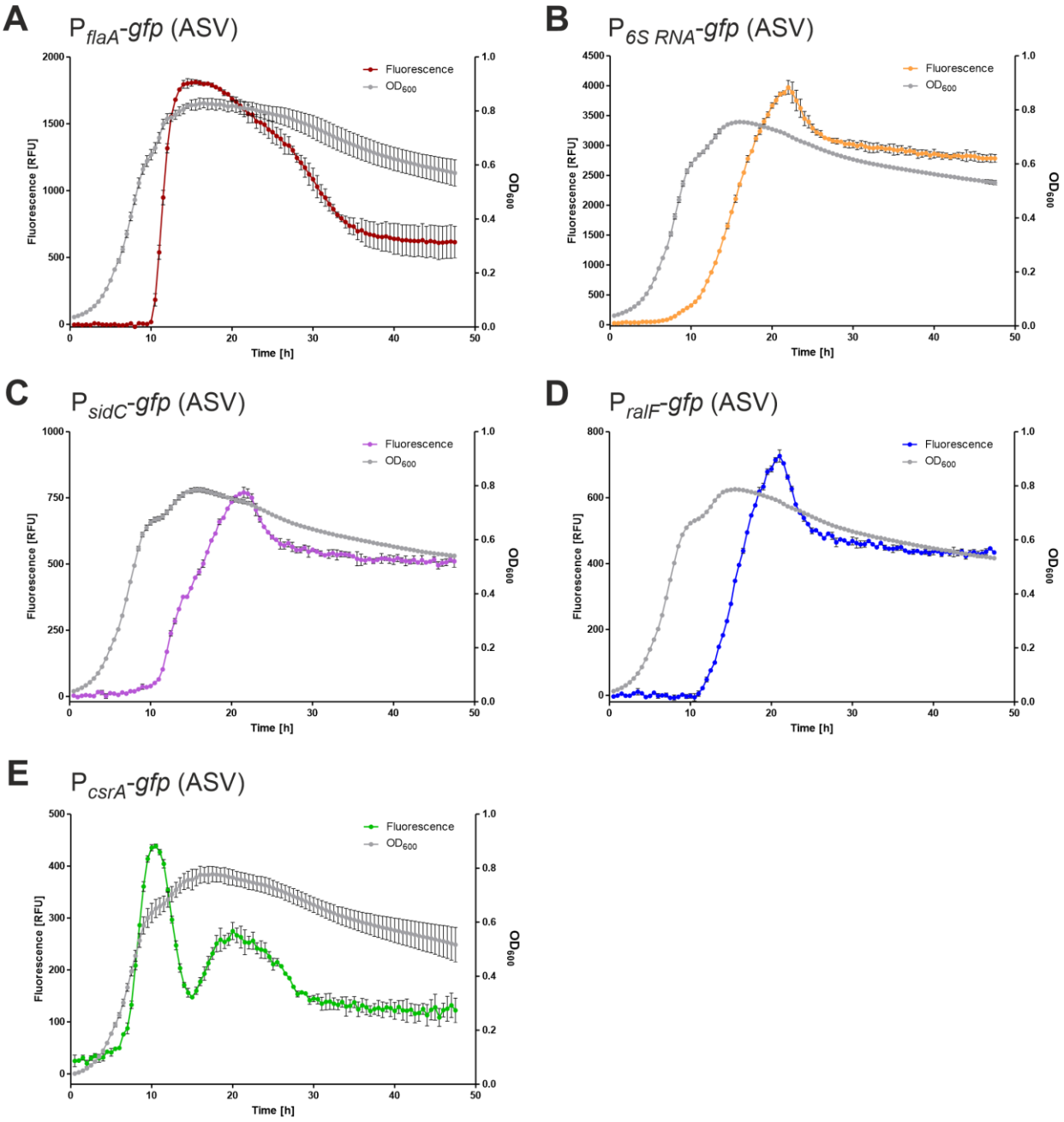

Figure S2.7. Gene expression kinetics of *L. pneumophila* JR32 in AYE medium using single promoter reporters.

L. pneumophila JR32 harbouring (**A**) P_{flaA}-*gfp* (pCM009), (**B**) P_{6SRNA}-*gfp* (pRH049), (**C**) P_{sidC}-*gfp* (pRH035), (**D**) P_{ralF}-*gfp* (pRH032) or (**E**) P_{csrA}-*gfp* (pRH031) reporter constructs were grown at 37 °C in AYE medium in microplates while orbitally shaking. GFP fluorescence (relative fluorescence units, RFU) at a gain of 50 and optical density at 600 nm (OD_{600}) were monitored over time using a microplate reader. The kinetics of the GFP fluorescence or OD_{600} values are shown and depicted by the left or right y-axis respectively. The data are means and standard deviations of technical triplicates and representative of three independent measurements.

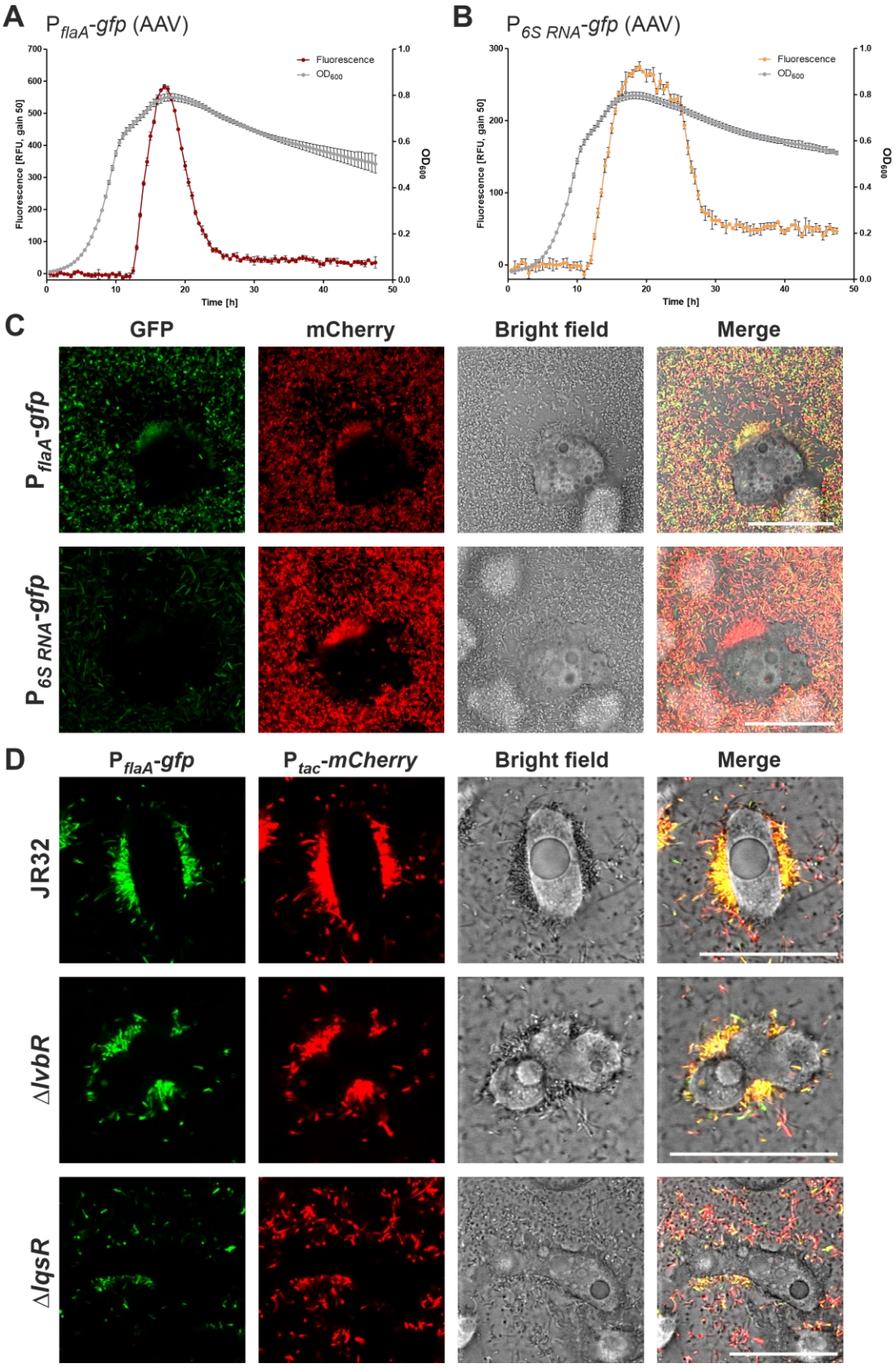
A
P flaA-gfp (AAV)
Fluorescence
OD600
Fluorescence [RFU, gain 50]
OD600
Time [h]
B
P 6S RNA-gfp (AAV)
Fluorescence
OD600
Fluorescence [RFU, gain 50]
OD600
Time [h]
C
GFP
mCherry
Bright field
Merge
P flaA-gfp
P 6S RNA-gfp
D
P flaA-gfp
P tac-mCherry
Bright field
Merge
JR32
ΔlvbR
ΔlqsR

Figure S2.8 (overleaf). Gene expression kinetics of *L. pneumophila* JR32 in AYE medium and in amoeba-adherent bacteria in biofilms using dual promoter reporters.
L. pneumophila JR32 harbouring (**A**) P_{flaA}-*gfp* (pSN7) or (**B**) P_{6SRNA}-*gfp* (pSN25) reporter constructs were grown at 37 °C in AYE medium within microplates while orbitally shaking. GFP fluorescence (relative fluorescence units, RFU) at a gain of 50 and optical density at 600 nm (OD_{600}) were monitored over time using a microplate reader. The kinetics of the GFP fluorescence (left y-axis) or OD_{600} (right y-axis) values are shown. The data are means and standard deviations of technical triplicates and representative of three independent measurements. (**C**, **D**) Biofilms of *L. pneumophila* JR32, Δ*lvbR* or Δ*lqsR* harbouring dual reporter plasmids expressing P_{tac}-*mcherry* (constitutive) and P_{flaA}-*gfp* (pSN7) or P_{6SRNA}-*gfp* (pSN25) were grown in AYE medium for 6 days. *A. castellanii* was added to preformed biofilms, and confocal microcopy images of amoebae with adherent bacterial clusters were acquired close to the bottom of microscopy dishes. The images shown are representative of 2–3 independent experiments. Scale bars, 30 µm.

Table S2.1. Oligonucleotides used in this study.

Oligonucleotide	Sequence 5' - 3' [a]	Comments
oRH040	CTTCCAGATGTATGCTCTTCTTTATGAGGCTGAGTTTTTAG	P_{lvbR}-*lvbR* (re) (into *Bsp*QI-site)
oRH041	CTTGCTGGCGTTCGGGGCGTGCTGATTGGTCC	P_{lvbR}-*lvbR* (fo) (into *Bsp*QI-site)
oRH128	GGAAACAGAATTCGAGCTCGTCTGGGATTTATAAAGATAAATTGC	P_{csrA} (fo) (into *Sac*I- and *Xba*I-site)
oRH129	CATATGTATATCTCCTTCTTAAATCTAGAGACTAAAATCTCCCTAACATAGC	P_{csrA} (re) (into *Sac*I- and *Xba*I-site)
oRH174	TGATCCGTCGATCGCCCGGGGATCCCTATCGACCTAACAAAGATAATACAGATTGCG	P_{flaA}-*flaA* (fo) (into *Bam*HI-site)
oRH175	CCGCATTACGCGTCTCGAGGATCCACCAGAACATTTAACCCATAAACCTTCC	P_{flaA}-*flaA* (re) (into *Bam*HI-site)
oRH180	CCGGGCATATGATCGATGGATCCGGTATTCATCTTCCTCAAACG	P_{ralF} (fo) (into *Bam*HI- and *Bgl*II-site)
oRH182	CCGGGCATATGATCGATGGATCCGTCTGGGATTTATAAAGATAAATTGC	P_{csrA} (fo) (into *Bam*HI- and *Bgl*II-site)
oRH210	GTGAAAAGTTCTTCTCCTTTAGATCTTTTCATGACTAAAATCTCCCTAACATAGC	P_{csrA} (re) (into *Bam*HI- and *Bgl*II-site)
oRH211	GTGAAAAGTTCTTCTCCTTTAGATCTTTTCATAATCTGCTCCTTTAGTCTGAG	P_{ralF} (re) (into *Bam*HI- and *Bgl*II-site)

oRH215	GGAAACAGAATTCGAGCTCCATGGCCTGGCTCCTCTC	P_{6SRNA} (fo) (into *Sac*I- and *Xba*I-site)
oRH216	CATATGTATATCTCCTTCTTAAATCTAGACTGGCCTCCAAAATTGTACTGTTG	P_{6SRNA} (re) (into *Sac*I- and *Xba*I-site)
oRH217	CCGGGCATATGATCGATGGATCCCGGGAACTCAATAAATCAAC	P_{sidC} (fo) (into *Bam*HI- and *Bgl*II-site)
oRH218	GTGAAAAGTTCTTCTCCTTTAGATCTTTTCATTTTCTAGTGTCTTGTTTATAAG	P_{sidC} (re) (into *Bam*HI- and *Bgl*II-site)

[a] Regions overlapping with destination vector are underlined.

Movie S2.1. Motility of *L. pneumophila* JR32.
Movie S2.2. Motility of *L. pneumophila* Δ*lvbR.*
Movie S2.3. Motility of *L. pneumophila* Δ*lqsR.*
Movie S2.4. *A. castellanii* migrating through JR32 biofilm.
Movie S2.5. *A. castellanii* migrating through Δ*lvbR* biofilm.
Movie S2.6. *A. castellanii* migrating through Δ*lqsR* biofilm.
Movie S2.7. *A. castellanii* migrating through Δ*lqsA* biofilm.
Movie S2.8. *A. castellanii* migrating through Δ*flaA* biofilm.
Movie S2.9. *A. castellanii* migrating through Δ*icmT* biofilm.
Movies available online along with the published paper.

2.8 Own contributions

SM analyzed promotor expression using a microplate reader (Fig. 2.2B), SM assessed *L. pneumophila* cluster formation on *A. castellanii* by flow cytometry (Fig. 2.6D, Fig. S2.5AB), SM analyzed promotor expression within bacterial clusters by flow cytometry (2.7BC, Fig. S2.5C), SM quantified *L. pneumophila* biofilm formation by flow cytometry (Fig. S2BC). SM visualized motility of *L. pneumophila* strains by fluorescence microscopy (Movies available online along with the published paper). SM prepared the corresponding Figures and contributed to writing the manuscript.

3. Chapter three – Nitric oxide signaling through three receptors regulates virulence, biofilm formation, and phenotypic heterogeneity of *Legionella pneumophila*

Nitric oxide signaling through three receptors regulates virulence, biofilm formation, and phenotypic heterogeneity of *Legionella pneumophila*

Sarah Michaelis[1], Tong Chen[1], Camille Schmid[1] and Hubert Hilbi[1*]
[1]Institute of Medical Microbiology, University of Zürich, Gloriastrasse 30, 8006 Zürich, Switzerland.

Running title: NO signaling in *Legionella*

Key words: Amoeba, Acanthamoeba, biofilm, cell-cell communication, flagellum, host-pathogen interaction, inter-kingdom signaling, intracellular replication, Legionella, macrophage, microcolony, nitric oxide, phenotypic heterogeneity, quorum sensing, timer.

Abbreviations: c-di-GMP, cyclic di-guanosine monophosphate; DKO/TKO, double/triple knockout; DPTA (dipropylenetriamine) NONOate, (Z)-1-[N-(3-aminopropyl)-N-(3-ammoniopropyl)amino]diazen-1-ium-1,2-diolate; GFP, green fluorescent protein; Hnox1, haem-nitric oxide/oxygen binding domain; Icm/Dot, intracellular multiplication/defective organelle trafficking; LAI-1, Legionella autoinducer-1; LCV, Legionella-containing vacuole; Lqs, Legionella quorum sensing; LvbR, Legionella virulence and biofilm regulator; NO, nitric oxide; NosP, NO sensing protein; SNP, sodium nitroprusside; T4SS, type IV secretion system.

*Correspondence: E-mail hilbi@imm.uzh.ch

Article published in: *Mbio* (2024): e00710-24

3.1 Abstract

The causative agent of Legionnaires' disease, *Legionella pneumophila*, is an environmental bacterium, which replicates in macrophages, parasitizes amoeba, and forms biofilms. *L. pneumophila* employs the *Legionella* quorum sensing (Lqs) system and the transcription factor LvbR to control various bacterial traits, including virulence and biofilm architecture. LvbR negatively regulates the nitric oxide (NO) receptor Hnox1, linking quorum sensing to NO signaling. Here, we assessed the response of *L. pneumophila* to NO and investigated bacterial receptors underlying this process. Chemical NO donors, such as dipropylenetriamine (DPTA) NONOate and sodium nitroprusside (SNP), delayed and reduced the expression of the promoters for flagellin (P_{flaA}) and the 6S small regulatory RNA (P_{6SRNA}). Marker-less *L. pneumophila* mutant strains lacking individual (Hnox1, Hnox2, or NosP) or all three NO receptors (triple knockout, TKO) grew like the parental strain in media. In the TKO strain, the reduction of P_{flaA} expression by DPTA NONOate was less pronounced, suggesting that the NO receptors are implicated in NO signaling. In the Δ*nosP* mutant, the *lvbR* promoter was upregulated, indicating that NosP negatively regulates LvbR. The single and triple NO receptor mutant strains were impaired for growth in phagocytes, and phenotypic heterogeneity of non-growing/growing bacteria in amoeba was regulated by the NO receptors. The single NO receptor and TKO mutant strains showed altered biofilm architecture and lack of response of biofilms to NO. In summary, we provide evidence that *L. pneumophila* regulates virulence, intracellular phenotypic heterogeneity, and biofilm formation through NO and three functionally non-redundant NO receptors, Hnox1, Hnox2, and NosP.

3.2 Importance

The highly reactive diatomic gas molecule nitric oxide (NO) is produced by eukaryotes and bacteria to promote short-range and transient signaling within and between neighboring cells. Despite its importance as an inter-kingdom and intra-bacterial signaling molecule, the bacterial response and the underlying components of the signaling pathways are poorly characterized. The environmental bacterium *Legionella pneumophila* forms biofilms and replicates in protozoan and mammalian phagocytes. *L. pneumophila* harbors three putative NO receptors, one of which crosstalks with the *Legionella* quorum sensing (Lqs)-LvbR network to regulate various bacterial traits, including virulence and biofilm architecture. In this study, we used pharmacological, genetic, and cell biological approaches to assess the response of *L. pneumophila* to NO and to demonstrate that the putative NO receptors are implicated in NO detection, bacterial replication in phagocytes, intracellular phenotypic heterogeneity, and biofilm formation.

3.3 Introduction

The causative agent of Legionnaires' disease, *Legionella pneumophila*, is an environmental bacterium, which colonizes biofilms (Abdel-Nour et al., 2013; Declerck, 2010) and replicates intracellularly in protozoa (Boamah et al., 2017; Hoffmann et al., 2014; Swart et al., 2018). Upon inhalation of *Legionella*-laden aerosols, the opportunistic pathogen reaches the lung and replicates in alveolar macrophages, thus triggering a fulminant pneumonia (Mondino et al., 2020; Newton et al., 2010). Many mechanistic aspects of

intracellular replication in protozoa and macrophages are evolutionarily conserved, and *L. pneumophila* is sophisticatedly adapted for its intracellular life (Hilbi and Buchrieser, 2022).

L. pneumophila orchestrates intracellular replication and other interactions with eukaryotic host cells through a type IV secretion system (T4SS) termed Icm/Dot (intracellular multiplication/defective organelle trafficking) (Böck et al., 2021; Ghosal et al., 2019; Kubori and Nagai, 2016). The Icm/Dot T4SS translocates the striking number of more than 300 different “effector” proteins, which manipulate a plethora of cellular processes and promote the formation of a membrane-bound, ER-associated replication compartment, the *Legionella*-containing vacuole (LCV) (Asrat et al., 2014; Finsel and Hilbi, 2015; Hubber and Roy, 2010; Lockwood et al., 2022; Personnic et al., 2016; Qiu and Luo, 2017; Steiner et al., 2018; Swart and Hilbi, 2020).

L. pneumophila inter-kingdom interactions are not only mediated by bacterial effector proteins, but also through the low molecular weight signaling molecule LAI-1 (*Legionella* autoinducer-1, 3-hydroxypentadecane-4-one), which is produced and detected by the Lqs (*Legionella* quorum sensing) system (Hochstrasser and Hilbi, 2017; Tiaden and Hilbi, 2012; Tiaden et al., 2010a) (**Fig. 3.1A**). LAI-1 and components of the Lqs system modulate the migration of *Dictyostelium discoideum* amoeba, macrophages, or epithelial cells (Simon et al., 2015), regulate the movement of *Acanthamoeba castellanii* amoeba through *L. pneumophila* biofilms (Hochstrasser et al., 2022), and promote intracellular replication of *L. pneumophila* in macrophages (Fan et al., 2023). The Lqs system also regulates many traits of *L. pneumophila*, including virulence (Hochstrasser and Hilbi, 2017; Personnic et al., 2018), motility (Schell et al., 2016b), phenotypic heterogeneity of bacterial subpopulations (Personnic et al., 2021; Personnic et al., 2019; Striednig et al., 2021), natural competence (Kessler et al., 2013), expression of a “genomic island” (Tiaden et al., 2010b), temperature-dependent cell density (Hochstrasser and Hilbi, 2022), and the switch from the replicative, non-virulent to the stationary, virulent and motile form (Hochstrasser and Hilbi, 2022; Tiaden et al., 2007).

The signaling molecule LAI-1 is produced by the pyridoxal-5′-phosphate (PLP)-dependent autoinducer synthase LqsA (Fan et al., 2023; Spirig et al., 2008; Tiaden et al., 2010b), secreted and delivered by bacterial outer membrane vesicles (Fan et al., 2023), and detected by the two orthologous *L. pneumophila* sensor histidine kinases LqsS (Schell et al., 2016b; Tiaden et al., 2010b) and LqsT (Kessler et al., 2013; Schell et al., 2016b) (**Fig. 3.1A**). Upon binding of LAI-1, LqsS and LqsT convergently relay a phosphorylation signal to the prototypic response regulator LqsR (Schell et al., 2016b; Tiaden et al., 2008; Tiaden et al., 2007). LqsR contains a canonical aspartate phosphate receiver domain, dimerizes upon sensor kinase-mediated phosphorylation, and possesses a putative nucleotide-binding output domain (Hochstrasser et al., 2020; Schell et al., 2014) (**Fig. 3.1A**).

The Lqs system is integrated into and crosstalks with other regulatory systems of *L. pneumophila*, such as sensor histidine kinase-response regulator two-component systems (Graham et al., 2023; Hochstrasser and Hilbi, 2017) and the cyclic di-guanosine monophosphate (c-di-GMP) signaling network (Hochstrasser and Hilbi, 2020) (**Fig. 3.1A**). The sensor kinase LqsS negatively regulates the pleiotropic transcription factor LvbR (*Legionella* virulence and biofilm regulator), which itself negatively regulates Hnox1 (haem-nitric

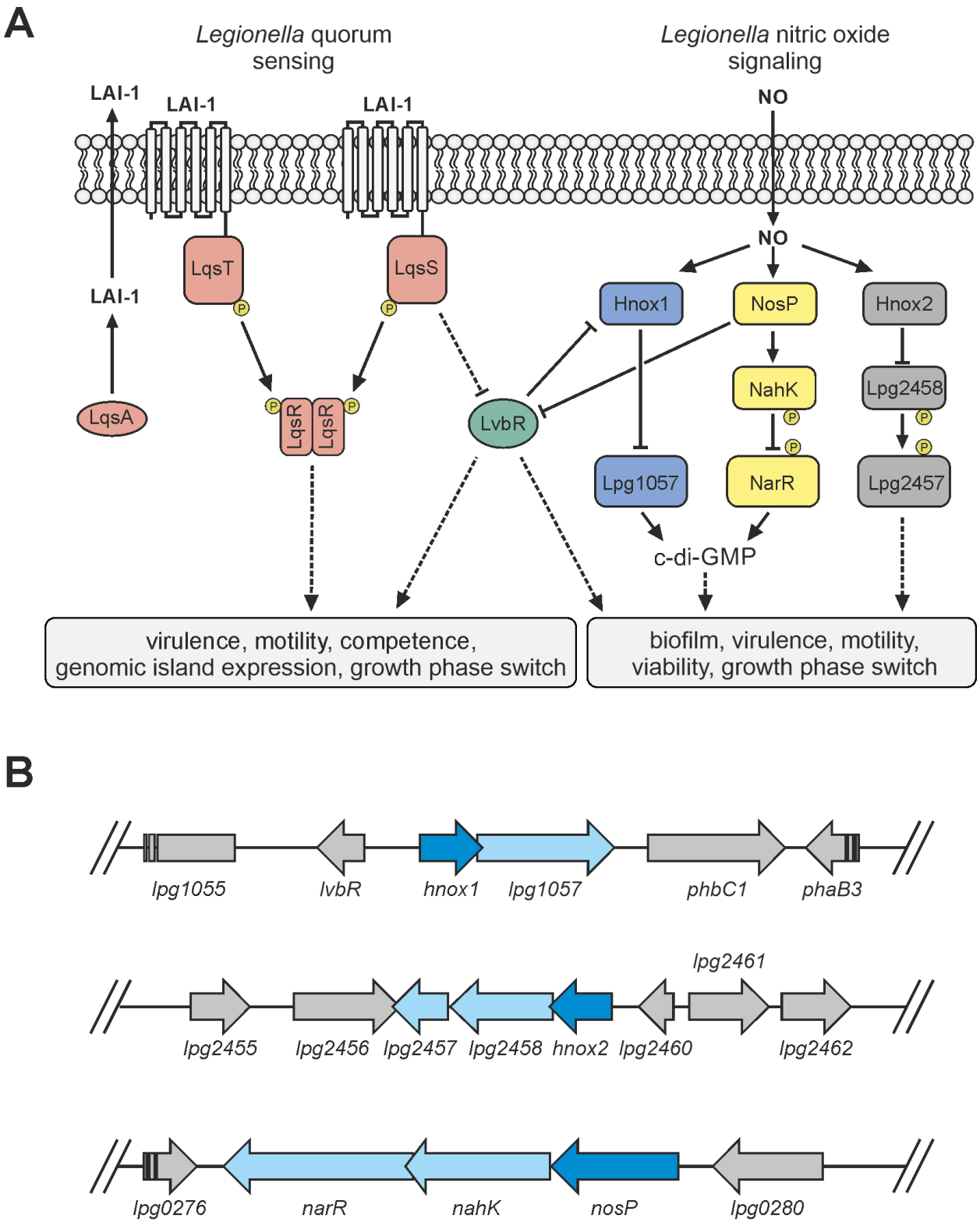
A
Legionella quorum sensing
Legionella nitric oxide signaling
LAI-1
LAI-1
LAI-1
LAI-1
NO
NO
LqsT
LqsS
LqsA
LqsR
LqsR
LvbR
Hnox1
NosP
Hnox2
NahK
Lpg2458
Lpg1057
NarR
Lpg2457
c-di-GMP
virulence, motility, competence, genomic island expression, growth phase switch
biofilm, virulence, motility, viability, growth phase switch
B
lpg1055
lvbR
hnox1
lpg1057
phbC1
phaB3
lpg2461
lpg2455
lpg2456
lpg2457
lpg2458
hnox2
lpg2460
lpg2462
lpg0276
narR
nahK
nosP
lpg0280

Figure 3.1. The *L. pneumophila* Lqs-LvbR regulatory network, NO signaling and genomic organization of NO receptors.
(**A**) The Lqs (*Legionella* quorum sensing) system produces, detects, and responds to the α-hydroxyketone compound LAI-1 (*Legionella* autoinducer-1) to regulate various traits of *L. pneumophila*. The Lqs system comprises the autoinducer synthase LqsA, the cognate membrane-bound sensor histidine kinases LqsS and LqsT, and the receiver domain-containing response regulator LqsR. The transcription factor LvbR (*Legionella* virulence and biofilm regulator) is regulated by LqsS, regulates the nitric oxide (NO) sensor Hnox1 and, through the diguanylate cyclase Lpg1057, cyclic di-guanosine monophosphate (c-di-GMP) signaling. The NO sensor NosP regulates LvbR and signals through the two-component system (TCS) NahK-NarR to regulate c-di-GMP levels. The NO sensor Hnox2 is upstream of a TCS comprising the histidine kinase Lpg2458 and the CheY-like single domain response regulator Lpg2457, the downstream signal of which is not known. (**B**) Genomic organization of the three NO receptor genes *nosP*, *hnox1*, and *hnox2*: *nosP* (*lpg0279*) forms an operon with *nahK* and *narR*, *hnox1* (*lpg1056*) with *lpg1057* (divergently transcribed from *lvbR*), and *hnox2* (*lpg2459*) with *lpg2458* and *lpg2457*, respectively.

oxide/oxygen binding domain) (Hochstrasser et al., 2019; Tiaden et al., 2010b), an inhibitor of the GGDEF/EAL domain-containing diguanylate cyclase (DGC) Lpg1057 (Carlson et al., 2010; Pecastaings et al., 2016) (**Fig. 3.1A**). Accordingly, LqsS likely promotes the production of c-di-GMP by negatively regulating a diguanylate cyclase inhibitor (Hochstrasser and Hilbi, 2020; Hochstrasser et al., 2019).

Another small molecule implicated in bacterial signaling is nitric oxide (NO). NO is a membrane-permeable diatomic gas, which is toxic at high (μM) concentrations and serves as a chemical cue for bacteria as well as for eukaryotic cells at low (nM-μM) concentrations (Arora et al., 2015; Cary et al., 2006). The Lqs system is linked to NO signaling through LqsS, LvbR, and the NO-binding protein Hnox1 (Carlson et al., 2010) (**Fig. 3.1A**). Purified Hnox1 and its homolog Hnox2 bind NO, and Hnox1 inhibits the DGC activity of purified Lpg1057 and reduces c-di-GMP production (Carlson et al., 2010). Analogously, purified NosP (NO sensing protein) binds NO, which activates autophosphorylation of the sensor kinase NahK (NosP-associated histidine kinase) and subsequent phospho-transfer to the response regulator NarR (NosP-associated response regulator) (Fischer et al., 2019) (**Fig. 3.1A**). NarR is a DGC/PDE (phosphodiesterase) bifunctional enzyme, which synthesizes and degrades c-di-GMP. Upon phosphorylation, the DGC activity is reduced, resulting in lower levels of c-di-GMP and impaired biofilm formation (Fischer et al., 2019; Hughes et al., 2019; Levet-Paulo et al., 2011; Pecastaings et al., 2016). While Hnox1 and NosP have been biochemically implicated in NO-binding and c-di-GMP signaling *in vitro*, the response of *L. pneumophila* to NO and the role of *L. pneumophila* NO sensors have been barely characterized *in vivo*.

In this study, we employ pharmacological, genetic, and cell biological approaches to determine the response of *L. pneumophila* to NO and to demonstrate that the putative NO receptors Hnox1, Hnox2, and NosP are implicated in NO detection by the pathogen, replication in phagocytes, phenotypic heterogeneity, and biofilm formation.

3.4 Results

3.4.1 Chemical NO generators regulate the *flaA* and *6SRNA* promoters in *L. pneumophila*.

The response of *L. pneumophila* to chemically produced NO has not been assessed in detail. To pharmacologically test whether *L. pneumophila* responds to NO, we employed the chemical NO generators sodium nitroprusside (SNP) (**Fig. S3.1A**) and dipropylenetriamine (DPTA) NONOate (**Fig. S3.1B**). SNP and DPTA NONOate release at a given concentration approximately 1/1000 (SNP) or 2/1000 (DPTA NONOate) NO molecules, respectively (i.e., 1 µM SNP = ~1 nM NO) (Barraud et al., 2009b). The compounds were used to study the effects of NO on the expression of *gfp* under control of the promoters for flagellin (P_{flaA}), the 6S small regulatory RNA (P_{6SRNA}), the effector protein SidC (P_{sidC}), or the NO receptor Hnox1 (P_{hnox1}), respectively.

SNP was added to *L. pneumophila* JR32 expressing *gfp* under control of P_{flaA}, P_{6SRNA}, P_{sidC}, or P_{hnox1}, and the relative fluorescence (RFU) normalized to bacterial counts was assessed in AYE medium (**Fig. 3.2A**). Under these conditions, 2.5 µM and 5 µM SNP dose-dependently delayed the production of GFP under the control of P_{flaA} or P_{6SRNA} but had no effect on the production of GFP under the control of P_{sidC} or P_{hnox1}. The SNP-dependent delay in P_{flaA}-controlled production of GFP was observed in the parental *L. pneumophila* strain JR32, as well as in the Δ*lqsR* mutant strain (**Fig. S3.2A**), which shows an overall reduced P_{flaA} expression (Schell et al., 2016b). Similar results were obtained upon quantifying the production of GFP under control of P_{flaA} (**Fig. S3.2BC**) or P_{6SRNA} (**Fig. S3.2DE**) by flow cytometry. After 20 h of growth, 2.5 µM and 5 µM SNP significantly reduced the production of GFP under the control of P_{flaA} or P_{6SRNA}, and after 22 h or 24 h of growth, 5 µM SNP was still effective.

To confirm the results obtained with SNP, we treated *L. pneumophila* JR32 expressing *gfp* under control of P_{flaA} with up to 400 µM of the NO-generating chemical DPTA NONOate in AYE medium (**Fig. 3.2B**). Under the conditions used, DPTA NONOate dose-dependently delayed the production of GFP under the control of P_{flaA}, similar to what was observed with SNP. Moreover, at a concentration of 400 µM, DPTA NONOate not only delayed P_{flaA}-dependent *gfp* expression but also significantly reduced the production of GFP (**Fig. 3.2B**). DPTA NONOate dissolved in PBS pH 5.0 quantitatively releases NO upon incubation at room temperature for 1 h. This “spent” DPTA NONOate no longer affected the production of P_{flaA}-controlled GFP (**Fig. 3.2C**), and therefore, the release of NO underlies the biological activity of the compound on *L. pneumophila*.

In a different approach, we tested the effect of DPTA NONOate on the expression of *gfp* under control of P_{flaA} in sessile microcolonies (**Fig. 3.2D**). Under these conditions, the treatment with DPTA NONOate also caused a dose-dependent delay in the P_{flaA}-dependent *gfp* expression in the course of 30 h of microcolony formation. In summary, the NO-generating compounds SNP and DPTA NONOate dose-dependently delay the expression of P_{flaA} or P_{6SRNA} in *L. pneumophila* grown in planktonic or sessile form in AYE medium. These results indicate that *L. pneumophila* detects and responds to NO in the nanomolar concentration range.

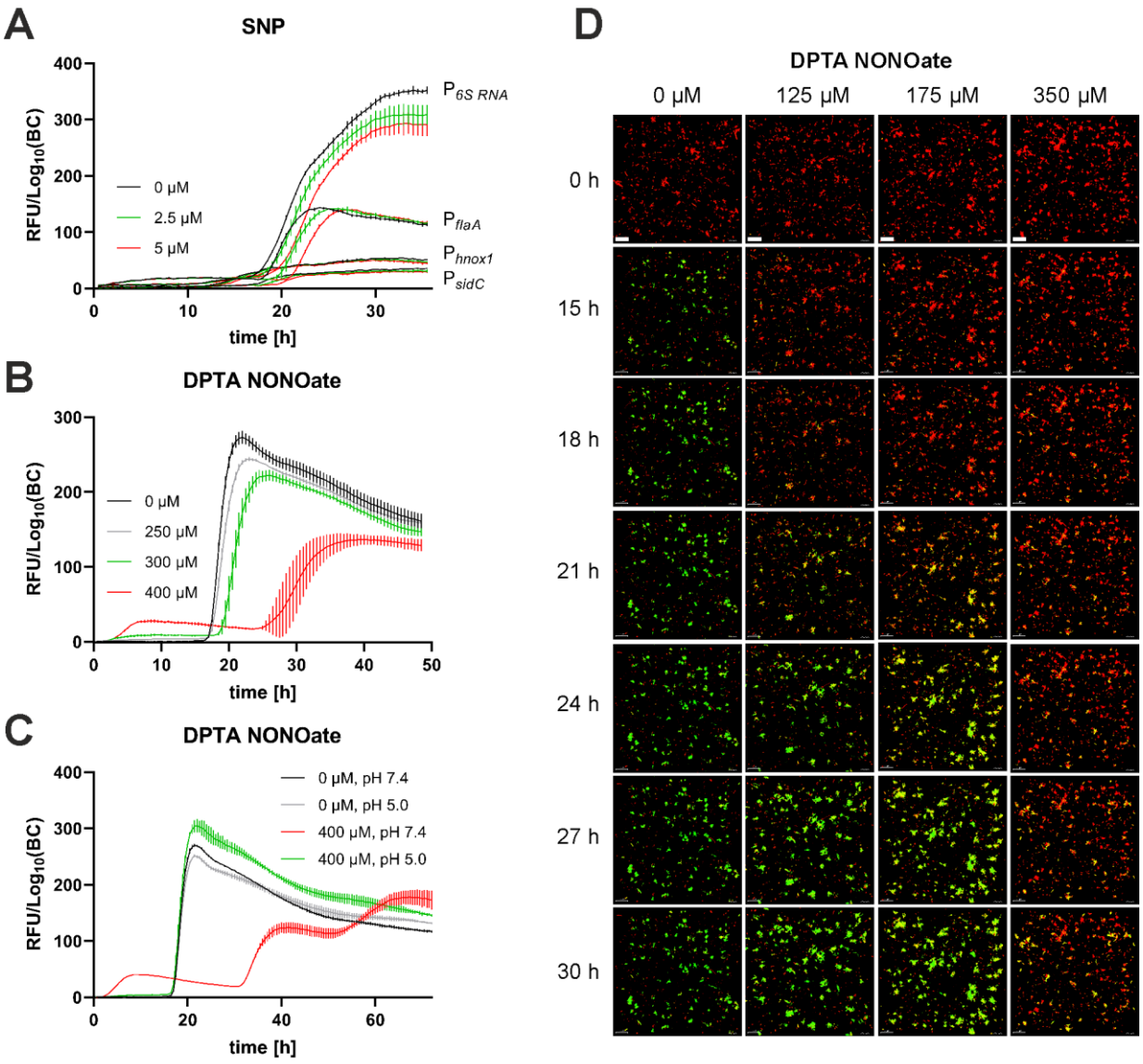

Figure 3.2. NO delays the expression of P*flaA*-*gfp* and P*6SRNA*-*gfp* in *L. pneumophila*.
L. pneumophila JR32 harboring (**A)** P*flaA*-*gfp* (pCM009), P*6SRNA*-*gfp* (pRH049), P*sidC*-*gfp* (pRH035), or P*hnox1*-*gfp* (pRH026) reporter constructs or (**B**, **C**) P*flaA*-*gfp* (pCM009) was grown in AYE medium for 18 h at 37°C and inoculated in AYE medium at an initial OD_{600} of 0.2. GFP fluorescence and OD_{600} were measured over time using a microplate reader. Promoter activity is inferred by *gfp* expression levels, denoted as relative fluorescence units divided by $\log_{10}$(bacterial counts) (RFU/Log_{10}(BC)). Strains were grown at 30°C (**A**) without (black) or with 2.5 µM (green) or 5.0 µM SNP (red), (**B**) without (black) or with 250 µM (grey), 300 µM (green), or 400 µM DPTA NONOate (red), or (**C**) without (black) or with 400 µM DPTA NONOate (red), or without (grey), or with 400 µM spent DPTA NONOate (green). Data shown (A-C) are means and standard deviations of technical triplicates and representative of three independent experiments. (**D**) *L. pneumophila* JR32 expressing P*tac*-*mCherry* and P*flaA*-*gfp* (pSN07) was grown in AYE medium for 21-22 h at 37°C, immobilized in AYE/0.5% agarose in 8-well ibidi dishes and let form microcolonies for 24 h at 30°C. After addition of DPTA NONOate (0, 125, 175 or 350 µM), P*tac*-*mCherry* and P*flaA*-*gfp* expression were recorded by time lapse microscopy for 30 h, and microcolony formation was analyzed by 3D reconstruction (Imaris). Scale bars: 20 µm. Data shown are means and standard deviations of technical triplicates and representative of three biological replicates.

3.4.2 Construction of marker-less *L. pneumophila* mutant strains lacking NO receptors.

The NO receptor genes localize to three different regions in the *L. pneumophila* genome, and each gene is organized in an operon (Hughes et al., 2019; Sahr et al., 2012) (**Fig. 3.1B**). The gene *hnox1* forms an operon with *lpg1057*, *hnox2* with *lpg2458* and *lpg2457*, and *nosP* with *nahK* and *narR*, respectively. Using *gfp* fusion constructs to analyze the expression of the NO receptor gene promoters revealed that in the *L. pneumophila* parental strain JR32, P_{hnox1} is expressed in the logarithmic growth phase showing a peak at the transition to the stationary growth phase, while P_{hnox2} and P_{nosP} are expressed to a lower extent and only in the stationary phase (**Fig. 3.3A**).

To assess the factors underlying the response of *L. pneumophila* to NO, we constructed and characterized marker-less mutant strains lacking individual (Hnox1, Hnox2, or NosP), two (double knockout, DKO), or all three (triple knockout, TKO) NO receptors. The NO receptor genes were deleted using a marker-less, non-polar knockout strategy (for details see the Materials and Methods section), allowing to not only generate the single knockout strains (Δ*hnox1*, Δ*hnox2*, Δ*nosP*), but also the double knockout (DKO, Δ*hnox1*-Δ*nosP*) and the triple knockout (TKO, Δ*hnox1*-Δ*nosP*-Δ*hnox2*) strain. The genomic deletions and lack of other mutations in the TKO mutant strain were verified by whole genome sequencing (data not shown). The NO single and triple knockout receptor mutant strains grew indistinguishable from the parental strain in AYE broth or minimal defined medium, MDM (**Fig. S3.3**), and the TKO deletion mutant did not differ in the expression of the stationary phase promoters P_{flaA} and P_{6SRNA}, or in the expression of the quorum sensing promoters P_{lqsA} and P_{lqsR} (**Fig. S3.4**). In contrast, the P_{lvbR} promoter was expressed only in the Δ*nosP* and TKO mutant strains but neither in the JR32 parental strain nor in the Δ*hnox1* or Δ*hnox2* mutants (**Fig. 3.3B**). Taken together, compared to the parental strain, *L. pneumophila* single and triple NO receptor knockout strains grow indistinguishable in complex and defined media, and the promoter expression studies reveal that the *flaA*, *6SRNA*, *lqsA* or *lqsR* genes are not regulated through the NO receptors, while *lvbR* is negatively regulated by NosP but neither by Hnox1 nor by Hnox2. Accordingly, NO-dependent regulation of LvbR specifically involves NosP (**Fig. 3.1A**).

3.4.3 *L. pneumophila* lacking NO receptors is less responsive to chemically generated NO.

To test whether the putative NO receptors Hnox1, Hnox2, or NosP mediate the response of *L. pneumophila* to NO, we exposed JR32 or the TKO mutant strain expressing P_{flaA}-*gfp* to DPTA NONOate in AYE broth (**Fig. 3.3C**). Upon treatment with 400 µM DPTA, both *L. pneumophila* strains showed a delayed GFP production; however, DPTA NONOate reduced the production of GFP in the parental strain JR32, while the reduction of GFP production by DPTA NONOate was absent in the TKO mutant strain.

In another approach, we compared the effect of DPTA NONOate on the production of GFP under control of P_{flaA} in sessile microcolonies formed by either the parental strain JR32 or the TKO mutant strain (**Fig. 3.3D**). Under these conditions, the treatment with 350 µM DPTA NONOate also caused a delayed GFP production in the strain JR32, while the reduction of GFP production by DPTA NONOate was diminished in the TKO mutant strain, in particular at later time points (27-39 h). Taken together, these results

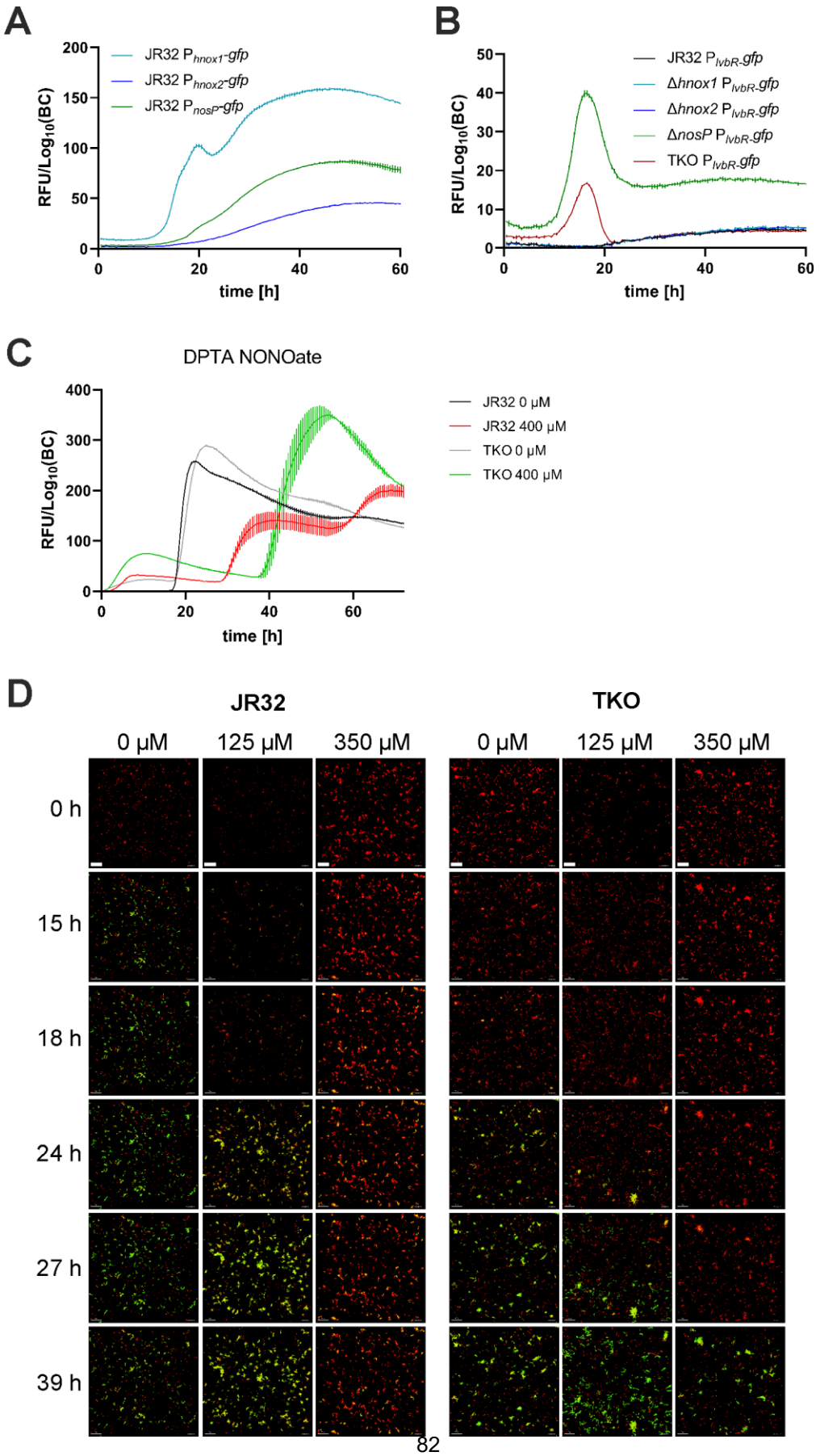
A
JR32 P hnox1-gfp
JR32 P hnox2-gfp
JR32 P nosP-gfp
RFU/Log10(BC)
time [h]
B
JR32 P lvbR-gfp
Δhnox1 P lvbR-gfp
Δhnox2 P lvbR-gfp
ΔnosP P lvbR-gfp
TKO P lvbR-gfp
RFU/Log10(BC)
time [h]
C
DPTA NONOate
JR32 0 µM
JR32 400 µM
TKO 0 µM
TKO 400 µM
RFU/Log10(BC)
time [h]
D
JR32
TKO
0 µM
125 µM
350 µM
0 h
15 h
18 h
24 h
27 h
39 h

Figure 3.3. *L. pneumophila* strains lacking NO receptors are less responsive to NO.
(**A**) *L. pneumophila* JR32 harboring P_{hnox1}-*gfp* (pRH026), P_{hnox2}-*gfp* (pCS031) and P_{nosP}-*gfp* (pCS032) or (**B**) *L. pneumophila* JR32, Δ*hnox1*, Δ*hnox2*, Δ*nosP*, and TKO mutant strains harboring P_{lvbR}-*gfp* (pRH023) were grown in AYE medium for 18 h at 37°C and inoculated in AYE medium at an initial OD_{600} of 0.2. Strains were grown at 30°C, and OD_{600} and GFP fluorescence were measured over time using a microplate reader. Promoter activity is inferred via *gfp* expression levels, denoted as relative fluorescence units divided by log_{10}(bacterial counts) (RFU/Log_{10}(BC)). Data shown are means and standard deviations of technical triplicates and representative of three independent experiments. (**C**) *L. pneumophila* JR32 (black/red) or TKO strains (grey/green) harboring P_{flaA}-*gfp* (pCM009) were grown in AYE medium for 18 h at 37°C and inoculated in AYE medium at an initial OD_{600} of 0.2. Strains were grown without (black/grey) or with 400 µM DPTA NONOate (red/green) at 30°C, and OD_{600} and GFP fluorescence were measured over time using a microplate reader. Promoter activity is inferred via *gfp* expression levels, denoted as relative fluorescence units divided by log_{10}(bacterial counts) (RFU/Log_{10}(BC)). Data shown are means and standard deviations of technical triplicates and representative of three independent experiments. (**D**) *L. pneumophila* JR32 or TKO mutants expressing P_{tac}-*mCherry* and P_{flaA}-*gfp* (pSN07) were grown in AYE medium for 21-22 h at 37°C, immobilized in AYE/0.5% agarose in 8-well ibidi dishes and let form microcolonies for 24 h at 30°C. After addition of DPTA NONOate (0, 125, or 350 µM), P_{tac}-*mCherry* and P_{flaA}-*gfp* expression were recorded by time lapse microscopy for 39 h, and microcolony formation was analyzed by 3D reconstruction (Imaris). Scale bars: 20 µm. Data shown are representative of three biological replicates.

indicate that the three NO receptors, Hnox1, Hnox2, and NosP, are indeed implicated in NO signaling in planktonic as well as sessile *L. pneumophila*.

3.4.4 *L. pneumophila* NO receptor mutant strains are impaired for intracellular replication in macrophages and amoebae.

Next, we sought to assess whether the NO receptors are implicated in virulence and host-pathogen interactions of *L. pneumophila*. To this end, we infected macrophages and amoebae with the parental strain or the single and triple NO receptor knockout strains. Upon infection of RAW 264.7 macrophages, the NO single knockout and TKO mutant strains grew significantly less efficiently compared to the parental strain JR32 (**Fig. 3.4A**). The mutant strains initiated growth later, followed by an apparently similar growth rate, and the growth defect of all mutants was comparable.

Similar results were obtained upon infection of the natural host amoeba, *A. castellanii*. The NO receptor single and triple knockout mutant strains grew significantly less efficiently compared to the parental strain JR32 (**Fig. 3.4B**). Upon growth in the amoebae, the initiation as well as the growth rate of the NO receptor mutant strains appeared to be impaired. The intracellular replication of the single mutant strains was restored to wild-type level upon re-introducing a single copy of the deleted gene into the genome of the mutant strains (**Fig. 3.4C**). Hence, the intracellular growth phenotype of the mutant strains is owed solely to the loss of the individual NO receptor genes and not due to second site or polar mutations. In contrast, re-introducing a single copy of the *hnox1*, *hnox2* or *nosP* genes into the genome of the TKO mutant strain did not revert the intracellular growth defect of the mutant (**Fig. 3.4D**). This result indicates that the three different NO receptors, Hnox1, Hnox2 and NosP have non-redundant functions. In summary, *L. pneumophila* single NO receptor mutant strains and the TKO mutant are impaired for intracellular growth in macrophages and amoebae, the growth defect of the single mutants is complemented by re-introducing

the corresponding gene into the mutant genome, and the TKO mutant cannot be complemented by single NO receptor genes.

3.4.5 Intracellular growth heterogeneity of *L. pneumophila* is regulated by NO signaling.

In eukaryotic host cells, the Lqs system regulates the size of the non-growing *L. pneumophila* persister subpopulation (Personnic et al., 2019; Striednig et al., 2021) as well as the heterogeneous expression of the stationary growth phase promoter P_{flaA} and LCV/host cell exit (Striednig et al., 2021). To test whether the NO receptors and NO signaling affect the ratio of growing/non-growing intracellular *L. pneumophila*, we employed the Timer system, a stable fluorescent reporter protein that slowly maturates from a green to a red fluorescent form, as a growth rate proxy (Claudi et al., 2014; Personnic et al., 2019).

In initial experiments, *A. castellanii* amoeba were infected with timer-producing *L. pneumophila* JR32 or TKO mutant strains, and the ratio of growing (green) versus non-growing (red) intracellular bacteria was assessed by confocal fluorescence microscopy (**Fig. 3.5A**). Using this approach, a larger portion of the intracellular TKO mutant bacteria appeared green (growing), compared to parental strain JR32. This finding supports the notion that NO signaling positively regulates the emergence of non-growing intracellular *L. pneumophila*. The finding also suggests that the TKO mutant bacteria might reach stationary growth phase later than JR32 bacteria, and thus, reflects the overall growth defect of the TKO mutant in macrophages (**Fig. 3.4A**) and *A. castellanii* (**Fig. 3.4B**).

In order to quantify the ratio of growing/non-growing intracellular *L. pneumophila*, we employed flow cytometry (**Fig. 3.5B-D**). *A. castellanii* amoeba were infected with timer-producing *L. pneumophila* JR32 or TKO mutant strains, and lysates of the infected amoebae were assessed for the intensity of GFP *versus* mCherry fluorescence (**Fig. 3.5B**) and bacterial counts *versus* log (GFP/mCherry) (**Fig. 3.5C**) to discriminate growing from non-growing *L. pneumophila*. This quantitative analysis revealed that compared to the JR32 parental strain, TKO mutant bacteria formed almost two-times fewer non-growers in the amoebae (**Fig. 3.5D**), indicating that NO signaling indeed positively regulates the ratio of non-growing to growing *L. pneumophila*. Taken together, these results reveal that NO signaling regulates intracellular phenotypic heterogeneity of *L. pneumophila* and the ratio of non-growing *versus* growing bacteria in amoebae.

3.4.6 *L. pneumophila* NO receptor mutant strains form mat-like biofilms.

To assess the role of the NO receptors for *L. pneumophila* biofilm formation, GFP-producing *L. pneumophila* JR32 or Δ*hnox1*, Δ*hnox2*, Δ*nosP*, DKO, or TKO mutant strains were seeded onto ibidi µ-dishes and left to form biofilms in AYE medium for 1, 2, and 3 days at 25°C without disturbance. Biofilm formation, including architecture and adherence to an abiotic surface, was analyzed by confocal microscopy (**Fig. 3.6**).

Under these conditions, the attachment of the parental JR32 strain and the NO receptor mutant strains to the abiotic dish surface was undistinguishable (**Fig. S3.5A**). However, the biofilm formed by the JR32 strain showed a “clustered” and “patchy” appearance, while the Δ*hnox1*, Δ*hnox2*, Δ*nosP*, DKO or TKO mutant strains formed a “mat-like” biofilm with a different 2D- and 3D-architecture (**Fig. 3.6A, S3.5B**).

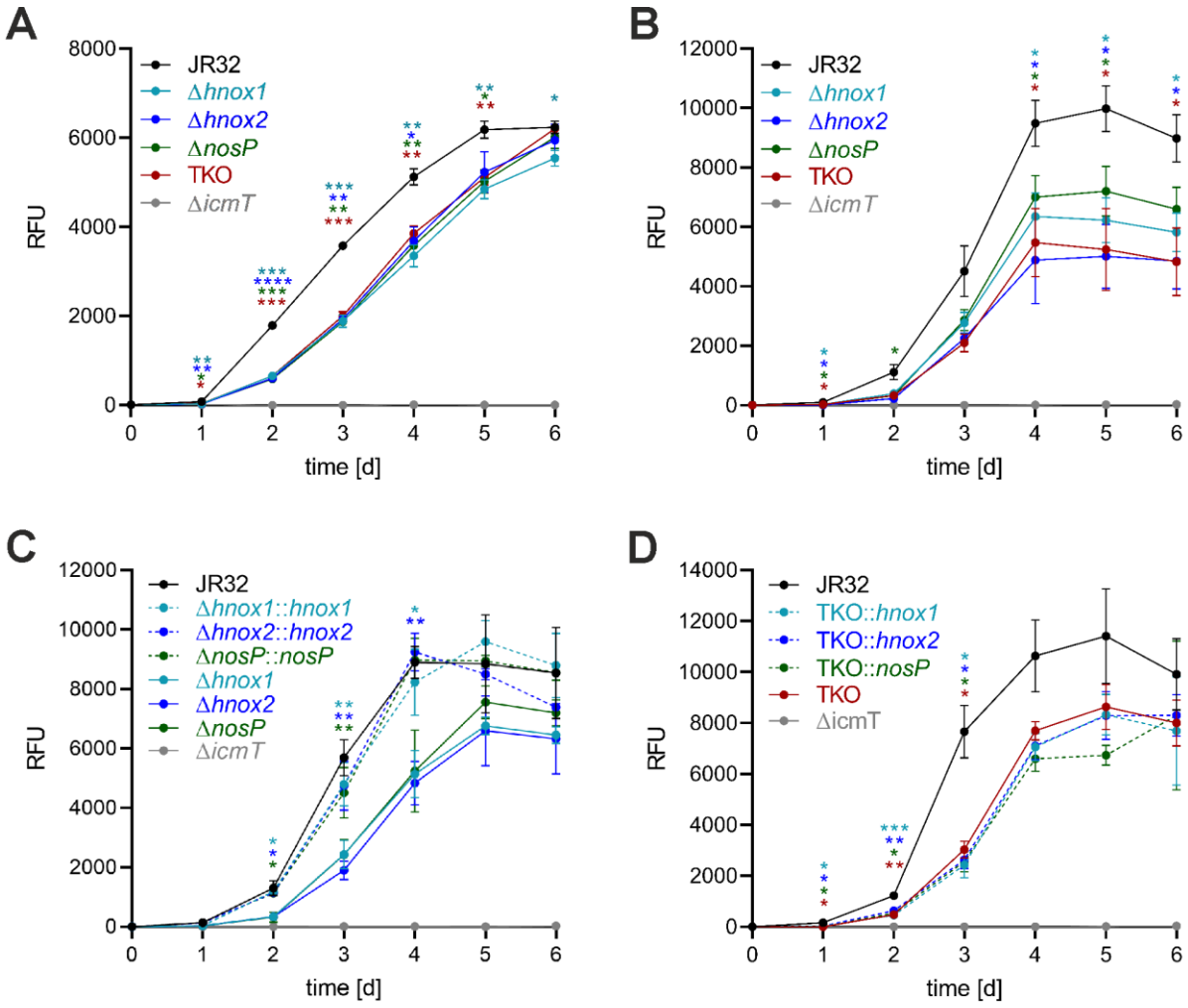

Figure 3.4. *L. pneumophila* NO receptor mutant strains are impaired for intracellular replication in macrophages and amoeba.

(**A**) RAW 264.7 macrophages were infected (MOI 1, 6 d) with GFP-producing *L. pneumophila* JR32, Δ*icmT*, Δ*hnox1*, Δ*hnox2*, Δ*nosP* or TKO mutant strains harboring pNT28. Intracellular replication was assessed by relative fluorescence units (RFU). *A. castellanii* amoebae were infected (MOI 1, 6 d) with GFP-producing *L. pneumophila* harboring pNT28, (**B**) strain JR32, Δ*icmT*, Δ*hnox1*, Δ*hnox2*, Δ*nosP* or TKO (**C**) strain JR32, the single NO receptor mutants or the complemented single mutants, or (**D**) strain JR32, the TKO mutant or TKO with single NO receptor genes. Intracellular replication was assessed by GFP production and expressed as relative fluorescent units (RFU). Data shown are means and standard deviation of technical triplicates and representative of three biological replicates (*$p < 0.05$, **$p < 0.01$, ***$p < 0.001$, ****$p < 0.0001$; two-way ANOVA).

Quantification of the biofilm mass by flow cytometry revealed that the biomass of the NO receptor mutant strain biofilms was larger than that of the parental strains at early times during biofilm formation (**Fig. 3.6B)**; yet, high resolution scanning electron microscopy (SEM) images of wild-type and TKO biofilms were similar (**Fig. S3.5C**). In summary, biofilms formed by *L. pneumophila* lacking one (Hnox1, Hnox2, NosP), two (DKO) or all three (TKO) NO receptors adopt a “mat-like” architecture morphologically distinct from the

"patchy" morphology of biofilms formed by the parental strain JR32, and the mutant biofilms contain more biomass.

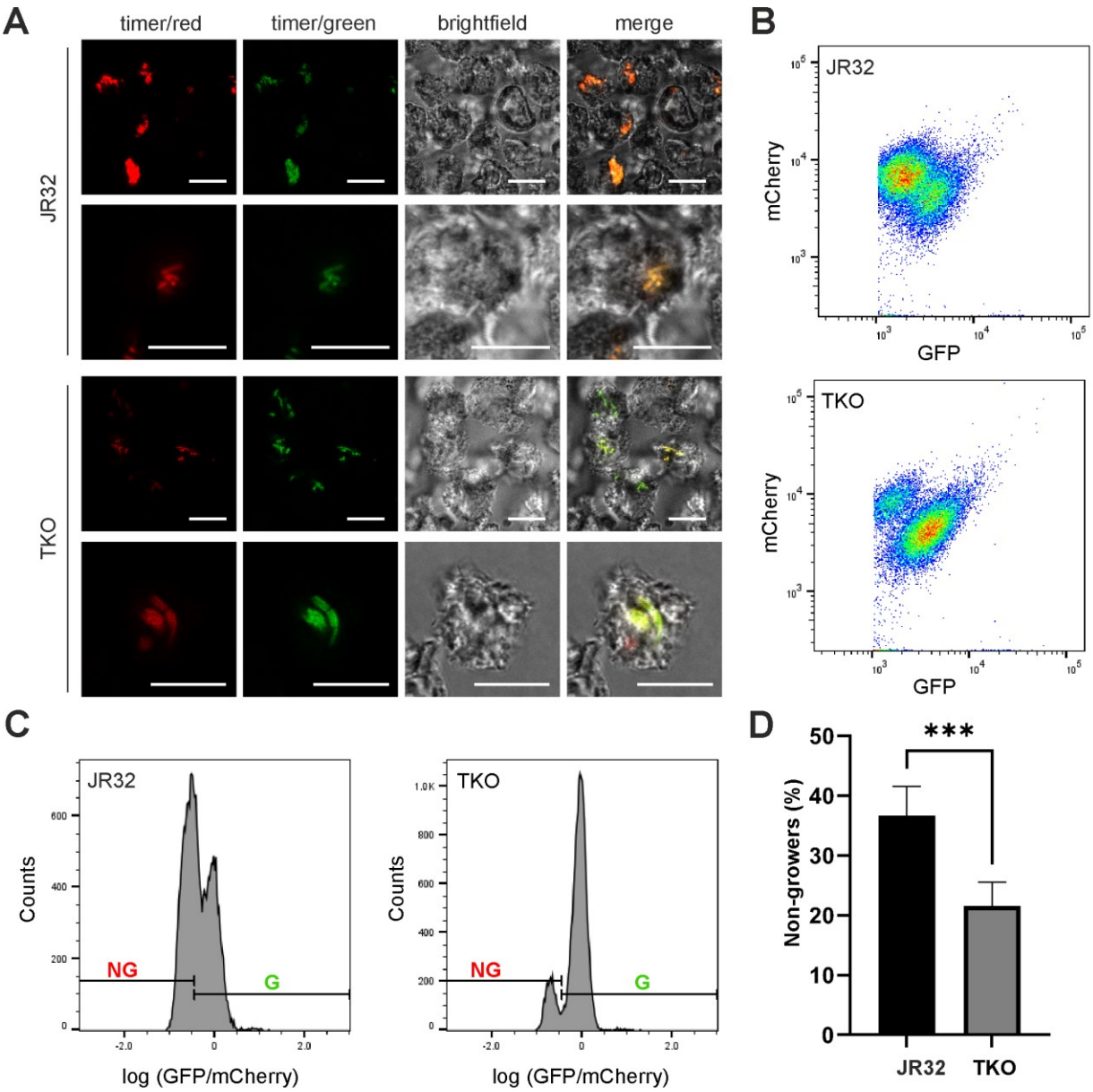

Figure 3.5. Phenotypic heterogeneity of *L. pneumophila* NO receptor mutant strains in amoeba. (**A**) *A. castellanii* amoeba were infected (MOI 1, 20 h) with timer-producing *L. pneumophila* JR32 or TKO mutant strains harboring pNP107. The phenotypic heterogeneity was assessed (**A**) by confocal fluorescence microscopy in intact cells (scale bars, 10 µm), or (**B-D**) by flow cytometry in lysates. The flow cytometry data is depicted as (**B**) pseudocolor graph showing mCherry *versus* GFP signal intensity, (**C**) bacterial counts *versus* log (GFP/mCherry) to discriminate non-growing from growing *L. pneumophila*, and (**D**) bar graph depicting the percentage of non-growing bacteria. Data shown are representative of (A) 2 or (B-D) 6 experiments and show (D) means and standard deviations of six biological replicates (***, $p < 0.001$; Student's *t*-test).

We also tested whether NO signaling affects the dispersal of *L. pneumophila* biofilms. To this end, we compared the effect of the chemical NO donor SNP on the dispersal of one day old biofilms formed by GFP-producing *L. pneumophila* JR32, single NO receptor or TKO mutant strains (**Fig. 3.6C**). Intriguingly, 10 µM SNP promoted the dispersal of a biofilm formed by the parental strain JR32, but not biofilms formed by single NO receptor or TKO mutant bacteria. These findings indicate a role of the NO receptors Hnox1, Hnox2, and NosP for NO signaling and dispersal of *L. pneumophila* biofilms and confirm a non-redundant function of the three NO receptors.

Biofilms are encased by a complex extracellular matrix. To assess whether NO signaling plays a role in formation of extracellular structures, we performed a sedimentation experiment, which previously has revealed the enhanced formation of extracellular filaments by the *L. pneumophila* Δ*lqsR* and Δ*lqsS* mutant strains (Kessler et al., 2013; Tiaden et al., 2010b). *L. pneumophila* JR32, single NO receptor mutants, TKO, and Δ*lqsR* mutant strains were grown on CYE agar plates, gently suspended in AYE medium and let sediment by gravity for 4 h at RT **(Fig. S3.6A**). Quantification of the sedimentation rate revealed that single NO receptor mutants sedimented like the parental JR32 strain (data not shown), while the TKO mutant strain sedimented significantly slower than JR32, albeit still faster than the Δ*lqsR* mutant **(Fig. S3.6B**). A high-resolution analysis by EM indicated that the TKO mutant formed a more extensive network of extracellular filaments **(Fig. 3.6D**), and therefore, the sedimentation rate of the *L. pneumophila* JR32, TKO, and Δ*lqsR* mutant strains is inversely correlated to the formation of extracellular filaments.

3.5 Discussion

In this study, we investigated the response of *L. pneumophila* to NO and characterized the bacterial receptors underlying this process. We found that the chemical NO donors SNP and DPTA NONOate delayed and reduced the expression of the promoters for flagellin (P_{flaA}) and the 6S small regulatory RNA (P_{6SRNA}) (**Fig. 3.2**). Compared to the parental *L. pneumophila* strain JR32, P_{flaA} expression was initially much less pronounced and delayed in presence of DPTA NONOate in the TKO strain, indicating that the NO receptors are implicated in NO signaling *in vivo* (**Fig. 3.3**). Moreover, the *L. pneumophila* single and triple NO receptor mutant strains were impaired for growth in macrophages and amoebae (**Fig. 3.4**) and the NO receptors regulated the intracellular phenotypic heterogeneity of *L. pneumophila* such that the non-growing subpopulation was larger in the parental strain compared to strains lacking the NO receptors (**Fig. 3.5**). Finally, the single and triple NO receptor mutant strains showed a mat-like biofilm architecture, and NO-dependent biofilm dispersal was dependent on the NO receptors (**Fig. 3.6**).

NO is a highly reactive free radical, has a lifetime of only a few seconds and diffuses freely across membranes. These characteristics render NO ideal for short-range and transient signaling within and between neighboring cells (Arora et al., 2015; Cary et al., 2006). Accordingly, NO signaling is implicated in intracellular replication of *L. pneumophila* in phagocytes (**Fig. 3.4**) as well as in biofilm dynamics (**Fig. 3.6**). These findings are consistent with the idea that NO signaling in the µm range is important for pathogen-host cell interactions as well as for bacterial cell-cell communication.

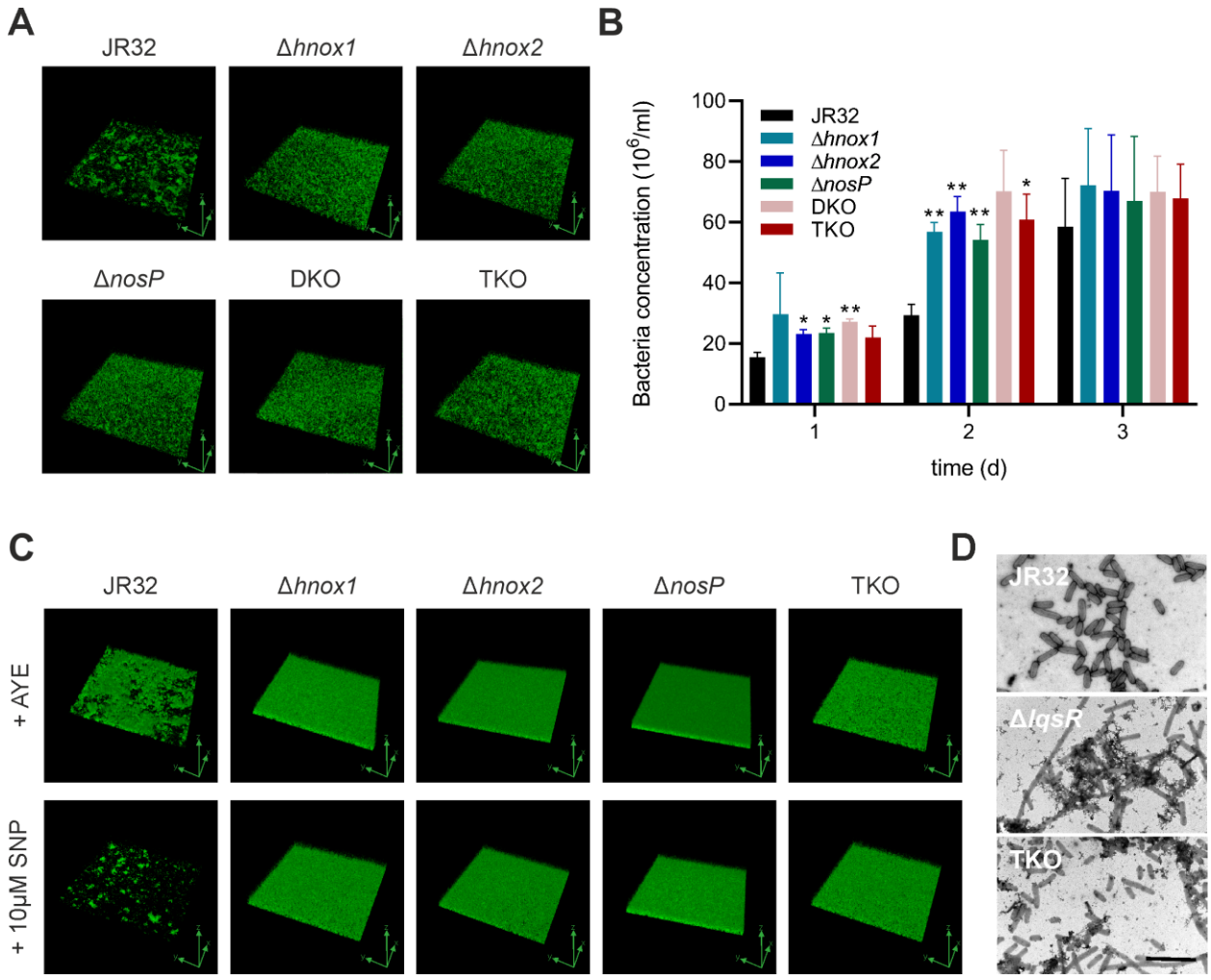

Figure 3.6. *L. pneumophila* NO receptor deletion strains form altered biofilms.
(**A**) Biofilms were initiated with exponential phase (18 h) GFP-producing *L. pneumophila* JR32, Δ*hnox1*, Δ*hnox2*, Δ*nosP*, or TKO mutant strains harboring pNT28 in ibiTreat microscopy dishes in AYE medium and grown at 25°C without mechanical disturbance for 24 h. Confocal fluorescence microscopy images are shown as 3D representations (green axes: xyz orientation, dimensions: 185 × 185 × 30 µm). The images shown are representative of 3 independent experiments. (**B**) Biofilms were initiated with exponential phase (18 h) GFP-producing *L. pneumophila* JR32 or TKO mutant strains harboring pNT28 in ibiTreat microscopy dishes in AYE medium and grown without mechanical disturbance at 25°C for 1-3 d. Biomass of resuspended bacteria was determined by flow cytometry through the ratio of GFP-producing *L. pneumophila* (identified by fluorescence vs. FSC) to beads population (identified by SSC vs. FSC). Data shown are means and standard deviation (bacteria/ml) of biological triplicates from 100'000 events of each biofilm suspension (*p < 0.05, **p < 0.01; two-way ANOVA). (**C**) Biofilms formed for 24 h by *L. pneumophila* JR32, single NO receptor mutants or the TKO mutant strain were treated or not with 10 µM SNP for another day. Dimensions (xyz): 185 × 185 × 30 µm. (**D**) Representative electron micrographs of *L. pneumophila* JR32, Δ*lqsR* or TKO after 5 h sedimentation in AYE medium. The samples were mounted on copper grids and stained with uranyl formate. Scale bars, 5 µm.

The NO receptor gene promoters P_{hnox1}, P_{hnox2} and P_{nosP} are differentially expressed upon growth of *L. pneumophila* in broth (**Fig. 3.3A**), and *L. pneumophila* mutant strains lacking individual NO receptors all

showed a similar defect in intracellular replication in macrophages and amoebae (**Fig. 3.4AB**). These findings suggest that the three different NO receptors, Hnox1, Hnox2 and NosP are non-redundant and might adopt specific functions during growth in media as well as during intracellular growth. Rather surprisingly, the TKO mutant also did not show a more severe intracellular growth phenotype than the three single NO receptor mutant strains. In agreement with a non-redundant function of the individual NO receptors, the TKO mutant strain was not complemented by the genomic integration of individual NO receptor genes (**Fig. 3.4D**). Furthermore, the single as well as the TKO mutant strains formed architecturally altered biofilms, which no longer dispersed following the administration of NO (**Fig. 3.6**). Accordingly, all three NO receptors are required for the response of *L. pneumophila* biofilms to NO, supporting the notion of non-redundant functions of the NO receptors.

Possible explanations for the observed non-redundancy of the three NO receptors are that the receptors obligatorily crosstalk among each other, and/or, they do not trigger the same downstream signaling pathway(s) regulating different features of *L. pneumophila*. As an example, NosP but neither Hnox1 nor Hnox2 negatively regulates the transcription factor LvbR (**Fig. 3.3B**). While additional pathways specific for an individual NO receptor are likely in operation, the second messenger c-di-GMP is a candidate for convergent signaling through the three NO receptors. The Hnox-1 (Carlson et al., 2010) and NosP (Fischer et al., 2019) signaling pathways have experimentally been shown to converge on modulating c-di-GMP; yet, for Hnox-2 the downstream second messenger(s) or signaling cascade is not known. In agreement with an important role of c-di-GMP signaling for *L. pneumophila*-host cell interactions, several proteins predicted to contain domains related to c-di-GMP synthesis, hydrolysis or recognition were found to modulate intracellular growth of *L. pneumophila* (Allombert et al., 2014; Levi et al., 2011).

Intriguingly, NO signaling regulates intracellular phenotypic heterogeneity of *L. pneumophila* by modulating the ratio of growing to non-growing bacteria (**Fig. 3.5**). Phenotypic heterogeneity underlies the formation of a virulent and motile *L. pneumophila* subpopulation, which preferentially exits the LCV and the amoeba host cell, and thus, seems to engage in “division of labor” (Striednig et al., 2021). The Lqs quorum sensing system and the LAI-1 signaling molecule modulate these aspects of phenotypic heterogeneity (Personnic et al., 2019; Striednig et al., 2021). We show here that in addition to quorum sensing, NO signaling also orchestrates intracellular phenotypic heterogeneity of *L. pneumophila*, and accordingly, governs short-distance division of labor of the pathogen.

Bacterial cell-cell communication in sessile communities also requires signaling in the µm range. Accordingly, NO signaling is occurring during microcolony formation (**Fig. 3.3D**) and is implicated in biofilm formation and dispersal of *L. pneumophila* (**Fig. 3.6**). The TKO mutant strain showed a “mat-like” rather than a “patchy” biofilm architecture (**Fig. 3.6AB**), and single NO receptor mutant or TKO biofilms no longer respond to NO (**Fig. 3.6C**). NO is commonly involved in the regulation of bacterial biofilms (Arora et al., 2015). Biofilm formation is frequently regulated by NO-binding H-NOX domain proteins and downstream signaling networks such as two-component systems or c-di-GMP metabolism (Plate and Marletta, 2013). Accordingly, several c-di-GMP metabolizing enzymes are involved in the regulation of *L. pneumophila*

biofilm formation (Carlson et al., 2010; Pecastaings et al., 2016). Specifically, the DGC Lpg1057/Lpl1054 has been implicated in NO-mediated c-di-GMP production (**Fig. 3.1A**) and effects on biofilms (Pecastaings et al., 2016).

The pleotropic transcription factor LvbR regulates the architecture of *L. pneumophila* biofilms such that the Δ*lvbR* mutant strain forms a "mat-like" biofilm (Hochstrasser et al., 2019), similar to the single NO receptor and TKO mutant strains (**Fig. 3.6**). NosP negatively regulates LvbR (**Fig. 3.3B**), apparently conflicting with the similar biofilm phenotypes of the corresponding mutant strains. The downstream targets of LvbR- and NO-mediated signaling seem to be complex and might involve c-di-GMP signaling. LvbR (Hochstrasser et al., 2019) as well as NosP (Fischer et al., 2019) positively regulate c-di-GMP signaling through Lpg1057 or NarR, respectively (**Fig. 3.1A**). Perhaps, under the conditions tested, these regulatory pathways are dominant over the negative regulation of LvbR by NosP. LvbR also downregulates flagellar genes in biofilms (Hochstrasser et al., 2019), and the chemical NO donors SNP and DPTA NONOate delayed and reduced the expression of the flagellin promoter (P_{flaA}) in planktonic and sessile *L. pneumophila* (**Figs. 3.2 and 3.3**). However, an *L. pneumophila* Δ*flaA* mutant strain forms "patchy" biofilms like the parental strain (Hochstrasser et al., 2019), and therefore, the flagellum does not account for the altered biofilm architecture of Δ*lvbR* and TKO mutant biofilms.

Beyond a similar biofilm morphology of *L. pneumophila* strains lacking the NO receptors or *lvbR*, there appears to be an intimate link between NO signaling and LvbR. On a transcriptional level, LvbR is a negative regulator of Hnox1, and consequently, reduces NO signaling. Reciprocally, the P_{lvbR} promoter is induced in absence of NO signaling in the Δ*nosP* and TKO mutant strains (**Fig. 3.3B**) but not in the parental strain JR32, while several other promoters (P_{flaA}, P_{6SRNA}, P_{lqsA} and P_{lqsR}) are not differentially regulated (**Fig. S3.4**). Since NosP-mediated signaling negatively regulates the Hnox1 inhibitor LvbR, NO signaling appears to be amplified by a positive feedback loop. However, this regulatory loop might not occur in all *L. pneumophila* strains, as P_{lvbR} was transiently expressed in several clinical and environmental *L. pneumophila* isolates (Hochstrasser and Hilbi, 2022).

The Lqs system regulates NO signaling through LvbR (Hochstrasser and Hilbi, 2020) (**Fig. 3.1A**), since the sensor kinase LqsS negatively regulates LvbR, which in turn negatively regulates Hnox1 (Hochstrasser et al., 2019; Tiaden et al., 2010b). Accordingly, the Lqs system is a positive regulator of NO signaling in *L. pneumophila*, representing a prototypical and novel regulation of NO signaling by quorum sensing. In *L. pneumophila*, NO regulates motility (P_{flaA}) dependent on the NO receptors (**Fig. 3.2 and 3.3**), but the NO receptors do not seem to regulate stress response (P_{6SRNA}) and components of the Lqs system (P_{lqsA}, P_{lqsR}) (**Fig. S3.4**). While in *L. pneumophila* quorum sensing regulates NO signaling, NO signaling regulates quorum sensing in other bacteria (Heckler and Boon, 2019).

NO signaling has been found to regulate quorum sensing in different bacteria, including pathogens of the genera *Vibrio* and *Pseudomonas* (Heckler and Boon, 2019). *Vibrio harveyi* shows a NO-dependent increase in bioluminescence, which is relayed through the pivotal quorum sensing histidine phosphotransfer protein LuxU (Henares et al., 2012). Binding of NO to the sensor H-NOX inhibits the cytosolic hybrid

histidine kinase HqsK, which in turn leads to dephosphorylation of the pivotal integrator of quorums sensing, LuxU, in *V. harveyi* (Henares et al., 2012) as well as in *Vibrio parahaemolyticus* (Ueno et al., 2019). Analogously, in *Vibrio cholerae*, binding of NO to the sensor NosP inhibits the cytosolic hybrid histidine kinase VpsS, which decreases the levels of phosphorylated LuxU (Hossain et al., 2018). Intriguingly, the effect of NO is only observed at low cell density, when the other three quorum sensing pathways converging on LuxU are not operational (Henares et al., 2012). NO has also been reported to reduce flagellum production and to enhance biofilm formation in an H-NOX-dependent manner in *V. harveyi* (Henares et al., 2013), while leading to biofilm dispersal of *V. cholerae* (Barraud et al., 2009b) and *Vibrio fischeri* (Thompson et al., 2019). Overall, the crosstalk between quorum sensing and NO signaling regulates virulence and biofilm formation in a number of human pathogens, including the genera *Legionella*, *Vibrio* and *Pseudomonas*.

In summary, we demonstrate in this study that *L. pneumophila* regulates virulence, intracellular phenotypic heterogeneity, and biofilm dynamics through NO and the three NO receptors, Hnox1, Hnox2 and NosP. Further studies will identify and characterize the molecular components underlying NO-dependent *L. pneumophila*-phagocyte inter-kingdom signaling, biofilm architecture and dynamics as well as phenotypic heterogeneity.

3.6 Materials and methods

3.6.1 Bacteria, eukaryotic cells, and growth conditions.

L. pneumophila strains (**Table 3.1**) were grown on CYE agar plates at 37°C for 2-4 d (Feeley et al., 1979) or in liquid cultures with *N*-(2-acetamido)-2-aminoethanesulfonic acid (ACES)-buffered yeast extract (AYE) medium (Horwitz, 1983) for 18-22 h on a wheel (80 rpm). AYE medium was supplemented with chloramphenicol (Cm; 5 µg/ml) to maintain plasmids if required.

To determine growth characteristics, *L. pneumophila* JR32 and the Δ*hnox1*, Δ*hnox2*, Δ*nosP*, the DKO, or the TKO mutant strains were grown for 18 h at 37°C in AYE medium, diluted to an initial OD_{600} of 0.2 in a black clear bottom 96-well plate (100 µl/well) and then incubated at 30°C while orbitally shaking. Growth was monitored in triplicates by measuring the absorbance at 600 nm (OD_{600}) in a microtiter plate reader (Synergy H1 Hybrid Reader BioTek, or Cytation 5 Hybrid Multi-Mode Reader, Agilent Technologies). Several independent Δ*hnox1*, Δ*hnox2*, Δ*nosP*, and TKO clones were tested.

A. castellanii (ATCC: 30234, lab collection) was cultured in proteose, yeast extract, glucose (PYG) medium (Moffat and Tompkins, 1992; Segal and Shuman, 1999) at 23°C using proteose from Becton Dickinson Biosciences and yeast extract from Difco. Murine RAW 264.7 macrophages (ATCC: TIB-71™, lab collection) were grown in RPMI 1640 medium (Life Technologies) supplemented with 10% fetal calf serum (FCS; Life Technologies) and 1% L-glutamine (Life Technologies) in a humidified atmosphere at 37°C in 5% CO_2.

3.6.2 Molecular cloning and generation of *L. pneumophila* scar-free deletion mutants.

Cloning was performed according to standard protocols, and plasmids were isolated using the NucleoSpin plasmid kit (Macherey-Nagel). DNA fragments were amplified using Q5 (NEB) or Phusion (Thermo scientific) high-fidelity DNA polymerase (NEB). DNA fragments were assembled via Gibson assembly using NEBuilder HiFi DNA assembly kit (NEB). DNA fragments were amplified using the primers listed in **Table S3.1**, and the plasmids used in this study are listed in **Table 3.1**. All constructs were verified by DNA sequencing.

The scar-free single or multiple NO receptor deletion mutants were generated by double homologous recombination. The genes of interest as well 1 kb of their upstream and downstream region were cloned into the suicide plasmid pSR47S (Merriam et al., 1997; Ren et al., 2006), and the relevant genes were deleted except for overlapping regions with adjacent genes in the case of *hnox1* and *hnox2*. For the construction of suicide plasmids, the gene of interest and ca. 1 kb of their upstream and downstream region were amplified using the primer pairs oSM124/oSM125 for *hnox1* (1'154'000-1'154'542 bp), oSM130/oSM131 for *nosP* (332'290-333'456 bp), or oSM134/oSM135 for *hnox2* (2'773'093-2'773'653 bp). The individual amplified fragments were then assembled with linearized pSR47S (generated by amplification using oSM113/oSM114) to yield pSM036, pSM037 and pSM038. These intermediate vectors were also used for the complementation by chromosomal reintegration of the NO receptor genes at the original site in the genome. The gene of interest was then deleted using vector linearization PCR with the primer pairs oSM126/oSM127 for Δ*hnox1*, oSM130/oSM131 for Δ*nosP* and oSM136/oSM137 for Δ*hnox2*, yielding pSM028, pSM031 and pSM032. In the case of *hnox1* and *hnox2*, overlapping regions with *lpg1057* or *lpg2458*, respectively, were not deleted and kept in the upstream fragments.

L. pneumophila JR32 was transformed with plasmid pSM028 for *hnox1*, pSM031 for *nosP* or pSM032 for *hnox2* deletion, yielding the strains SM01, SM02, and SM03. Co-integrates were selected on CYE plates supplemented with kanamycin (Km; 20 µg/ml). Single colonies were picked and streaked on CYE plates to allow for a second recombination event, followed by streaking single colonies on freshly prepared CYE plates supplemented with 5-10% sucrose. Single colonies were then patched on CYE with and without Km plates. The correct genomic deletion in Km sensitive clones was verified by colony PCR and sequencing. The TKO was generated by transforming Δ*hnox1* with pSM031 and performing the selection process to yield a double knockout mutant Δ*hnox1*-Δ*nosP* (SM04), which subsequently was transformed with pSM032 and subjected to the selection process a third time to yield the TKO strain (SM05). The genomic deletions of the TKO mutant strain and lack of other mutations were validated by whole genome sequencing.

Plasmids pCS031 and pCS032 harboring a transcriptional P_{hnox2}- or P_{nosP}-*gfp* fusion were constructed by PCR amplification of the promoters for *hnox2* (200 bp) or *nosP* (200 bp) using the primer pair oCS103/104 or oCS105/106 and cloned into the SacI and XbaI sites of pCM009 (Schell et al., 2016b) using the NEBuilder HiFi DNA assembly reaction.

To construct the plasmids pSM015, pSM016, and pSM017 harboring *hnox1*, *nosP*, or *hnox2* under control of their own promoters, the corresponding gene regions were amplified together with their putative

native promoter regions (600 bp upstream) using Phusion polymerase, JR32 genomic DNA as a template, and the primer pairs oSM059/oSM060, oSM061/oSM062 and oSM063/oSM064, respectively. The PCR products were purified and cloned into pNT31 (constitutively expressing *gfp*), previously digested with BamH1 and Xho1. These plasmids were used for complementation assays but did not restore the phenotype of the parental strain JR32.

Bacterial growth and GFP production were monitored in triplicates by measuring the absorbance at 600 nm (OD_{600}) and fluorescence (excitation, 485 nm; emission, 528 nm; gain, 50) using a microtiter plate reader. Promoter activity was inferred by *gfp* expression levels, denoted as relative fluorescence units divided by $\log_{10}$(bacterial counts).

3.6.3 Expression of GFP reporter constructs in *L. pneumophila*.

Promoter expression was assessed by plate reader and quantified by flow cytometry as described (Hochstrasser and Hilbi, 2022). Briefly, *L. pneumophila* strains (JR32, Δ*hnox1*, Δ*hnox2*, Δ*nosP* or TKO) harboring P_{flaA}-, P_{6SRNA}-, P_{sidC}-, P_{hnox1}-, P_{hnox2}-, P_{nosP}-, P_{lvbR}-, P_{lqsR}- or P_{lqsA}-*gfp* (ASV) fusion reporter plasmids (pCM009, pRH049, pRH035, pRH026, pCS031, pCS032, pRH023, pRH037 or pRH038) were grown for 3 d on CYE/Cm agar plates followed by growth in AYE/Cm (5 µg/ml) on a rotating wheel (80 rpm) at 37°C for 18 h. On the day of the experiment, fresh stock solutions and dilution series of the chemical NO generators were prepared. For SNP, a 100 mM stock solution was prepared directly in AYE medium. For DPTA NONOate, 40 mM stock solutions were prepared, either in PBS pH 7.4 or in PBS pH 5.0 (for spent DPTA NONOate), adjusted by adding HCl. As DTPA NONOate is sensitive to moisture and should be kept sealed, a new 10 mg vial was used for each experiment. At the concentrations used (5 µM SNP, 400 µM DPTA NONOate), we did not observe effects of the pharmacological NO donors on survival of *L. pneumophila* but there was a slightly prolonged lag phase.

Bacterial strains from overnight cultures were subsequently inoculated in a black, clear bottom 96-well plate (100 ml/well, polystyrene) at an initial OD_{600} of 0.2 in AYE/Cm (5 µg/ml) supplemented or not with the NO generators to reach the final concentrations indicated for SNP (0, 2.5 or 5 µM), DPTA NONOate (0, 250, 300 or 400 µM), or spent DPTA NONOate (0 or 400 µM), and the strains were incubated at 30°C while orbitally shaking. Bacterial growth and GFP production were monitored in triplicates by measuring the OD_{600} and fluorescence (excitation, 485 nm; emission, 528 nm; gain, 50) with a microplate reader. Blank values (AYE medium) were subtracted from all samples and promoter activity was inferred by *gfp* expression levels, denoted as relative fluorescence units (RFU) divided by $\log_{10}$(bacterial counts).

To quantify promoter expression by flow cytometry, *L. pneumophila* JR32 strain harboring P_{flaA}- or P_{6SRNA}-*gfp* (ASV) fusion reporter plasmids (pCM009, or pRH049) were grown at 37°C in AYE/Cm (5 µg/ml) supplemented with SNP to reach a final concentration of 0, 2.5 and 5 µM SNP from a freshly prepared 100 mM stock solution in AYE. Every 2 h from 18-28 h, the bacteria were fixed with 4% paraformaldehyde (PFA) for 1 h at room temperature (RT) and subsequently stained with 1 µg/ml DAPI for 45 min at RT in the dark. The GFP-positive population was quantified using a Fortessa II flow cytometer and Diva software. The bacterial population was identified employing a forward (FSC, 650 V) and sideward scatter (SSC, 240 V)

gating, with a threshold of 200 each, examined for DAPI stain (Vio 450_50, 700 V) and GFP production (Blue 530_30, 600 V), and 10'000 events per sample were recorded. The data were analyzed with the software FlowJo. The GFP-positive population was gated using a GFP control and a DAPI control as reference. The strain JR32/pNT028, constitutively producing GFP, served as the GFP control, and the parental JR32 strain as the DAPI control.

3.6.4 Microcolony growth.

Microcolony growth of *L. pneumophila* and bacterial GFP production was assessed as described (Personnic et al., 2021). Briefly, *L. pneumophila* strains (JR32, TKO) carrying the dual reporter P_{tac}-*mcherry*/P_{flaA}-*gfp* (pSN7) were grown on CYE agar plates supplemented with Cm (5 µg/ml) at 37°C for 2 d. Bacterial lawns were used to inoculate AYE medium/Cm (5 µg/ml) at an OD_{600} of 0.1 and grown on a wheel (80 rpm) for ca. 21-22 h. Stationary phase bacteria were embedded in AYE medium/0.5% agarose/Cm (5 µg/ml) at an OD_{600} of 0.1 and poured into chambered coverslips (ibidi 8-well µ-slide). After solidification, bacteria were allowed to grow over night at 30°C to form microcolonies. The next day, DPTA NONOate was freshly dissolved in PBS and added to the wells at the final concentrations indicated (0, 125, 175 or 350 µM). Microcolony formation was monitored by confocal microscopy at 30°C. To generate 3D images, 100-200 slices were recorded.

3.6.5 Biofilm formation and dispersal.

The formation and quantification of biofilm by *L. pneumophila* was determined as described previously (Hochstrasser and Hilbi, 2022; Hochstrasser et al., 2019). Briefly, GFP-producing *L. pneumophila* strains (pNT28) were grown for 3 d on CYE/Cm agar plates, followed by growth in AYE/Cm on a rotating wheel (80 rpm) at 37°C for 18 h. The bacteria were diluted to an OD_{600} of 0.3 in AYE/Cm, 2 ml were placed into an ibiTreat microscopy dish (ibidi) and incubated at 25°C for 24 h while avoiding mechanical disturbance. The biofilm architecture was monitored by confocal fluorescence microscopy (Leica TCS SP8 X CLSM, objective: HC PL APO CS2, 63x/1.4-0.60 oil; Leica Microsystems) by acquiring images at the dish bottom (0 µm, attachment layer) or at a level of 4 µm above the dish bottom and the 3D-images were generated using ImageJ. To assess biofilm dispersal upon addition of NO, a final concentration of 10 µM SNP dissolved in 1 ml AYE was carefully added to one day old biofilms. Biofilms were then incubated for another day at 25°C before images were acquired by confocal fluorescence microscopy as described.

Biofilm formation was quantified as described (Hochstrasser and Hilbi, 2022). Briefly, GFP-producing *L. pneumophila* strains (pNT28) were left to form biofilms at 25°C for 3 d. The biofilms were resuspended by excessive pipetting, transferred into a falcon tube, excessively vortexed, and the OD_{600} was determined (usually 3.3-4.1). Subsequently, the suspension was diluted 1:100 (2 µl beads:200 µl bacteria) with a well-mixed microsphere standard suspension (Bacteria counting kit, Invitrogen). The biofilm mass (bacteria/ml, 10^5 events) was quantified using a Fortessa II flow cytometer and Diva software. Before measuring, samples were vortexed for 8 sec. Bacteria and microsphere standard were determined employing a forward (FSC, 650V) and sideward scatter (SSC, 230V), with a threshold of 200 each, *L. pneumophila* was identified

by GFP production (Blue 530_30: 350V). The data were analyzed with the software FlowJo. The gating protocol was as follows: beads were identified using a control sample (AYE/Cm without bacteria) supplemented with beads as a reference (gate 1, FSC *vs*. SSC). The number of events counted in the microsphere gate provides an accurate estimate of the volume analyzed. The *Legionella* populations were depicted in pseudocolor graphs (gate 2, GFP *vs*. FSC) using a resuspended biofilm sample (of *L. pneumophila* strain JR32) without beads as a reference. Bacterial density in the biofilm was determined from the ratio of *L. pneumophila* (gate 2) to beads (gate 1).

The *L. pneumophila* biofilm structure was assessed by scanning electron microscopy (SEM) (Tiaden et al., 2010b). One day old biofilms were fixed with glutaraldeyde (2.5%) in cacodylate buffer, followed by treatment with Dulbecco's PBS (pH 7.35), 1% osmium, Dulbecco's PBS (pH 7.35), 70% ethanol, 100% ethanol and hexamethyldisilazane. After drying, the samples were covered with platinum and imaged by SEM.

3.6.6 Sedimentation and formation of extracellular filaments.

The sedimentation behavior of different *L. pneumophila* strains was assessed as published (Kessler et al., 2013; Tiaden et al., 2010b). Briefly, to analyze sedimentation, *L. pneumophila* strains (JR32, TKO, Δ*lqsR*) constitutively producing GFP (pNT28) were grown for 4 d on CYE agar plates, gently (without vortexing) suspended in AYE medium to a final OD_{600} of 5.0 and let sediment by gravity for 4-6 h at RT. The sedimentation rate was visualized by recording the bacterial fluorescence using a UV lamp and quantified as mm per h.

The appearance of the *L. pneumophila* strains during sedimentation was also assessed by EM (Tiaden et al., 2010b). To this end, samples were taken after 5 h of sedimentation, mounted on copper grids, stained with uranyl formate and viewed with the FEI G2 Tecnai spirit electron microscope.

3.6.7 Intracellular replication of *L. pneumophila* in macrophages.

Intracellular replication of *L. pneumophila* in macrophages was determined as published (Personnic et al., 2019; Steiner et al., 2017). Briefly, RAW 264.7 macrophages were cultivated in supplemented RPMI 1640 medium, diluted the day before infection and seeded in 96-well plates (7×10^4 cells per well). GFP-producing *L. pneumophila* strains (pNT28) were inoculated at an OD_{600} of 0.1 in AYE/Cm (5 µg/ml), grown to early stationary phase at 37°C and diluted in supplemented RPMI to yield a final MOI of 1. The infection was synchronized by centrifugation (400 × *g*, 10 min, RT). After 1.5 h, the infected cells were washed with supplemented RPMI medium, the plates were incubated at 37°C with 5% CO_2 in a humidified atmosphere, and intracellular bacterial replication was assessed by measuring GFP production with a plate reader.

3.6.8 Intracellular replication of *L. pneumophila* in *A. castellanii*.

Intracellular replication of *L. pneumophila* in *A. castellani* was determined as published (Hochstrasser et al., 2019). Briefly, the amoebae were seeded in PYG in a black clear bottom 96-well plate (2×10^4 cells/well) and left to adhere at 30°C for 24 h (cell numbers approximately doubled in this time). The media and non-adherent amoeba were aspirated, and adherent amoeba were washed with Ac buffer. GFP-producing *L.*

pneumophila (pNT28) was grown in AYE media supplemented with Cm (5 µg/ml) for 21-22 h at 37°C to early stationary phase (OD_{600} ca. 5, ~2 × 10^9 bacteria/mL). The cultures were routinely checked under the microscope (motile, non-filamentous bacteria). Cultures were diluted in Ac buffer to the desired density and used to infect the amoeba at an MOI of 1. The infection was synchronized by centrifugation (400 × *g*, 10 min, RT) and then incubated at 30°C. Intracellular bacterial replication was assessed by measuring GFP production with a plate reader.

To assess phenotypic heterogeneity, *A. castellanii* were infected with *L. pneumophila* JR32 or TKO carrying pNP107 as described above, except that culture-treated 6-well plates (VWR) were used with 8.5 × 10^5 amoeba seeded per well. The amoebae were infected at an MOI of 1, centrifuged (1000 × *g*, 10 min, RT) and incubated at 30°C for 24 h. For visualization of phenotypic heterogeneity by confocal fluorescence microscopy (Leica SP8 inverse, 63× oil objective), the infected amoebae were collected and fixed with 4% PFA (1 h), washed twice with PBS, transferred to an 18-well µ-slide dish (Ibidi) and immobilized by adding a layer of PBS/0.5% agarose.

For flow cytometry analysis of phenotypic heterogeneity, the infected amoebae were collected, lysed with 0.1% Triton TX-100 (Sigma) in 150 mM NaCl (30 min, RT), pelleted, fixed with 4% PFA (1 h), washed twice with PBS and finally collected in 0.5 ml PBS and stored at 4°C until use. A Fortessa II flow cytometer and Diva software were used to record the relevant spectral parameters. Bacterial populations were identified employing a forward (FSC, 650 V) and sideward scatter (SSC, 300 V) gating, each with a threshold of 200. The bacterial population was further examined for GFP (Blue 530_30, 700 V) and mCherry production (YG 610/20, 700V). Approximately 2 × 10^4 GFP-positive bacteria per sample were recorded. The data was analyzed using FlowJo software. The gating protocol was as follows: 1) The bacterial population was defined in a SSC-H and FSC-H pseudocolor graph, 2) GFP-positive bacteria were determined in a GFP-H vs FSC-H graph, 3) the spectral properties collected using the Timer reporter were analysed by calculating log(<Param name=”Blue 530_30-H”/>/<Param name= “YG 610_20-H”/>) and defining a growers/non-growers gate in a histogram.

3.6.9 Statistics and data availability.

Statistics were determined by a Student's *t*-test or two-way ANOVA on the means and standard deviations of three replicates, using untreated bacteria as reference value in pharmacological experiments, or compared to *L. pneumophila* JR32-infected host cells in infection experiments. The statistical analysis was performed using the GraphPad Prism (Version 9.5.1) software, and differences were deemed statistically significant when the *p*-value was less than 0.05. All data are contained within the manuscript.

3.7 Acknowledgements

The work was supported by the Swiss National Science Foundation (SNF; 31003A_175557, 310030_200706). We would like to thank Kenny Jungfer (Department of Biochemistry, UZH) for his enthusiastic help with the electron microscopy, which was performed at the Center for Microscopy and Image Analysis, UZH. We would also like to thank Helena Seth-Smith and Adrian Egli (Institute of Medical

Microbiology, UZH) for whole genome sequencing of the TKO mutant strain. The plasmid pSR47S was kindly provided by Manuela Hospenthal (ETH Zürich). The authors declare no conflict of interest.

3.8 Supporting Information

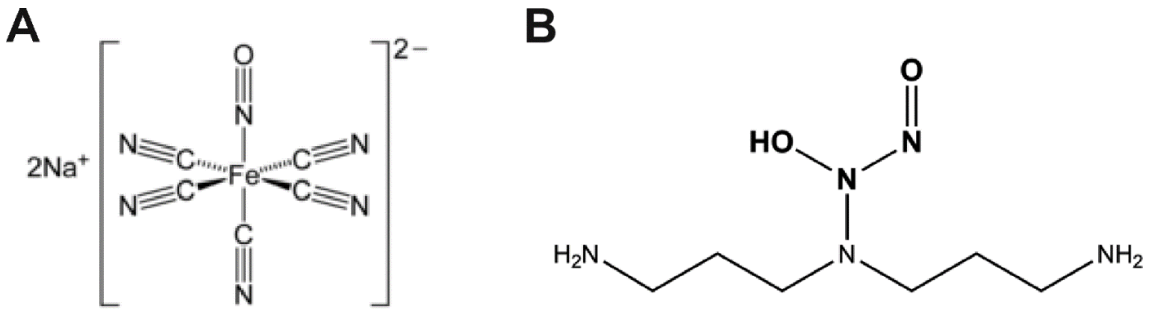

Figure S3.1. Chemical structures of NO donors used in this study.
The chemical structures of the NO donors (**A**) sodium nitroprusside (SNP) and (**B**) dipropylenetriamine (DPTA) NONOate. The NO groups released by DPTA NONOate are shown in bold.

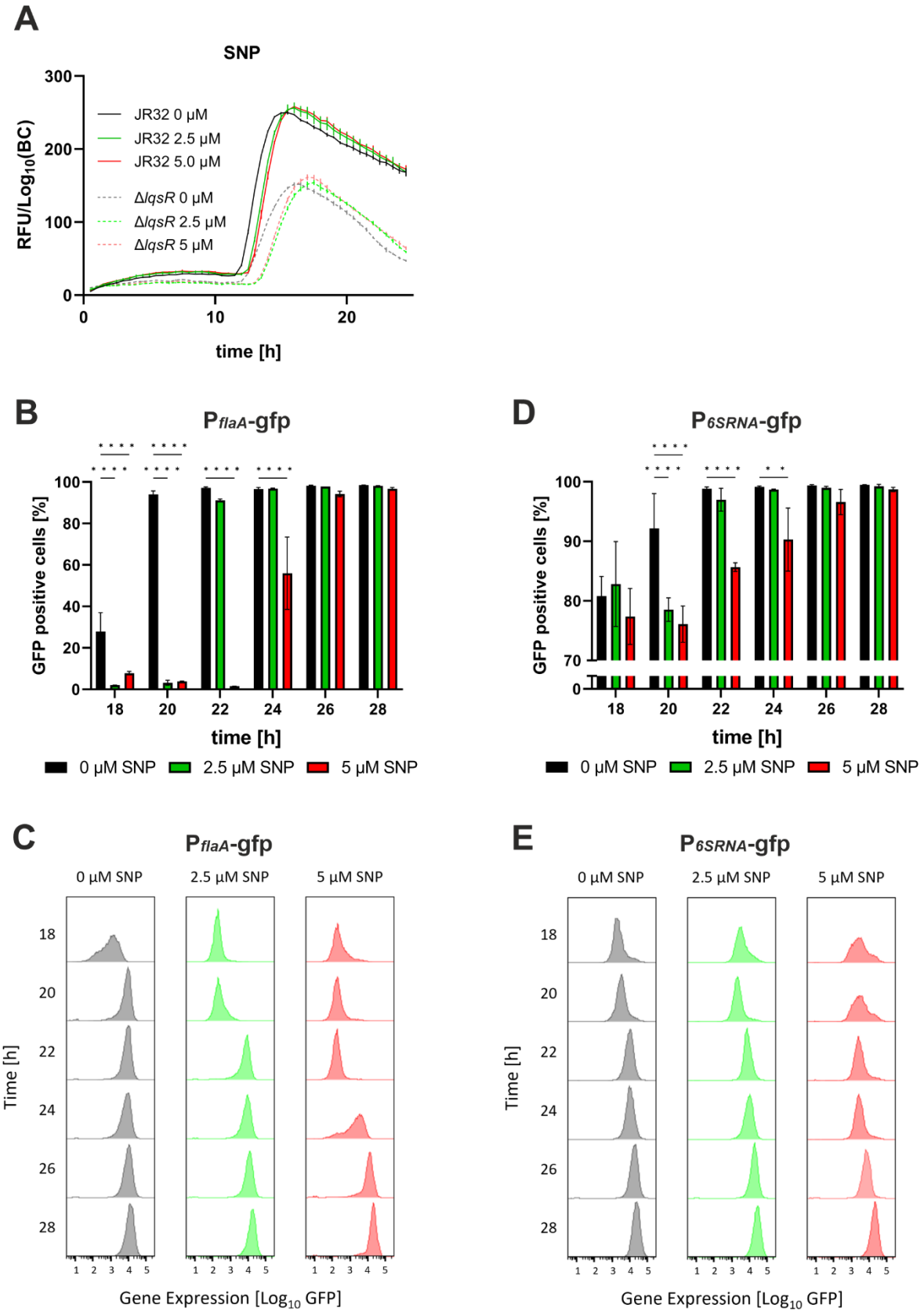
A
SNP
RFU/Log10(BC)
JR32 0 µM
JR32 2.5 µM
JR32 5.0 µM
ΔlqsR 0 µM
ΔlqsR 2.5 µM
ΔlqsR 5 µM
time [h]
B
PflaA-gfp
GFP positive cells [%]
time [h]
0 µM SNP
2.5 µM SNP
5 µM SNP
D
P6SRNA-gfp
GFP positive cells [%]
time [h]
0 µM SNP
2.5 µM SNP
5 µM SNP
C
PflaA-gfp
0 µM SNP
2.5 µM SNP
5 µM SNP
Time [h]
Gene Expression [Log10 GFP]
E
P6SRNA-gfp
0 µM SNP
2.5 µM SNP
5 µM SNP
Time [h]
Gene Expression [Log10 GFP]

Figure S3.2 (overleaf)**. Effect of SNP on P_{flaA}-*gfp* or P_{6SRNA}-*gfp* expression in *L. pneumophila*.**
(**A**) *L. pneumophila* JR32 or Δ*lqsR* harboring the P_{flaA}-*gfp* (pCM009) reporter construct were grown in AYE medium for 18 h at 37°C, inoculated in AYE medium at an initial OD_{600} of 0.2 and were grown at 30°C without (black) or with 2.5 µM (green) or 5.0 µM SNP (red). GFP fluorescence and OD_{600} were measured over time using a microplate reader. Promoter activity is inferred by *gfp* expression levels, denoted as relative fluorescence units divided by Log_{10}(bacterial counts) (RFU/Log_{10}(BC)). Data shown are means and standard deviations of technical triplicates and representative of two independent experiments. *L. pneumophila* JR32 strains harboring (**B**, **C**) P_{flaA}-*gfp* (pCM009) or (**D**, **E**) P_{6SRNA}-*gfp* (pRH049) were grown in AYE medium without addition (black) or supplemented with 2.5 µM (green) or 5.0 µM of SNP (red). Every 2 h from 18-28 h, the bacteria were fixed with PFA and stained with DAPI. The GFP signal was determined by flow cytometry. (**B**, **D**) Percentage of GFP-positive cells after restrictive gating of the bacterial population at every timepoint. Data shown are means and standard deviations of biological triplicates (*$p < 0.05$, **$p < 0.01$, ***$p < 0.001$, ****$p < 0.0001$; two-way ANOVA). (**C**, **E**) Representative histogram of the GFP signal of the whole bacterial population at every timepoint.

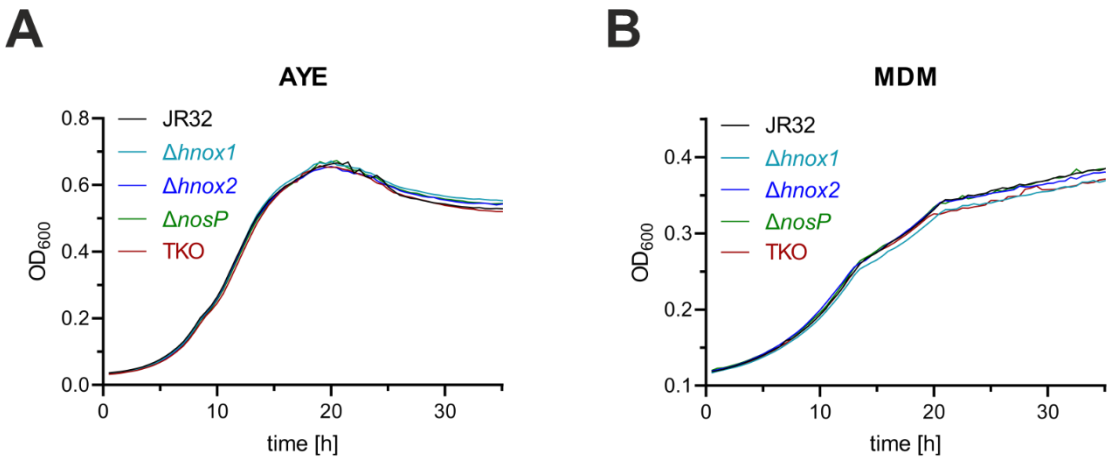

Figure S3.3. Growth of *L. pneumophila* NO receptor deletion strains in medium.
L. pneumophila JR32, Δ*hnox1*, Δ*hnox2*, Δ*nosP* or the TKO mutant strains were grown in (**A**) AYE medium or (**B**) minimal defined medium (MDM), and OD_{600} was monitored over time. Data shown are means and standard deviations of technical triplicates and representative of three independent experiments.

Figure S4

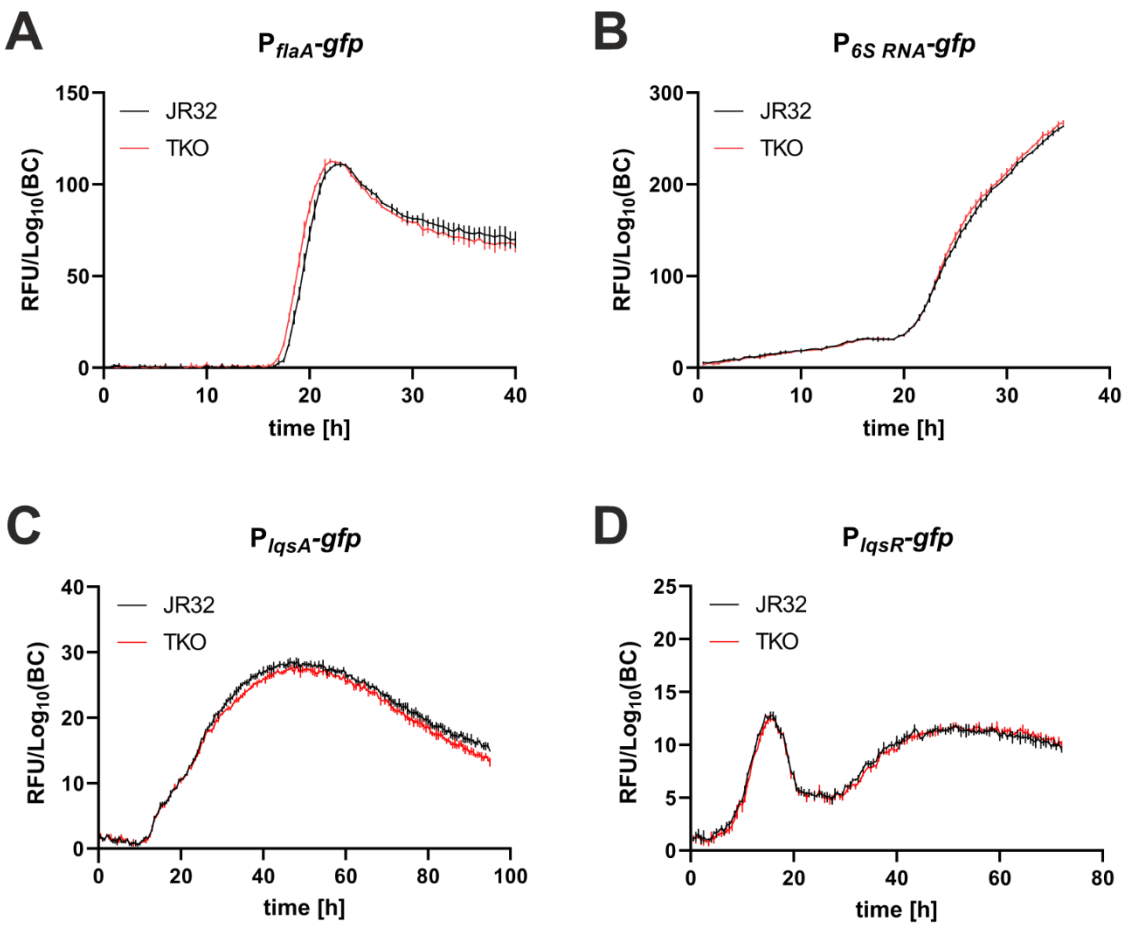

Figure S3.4. **Promoter activity in *L. pneumophila* JR32 and TKO mutants.**
L. pneumophila JR32 or TKO mutants harboring (**A**) P*flaA*-*gfp* (pCM009), (**B**) P*6SRNA*-*gfp* (pRH049), (**C**) P*lqsA*-*gfp* (pRH038), or (**D**) P*lqsR*-*gfp* (pRH037) were grown in AYE medium, and GFP fluorescence was monitored over time. Promoter activity is inferred from *gfp* expression levels, denoted as relative fluorescence units divided by $\log_{10}$(bacterial counts) (RFU/$\log_{10}$(BC)). Data shown are means and standard deviations of technical triplicates and representative of three independent experiments each.

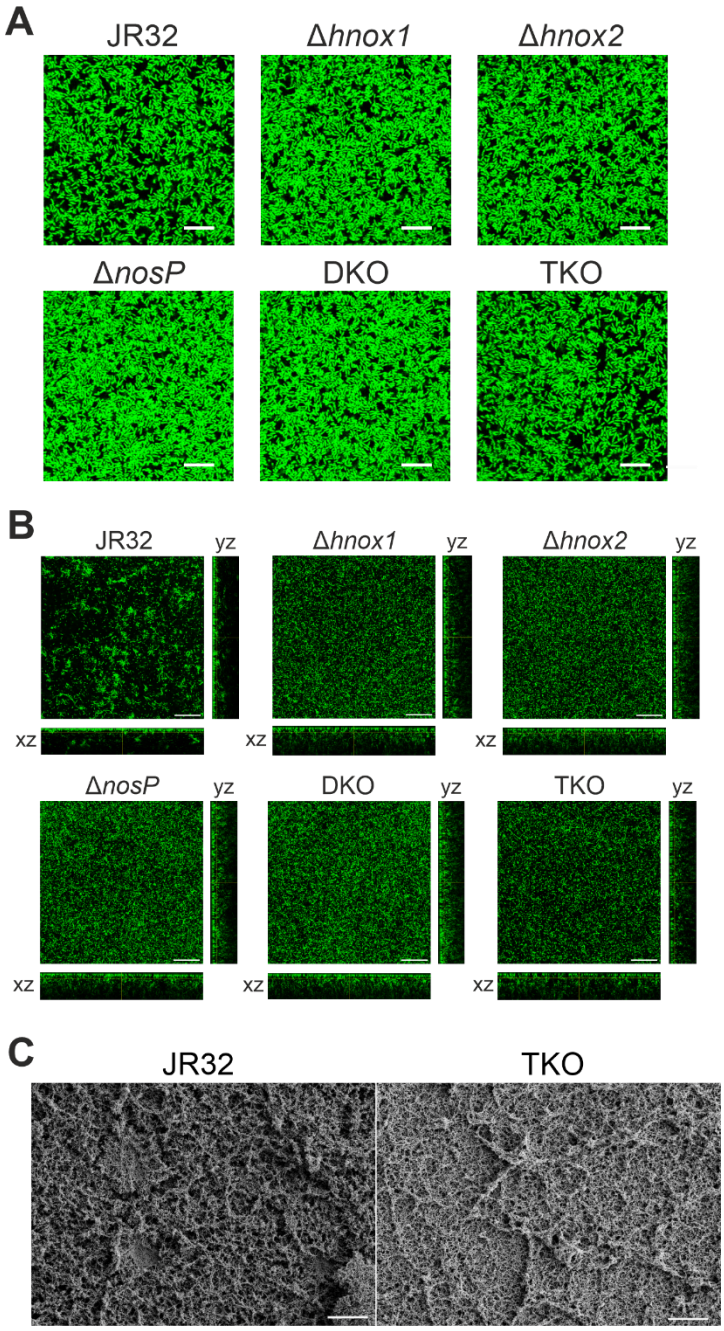

Figure S3.5. Biofilm formation of *L. pneumophila* TKO mutant strain.
(**A**) Exponential phase (18 h) GFP-producing *L. pneumophila* JR32, Δ*hnox1*, Δ*hnox2*, Δ*nosP* or TKO mutant strains harboring pNT28 were grown in ibiTreat microscopy dishes in AYE medium for 24 h. Confocal microscopy pictures were obtained (**A**) at the dish bottom (0 µm) to determine attachment of the strains to an abiotic surface and (**B**) at 4 µm above dish bottom (shown as cross-section of the xz and yz profile generated from z-stacks). Scale bars, 10 µm (A), 30 µm (B). The images shown are representative of at least 3 independent experiments. (**C**) Electron micrographs of *L. pneumophila* JR32 and TKO mutant biofilms. Biofilms grown for 24 h were fixed with glutaraldehyde (2.5%) in cacodylate buffer, dehydrated, dried, and coated with platinum before imaging by scanning electron microscopy. Scale bars, 60 µm.

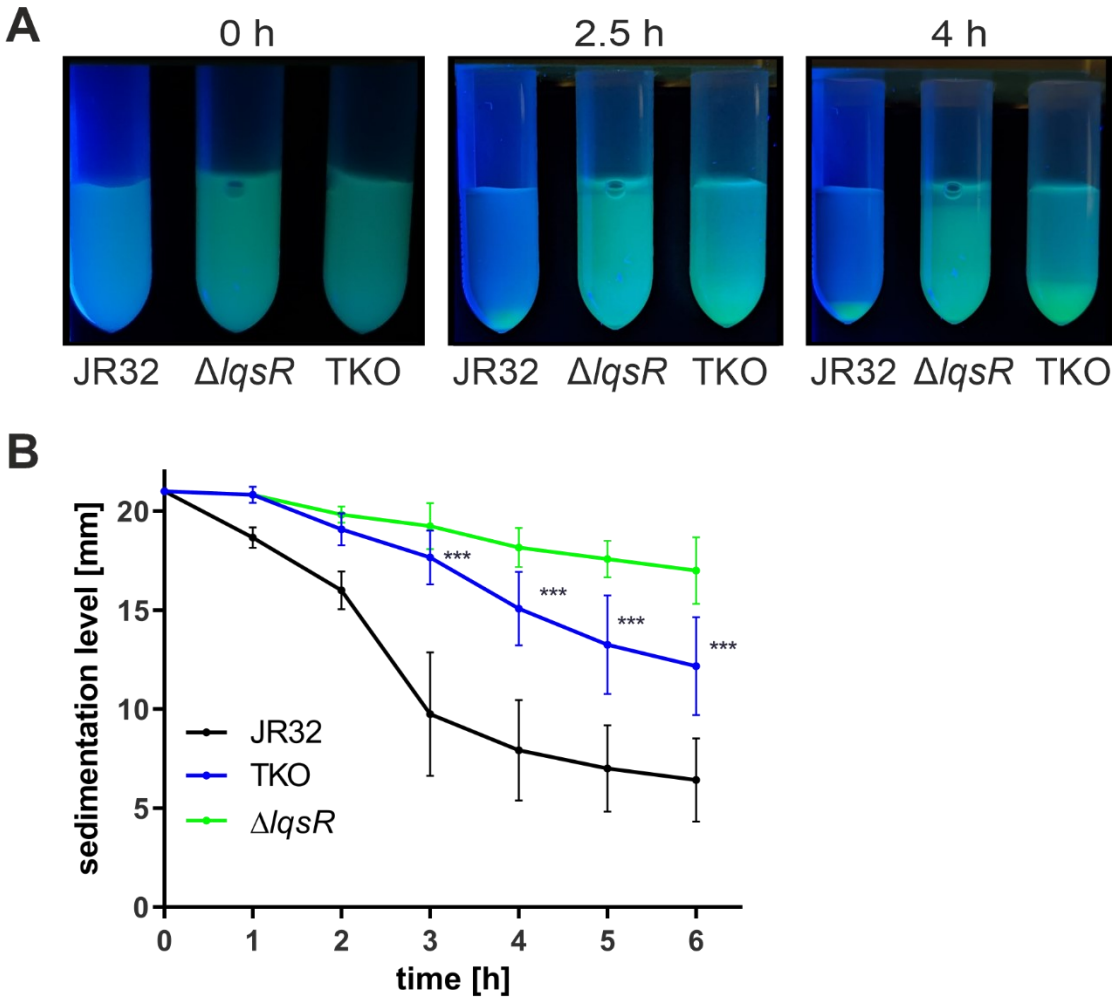

Figure S3.6. Sedimentation and formation of extracellular filaments of *L. pneumophila* TKO mutant strain.

(**A**) GFP-producing *L. pneumophila* JR32, Δ*lqsR* or TKO harboring pNT28 were grown for 4 d on CYE agar plates, gently suspended in AYE medium at an OD_{600} of 5.0 and let sediment at room temperature for the time indicated. Sedimentation was visualized by recording the bacterial fluorescence using a UV lamp. (**B**) Sedimentation kinetics (mm) over a period of 6 h. Data shown are means and standard deviations of six biological replicates (***, $p < 0.001$; two-way ANOVA comparing JR32 and TKO).

Table S3.1. Oligonucleotides used in this study.

Oligonu-cleotide	Sequence 5' - 3' [a]	Comments
oCS103	CAGGAAACAGAATTCGAGCTCAACAGGGGAATATCAGAAAAGTAG	Amplification of P_{hnox2}, overlap to pCM009 (fo)
oCS104	GCTCATATGTATATCTCCTTCTTAAATCTAGAGATGTTTTATATCAATTGATTAATACTATAAGTATAG	Amplification of P_{hnox2}, overlap to pCM009 (rev)
oCS105	CAGGAAACAGAATTCGAGCTCGCAACTTTAAAAAATGGCAAAATC	Amplification of P_{nosP} , overlap to pCM009 (fo)
oCS106	GCTCATATGTATATCTCCTTCTTAAATCTAGAATTGCTGTGACTTGGATTTATC	Amplification of P_{nosP} , overlap to pCM009 (rev)
oSM059	GTCGATCGCCCGG***GGATCC***AGTTTTTAGTTATTTTCCTCTTGAAG	Amplification of $P_{lpg1056}$-*lpg1056* (fo)
oSM060	CATTACGCGT***CTCGAG***GATCCTCACTCAAAGGTAATCTCCA	Amplification of $P_{lpg1056}$-*lpg1056* (rev)
oSM061	GTCGATCGCCCGG***GGATCC***GTATCTGAAAAATTATTGGGCAATTG	Amplification of $P_{lpg0279}$-*lpg0279* (fo)
oSM062	CATTACGCGT***CTCGAG***GATCCTTATGGACTCTCTAACAGGGTC	Amplification of $P_{lpg0279}$-*lpg0279* (rev)
oSM063	GTCGATCGCCCGG***GGATCC***TATATACAAAAATTAAAAGAAATGTTTACTCAAATG	Amplification of $P_{lpg2459}$-*lpg2459* (fo)
oSM064	CATTACGCGT***CTCGAG***GATCCTCACTCATCAGGATCGCC	Amplification of $P_{lpg2459}$-*lpg2459* (rev)
oSM113	GGATCCCCCGGGCTGCAGGAATTCG	pSR47S linearization (fo)
oSM114	CCACTAGTTCTAGAGCGGCCGCC	pSR47S linearization (re)
oSM124	GCTGGAGCTCCACCGCGGTGGCGGCCGCTCTAGAACTAGTGGTGTCCTTTTTATTGTTTTCCTGC	*hnox1* ± 950 bp with overlap to pSR47S (fo)
oSM125	GGTATCGATAAGCTTGATATCGAATTCCTGCAGCCCGGGGGATCCACCCATTCACCAATTGGAATAATC	*hnox1* ± 950 bp with overlap to pSR47S (re)
oSM126	CTGAAGACCATAGATGATCATTGTCGTTTGGAGATTACCTTTGAGTG	Exclusion of *hnox1* from pSM036 (fo)
oSM127	GACAATGATCATCTATGGTCTTCAGCATAAAACAAATCTTTAAATCCC	Exclusion of *hnox1* from pSM036 (re)
oSM130	GCTGGAGCTCCACCGCGGTGGCGGCCGCTCTAGAACTAGTGGTCTCTCACCTTGGCAGC	*nosP* ± 999 bp with overlap to pSR47S (fo)

oSM131	GGTATCGATAAGCTTGATATCGAATTCCTGCAGCCCGGGGGATCCGCATTAAGAATCACATCATGGATTG	*nosP* ± 999 bp with overlap to pSR47S (re)
oSM132	CAAGTCACAGCAATACCAAAAAGGAATTCAGTAATAATGACAGAAATG	Exclusion of *nosP* from pSM037 (fo)
oSM133	ATTCCTTTTTGGTATTGCTGTGACTTGGATTTATCTTATGATTAATTATAG	Exclusion of *nosP* from pSM037 (re)
oSM134	GCTGGAGCTCCACCGCGGTGGCGGCCGCTCTAGAACTAGTGGGTAATGATTTGGGGTAAGTTGATAG	*hnox2* ± 950 bp with overlap to pSR47S (fo)
oSM135	GGTATCGATAAGCTTGATATCGAATTCCTGCAGCCCGGGGGATCCAGTAATTTGGCCGTTGGC	*hnox2* ± 950 bp with overlap to pSR47S (re)
oSM136	CAATTGATATAAAACATCCTGATGAGTGATTATGAAGTATTGTTACG	Exclusion of *hnox2* from pSM038 (fo)
oSM137	CATAATCACTCATCAGGATGTTTTATATCAATTGATTAATACTATAAGTATAGTCG	Exclusion of *hnox2* from pSM038 (re)

[a] Restriction sites are in italics and bold, regions overlapping with destination vector pCM009 or pSR47S are underlined.

3.9 Own contributions

SM designed NO-receptor mutants and complementation plasmids (SM01-05; pSM15-17, 28, 31-32, 36-38). SM analyzed microcolony formation of the parental strain (Fig. 3.2D) and the TKO mutant (Fig. 3.3D) in absence or presence of DPTA NONOate by fluorescence microscopy. SM performed infection experiments of RAW 264.7 macrophages (Fig. 3.4A). SM quantified intracellular growth heterogeneity by flow cytometry (Fig. 3.5B-D). SM quantified biofilm mass by flow cytometry (Fig. 3.6B). SM visualized biofilms by scanning electron microscopy (Fig. S3.5C). SM analyzed sedimentation of *L. pneumophila* strains (Fig. S3.6A) and provided samples for electron microscopy (Fig. 3.6D). SM prepared the corresponding Figures and contributed to writing the manuscript.

4. Chapter four- General discussion

4.1 *Legionella*-amoeba interactions in biofilms

L. pneumophila can be found in natural and anthropogenic freshwater environments where it colonizes biofilms. Biofilms are complex, natural assemblies of microorganisms that can develop at the solid-water interface (substrate-associated biofilms) and at the water-air interface (floating biofilms) (Declerck, 2010). Within such biofilms, *L. pneumophila* likely encounters free-living amoebae, which feed on bacteria, fungi and algae (Greub and Raoult, 2004). Here, we discovered and characterized interactions between *L. pneumophila* and the amoeba *A. castellanii* within biofilms. Our main findings include (I) that LvbR, LqsR, FlaA, the IcmT/Dot T4SS and the effector LegG1 promote the migration of *A. castellanii* through *L. pneumophila* biofilms, and (II) that *L. pneumophila* forms clusters on the surface of *A. castellanii* within biofilms. Moreover, we found that cluster formation is regulated by LqsR, LvbR and FlaA and that amoeba-adherent *L. pneumophila* clusters express motility and virulence genes.

4.1.1 *A. castellanii* migration through *L. pneumophila* biofilms

L. pneumophila utilizes a regulatory network comprising the *Legionella* quorum sensing system (Lqs) and the pleiotropic transcription factor LvbR to control a wide range of traits such as bacterial motility, virulence, and biofilm architecture (**Fig. 1.3; Chapter 1.1.5**). In this study, we analyzed the migration of *A. castellanii* through different *L. pneumophila* mono species biofilms by quantifying the migration distance and velocity of amoebae. We discovered that the response regulator LqsR as well as the transcription factor LvbR, the main flagellum protein FlaA, the Icm/Dot type IV secretion system and the effector LegG1 (*lpg1976*) promote the migration of *A. castellanii* through *L. pneumophila* biofilms, as amoebae migrated more slowly through biofilms of *L. pneumophila* lacking the corresponding factors (**Fig. 2.4 and 2.5; Chapter 2.3.2 and 2.3.3**).

Previous studies in our group have shown that the pleiotropic transcription factor LvbR links the Lqs and c-di-GMP regulatory networks to control biofilm architecture and virulence. Specifically, *L. pneumophila* lacking LvbR was found to accumulate less sessile biomass and formed homogeneous, mat-like biofilms. In contrast, the parental strain developed biofilms that where characterized by compact bacterial clusters (Hochstrasser et al., 2019). Since LvbR was identified to promote amoeba migration, this suggests that the biofilm architecture might be a factor that influences the migration behavior of *A. castellanii.* Migration could be facilitated in patchy biofilms with interspersed clusters, allowing the amoebae to move faster and to cover greater distances. However, investigations of the biofilm architecture in absence of *A. castellanii* showed that the quorum sensing mutants Δ*lqsR* and Δ*lqsA* as well as the mutants Δ*icmT* and Δ*flaA* form patchy biofilms, morphologically similar to the parental strain (**Fig. 2.3; Chapter 2.3.1**). Therefore, the biofilm architecture does not seem to correlate with the migration behavior of amoebae.

Extracellular polymeric substances (EPS) are biopolymers of microbial origin that co-determine the living conditions of the biofilm organisms, e.g., by influencing porosity, density, water content and mechanical stability. EPS comprise polysaccharides, proteins, glycoprotein, glycolipids and in some cases

extracellular DNA (Flemming et al., 2007). To date, not much is known about EPS formation by *Legionella*. One study reported that biofilms showed a mycelial mat-like structure and a thin layer of a ruthenium red-stainable substance (possibly polysaccharides) (Piao et al., 2006). Furthermore, the sensor kinase LqsS and the response regulator LqsR were shown to control sedimentation and extracellular filaments of *L. pneumophila* (Tiaden et al., 2010b). Future studies could focus on the characterization of these extracellular filaments. Fractions of EPS (e.g., proteins, saccharides) can be analyzed with colorimetric methods, e.g., the Lowry method, the bicinchoninic acid (BCA) assay and the phenol sulfuric acid method (Felz et al., 2019).This could help to identify components that mediate the migration behavior of amoebae in *L. pneumophila* biofilms.

4.1.2 *L. pneumophila* cluster formation on *A. castellanii*

Our studies on *Legionella*-amoebae interactions within biofilms also revealed that *L. pneumophila* forms bacterial aggregates on the surface of *A. castellanii* (**Fig. 2.6; Chapter 2.3.4**). The bacterial clusters preferentially decorated the lagging end of the moving amoebae. Furthermore, trails of migrating amoebae were visible in the biofilms formed by the parental strain JR32 (**Movie S2.4; Chapter 2.3.2**). In biofilms formed by the Δ*lvbR* mutant bacterial clusters were barely present and much smaller. Interestingly, *L. pneumophila* did not form clusters in biofilms produced by the Δ*lqsR* and the Δ*flaA* mutant strains, indicating that the formation of bacterial clusters depends on the corresponding proteins (**Fig. 2.6; Chapter 2.3.4**). We further characterized amoeba-adherent *L. pneumophila* clusters by analyzing the activity of promoters serving as prototypic proxies for motility (P_{flaA}), virulence (P_{sidC}, P_{ralF}), stress response (P_{6SRNA}) or replication (P_{csrA}). These investigations revealed that amoeba-adherent *L. pneumophila* clusters express motility (P_{flaA}) and virulence genes (P_{sidC}, P_{ralF}), whereas P_{6SRNA} and P_{csrA} were less or not active (**Fig. 2.7; Chapter 2.3.5**).

In future experiments, the timer reporter as a readout for the growth rate could be examined for its expression in the bacterial clusters on amoebae. This could reveal whether bacterial cluster formation on the surface of amoebae is a random process or regulated by the growth phase of *L. pneumophila*. Moreover, cluster formation and amoeba migration in biofilms formed by the mutants Δ*hnox1*, Δ*hnox2* or Δ*nosP* could be investigated. The three NO receptor mutants all form mat-like biofilms (**Fig. 3.6; Chapter 3.4.6**). It would be interesting to see whether these mutants also exhibit the same bacterial clusters and amoebae migration phenotype as the Δ*lvbR, Δlqs*R *or* Δ*flaA* mutant strains, especially since our investigations revealed that one of the NO receptors, NosP, negatively regulates LvbR (**Fig. 3.3B; Chapter 3.4.2**).

Adhesion to host cells is considered an essential step for infection by *L. pneumophila*. However, only a few mediators of *L. pneumophila* adherence to host cells are known (Chang et al., 2005; Duncan et al., 2011). The *Legionella* collagen-like protein (Lcl) was shown to play a role in *L. pneumophila* adhesion and invasion of host cells. The corresponding gene, *lpg2644*, encodes an outer membrane motif and contains a collagen-like repeat region (Vandersmissen et al., 2010). Moreover, Lcl of *L. pneumophila* was shown to play a role in biofilm formation, as a Δ*lpg2644* mutant was impaired in biofilm formation (Duncan et al.,

2011). Interestingly our results from comparative proteomics revealed that Lcl was less abundant in biofilms formed by the Δ*lvbR* mutant compared to the parental strain (**Fig. S2.1; Chapter 2.7**). Consequently, lower amounts of Lcl in the Δ*lvbR* mutant may contribute to the mat-like architecture of the Δ*lvbR* strain or to the reduced cluster formation of this mutant.

Other factors that mediate *L. pneumophila* adhesion to host cells include LaiA, RtxA, Hsp60 and $PilE_L$. The *L. pneumophila* gene *rtxA*, encodes a "repeats in structural toxin" (RTX) and has been shown to be involved in adherence, cytotoxicity, pore formation, intracellular replication, and virulence in mice (Cirillo et al., 2001). Another molecule reported to be involved in adhesion is called *L. pneumophila* adhesion molecule homologous with integrin analogue of *S. cerevisiae* (LaiA) (Chang et al., 2005). Furthermore, the chaperonin Hsp60 is displayed on the surface of virulent *L. pneumophila* and has been shown to mediate invasion in a HeLA cell model (Garduño et al., 1998). In addition, a gene in *L. pneumophila* with homology to the type IV pilin genes ($pilE_L$) was found to be involved in adherence to human epithelial cells, macrophages and *Acanthamoeba polyphaga* (Stone and Kwaik, 1998). In further studies, the potential involvement of the adhesion mediators in bacterial cluster formation on *A. castellanii* could be analyzed. To measure the promoter activity of these genes within bacterial clusters, fluorescent reporters of P_{lcl}, P_{laiA}, P_{rtxA}, P_{hsp60} and P_{pilEL} could be cloned. In addition, knockout mutants (Δ*lcL*, Δ*laiA*, Δ*rtxA*, Δ*hsp60* and Δ$pilE_L$) could be generated and examined for their ability to form bacterial clusters on the amoeba.

Bacterial cluster formation on the surface of *A. castellanii* has been previously reported. In fact, *A. castellanii* forms large aggregates of densely packed *Listeria monocytogenes* on its surface, so called "backpacks" to capture and feed on the bacteria (Doyscher et al., 2013). The assembly of backpacks was suggested to be dependent on bacterial motility. Since *L. monocytogenes* is Gram-positive and *L. pneumophila* is Gram-negative, the bacterial cell wall does not seem to determine the formation of backpacks. Later, it was discovered that the dynamics of *L. monocytogenes* capturing by *A. castellanii* are controlled by random encounters, which are further enhanced by bacterial motility. In addition, a role for amoeboid locomotion in the assembly of trapped bacteria into backpacks was suggested (de Schaetzen et al., 2022). Our studies on amoeba-*L. pneumophila* interactions in biofilms showed that LvbR, LqsR and the major flagellar component flagellin (FlaA/FliC) determine the formation of *L. pneumophila* clusters on *A. castellanii.* (**Fig. 2.6; Chapter 2.3.4**). In addition, our results from comparative proteomics revealed that FlaA (Lpg1340) is depleted in biofilms formed by the Δ*lvbR* or the Δ*lqsR* mutant strains (**Fig. S2.1; Chapter 2.7**). Furthermore, the expression of a P_{flaA}-*gfp* reporter construct was delayed and downregulated in the Δ*lvbR* and Δ*lqsR* mutant strains (**Fig. 2.2C; Chapter 2.3.1**) and the mutants showed reduced motility in AYE medium (**Movies S2.2 and S2.3; Chapter 2.7**). Taken together, the results indicate that LqsR and LvbR function as positive regulators of FlaA production and *flaA* transcription. Hence, the formation of clusters on *A. castellanii* seems to depend on or be promoted by bacterial motility or the flagellum in *L. monocytogenes* as well as in *L. pneumophila*. However, in contrast to *L. pneumophila*, *L. monocytogenes* does not seem to be able to infect *A. catellanii*. Instead, backpacking appears to be an effective strategy of the amoebae to capture bacteria, which are subsequently phagocytosed and digested (Doyscher et al.,

2013). For *L. pneumophila*, the function of clusters formation on amoebae remains unclear and requires further investigation. However, it is possible that *Legionella* uses the formation of cluster to its own advantage, e.g., to promote its uptake into the host cell or to spread within the biofilm.

Considering the fact that *L. pneumophila* is highly fastidious when being cultivated in the laboratory, it is expected that the bacterium colonizes pre-established microbial structures under natural conditions, where biofilms mostly occur as complex, species-rich communities (Declerck, 2010). Under dynamic flow conditions *L. pneumophila* does not form robust biofilms (Mampel et al., 2006). However, *L. pneumophila* seems to be able to colonize biofilms formed by certain bacteria such as *Microbacterium* sp., while other species such as *Klebsiella pneumoniae* decreased the persistence of *L. pneumophila* in a flow chamber system. These findings suggest that specific interactions between *L. pneumophila* and other bacteria modulate colonization (Mampel et al., 2006). Since biofilms often occur as complex multispecies communities, it would be interesting to investigate bacterial cluster formation of *L. pneumophila* and amoeba migration in a more realistic experimental set-up with biofilms containing additional bacterial species.

L. pneumophila, *Mycobacterium avium*, *Pseudomonas aeruginosa* and many other bacterial species belong to the group of amoeba-resistant bacteria. Amoebae function as an important reservoir for these microorganisms and may protect them from antibacterial treatment, e.g., with chlorine, antibiotics, or biocides. While some of these pathogens are considered as endosymbionts, others such as *Legionella* spp. lyse their host cells (Greub and Raoult, 2004). In our study, we investigated the interactions between the amoeba *A. castellanii* and *L. pneumophila* within biofilms, which were characterized by the formation of bacterial clusters on the surface of the amoeba. Further investigations on EPS components could help to identify factors that account for the differential migration behavior of amoeba in biofilms formed by distinct *L. pneumophila* (mutant) strains. In addition, the role of adhesins in amoeba migration and bacterial cluster formation could be investigated. Since *Legionella*-amoeba interactions in biofilms may contribute to the survival and proliferation of the pathogen, a detailed knowledge of these interactions is important to provide a scientific background for the development of efficient control measures.

4.2 Nitric oxide signaling in *L. pneumophila*

Nitric oxide (NO) is an uncharged highly diffusible gas molecule with one unpaired electron, that is, NO is a radical molecule. The diatomic gas functions as a cytotoxic agent at high (micromolar) concentrations and acts as a signaling molecule at low (nanomolar) concentrations (Derbyshire and Marletta, 2009; Sasaki et al., 2016). Bacteria may be exposed to NO from endogenous (e.g., denitrification) or exogenous sources (e.g., produced by the NO synthases of the host cell). Eukaryotes employ the NO receptor soluble guanylyl cyclase (sGC), , which responds to picomolar amounts of NO. sGC comprises a heme-binding domain, that is a member of the H-NOX (heme-nitric oxide and oxygen binding domain) family (Williams and Boon, 2019). H-NOX proteins are also encoded in bacterial genomes. In fact, over 250 bacterial species are known to contain H-NOX proteins (Plate and Marletta, 2013). More recently, an additional bacterial NO-

sensor was discovered, termed NO sensor protein (NosP), which is more widely conserved among bacteria and has been found in more than 800 bacterial species (Williams and Boon, 2019).

The facultative intracellular, opportunistic pathogen *L. pneumophila* possesses both H-NOX and NosP NO sensors. In fact, the *L. pneumophila* genome encodes two H-NOX proteins: Hnox1 and Hnox2 (Carlson et al., 2010). Interestingly, the pleiotropic *Legionella* transcription factor LvbR was found to negatively regulate the expression of the NO receptor Hnox1, thereby linking quorum sensing to NO signaling (Hochstrasser et al., 2019). In this work, we investigated the response of *L. pneumophila* to NO and the bacterial receptors involved in NO-signaling using pharmacological, genetic and cell biological methods. Our main findings include: (I) Chemical NO donors delay and reduce the expression of the promoters P_{flaA} and P_{6SRNA}, (II) in a marker-less *L. pneumophila* mutant lacking *hnox1*, *hnox2* and *nosP* (triple knockout, TKO), the reduction of P_{flaA} expression by NO is less pronounced, (III) the *lvbR* promoter is upregulated in a mutant lacking the NO receptor NosP, (IV) the NO receptor mutant strains are impaired for intracellular replication in macrophages and amoebae, (V) the intracellular growth heterogeneity in amoeba is regulated by NO signaling, and (VI) the NO receptor mutants form mat-like biofilms and are no longer responsive to NO.

4.2.1 Nitric oxide modulates *flaA* and *6SRNA* promoter expression in *L. pneumophila*

To study the effects of NO on biological targets NO releasing agents are often employed as an experimental tool (Schröder, 2006). Major classes of current NO donors have different structures, chemical reactivities and NO-release kinetics (Wang et al., 2002). In this study, two different chemical NO generators were employed to assess the response of *L. pneumophila* to NO. One of the pharmacological NO donors we used is the metal nitrosyl compound sodium nitroprusside ($Na_2[Fe(CN)_5NO]$, SNP). SNP has been used for many decades in a clinical context to reduce blood pressure. During SNP decomposition, in addition to NO, other biologically active products such as cyanide and free iron are generated in addition to NO (Kim et al., 2006; Schröder, 2006; Wang et al., 2002). Therefore, caution is required when interpreting biological effects of SNP as a result of NO release. In previous studies, the release of NO from SNP in solution was quantified with an NO electrode. Accordingly, an approximately 1000-fold linear relationship between the NO donor concentrations and the NO levels can be expected (Barraud et al., 2009a; Barraud et al., 2009b).

A different class of NO donors comprise the so called “NONOates” (1-substituted diazen-1-ium-1,2-diolates). DPTA NONOate ((*Z*)-1-[*N*-(3-Aminopropyl)-N-(3-ammoniopropyl)amino]diazen-1-ium-1,2-diolate) is an NO donor that dissociates in a pH-dependent process, with a half-life of three hours at 37 °C (Keefer et al., 1996). Choosing a proper control when performing experiments with NO donors is critical. In our study, we allowed the compound to decompose before adding it to the bacterial sample, by dissolving it in phosphate buffered saline (PBS) at a low pH of 5.0 (instead of pH 7.4). The “spent” DPTA NONOate was used as a control and is supposed to contain all decomposition by-products.

To investigate the response of *L. pneumophila* to pharmacological generated NO, we used both NO donors, SNP and DPTA NONOate. In particular, we measured the effect of chemically generated NO on the expression of *gfp* under control of the promoters for flagellin (P_{flaA}), the 6S small regulatory RNA

(P_{6SRNA}), the effector protein SidC (P_{sidC}), or the NO receptor Hnox1 (P_{hnox1}) (**Fig. 3.2A; Chapter 3.4.1**). Interestingly, SNP dose-dependently delayed the expression of P_{flaA} and P_{6RNA} but had no effect on the production of *gfp* under the control of P_{sidC} or P_{hnox1}. Confirmatory results were obtained by quantifying GFP production under control of P_{flaA} or P_{6SRNA} by flow cytometry (**Fig. S.3.2B-E; Chapter 3.7**). To validate these results, we employed another NO donor and examined the expression of P_{flaA}-*gfp* in the presence of DPTA NONOate (**Fig. 3.2B; Chapter 3.4.1**). Also in this case, DPTA NONOate delayed the production of GFP under the control P_{flaA} in a dose-dependent manner. In addition, at a concentration of 400 µM DPTA NONOate, GFP production was reduced. In contrast, "spent" DPTA NONOate, which was used as a control, had no effect on the production of P_{flaA}-GFP (**Fig. 3.2C; Chapter 3.4.1**). Furthermore, we studied the effect of DPTA NONOate on the expression of *gfp* under control of P_{flaA} in sessile microcolonies (**Fig. 3.2D; Chapter 3.4.1**). Again, the treatment with DPTA NONOate caused a dose-dependent delay in P_{flaA}-*gfp* expression. Together, the results indicate that the pharmacological NO donors delay and reduce the expression of P_{flaA}.

In future experiments, it would be interesting to study the NO-concentration within *L. pneumophila*. So far, the NO release form chemical NO donors and the amount of NO that enters bacteria can only be estimated. The iGEM (internationally genetically engineered machine) team IBD NanoBiotics 2022 at the University of Zurich, has engineered probiotic *E. coli* Nissle 1917 strains with genetic circuits designed to secrete anti-TNF-α nanobodies in response to NO. TNF-α is a pro-inflammatory cytokine that regulates the secretion of the inflammation marker NO by gut epithelial cells. Accordingly, the engineered *E. coli* strain constitutes a negative feedback loop that represses TNF-α stimuli to repress inflammatory responses. The designed NO sensory system was inspired by the naturally occurring NOR-pNorV NO sensing unit from *E. coli*, a NO sensitive transcription regulatory unit that controls NO detoxification pathways (Chen et al., 2021). The iGEM team developed a promoter construct (pNorVβ) that can induce GFP expression in *E. coli* Nissle 1917 upon induction with the NO donor DETA/NO in a concentration-dependent manner (EC_{50} of ca. 335 µM DETA/NO) (unpublished).

Similar biosensors could be developed for use in *L. pneumophila* to quantify NO released by chemical NO donors or NO-producing host cells. In fact, reporter constructs that allow to determine the intracellular concentration and maybe even localization of NO in the bacteria would be a very helpful tool to investigate NO-dependent signaling pathways in *L. pneumophila.*

4.2.2 The expression of the promoters *flaA* and *lvbR* is regulated by NO receptors

To characterize the pathways underlying NO-signaling, we constructed marker-less *L. pneumophila* mutant strains lacking the NO receptors Hnox1, Hnox2 and NosP. The *hnox1* gene of *L. pneumophila* localizes adjacent to a diguanylate cyclase gene. The hnox2 gene is located adjacent to a histidine kinase and a single domain response regulator (Carlson et al., 2010). H-NOX proteins are often encoded by genes in a putative operon and upstream of a predicted histidine kinase in facultative aerobes. For instance, an H-NOX protein from *Shewanella oneidensis* (SO2144) was shown to interact directly with a sensor histidine kinase

(SO2145). Furthermore, it was found that the *S. oneidensis* H-NOX protein binds NO (but not O_2) and in this form inhibits the autophosphorylation of the histidine kinase (Price et al., 2007).

The third *L. pneumophila* NO sensor, NosP (Lpg0279) is encoded in a putative operon with a histidine kinase NahK (Lpg0278) and the c-di-GMP-metabolizing response regulator NarR (Lpg0277) (Fischer et al., 2019). In general, *nosP genes* exhibit similar operon arrangements as *hnox* genes, and are predicated to be co-cistronic with genes encoding methyl-accepting chemotaxis proteins, histidine kinases, and c-di-GMP metabolizing enzymes (Bacon et al., 2017).

To generate single (Δ*hnox1*, Δ*hnox2*, Δ*nosP*), double (Δ*hnox1*Δ*nosP*) and triple knockout mutant (Δ*hnox1*Δ*hnox2*Δ*nosP*) strains, the suicide plasmid pSR47S was used. The scar-free genomic deletion method was established in our laboratory as part of this project and has the advantage that it allows to delete several genes without inserting antibiotic resistance cassettes into the genome. In the Δ*hnox1 and* Δ*hnox2* mutants the overlapping regions with adjacent genes were kept. The single and triple knockout strains all grew like the parental strain in AYE and minimal defined (MDM) medium (**Fig. S3.3; Chapter 3.7**). Interestingly, the P_{lvbR} promoter was only expressed in the Δ*nosP* mutant and the TKO mutant, but not in the parental strain or the Δ*hnox1* and Δ*hnox2* mutant strains, indicating that NosP negatively regulates LvbR (**Fig. 3.3B; Chapter 3.4.2**). It has already been shown in *L. pneumophila* that the transcription factor LvbR links the Lqs and the c-di-GMP regulatory network by inhibiting the transcription of the NO receptor Hnox1 (Hochstrasser et al., 2019). In other bacterial species, including *Vibrio harveyi*, a number of traits such as bioluminescence and motility were shown to be regulated by an NO-mediated quorum sensing pathway (Heckler and Boon, 2019).

Furthermore, we exposed the TKO mutant and the parental strain expressing P_{flaA}-*gfp* to DPTA NONOate. Following treatment with the NO donor both strains showed a delay in GFP production. Yet, in the TKO strain the reduction of P_{flaA} expression by DPTA NONOate was absent, indicating that the NO receptors are involved in NO signaling (**Fig. 3.3C; Chapter 3.4.3**). Similar results were obtained when the effect of DPTA NONOate on P_{flaA}-*gfp* expression was examined in microcolonies formed by the parental strain and the TKO mutant (**Fig. 3.3D; Chapter 3.4.3**). Here, the treatment with DPTA caused a delay of GFP production, however, the reduction of GFP by the NO donor was reduced in the TKO strain at later time points. Taken together, these results suggest that the NO receptors are involved in NO signaling by regulating the expression of P_{flaA}-*gfp*. It would be interesting to test whether the regulation of the *flaA* promoter is also reflected in the mobility behavior of the mutants. Low concentrations of NO have been shown to regulate motility in other microorganisms, including *P. aeruginosa* (Barraud et al., 2006). To assess the effects of NO on motility, the bacteria were exposed to the NO donors SNP and S-nitroso-l-glutathione (GSNO), and the NO scavenger 2-phenyl-4,4,5,5-tetramethylimidazoline-1-oxyl-3-oxide (PTIO) was also employed. Both swimming and swarming mobility were enhanced by the NO donors, while the effects were abolished in presence of the NO scavenger (Barraud et al., 2006). Similar experiments were performed to investigate the effects of synthetic LAI-1 on *L. pneumophila* motility (Schell et al., 2016). To this end, migration distance and velocity of single bacteria were quantified, in different genetic background

and in the presence or absence of LAI-1. Analogous experiments with chemical NO donors would reveal whether NO-signaling directly affects motility or whether it is only involved in regulating the promoter activity of *flaA*.

4.2.3 *L. pneumophila* NO receptors regulate intracellular replication and heterogeneity

To further characterize the functions of the *L. pneumophila* NO receptors, we investigated if the NO receptors are involved in host-pathogen interactions. For this purpose, we infected RAW 264.7 macrophages and *A. castellanii* with the single and the triple NO receptor mutant strains. In macrophages and *A. castellanii*, all NO receptor mutants were impaired for intracellular replication compared to the parental strain (**Fig. 3.4AB; Chapter 3.4.4**). The intracellular replication phenotype of the deletion mutants Δ*hnox1*, Δ*hnox2* and Δ*nosP* in *A. castellanii* could be restored wild-type levels by introducing a single copy of the deleted gene into the genome (**Fig. 3.4C; Chapter 3.4.4**). Remarkably, however, the growth defect of the triple mutant could not be complemented by re-introducing the single NO receptor genes, suggesting that the three NO receptors have non-redundant functions (**Fig. 3.4D; Chapter 3.4.4**). Future experiments could address the question whether host cell-derived NO regulates the intracellular fate of *L. pneumophila*. To this end, bone marrow-derived macrophages from mice that lack functional iNOS (inducible NO synthase) could be obtained and infected with *L. pneumophila* wild-type or NO receptor mutant strains. In addition, NO within phagocytes could be quantified using the membrane permeable fluorescent dye 4,5-diaminofuorescein (DAF-2) (Kojima et al., 1998).

Previous studies in our laboratory have shown that the Lqs system regulates the formation of virulent *Legionella* persisters within infected cells and, towards the end of an infection cycle, the formation of a transmissive subpopulation at the periphery of the LCV (Personnic et al., 2019; Striednig et al., 2021). Using the timer reporter as a proxy for the growth rate, we investigated in this study whether the NO receptors influence the ratio of growing to non-growing intracellular *L. pneumophila*. For this purpose, we infected *A. castellanii* with timer-producing *L. pneumophila* wild-type and the TKO mutant and assessed the ratio of growing (green) and non-growing (red) intracellular bacteria by microscopy (**Fig. 3.5A; Chapter 3.4.5**). In the TKO, a larger portion of the intracellular bacteria appeared to be growing than in the parental strain, indicating that NO signaling positively regulates the emergence of non-growing intracellular bacteria. In addition, quantification by flow cytometry revealed that NO-signaling positively regulates the ratio of non-growing to growing *L. pneumophila* (**Fig. 3.5B-D; Chapter 3.4.5**). Taken together, we showed, that phenotypic heterogeneity of non-growing/growing bacteria in amoeba was regulated by the NO receptors. In future studies, the non-growing *L. pneumophila* subpopulation could be characterized in more detail. It would be interesting to assess whether the non-growing bacteria are antibiotic resistant (persisters) and whether this subpopulation is virulent and motile.

Macrophages produce iNOS to generate NO as part of the immune response against intracellular pathogens. The gene expression of iNOS depends on lipopolysaccharides (LPS) and various pro-inflammatory cytokines including tumor necrosis factor alpha (TNF-α) and interferon-γ (IFN-γ) (Salim et al., 2016). Previous studies in our laboratory have shown that the activation of macrophages by the pro-

inflammatory cytokine IFN-γ leads to an increase in antibiotic-tolerant *L. pneumophila* persisters, likely due to a higher portion of intracellular non-growers as compared with naïve macrophages (Personnic et al., 2019). Further studies could investigate whether prior activation with IFN-γ also modulates the ratio of intracellular growers to non-growers in macrophages infected with the *L. pneumophila* NO receptor mutants.

4.2.4 The *L. pneumophila* NO receptors regulate biofilm architecture

In water systems, *Legionella* often colonizes biofilms, microbial communities that are embedded in extracellular polymeric substances (EPS) (Taylor et al., 2009). The association with biofilms can be advantageous for bacteria by providing high tolerance to biocides, antibiotics, and host defenses (Barraud et al., 2009b). Several studies have shown that non-toxic NO concentrations can induce biofilm dispersal (Williams and Boon, 2019). For instance, the exposure to low concentrations of NO donors induced removal of biofilms formed by Gram-positive bacteria (*Staphylococcus epidermis*, *Bacillus licheniformis*), Gram-negative bacteria (*Serratia marcescens*, *Vibrio cholerae*, *Fusobacterium nucleatum*, *Escherichia coli*) and yeast (*Candida albicans*) (Barraud et al., 2009b). In many species this happens via binding of NO to the sensors NosP or H-NOX, which seems to trigger a downstream response based on changes in the c-di-GMP level and/or the modulation of quorum sensing (Williams and Boon, 2019).

In this study, we investigated the role of the three NO receptors Hnox1, Hnox2 and NosP for *L. pneumophila* biofilm formation. Interestingly, the single NO receptor and TKO mutant strains showed an altered biofilm phenotype, reflected in a “matt-like” architecture (**Fig. 3.6A; Chapter 3.4.6**). Biofilms formed by the parental strain exhibited a “patchy” architecture, which has been reported before (Hochstrasser et al., 2019). In addition, the biomass of biofilms formed by the NO receptor mutants was larger compared to the parental strain (**Fig. 3.6B; Chapter 3.4.6**). Moreover, we investigated whether *L. pneumophila* NO signaling is involved in regulating biofilm dispersal. To this end, we exposed the biofilms to chemically generated NO by adding the NO donor SNP. Interestingly, SNP caused dispersal of the biofilm formed by the parental strain, while biofilms formed by the NO receptor mutants did not respond to the addition of the NO donor (**Fig. 3.6C; Chapter 3.4.6**). Taken together, the findings suggest that the NO receptors are involved in NO signaling and the regulation of biofilm dispersal.

The Δ*hnox1* mutant has been previously shown to display a hyper-biofilm phenotype. Consistent with the Hnox1 regulation of the GGDEF-EAL protein Lpg1057, the additional deletion of *lpg1057* in the Δ*hnox1* background resulted in reversion of the hyper-biofilm phenotype back to the wild-type level. Furthermore, overexpression of Lpg1057, resulted in a hyper-biofilm phenotype (Carlson et al., 2010). Experiments in the *L. pneumophila* Lens strain revealed that Lpl1054 (Lpg1057 in *L. pneumophila* Philadelphia 1) is a positive regulator of biofilm formation as the Δ*lpl1054* strain formed thinner biofilms compared to the wild-type. However, the measured intracellular concentration of c-di-GMP of the Δ*lpl1054* mutant was not significantly different from the wild-type (Pecastaings et al., 2016). This raises the question about the relationship between c-di-GMP levels and biofilm formation in *L. pneumophila.* Following the scheme, the presence and detection of NO (by the NO receptors Hnox1 and NosP) and the bacterial c-di-GMP level are

inversely correlated (**Fig. 1.4; Chapter 1.1.6**). The correlation between high c-di-GMP concentrations and biofilm formation has been shown in many bacterial species including *P. aeruginosa* and *Salmonella enterica* serovar Typhimurium (Valentini and Filloux, 2016). In our studies, the addition of the chemical NO donor SNP caused biofilm dispersal of the parental strain (**Fig. 3.6C; Chapter 3.4.6**). This could be due to reduced c-di-GMP levels in response to NO, as low levels of intracellular c-di-GMP have been shown to correlate with motility or biofilm dispersal in other bacteria (Fischer et al., 2019; Valentini and Filloux, 2016). Future studies could investigate the intracellular c-di-GMP levels of *L. pneumophila* biofilms formed by the wild-type or the NO receptor mutants in absence and presence of NO. A golden standard for the identification and quantification of c-di-GMP is the analysis of bacterial extracts via LC/MS/MS, which is highly sensitive (Irie and Parsek, 2014; Rybtke et al., 2017). Recently, a novel biosensor has been developed that allows to monitor c-di-GMP levels in *Caulobacter crescentus* and *P. aeruginosa* and could potentially become a useful tool to study the function and mechanisms of c-di-GMP in a variety of bacteria. To generate the biosensor, the C-terminal c-di-GMP binding domain (CTD) of the transcription factor BldD ($BldD^{CTD}$) was fused to both termini of a circularly permuted enhanced green fluorescent protein (cpEGFP). BldD is monomeric in absence of c-di-GMP but dimerizes in the presence of the second messenger. Upon dimerization, the cpEGFP moiety undergoes a conformational change that leads to an increased fluorescence intensity (Kaczmarczyk et al., 2022). Furthermore, RNA-based fluorescent biosensors have been developed to monitor population dynamics of c-di-GMP signaling by flow cytometry (Yeo et al., 2017). The quantification of intracellular c-di-GMP levels in the mutant strains and upon NO exposure will contribute to the understanding of the NO singling regulatory networks and biofilm dynamics in *L. pneumophila*.

4.2.5 NO and LAI-1 regulate the promotor expression of *flaA* in *L. pneumophila*

In our studies, we have shown that chemically generated NO delays the promoter expression of *flaA* in *L. pneumophila* (**Fig. 3.2; Chapter 3.4.1**). A mutant lacking the three NO receptors exhibited a different P_{flaA}-*gfp* expression pattern compared to the parental strain when being treated with DPTA NONOate, suggesting that the receptors are involved in NO signaling (**Fig. 3.3CD; Chapter 3.4.3**). Furthermore, addition of the NO donor SNP to biofilms promoted dispersal of biofilms formed by the parental strain, while biofilms formed by the NO receptor mutants were not affected (**Fig. 3.6C; Chapter 3.4.6**). Taken together, the findings suggest that NO signaling is involved in the regulation of bacterial motility by altering the expression of the *flaA* promotor and by promoting biofilm dispersal.

The small AHK quorum sensing molecule LAI-1 is synthesized by the autoinducer synthase LqsA and involved in mediating bacterial cell-cell communication (intra-species) and pathogen-host cell signaling (inter-kingdom) (Hochstrasser and Hilbi, 2017). Synthetic LAI-1 was shown to promote the motility of *L. pneumophila* by signaling through LqsS/LqsT and LqsR (Schell et al., 2016b). Moreover, LAI-1 was shown to modulate migration of eukaryotic cells (amoebae or macrophages) through an IQGAP1-Cdc42-ARHGEF9-dependant pathway (Simon et al., 2015). However, the eukaryotic LAI-1 receptor(s) has not been identified yet.

In follow-up experiments, we investigated the effects of LAI-1 alone and in combination with SNP on P_{flaA}-*gfp* expression in broth. Since LAI-1 must be dissolved in DMSO, a corresponding control was included. As previously reported in this study, the presence of the NO donor SNP delayed the expression of P_{flaA}-*gfp*. Interestingly, the presence of LAI-1 also caused a delay in the expression of *gfp* under control of the *flaA* promoter, which was even more pronounced compared to SNP. Furthermore, the effects of SNP and LAI-1 were found to be additive, as the delay of P_{fla}-*gfp* expression in presence of LAI-1 was enhanced by the combined treatment with SNP (**Fig. 4.1**).

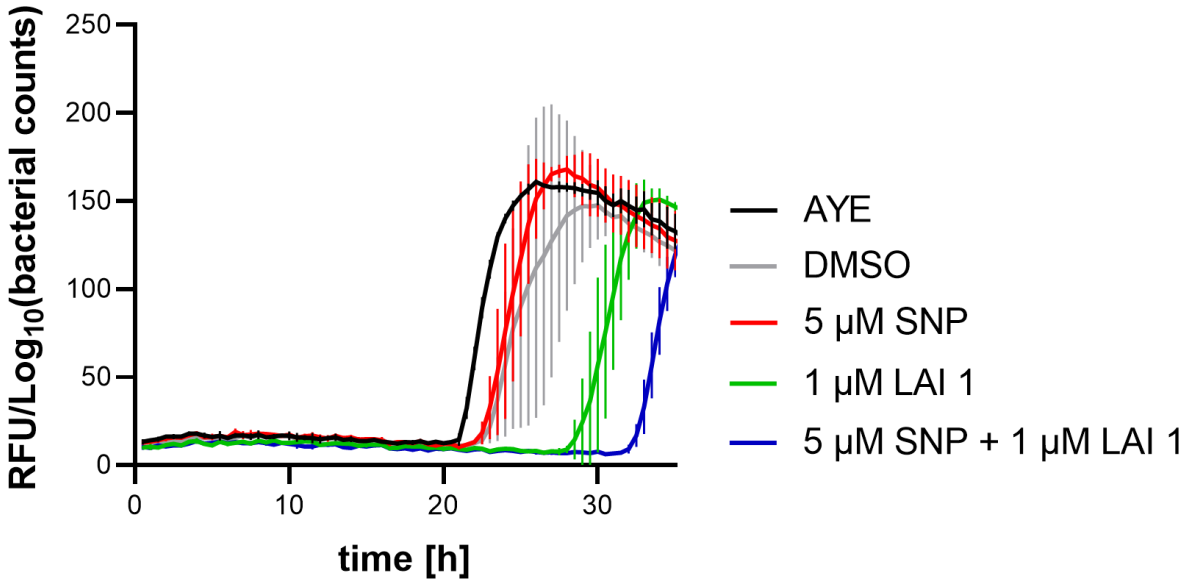

Figure 4.1. LAI-1 and SNP regulate P_{flaA}-*gfp* expression of *L. pneumophila* JR32 in broth.
Bacteria were grown in a microtiter plate in AYE medium, supplemented with 1 µM LAI-1 and 5 µM SNP, or not. The culture density at 600 nm (OD_{600}) and the GFP fluorescence (relative fluorescence units, RFU) were measured every 30 minutes. The Log_{10}(bacterial counts)/OD_{600} values are plotted versus time. The expression of P_{flaA}-*gfp* was delayed in the presence of LAI-1 and the shift was enhanced upon addition of SNP.

Thus, while NO and LAI-1 target different *L. pneumphila* receptors, the signaling molecules share downstream pathway(s) regulating the promoter expression of *flaA*. Two of the *L. pneumophila* NO receptors, NosP and Hnox1, are upstream of the c-di-GMP regulatory network. Quorum sensing and c-di-GMP signaling regulate some of the same processes, such as biofilm formation or virulence, suggesting that these pathways are linked (Camilli and Bassler, 2006). Although a direct link, has not yet been reported, there appears to be at least indirect interactions. In *V. cholerae*, e.g., the quorum sensing-regulated activator AphA regulates the expression of genes containing GGDEF and EAL domains (Camilli and Bassler, 2006; Kovacikova et al., 2005). Previous studies in *L. pneumophila* have shown that the pleiotropic transcription factor LvbR links the Lqs and c-di-GMP regulatory network to control biofilm architecture and virulence (Hochstrasser et al., 2019). Moreover, our investigations revealed that the NO receptor NosP

negatively regulates the expression of *lvbR* (**Fig. 3.3B; Chapter 3.4.2**). Whether LAI-1 and NO target independent pathways that mediate similar processes or whether the pathways converge to regulate motility remains to be investigated.

4.3 Concluding remarks

In this study, we have shown that the Lqs-LvbR network, FlaA and the Icm/Dot T4SS regulate the migration of *A. castellanii* through *L. pneumophila* biofilms. Furthermore, we observed that the Lqs-LvbR network and FlaA control the formation of bacterial clusters on the amoebae. Our data provides new insights into the interactions between *Legionella* and amoebae within biofilms and allowed the identification of components underlying amoebae migration and the formation of bacterial clusters. Interactions between *Legionella* and amoebae in biofilms could contribute to the survival and spread of *L. pneumophila* in water systems. A detailed understanding of the functions and mechanisms underlying the migration behavior of amoebae and the formation of bacterial clusters on the amoeba surface is therefore required and will be investigated in future studies.

Inter-kingdom signaling is an important, but still largely unexplored area in the field of pathogen-host interactions. As a facultative intracellular pathogen, *L. pneumophila* is likely exposed to host cell derived NO. Our studies on NO signaling have shown that *L. pneumophila* regulates virulence, intracellular phenotypic heterogeneity, and biofilm formation through NO and the three functionally non-redundant NO receptors Hnox1, Hnox2 and NosP. Follow-up experiments revealed that NO and LAI-1 additively affect the promoter expression of *flaA.* Further studies will identify and characterize the molecular components underlying NO- and LAI-1-dependent (inter-kingdom) signaling and will contribute to a better understanding of pathogen-host cell interactions.

Publications

- Enea Maffei, Aisylu Shaidullina, Marco Burkolter, Yannik Heyer, Fabienne Estermann, Valentin Druelle, Patrick Sauer, Luc Willi, **Sarah Michaelis**, Hubert Hilbi, David S. Thaler and Alexander Harms. Systematic exploration of *Escherichia coli* phage–host interactions with the BASEL phage collection. *PLoS biology* (2021), *19*(11), e3001424.
- Ramon Hochstrasser, **Sarah Michaelis**, Sabrina Brülisauer, Thomas Sura, Mingzhen Fan, Sandra Maaß, Dörte Becher and Hubert Hilbi. Migration of *Acanthamoeba* through *Legionella* biofilms is regulated by bacterial quorum sensing, effector proteins and the flagellum. *Environ Microbiol.* (2022), *24*(8), 3672-3692.
- **Sarah Michaelis**, Tong Chen, Camille Schmid and Hubert Hilbi. Nitric oxide signaling through three receptors regulates virulence, biofilm formation, and phenotypic heterogeneity of *Legionella pneumophila*. *mBio* (2024), e00710-24.
- **Sarah Michaelis**, Laura Gomez-Valero, Tong Chen, Camille Schmid, Carmen Buchrieser and Hubert Hilbi. The ins and outs of *Legionella* autoinducer and nitric oxide signaling. *MMBR* (2024). Status: Submitted.

References

Abdel-Nour, M., Duncan, C., Low, D.E., and Guyard, C. (2013). Biofilms: the stronghold of *Legionella pneumophila*. Int J Mol Sci *14*, 21660-21675.

Abu Khweek, A., and Amer, A.O. (2018). Factors Mediating Environmental Biofilm Formation by *Legionella pneumophila*. Front Cell Infect Microbiol *8*, 38.

Abu Kwaik, Y. (1996). The phagosome containing *Legionella pneumophila* within the protozoan *Hartmannella vermiformis* is surrounded by the rough endoplasmic reticulum. Applied and environmental microbiology *62*, 2022-2028.

Ackermann, M. (2013). Microbial individuality in the natural environment. The ISME journal *7*, 465-467.

Ackermann, M. (2015). A functional perspective on phenotypic heterogeneity in microorganisms. Nature reviews Microbiology *13*, 497-508.

Albert-Weissenberger, C., Sahr, T., Sismeiro, O., Hacker, J., Heuner, K., and Buchrieser, C. (2010). Control of flagellar gene regulation in *Legionella pneumophila* and its relation to growth phase. J Bacteriol *192*, 446-455.

Allombert, J., Jaboulay, C., Michard, C., Andrea, C., Charpentier, X., Vianney, A., and Doublet, P. (2021). Deciphering *Legionella* effector delivery by Icm/Dot secretion system reveals a new role for c-di-GMP signaling. J Mol Biol *433*, 166985.

Allombert, J., Lazzaroni, J.C., Bailo, N., Gilbert, C., Charpentier, X., Doublet, P., and Vianney, A. (2014). Three antagonistic cyclic di-GMP-catabolizing enzymes promote differential Dot/Icm effector delivery and intracellular survival at the early steps of *Legionella pneumophila* infection. Infect Immun *82*, 1222-1233.

Arora, D.P., Hossain, S., Xu, Y., and Boon, E.M. (2015). Nitric Oxide Regulation of Bacterial Biofilms. Biochemistry *54*, 3717-3728.

Asrat, S., de Jesus, D.A., Hempstead, A.D., Ramabhadran, V., and Isberg, R.R. (2014). Bacterial pathogen manipulation of host membrane trafficking. Annual review of cell and developmental biology *30*, 79-109.

Aurass, P., Gerlach, T., Becher, D., Voigt, B., Karste, S., Bernhardt, J., Riedel, K., Hecker, M., and Flieger, A. (2016). Life stage-specific proteomes of *Legionella pneumophila* reveal a highly differential abundance of virulence-associated Dot/Icm effectors. Mol Cell Proteomics *15*, 177-200.

Avery, S.V. (2006). Microbial cell individuality and the underlying sources of heterogeneity. Nature Reviews Microbiology *4*, 577-587.

Bacon, B., Nisbett, L.-M., and Boon, E. (2017). Bacterial haemoprotein sensors of NO: H-NOX and NosP. Advances in microbial physiology *70*, 1-36.

Bai, L., Yang, W., and Li, Y. (2023). Clinical and laboratory diagnosis of *Legionella* pneumonia. In Diagnostics (Basel), pp. 280.

Barraud, N., Hassett, D.J., Hwang, S.-H., Rice, S.A., Kjelleberg, S., and Webb, J.S. (2006). Involvement of nitric oxide in biofilm dispersal of *Pseudomonas aeruginosa*. Journal of bacteriology *188*, 7344-7353.

Barraud, N., Schleheck, D., Klebensberger, J., Webb, J.S., Hassett, D.J., Rice, S.A., and Kjelleberg, S. (2009a). Nitric oxide signaling in *Pseudomonas aeruginosa* biofilms mediates phosphodiesterase activity, decreased cyclic di-GMP levels, and enhanced dispersal. Journal of bacteriology *191*, 7333-7342.

Barraud, N., Storey, M.V., Moore, Z.P., Webb, J.S., Rice, S.A., and Kjelleberg, S. (2009b). Nitric oxide-mediated dispersal in single- and multi-species biofilms of clinically and industrially relevant microorganisms. Microb Biotechnol *2*, 370-378.

Bassler, B.L., and Losick, R. (2006). Bacterially speaking. Cell *125*, 237-246.

Benin, A.L., Benson, R.F., Arnold, K.E., Fiore, A.E., Cook, P.G., Williams, L.K., Fields, B., and Besser, R.E. (2002). An outbreak of travel-associated Legionnaires disease and Pontiac fever: the need for enhanced surveillance of travel-associated legionellosis in the United States. The Journal of infectious diseases *185*, 237-243.

Berman, J.J. (2019). Taxonomic guide to infectious diseases: understanding the biologic classes of pathogenic organisms (Academic Press).

Best, A., and Kwaik, Y.A. (2019). Nutrition and bipartite metabolism of intracellular pathogens. Trends in microbiology *27*, 550-561.

Bigot, R., Bertaux, J., Frere, J., and Berjeaud, J.M. (2013). Intra-amoeba multiplication induces chemotaxis and biofilm colonization and formation for *Legionella*. PLoS One *8*, e77875.

Boamah, D.K., Zhou, G., Ensminger, A.W., and O'Connor, T.J. (2017). From many hosts, one accidental pathogen: the diverse protozoan hosts of *Legionella*. Frontiers in cellular and infection microbiology *7*, 477.

Böck, D., Hüsler, D., Steiner, B., Medeiros, J.M., Welin, A., Ramomska, K.A., Hardt, W.D., Pilhofer, M., and Hilbi, H. (2021). The polar *Legionella* Icm/Dot T4SS establishes distinct contact sites with the pathogen vacuole membrane. mBio *12*, e02180-02121.

Bogdan, C. (2001). Nitric oxide and the immune response. Nat Immunol *2*, 907-916.

Bogdan, C., Rollinghoff, M., and Diefenbach, A. (2000). The role of nitric oxide in innate immunity. Immunological reviews *173*, 17-26.

Bonn, F., Bartel, J., Buttner, K., Hecker, M., Otto, A., and Becher, D. (2014). Picking vanished proteins from the void: how to collect and ship/share extremely dilute proteins in a reproducible and highly efficient manner. Analytical chemistry *86*, 7421-7427.

Boon, E.M., Davis, J.H., Tran, R., Karow, D.S., Huang, S.H., Pan, D., Miazgowicz, M.M., Mathies, R.A., and Marletta, M.A. (2006). Nitric oxide binding to prokaryotic homologs of the soluble guanylate cyclase β1 H-NOX domain. Journal of biological chemistry *281*, 21892-21902.

Boon, E.M., Huang, S.H., and Marletta, M.A. (2005). A molecular basis for NO selectivity in soluble guanylate cyclase. Nature chemical biology *1*, 53-59.

Boon, E.M., and Marletta, M.A. (2005). Ligand specificity of H-NOX domains: from sGC to bacterial NO sensors. Journal of inorganic biochemistry *99*, 892-902.

Brameyer, S., Plener, L., Muller, A., Klingl, A., Wanner, G., and Jung, K. (2018). Outer membrane vesicles facilitate trafficking of the hydrophobic signaling molecule CAI-1 between *Vibrio harveyi* cells. Journal of bacteriology *200*.

Brenner, D.J., Steigerwalt, A.G., and McDade, J.E. (1979). Classification of the Legionnaires' disease bacterium: *Legionella pneumophila*, genus novum, species nova, of the family *Legionellaceae*, familia nova. Annals of internal medicine *90*, 656-658.

Brombacher, E., Urwyler, S., Ragaz, C., Weber, S.S., Kami, K., Overduin, M., and Hilbi, H. (2009). Rab1 guanine nucleotide exchange factor SidM is a major phosphatidylinositol 4-phosphate-binding effector protein of *Legionella pneumophila*. Journal of biological chemistry *284*, 4846-4856.

Brüggemann, H., Hagman, A., Jules, M., Sismeiro, O., Dillies, M.A., Gouyette, C., Kunst, F., Steinert, M., Heuner, K., Coppee, J.Y.*, et al.* (2006). Virulence strategies for infecting phagocytes deduced from the in vivo transcriptional program of *Legionella pneumophila*. Cell Microbiol *8*, 1228-1240.

Byrne, B., and Swanson, M.S. (1998). Expression of *Legionella pneumophila* virulence traits in response to growth conditions. Infection and immunity *66*, 3029-3034.

Camilli, A., and Bassler, B.L. (2006). Bacterial small-molecule signaling pathways. Science *311*, 1113-1116.

Carlson, H.K., Vance, R.E., and Marletta, M.A. (2010). H-NOX regulation of c-di-GMP metabolism and biofilm formation in *Legionella pneumophila*. Mol Microbiol *77*, 930-942.

Cary, S.P., Winger, J.A., Derbyshire, E.R., and Marletta, M.A. (2006). Nitric oxide signaling: no longer simply on or off. Trends Biochem Sci *31*, 231-239.

Chahin, A., and Opal, S.M. (2017). Severe pneumonia caused by *Legionella pneumophila*: differential diagnosis and therapeutic considerations. Infectious Disease Clinics *31*, 111-121.

Chang, B., Kura, F., Amemura-Maekawa, J., Koizumi, N., and Watanabe, H. (2005). Identification of a novel adhesion molecule involved in the virulence of *Legionella pneumophila*. Infection and immunity *73*, 4272-4280.

Charpentier, X., Kay, E., Schneider, D., and Shuman, H.A. (2011). Antibiotics and UV radiation induce competence for natural transformation in *Legionella pneumophila*. Journal of bacteriology *193*, 1114-1121.

Chen, X.J., Wang, B., Thompson, I.P., and Huang, W.E. (2021). Rational design and characterization of nitric oxide biosensors in *E. coli Nissle* 1917 and mini SimCells. ACS Synthetic Biology *10*, 2566-2578.

Cirillo, S.L., Bermudez, L.E., El-Etr, S.H., Duhamel, G.E., and Cirillo, J.D. (2001). *Legionella pneumophila* entry gene *rtxA* is involved in virulence. Infection and immunity *69*, 508-517.

Claudi, B., Sprote, P., Chirkova, A., Personnic, N., Zankl, J., Schurmann, N., Schmidt, A., and Bumann, D. (2014). Phenotypic variation of *Salmonella* in host tissues delays eradication by antimicrobial chemotherapy. Cell *158*, 722-733.

Correia, A.M., Ferreira, J.S., Borges, V., Nunes, A., Gomes, B., Capucho, R., Goncalves, J., Antunes, D.M., Almeida, S., Mendes, A.*, et al.* (2016). Probable Person-to-Person Transmission of Legionnaires' Disease. The New England journal of medicine *374*, 497-498.

Cunha, B.A., Burillo, A., and Bouza, E. (2016). Legionnaires' disease. The Lancet *387*, 376-385.

Dalebroux, Z.D., Edwards, R.L., and Swanson, M.S. (2009). SpoT governs *Legionella pneumophila* differentiation in host macrophages. Molecular microbiology *71*, 640-658.

Davey, M.E., and O'Toole G, A. (2000). Microbial biofilms: from ecology to molecular genetics. Microbiol Mol Biol Rev *64*, 847-867.

De Buck, E., Maes, L., Meyen, E., Van Mellaert, L., Geukens, N., Anne, J., and Lammertyn, E. (2005). Legionella pneumophila Philadelphia-1 tatB and tatC affect intracellular replication and biofilm formation. Biochem Biophys Res Commun *331*, 1413-1420.

de Felipe, K.S., Glover, R.T., Charpentier, X., Anderson, O.R., Reyes, M., Pericone, C.D., and Shuman, H.A. (2008). *Legionella* eukaryotic-like type IV substrates interfere with organelle trafficking. PLoS Pathog *4*, e1000117.

de Schaetzen, F., Fan, M., Alcolombri, U., Peaudecerf, F.J., Drissner, D., Loessner, M.J., Stocker, R., and Schuppler, M. (2022). Random encounters and amoeba locomotion drive the predation of *Listeria monocytogenes* by *Acanthamoeba castellanii*. Proceedings of the National Academy of Sciences *119*, e2122659119.

Declerck, P. (2010). Biofilms: the environmental playground of *Legionella pneumophila*. Environ Microbiol *12*, 557-566.

Declerck, P., Behets, J., Margineanu, A., van Hoef, V., De Keersmaecker, B., and Ollevier, F. (2009). Replication of *Legionella pneumophila* in biofilms of water distribution pipes. Microbiol Res *164*, 593-603.

Declerck, P., Behets, J., van Hoef, V., and Ollevier, F. (2007). Replication of *Legionella pneumophila* in floating biofilms. Curr Microbiol *55*, 435-440.

Delgado, M.G., Rivera, C.A., and Lennon-Dumenil, A.M. (2022). Macropinocytosis and Cell Migration: Don't Drink and Drive… Subcell Biochem *98*, 85-102.

Derbyshire, E.R., and Marletta, M.A. (2009). Biochemistry of soluble guanylate cyclase. cGMP: Generators, Effectors and Therapeutic Implications, 17-31.

Di Paolo, G., and De Camilli, P. (2006). Phosphoinositides in cell regulation and membrane dynamics. Nature *443*, 651-657.

Dietrich, C., Heuner, K., Brand, B.C., Hacker, J., and Steinert, M. (2001). Flagellum of *Legionella pneumophila* positively affects the early phase of infection of eukaryotic host cells. Infection and immunity *69*, 2116-2122.

Doebbeling, B.N., and Wenzel, R.P. (1987). The epidemiology of *Legionella pneumophila* infections. Paper presented at: Seminars in Respiratory Infections.

Donaldson, J.G., and Jackson, C.L. (2000). Regulators and effectors of the ARF GTPases. Current opinion in cell biology *12*, 475-482.

Dondero Jr, T.J., Rendtorff, R.C., Mallison, G.F., Weeks, R.M., Levy, J.S., Wong, E.W., and Schaffner, W. (1980). An outbreak of Legionnaires' disease associated with a contaminated air-conditioning cooling tower. New England Journal of Medicine *302*, 365-370.

Doyscher, D., Fieseler, L., Dons, L., Loessner, M.J., and Schuppler, M. (2013). *Acanthamoeba* feature a unique backpacking strategy to trap and feed on *Listeria monocytogenes* and other motile bacteria. Environ Microbiol *15*, 433-446.

Duncan, C., Prashar, A., So, J., Tang, P., Low, D.E., Terebiznik, M., and Guyard, C. (2011). Lcl of *Legionella pneumophila* is an immunogenic GAG binding adhesin that promotes interactions with lung epithelial cells and plays a crucial role in biofilm formation. Infection and immunity *79*, 2168-2181.

Dupuy, M., Binet, M., Bouteleux, C., Herbelin, P., Soreau, S., and Hechard, Y. (2016). Permissiveness of freshly isolated environmental strains of amoebae for growth of *Legionella pneumophila*. FEMS microbiology letters *363*, fnw022.

Duron, O., Doublet, P., Vavre, F., and Bouchon, D. (2018). The importance of revisiting *Legionellales* diversity. Trends in parasitology *34*, 1027-1037.

Escoll, P., Mondino, S., Rolando, M., and Buchrieser, C. (2016). Targeting of host organelles by pathogenic bacteria: a sophisticated subversion strategy. Nature reviews Microbiology *14*, 5-19.

Escoll, P., Platon, L., Drame, M., Sahr, T., Schmidt, S., Rusniok, C., and Buchrieser, C. (2021). Reverting the mode of action of the mitochondrial F(O)F(1)-ATPase by *Legionella pneumophila* preserves its replication niche. eLife *10*.

Escoll, P., Song, O.R., Viana, F., Steiner, B., Lagache, T., Olivo-Marin, J.C., Impens, F., Brodin, P., Hilbi, H., and Buchrieser, C. (2017). *Legionella pneumophila* modulates mitochondrial dynamics to trigger metabolic repurposing of infected macrophages. Cell Host Microbe *22*, 302-316 e307.

Fan, M., Kiefer, P., Charki, P., Hedberg, C., Seibel, J., Vorholt, J.A., and Hilbi, H. (2023). The *Legionella* autoinducer LAI-1 is delivered by outer membrane vesicles to promote interbacterial and interkingdom signaling. Journal of Biological Chemistry *299*.

Fardeau, M.-L., Salinas, M.B., L'Haridon, S., Jeanthon, C., Verhé, F., Cayol, J.-L., Patel, B.K., Garcia, J.-L., and Ollivier, B. (2004). Isolation from oil reservoirs of novel thermophilic anaerobes phylogenetically related to *Thermoanaerobacter subterraneus*: reassignment of *T. subterraneus*, *Thermoanaerobacter yonseiensis*, *Thermoanaerobacter tengcongensis* and *Carboxydibrachium pacificum* to *Caldanaerobacter subterraneus* gen. nov., sp. nov., comb. nov. as four novel subspecies. International Journal of Systematic and Evolutionary Microbiology *54*, 467-474.

Faucher, S.P., Friedlander, G., Livny, J., Margalit, H., and Shuman, H.A. (2010). *Legionella pneumophila* 6S RNA optimizes intracellular multiplication. Proc Natl Acad Sci U S A *107*, 7533-7538.

Feeley, J.C., Gibson, R.J., Gorman, G.W., Langford, N.C., Rasheed, J.K., Mackel, D.C., and Baine, W.B. (1979). Charcoal-yeast extract agar: primary isolation medium for *Legionella pneumophila*. J Clin Microbiol *10*, 437-441.

Felz, S., Vermeulen, P., van Loosdrecht, M.C., and Lin, Y.M. (2019). Chemical characterization methods for the analysis of structural extracellular polymeric substances (EPS). Water Research *157*, 201-208.

Fields, B.S. (1996). The molecular ecology of *Legionellae*. Trends Microbiol *4*, 286-290.

Fields, B.S., Benson, R.F., and Besser, R.E. (2002). *Legionella* and Legionnaires' disease: 25 years of investigation. Clin Microbiol Rev *15*, 506-526.

Finsel, I., and Hilbi, H. (2015). Formation of a pathogen vacuole according to *Legionella pneumophila*: how to kill one bird with many stones. Cell Microbiol *17*, 935-950.

Fischer, F.B., Schmutz, C., Gaia, V., and Mäusezahl, D. (2020). Legionnaires' disease on the rise in Switzerland: A denominator-based analysis of national diagnostic data, 2007–2016. International journal of environmental research and public health *17*, 7343.

Fischer, J.T., Hossain, S., and Boon, E.M. (2019). NosP Modulates Cyclic-di-GMP Signaling in *Legionella pneumophila*. Biochemistry *58*, 4325-4334.

Flemming, H.-C., Neu, T.R., and Wozniak, D.J. (2007). The EPS matrix: the "house of biofilm cells". Journal of bacteriology *189*, 7945-7947.

Fliermans, C.B., Cherry, W.B., Orrison, L.H., Smith, S.J., Tison, D.L., and Pope, D.H. (1981). Ecological distribution of *Legionella pneumophila*. Appl Environ Microbiol *41*, 9-16.

Forsbach-Birk, V., McNealy, T., Shi, C., Lynch, D., and Marre, R. (2004). Reduced expression of the global regulator protein CsrA in *Legionella pneumophila* affects virulence-associated regulators and growth in Acanthamoeba castellanii. International journal of medical microbiology *294*, 15-25.

Fraser, D.W., Tsai, T.R., Orenstein, W., Parkin, W.E., Beecham, H.J., Sharrar, R.G., Harris, J., Mallison, G.F., Martin, S.M., McDade, J.E.*, et al.* (1977). Legionnaires' disease: description of an epidemic of pneumonia. N Engl J Med *297*, 1189-1197.

Fu, J., Zhou, M., Gritsenko, M.A., Nakayasu, E.S., Song, L., and Luo, Z.Q. (2022). *Legionella pneumophila* modulates host energy metabolism by ADP-ribosylation of ADP/ATP translocases. eLife *11*, e73611.

Fuqua, C., and Greenberg, E.P. (2002). Listening in on bacteria: acyl-homoserine lactone signalling. Nature reviews Molecular cell biology *3*, 685-695.

Galka, F., Wai, S.N., Kusch, H., Engelmann, S., Hecker, M., Schmeck, B., Hippenstiel, S., Uhlin, B.E., and Steinert, M. (2008). Proteomic characterization of the whole secretome of *Legionella pneumophila* and functional analysis of outer membrane vesicles. Infect Immun *76*, 1825-1836.

Garcia-Rodriguez, F.J., Buchrieser, C., and Escoll, P. (2023). *Legionella* and mitochondria, an intriguing relationship. Int Rev Cell Mol Biol *374*, 37-81.

Garcia-Vidal, C., Labori, M., Viasus, D., Simonetti, A., Garcia-Somoza, D., Dorca, J., Gudiol, F., and Carratala, J. (2013). Rainfall is a risk factor for sporadic cases of *Legionella pneumophila* pneumonia. PLoS One *8*, e61036.

Garduño, R.A., Garduño, E., and Hoffman, P.S. (1998). Surface-associated hsp60 chaperonin of *Legionella pneumophila* mediates invasion in a HeLa cell model. Infection and immunity *66*, 4602-4610.

Ghosal, D., Jeong, K.C., Chang, Y.W., Gyore, J., Teng, L., Gardner, A., Vogel, J.P., and Jensen, G.J. (2019). Molecular architecture, polar targeting and biogenesis of the *Legionella* Dot/Icm T4SS. Nat Microbiol *4*, 1173-1182.
Glick, T.H., Gregg, M.B., Berman, B., Mallison, G., Rhodes, W.W., Jr., and Kassanoff, I. (1978). Pontiac fever. An epidemic of unknown etiology in a health department: I. Clinical and epidemiologic aspects. American journal of epidemiology *107*, 149-160.
Gomez-Valero, L., Rusniok, C., Carson, D., Mondino, S., Perez-Cobas, A.E., Rolando, M., Pasricha, S., Reuter, S., Demirtas, J., Crumbach, J.*, et al.* (2019). More than 18,000 effectors in the *Legionella* genus genome provide multiple, independent combinations for replication in human cells. Proc Natl Acad Sci U S A *116*, 2265-2273.
Graham, C.I., MacMartin, T.L., de Kievit, T.R., and Brassinga, A.K.C. (2023). Molecular regulation of virulence in *Legionella pneumophila*. Molecular microbiology.
Greub, G., and Raoult, D. (2004). Microorganisms resistant to free-living amoebae. Clin Microbiol Rev *17*, 413-433.
Grimbergen, A.J., Siebring, J., Solopova, A., and Kuipers, O.P. (2015). Microbial bet-hedging: the power of being different. Curr Opin Microbiol *25*, 67-72.
Gudiol, C., Verdaguer, R., Angeles Domínguez, M., Fernández-Sevilla, A., and Carratalà, J. (2007). Outbreak of Legionnaires' disease in immunosuppressed patients at a cancer centre: usefulness of universal urine antigen testing and early levofloxacin therapy. Clinical microbiology and infection *13*, 1125-1128.
Haiko, J., and Westerlund-Wikstrom, B. (2013). The role of the bacterial flagellum in adhesion and virulence. Biology (Basel) *2*, 1242-1267.
Hall-Stoodley, L., Costerton, J.W., and Stoodley, P. (2004). Bacterial biofilms: from the natural environment to infectious diseases. Nature reviews Microbiology *2*, 95-108.
Haneburger, I., and Hilbi, H. (2013). Phosphoinositide lipids and the *Legionella* pathogen vacuole. Molecular Mechanisms in Legionella Pathogenesis, 155-173.
Haupt, T.E., Heffernan, R.T., Kazmierczak, J.J., Nehls-Lowe, H., Rheineck, B., Powell, C., Leonhardt, K.K., Chitnis, A.S., and Davis, J.P. (2015). An outbreak of legionnaires disease associated with a decorative water wall fountain in a hospital. Infection Control & Hospital Epidemiology *33*, 185-191.
Heckler, I., and Boon, E.M. (2019). Insights into nitric oxide modulated quorum sensing pathways. Frontiers in microbiology *10*, 2174.
Henares, B.M., Higgins, K.E., and Boon, E.M. (2012). Discovery of a nitric oxide responsive quorum sensing circuit in *Vibrio harveyi*. ACS chemical biology *7*, 1331-1336.
Henares, B.M., Xu, Y., and Boon, E.M. (2013). A nitric oxide-responsive quorum sensing circuit in *Vibrio harveyi* regulates flagella production and biofilm formation. Int J Mol Sci *14*, 16473-16484.
Hengge, R. (2009). Principles of c-di-GMP signalling in bacteria. Nature reviews Microbiology *7*, 263-273.
Henke, J.M., and Bassler, B.L. (2004). Three parallel quorum-sensing systems regulate gene expression in *Vibrio harveyi*. Journal of bacteriology *186*, 6902-6914.
Herran, B., Greve, P., Berjeaud, J.M., Bertaux, J., and Crepin, A. (2021). *Legionella* spp. all ears? The broad occurrence of quorum sensing elements outside *Legionella pneumophila*. Genome Biol Evol.
Higgins, D.A., Pomianek, M.E., Kraml, C.M., Taylor, R.K., Semmelhack, M.F., and Bassler, B.L. (2007). The major *Vibrio cholerae* autoinducer and its role in virulence factor production. Nature *450*, 883-886.
Hilbi, H., and Buchrieser, C. (2022). Microbe Profile: *Legionella pneumophila* - a copycat eukaryote. Microbiology (Reading) *168*, doi: 10.1099/mic.1090.001142.
Hilbi, H., Hoffmann, C., and Harrison, C.F. (2011). *Legionella* spp. outdoors: colonization, communication and persistence. Environ Microbiol Rep *3*, 286–296.
Hilbi, H., Segal, G., and Shuman, H.A. (2001). Icm/Dot-dependent upregulation of phagocytosis by *Legionella pneumophila*. Mol Microbiol *42*, 603-617.
Hilbi, H., Weber, S.S., Ragaz, C., Nyfeler, Y., and Urwyler, S. (2007). Environmental predators as models for bacterial pathogenesis. Environ Microbiol *9*, 563-575.
Hindre, T., Bruggemann, H., Buchrieser, C., and Hechard, Y. (2008). Transcriptional profiling of *Legionella pneumophila* biofilm cells and the influence of iron on biofilm formation. Microbiology *154*, 30-41.
Hochstrasser, R., and Hilbi, H. (2017). Intra-species and inter-kingdom signaling of *Legionella pneumophila*. Front Microbiol *8*, 79.
Hochstrasser, R., and Hilbi, H. (2019). Migration of *Acanthamoeba castellanii* through *Legionella* biofilms. Methods Mol Biol *1921*, 79-89.

Hochstrasser, R., and Hilbi, H. (2020). *Legionella* quorum sensing meets cyclic-di-GMP signaling. Curr Opin Microbiol *55*, 9-16.
Hochstrasser, R., and Hilbi, H. (2022). The *Legionella* Lqs-LvbR regulatory network controls temperature-dependent growth onset and bacterial cell density. Appl Environ Microbiol, aem0237021.
Hochstrasser, R., Hutter, C.A.J., Arnold, F.M., Barlocher, K., Seeger, M.A., and Hilbi, H. (2020). The structure of the *Legionella* response regulator LqsR reveals amino acids critical for phosphorylation and dimerization. Mol Microbiol *113*, 1070-1084.
Hochstrasser, R., Kessler, A., Sahr, T., Simon, S., Schell, U., Gomez-Valero, L., Buchrieser, C., and Hilbi, H. (2019). The pleiotropic *Legionella* transcription factor LvbR links the Lqs and c-di-GMP regulatory networks to control biofilm architecture and virulence. Environ Microbiol *21*, 1035-1053.
Hochstrasser, R., Michaelis, S., Brulisauer, S., Sura, T., Fan, M., Maass, S., Becher, D., and Hilbi, H. (2022). Migration of *Acanthamoeba* through *Legionella* biofilms is regulated by the bacterial Lqs-LvbR network, effector proteins and the flagellum. Environmental microbiology *24*, 3672-3692.
Hoffmann, C., Harrison, C.F., and Hilbi, H. (2014). The natural alternative: protozoa as cellular models for Legionella infection. Cell Microbiol *16*, 15-26.
Hornung, C., Poehlein, A., Haack, F.S., Schmidt, M., Dierking, K., Pohlen, A., Schulenburg, H., Blokesch, M., Plener, L., Jung, K.*, et al.* (2013). The Janthinobacterium sp. HH01 genome encodes a homologue of the *V. cholerae* CqsA and *L. pneumophila* LqsA autoinducer synthases. PLoS One *8*, e55045.
Horwitz, M.A. (1983). Formation of a novel phagosome by the Legionnaires' disease bacterium (*Legionella pneumophila*) in human monocytes. J Exp Med *158*, 1319-1331.
Hossain, S., Heckler, I., and Boon, E.M. (2018). Discovery of a nitric oxide responsive quorum sensing circuit in *Vibrio cholerae*. ACS chemical biology *13*, 1964-1969.
Hsu, B.-M., Huang, C.-C., Chen, J.-S., Chen, N.-H., and Huang, J.-T. (2011). Comparison of potentially pathogenic free-living amoeba hosts by *Legionella* spp. in substrate-associated biofilms and floating biofilms from spring environments. Water research *45*, 5171-5183.
Hubber, A., and Roy, C.R. (2010). Modulation of host cell function by *Legionella pneumophila* type IV effectors. Annu Rev Cell Dev Biol *26*, 261-283.
Hughes, E.D., Byrne, B.G., and Swanson, M.S. (2019). A Two-Component System That Modulates Cyclic di-GMP Metabolism Promotes *Legionella pneumophila* Differentiation and Viability in Low-Nutrient Conditions. Journal of bacteriology *201*.
Hüsler, D., Stauffer, P., and Hilbi, H. (2023a). Tapping lipid droplets: A rich fat diet of intracellular bacterial pathogens. Molecular microbiology *120*, 194-209.
Hüsler, D., Stauffer, P., Keller, B., Bock, D., Steiner, T., Ostrzinski, A., Vormittag, S., Striednig, B., Swart, A.L., Letourneur, F.*, et al.* (2023b). The large GTPase Sey1/atlastin mediates lipid droplet- and FadL-dependent intracellular fatty acid metabolism of *Legionella pneumophila*. eLife *12*, e85142.
Hüsler, D., Steiner, B., Welin, A., Striednig, B., Swart, A.L., Molle, V., Hilbi, H., and Letourneur, F. (2021). *Dictyostelium* lacking the single atlastin homolog Sey1 shows aberrant ER architecture, proteolytic processes and expansion of the *Legionella*-containing vacuole. Cell Microbiol *23*, e13318.
Huws, S.A., McBain, A.J., and Gilbert, P. (2005). Protozoan grazing and its impact upon population dynamics in biofilm communities. J Appl Microbiol *98*, 238-244.
Ingmundson, A., Delprato, A., Lambright, D.G., and Roy, C.R. (2007). *Legionella pneumophila* proteins that regulate Rab1 membrane cycling. Nature *450*, 365-369.
Irie, Y., and Parsek, M.R. (2014). LC/MS/MS-based quantitative assay for the secondary messenger molecule, c-di-GMP. *Pseudomonas* Methods and Protocols, 271-279.
Isberg, R.R., O'Connor, T.J., and Heidtman, M. (2009). The *Legionella pneumophila* replication vacuole: making a cosy niche inside host cells. Nat Rev Microbiol *7*, 13-24.
Iyer, L.M., Anantharaman, V., and Aravind, L. (2003). Ancient conserved domains shared by animal soluble guanylyl cyclases and bacterial signaling proteins. BMC genomics *4*, 1-8.
Jager, J., Keese, S., Roessle, M., Steinert, M., and Schromm, A.B. (2015). Fusion of *Legionella pneumophila* outer membrane vesicles with eukaryotic membrane systems is a mechanism to deliver pathogen factors to host cell membranes. Cell Microbiol *17*, 607-620.
Jahan, N., Potter, J.A., Sheikh, M.A., Botting, C.H., Shirran, S.L., Westwood, N.J., and Taylor, G.L. (2009). Insights into the biosynthesis of the *Vibrio cholerae* major autoinducer CAI-1 from the crystal structure of the PLP-dependent enzyme CqsA. J Mol Biol *392*, 763-773.
Jenal, U., Reinders, A., and Lori, C. (2017). Cyclic di-GMP: second messenger extraordinaire. Nature Reviews Microbiology *15*, 271-284.

Jung, A.L., Herkt, C.E., Schulz, C., Bolte, K., Seidel, K., Scheller, N., Sittka-Stark, A., Bertrams, W., and Schmeck, B. (2017). *Legionella pneumophila* infection activates bystander cells differentially by bacterial and host cell vesicles. Sci Rep *7*, 6301.

Jung, A.L., Stoiber, C., Herkt, C.E., Schulz, C., Bertrams, W., and Schmeck, B. (2016). *Legionella pneumophila*-derived outer membrane vesicles promote bacterial replication in macrophages. PLoS Pathog *12*, e1005592.

Kaczmarczyk, A., van Vliet, S., Jakob, R.P., Reinders, A., Klotz, A., Maier, T., and Jenal, U. (2022). A novel biosensor reveals dynamic changes of C-di-GMP in differentiating cells with ultra-high temporal resolution. Biorxiv, 2022.2010. 2018.512705.

Kagan, J.C., and Roy, C.R. (2002). *Legionella* phagosomes intercept vesicular traffic from endoplasmic reticulum exit sites. Nature cell biology *4*, 945-954.

Kagan, J.C., Stein, M.-P., Pypaert, M., and Roy, C.R. (2004). *Legionella* subvert the functions of Rab1 and Sec22b to create a replicative organelle. The Journal of experimental medicine *199*, 1201-1211.

Katz, S.M., and Hammel, J.M. (1987). The effect of drying, heat, and pH on the survival of *Legionella pneumophila*. Annals of Clinical & Laboratory Science *17*, 150-156.

Keefer, L.K., Nims, R.W., Davies, K.M., and Wink, D.A. (1996). "NONOates"(1-substituted diazen-1-ium-1, 2-diolates) as nitric oxide donors: convenient nitric oxide dosage forms. In Methods in enzymology (Elsevier), pp. 281-293.

Kelly, R.C., Bolitho, M.E., Higgins, D.A., Lu, W., Ng, W.L., Jeffrey, P.D., Rabinowitz, J.D., Semmelhack, M.F., Hughson, F.M., and Bassler, B.L. (2009). The *Vibrio cholerae* quorum-sensing autoinducer CAI-1: analysis of the biosynthetic enzyme CqsA. Nature chemical biology *5*, 891-895.

Kessler, A., Schell, U., Sahr, T., Tiaden, A., Harrison, C., Buchrieser, C., and Hilbi, H. (2013). The *Legionella pneumophila* orphan sensor kinase LqsT regulates competence and pathogen-host interactions as a component of the LAI-1 circuit. Environ Microbiol *15*, 646-662.

Kim, H.J., Tsoy, I., Park, M.K., Lee, Y.S., Lee, J.H., Seo, H.G., and Chang, K.C. (2006). Iron released by sodium nitroprusside contributes to heme oxygenase-1 induction via the cAMP-protein kinase A-mitogen-activated protein kinase pathway in RAW 264.7 cells. Molecular pharmacology *69*, 1633-1640.

Kojima, H., Nakatsubo, N., Kikuchi, K., Urano, Y., Higuchi, T., Tanaka, J., Kudo, Y., and Nagano, T. (1998). Direct evidence of NO production in rat hippocampus and cortex using a new fluorescent indicator: DAF-2 DA. Neuroreport *9*, 3345-3348.

Kovacikova, G., Lin, W., and Skorupski, K. (2005). Dual regulation of genes involved in acetoin biosynthesis and motility/biofilm formation by the virulence activator AphA and the acetate-responsive LysR-type regulator AlsR in *Vibrio cholerae.* Molecular microbiology *57*, 420-433.

Kubori, T., Lee, J., Kim, H., Yamazaki, K., Nishikawa, M., Kitao, T., Oh, B.H., and Nagai, H. (2022). Reversible modification of mitochondrial ADP/ATP translocases by paired *Legionella* effector proteins. Proc Natl Acad Sci U S A *119*, e2122872119.

Kubori, T., and Nagai, H. (2016). The Type IVB secretion system: an enigmatic chimera. Curr Opin Microbiol *29*, 22-29.

Kuiper, M.W., Wullings, B.A., Akkermans, A.D., Beumer, R.R., and van der Kooij, D. (2004). Intracellular proliferation of *Legionella pneumophila* in *Hartmannella vermiformis* in aquatic biofilms grown on plasticized polyvinyl chloride. Appl Environ Microbiol *70*, 6826-6833.

Lau, H.Y., and Ashbolt, N.J. (2009). The role of biofilms and protozoa in *Legionella* pathogenesis: implications for drinking water. J Appl Microbiol *107*, 368-378.

Letunic, I., and Bork, P. (2007). Interactive Tree Of Life (iTOL): an online tool for phylogenetic tree display and annotation. Bioinformatics *23*, 127-128.

Levet-Paulo, M., Lazzaroni, J.C., Gilbert, C., Atlan, D., Doublet, P., and Vianney, A. (2011). The atypical two-component sensor kinase Lpl0330 from Legionella pneumophila controls the bifunctional diguanylate cyclase-phosphodiesterase Lpl0329 to modulate bis-(3'-5')-cyclic dimeric GMP synthesis. J Biol Chem *286*, 31136-31144.

Levi, A., Folcher, M., Jenal, U., and Shuman, H.A. (2011). Cyclic diguanylate signaling proteins control intracellular growth of *Legionella pneumophila*. MBio *2*, e00316-00310.

Levin, T.C., Goldspiel, B.P., and Malik, H.S. (2019). Density-dependent resistance protects *Legionella pneumophila* from its own antimicrobial metabolite, HGA. eLife *8*, e46086.

Li, J., Azam, F., and Zhang, S. (2016). Outer membrane vesicles containing signalling molecules and active hydrolytic enzymes released by a coral pathogen Vibrio shilonii AK1. Environmental microbiology *18*, 3850-3866.
Li, L., Stoeckert, C.J., Jr., and Roos, D.S. (2003). OrthoMCL: identification of ortholog groups for eukaryotic genomes. Genome research *13*, 2178-2189.
Lockwood, D.C., Amin, H., Costa, T.R.D., and Schroeder, G.N. (2022). The *Legionella pneumophila* Dot/Icm type IV secretion system and its effectors. Microbiology (Reading) *168*, doi: 10.1099/mic.1090.001187.
Lu, H., and Clarke, M. (2005). Dynamic properties of Legionella-containing phagosomes in *Dictyostelium* amoebae. Cell Microbiol *7*, 995-1007.
Lucas, C.E., Brown, E., and Fields, B.S. (2006). Type IV pili and type II secretion play a limited role in *Legionella pneumophila* biofilm colonization and retention. Microbiology *152*, 3569-3573.
Maass, S., Sievers, S., Zuhlke, D., Kuzinski, J., Sappa, P.K., Muntel, J., Hessling, B., Bernhardt, J., Sietmann, R., Volker, U.*, et al.* (2011). Efficient, global-scale quantification of absolute protein amounts by integration of targeted mass spectrometry and two-dimensional gel-based proteomics. Analytical chemistry *83*, 2677-2684.
MacMicking, J., Xie, Q.W., and Nathan, C. (1997). Nitric oxide and macrophage function. Annual review of immunology *15*, 323-350.
Mallegol, J., Duncan, C., Prashar, A., So, J., Low, D.E., Terebeznik, M., and Guyard, C. (2012). Essential roles and regulation of the *Legionella pneumophila* collagen-like adhesin during biofilm formation. PLoS One *7*, e46462.
Mampel, J., Spirig, T., Weber, S.S., Haagensen, J.A.J., Molin, S., and Hilbi, H. (2006). Planktonic replication is essential for biofilm formation by *Legionella pneumophila* in a complex medium under static and dynamic flow conditions. Appl Environ Microbiol *72*, 2885-2895.
Manske, C., and Hilbi, H. (2014). Metabolism of the vacuolar pathogen *Legionella* and implications for virulence. Frontiers in cellular and infection microbiology *4*, 125.
Manske, C., Schell, U., and Hilbi, H. (2016). Metabolism of *myo*-inositol by *Legionella pneumophila* promotes infection of amoebae and macrophages. Appl Environ Microbiol *82*, 5000-5014.
Marrie, T.J., Costain, N., La Scola, B., Patrick, W., Forgie, S., Xu, Z., and McNeil, S.A. (2012). The role of atypical pathogens in community-acquired pneumonia. Paper presented at: Seminars in respiratory and critical care medicine (Thieme Medical Publishers).
Mashburn, L.M., and Whiteley, M. (2005). Membrane vesicles traffic signals and facilitate group activities in a prokaryote. Nature *437*, 422-425.
Matz, C., and Kjelleberg, S. (2005). Off the hook--how bacteria survive protozoan grazing. Trends Microbiol *13*, 302-307.
McDade, J.E., Shepard, C.C., Fraser, D.W., Tsai, T.R., Redus, M.A., and Dowdle, W.R. (1977). Legionnaires' disease: isolation of a bacterium and demonstration of its role in other respiratory disease. N Engl J Med *297*, 1197-1203.
Merriam, J.J., Mathur, R., Maxfield-Boumil, R., and Isberg, R.R. (1997). Analysis of the *Legionella pneumophila* flil gene: intracellular growth of a defined mutant defective for flagellum biosynthesis. Infect Immun *65*, 2497-2501.
Michaelis, S., Chen, T., Schmid, C., and Hilbi, H. (2024). Nitric oxide signaling through three receptors regulates virulence, biofilm formation, and phenotypic heterogeneity of *Legionella pneumophila*. MBio *accepted*.
Michel, T., and Feron, O. (1997). Nitric oxide synthases: which, where, how, and why? The Journal of clinical investigation *100*, 2146-2152.
Miller, M.B., Skorupski, K., Lenz, D.H., Taylor, R.K., and Bassler, B.L. (2002). Parallel quorum sensing systems converge to regulate virulence in *Vibrio cholerae*. Cell *110*, 303-314.
Minh, B.Q., Schmidt, H.A., Chernomor, O., Schrempf, D., Woodhams, M.D., von Haeseler, A., and Lanfear, R. (2020). IQ-TREE 2: New Models and Efficient Methods for Phylogenetic Inference in the Genomic Era. Molecular biology and evolution *37*, 1530-1534.
Moffat, J.F., and Tompkins, L.S. (1992). A quantitative model of intracellular growth of *Legionella pneumophila* in *Acanthamoeba castellanii*. Infection and immunity *60*, 296-301.
Molofsky, A.B., and Swanson, M.S. (2003). *Legionella pneumophila* CsrA is a pivotal repressor of transmission traits and activator of replication. Molecular microbiology *50*, 445-461.

Molofsky, A.B., and Swanson, M.S. (2004). Differentiate to thrive: lessons from the *Legionella pneumophila* life cycle. Mol Microbiol *53*, 29-40.
Mondino, S., Schmidt, S., Rolando, M., Escoll, P., Gomez-Valero, L., and Buchrieser, C. (2020). Legionnaires' Disease: State of the Art Knowledge of Pathogenesis Mechanisms of *Legionella*. Annual review of pathology *15*, 439-466.
Moronta, E.C. (2022). *Legionella*, *Chlamydia* and *Chlamydophila*. In Encyclopedia of Infection and Immunity (Elsevier), pp. 737-748.
Murga, R., Forster, T.S., Brown, E., Pruckler, J.M., Fields, B.S., and Donlan, R.M. (2001). Role of biofilms in the survival of *Legionella pneumophila* in a model potable-water system. Microbiology *147*, 3121-3126.
Nagai, H., Kagan, J.C., Zhu, X., Kahn, R.A., and Roy, C.R. (2002). A bacterial guanine nucleotide exchange factor activates ARF on *Legionella* phagosomes. Science *295*, 679-682.
Neunuebel, M.R., Chen, Y., Gaspar, A.H., Backlund, P.S., Jr., Yergey, A., and Machner, M.P. (2011). De-AMPylation of the small GTPase Rab1 by the pathogen *Legionella pneumophila*. Science *333*, 453-456.
Newton, H.J., Ang, D.K., van Driel, I.R., and Hartland, E.L. (2010). Molecular pathogenesis of infections caused by *Legionella pneumophila*. Clin Microbiol Rev *23*, 274-298.
Ng, W.L., and Bassler, B.L. (2009). Bacterial quorum-sensing network architectures. Annual review of genetics *43*, 197-222.
Nisbett, L.-M., and Boon, E.M. (2016). Nitric oxide regulation of H-NOX signaling pathways in bacteria. Biochemistry *55*, 4873-4884.
Oliva, G., Sahr, T., and Buchrieser, C. (2018). The life cycle of *L. pneumophila*: Cellular differentiation is linked to virulence and metabolism. Frontiers in cellular and infection microbiology *8*, 3.
Papenfort, K., and Bassler, B.L. (2016). Quorum sensing signal-response systems in Gram-negative bacteria. Nature reviews Microbiology *14*, 576-588.
Papenfort, K., Silpe, J.E., Schramma, K.R., Cong, J.P., Seyedsayamdost, M.R., and Bassler, B.L. (2017). A *Vibrio cholerae* autoinducer-receptor pair that controls biofilm formation. Nature chemical biology *13*, 551-557.
Pecastaings, S., Allombert, J., Lajoie, B., Doublet, P., Roques, C., and Vianney, A. (2016). New insights into *Legionella pneumophila* biofilm regulation by c-di-GMP signaling. Biofouling *32*, 935-948.
Pecastaings, S., Berge, M., Dubourg, K.M., and Roques, C. (2010). Sessile *Legionella pneumophila* is able to grow on surfaces and generate structured monospecies biofilms. Biofouling *26*, 809-819.
Pellicena, P., Karow, D.S., Boon, E.M., Marletta, M.A., and Kuriyan, J. (2004). Crystal structure of an oxygen-binding heme domain related to soluble guanylate cyclases. Proceedings of the National Academy of Sciences *101*, 12854-12859.
Pereira, C.S., Thompson, J.A., and Xavier, K.B. (2013). AI-2-mediated signalling in bacteria. FEMS Microbiol Rev *37*, 156-181.
Personnic, N., Bärlocher, K., Finsel, I., and Hilbi, H. (2016). Subversion of retrograde trafficking by translocated pathogen effectors. Trends Microbiol *24*, 450-462.
Personnic, N., Striednig, B., and Hilbi, H. (2018). *Legionella* quorum sensing and its role in pathogen-host interactions. Curr Opin Microbiol *41*, 29-35.
Personnic, N., Striednig, B., and Hilbi, H. (2021). Quorum sensing controls persistence, resuscitation, and virulence of *Legionella* subpopulations in biofilms. ISME J *15*, 196-210.
Personnic, N., Striednig, B., Lezan, E., Manske, C., Welin, A., Schmidt, A., and Hilbi, H. (2019). Quorum sensing modulates the formation of virulent *Legionella* persisters within infected cells. Nat Commun *10*, 5216.
Petrova, O.E., and Sauer, K. (2012). Sticky situations: key components that control bacterial surface attachment. J Bacteriol *194*, 2413-2425.
Piao, Z., Sze, C.C., Barysheva, O., Iida, K.-i., and Yoshida, S.-i. (2006). Temperature-regulated formation of mycelial mat-like biofilms by *Legionella pneumophila*. Applied and environmental microbiology *72*, 1613-1622.
Plate, L., and Marletta, M.A. (2013). Nitric oxide-sensing H-NOX proteins govern bacterial communal behavior. Trends Biochem Sci *38*, 566-575.
Pohl, N., Solbach, M.D., and Dumack, K. (2021). The wastewater protist *Rhogostoma minus* (*Thecofilosea*, *Rhizaria*) is abundant, widespread, and hosts *Legionellales*. Water research *203*, 117566.

Price, M.S., Chao, L.Y., and Marletta, M.A. (2007). *Shewanella oneidensis* MR-1 H-NOX regulation of a histidine kinase by nitric oxide. Biochemistry *46*, 13677-13683.
Qiu, J., and Luo, Z.Q. (2017). *Legionella* and *Coxiella* effectors: strength in diversity and activity. Nat Rev Microbiol *15*, 591-605.
Qiu, J., Sheedlo, M.J., Yu, K., Tan, Y., Nakayasu, E.S., Das, C., Liu, X., and Luo, Z.Q. (2016). Ubiquitination independent of E1 and E2 enzymes by bacterial effectors. Nature *533*, 120-124.
Ragaz, C., Pietsch, H., Urwyler, S., Tiaden, A., Weber, S.S., and Hilbi, H. (2008). The *Legionella pneumophila* phosphatidylinositol-4 phosphate-binding type IV substrate SidC recruits endoplasmic reticulum vesicles to a replication-permissive vacuole. Cellular microbiology *10*, 2416-2433.
Ren, T., Zamboni, D.S., Roy, C.R., Dietrich, W.F., and Vance, R.E. (2006). Flagellin-deficient *Legionella* mutants evade caspase-1- and Naip5-mediated macrophage immunity. PLoS Pathog *2*, e18.
Robinson, C.G., and Roy, C.R. (2006). Attachment and fusion of endoplasmic reticulum with vacuoles containing *Legionella pneumophila*. Cell Microbiol *8*, 793-805.
Rogers, J., Dowsett, A., Dennis, P., Lee, J., and Keevil, C. (1994). Influence of plumbing materials on biofilm formation and growth of *Legionella pneumophila* in potable water systems. Applied and environmental microbiology *60*, 1842-1851.
Roig, J., Domingo, C., and Morera, J. (1994). Legionnaires' disease. Chest *105*, 1817-1825.
Rojas-Hernandez, S., Rodriguez-Monroy, M.A., Moreno-Fierros, L., Jarillo-Luna, A., Carrasco-Yepez, M., Miliar-Garcia, A., and Campos-Rodriguez, R. (2007). Nitric oxide production and nitric oxide synthase immunoreactivity in *Naegleria fowleri*. Parasitology research *101*, 269-274.
Rolando, M., Sanulli, S., Rusniok, C., Gomez-Valero, L., Bertholet, C., Sahr, T., Margueron, R., and Buchrieser, C. (2013). *Legionella pneumophila* effector RomA uniquely modifies host chromatin to repress gene expression and promote intracellular bacterial replication. Cell Host Microbe *13*, 395-405.
Romling, U., Galperin, M.Y., and Gomelsky, M. (2013). Cyclic di-GMP: the first 25 years of a universal bacterial second messenger. Microbiology and molecular biology reviews : MMBR *77*, 1-52.
Ronn, R., McCaig, A.E., Griffiths, B.S., and Prosser, J.I. (2002). Impact of protozoan grazing on bacterial community structure in soil microcosms. Appl Environ Microbiol *68*, 6094-6105.
Rothmeier, E., Pfaffinger, G., Hoffmann, C., Harrison, C.F., Grabmayr, H., Repnik, U., Hannemann, M., Wölke, S., Bausch, A., Griffiths, G.*, et al.* (2013). Activation of Ran GTPase by a *Legionella* effector promotes microtubule polymerization, pathogen vacuole motility and infection. PLoS Pathog *9*, e1003598.
Rowbotham, T.J. (1980). Preliminary report on the pathogenicity of *Legionella pneumophila* for freshwater and soil amoebae. J Clin Pathol *33*, 1179-1183.
Roy, C.R., Berger, K.H., and Isberg, R.R. (1998). *Legionella pneumophila* DotA protein is required for early phagosome trafficking decisions that occur within minutes of bacterial uptake. Molecular microbiology *28*, 663-674.
Rybtke, M., Chua, S.L., Yam, J.K.H., Givskov, M., Yang, L., and Tolker-Nielsen, T. (2017). Gauging and visualizing c-di-GMP levels in *Pseudomonas aeruginosa* using fluorescence-based biosensors. c-di-GMP Signaling: Methods and Protocols, 87-98.
Sadosky, A.B., Wiater, L.A., and Shuman, H.A. (1993). Identification of *Legionella pneumophila* genes required for growth within and killing of human macrophages. Infection and immunity *61*, 5361-5373.
Sahr, T., Brüggemann, H., Jules, M., Lomma, M., Albert-Weissenberger, C., Cazalet, C., and Buchrieser, C. (2009). Two small ncRNAs jointly govern virulence and transmission in *Legionella pneumophila*. Molecular microbiology *72*, 741-762.
Sahr, T., Escoll, P., Rusniok, C., Bui, S., Pehau-Arnaudet, G., Lavieu, G., and Buchrieser, C. (2022). Translocated Legionella pneumophila small RNAs mimic eukaryotic microRNAs targeting the host immune response. Nature communications *13*, 762.
Sahr, T., Rusniok, C., Dervins-Ravault, D., Sismeiro, O., Coppee, J.Y., and Buchrieser, C. (2012). Deep sequencing defines the transcriptional map of *L. pneumophila* and identifies growth phase-dependent regulated ncRNAs implicated in virulence. RNA Biol *9*, 503-519.
Sahr, T., Rusniok, C., Impens, F., Oliva, G., Sismeiro, O., Coppee, J.-Y., and Buchrieser, C. (2017). The *Legionella pneumophila* genome evolved to accommodate multiple regulatory mechanisms controlled by the CsrA-system. PLoS genetics *13*, e1006629.
Salim, T., Sershen, C.L., and May, E.E. (2016). Investigating the role of TNF-α and IFN-γ activation on the dynamics of iNOS gene expression in LPS stimulated macrophages. PloS one *11*, e0153289.

Sasaki, Y., Oguchi, H., Kobayashi, T., Kusama, S., Sugiura, R., Moriya, K., Hirata, T., Yukioka, Y., Takaya, N., and Yajima, S. (2016). Nitrogen oxide cycle regulates nitric oxide levels and bacterial cell signaling. Scientific reports *6*, 22038.

Sauer, K., Stoodley, P., Goeres, D.M., Hall-Stoodley, L., Burmolle, M., Stewart, P.S., and Bjarnsholt, T. (2022). The biofilm life cycle: expanding the conceptual model of biofilm formation. Nature reviews Microbiology *20*, 608-620.

Schator, D., Mondino, S., Berthelet, J., Di Silvestre, C., Ben Assaya, M., Rusniok, C., Rodrigues-Lima, F., Wehenkel, A., Buchrieser, C., and Rolando, M. (2023). *Legionella* para-effectors target chromatin and promote bacterial replication. Nature communications *14*, 2154.

Schell, U., Kessler, A., and Hilbi, H. (2014). Phosphorylation signalling through the *Legionella* quorum sensing histidine kinases LqsS and LqsT converges on the response regulator LqsR. Mol Microbiol *92*, 1039-1055.

Schell, U., Simon, S., and Hilbi, H. (2016a). Inflammasome Recognition and Regulation of the *Legionella* Flagellum. Curr Top Microbiol Immunol *397*, 161-181.

Schell, U., Simon, S., Sahr, T., Hager, D., Albers, M.F., Kessler, A., Fahrnbauer, F., Trauner, D., Hedberg, C., Buchrieser, C*., et al.* (2016b). The alpha-hydroxyketone LAI-1 regulates motility, Lqs-dependent phosphorylation signalling and gene expression of *Legionella pneumophila*. Mol Microbiol *99*, 778-793.

Schröder, H. (2006). No nitric oxide for HO-1 from sodium nitroprusside. Molecular pharmacology *69*, 1507-1509.

Schroter, L., and Dersch, P. (2019). Phenotypic Diversification of Microbial Pathogens-Cooperating and Preparing for the Future. J Mol Biol *431*, 4645-4655.

Schwechheimer, C., and Kuehn, M.J. (2015). Outer-membrane vesicles from Gram-negative bacteria: biogenesis and functions. Nature reviews Microbiology *13*, 605-619.

Segal, G., Russo, J.J., and Shuman, H.A. (1999). Relationships between a new type IV secretion system and the *icm*/*dot* virulence system of *Legionella pneumophila*. Mol Microbiol *34*, 799-809.

Segal, G., and Shuman, H.A. (1998). Intracellular multiplication and human macrophage killing by *Legionella pneumophila* are inhibited by conjugal components of IncQ plasmid RSF1010. Mol Microbiol *30*, 197-208.

Segal, G., and Shuman, H.A. (1999). *Legionella pneumophila* utilizes the same genes to multiply within *Acanthamoeba castellanii* and human macrophages. Infection and immunity *67*, 2117-2124.

Sethi, K.K., and Brandis, H. (1983). Direct demonstration and isolation of *Legionella pneumophila* (serogroup 1) from bathroom water specimens in a hotel. Zentralblatt fur Bakteriologie, Mikrobiologie und Hygiene 1 Abt Originale B, Hygiene *177*, 402-405.

Shank, E.A., and Kolter, R. (2009). New developments in microbial interspecies signaling. Curr Opin Microbiol *12*, 205-214.

Shevchuk, O., Jager, J., and Steinert, M. (2011). Virulence properties of the *Legionella pneumophila* cell envelope. Frontiers in microbiology *2*, 74.

Simmering, J.E., Polgreen, L.A., Hornick, D.B., Sewell, D.K., and Polgreen, P.M. (2017). Weather-dependent risk for Legionnaires' disease, United States. Emerg Infect Dis *23*, 1843-1851.

Simon, S., Schell, U., Heuer, N., Hager, D., Albers, M.F., Matthias, J., Fahrnbauer, F., Trauner, D., Eichinger, L., Hedberg, C*., et al.* (2015). Inter-kingdom signaling by the *Legionella* quorum sensing molecule LAI-1 modulates cell migration through an IQGAP1-Cdc42-ARHGEF9-dependent pathway. PLoS Pathog *11*, e1005307.

Simon, S., Wagner, M.A., Rothmeier, E., Müller-Taubenberger, A., and Hilbi, H. (2014). Icm/Dot-dependent inhibition of phagocyte migration by *Legionella* is antagonized by a translocated Ran GTPase activator. Cell Microbiol *16*, 977-992.

Solomon, J.M., and Isberg, R.R. (2000). Growth of *Legionella pneumophila* in *Dictyostelium discoideum*: a novel system for genetic analysis of host-pathogen interactions. Trends Microbiol *8*, 478-480.

Spirig, T., Tiaden, A., Kiefer, P., Buchrieser, C., Vorholt, J.A., and Hilbi, H. (2008). The *Legionella* autoinducer synthase LqsA produces an α-hydroxyketone signaling molecule. J Biol Chem *283*, 18113-18123.

Spitalny, K.C., Vogt, R.L., Orciari, L.A., Witherell, L.E., Etkind, P., and Novick, L.F. (1984). Pontiac fever associated with a whirlpool spa. American journal of epidemiology *120*, 809-817.

Sreelatha, A., Nolan, C., Park, B.C., Pawlowski, K., Tomchick, D.R., and Tagliabracci, V.S. (2020). A *Legionella* effector kinase is activated by host inositol hexakisphosphate. J Biol Chem *295*, 6214-6224.

Steele, T.W., Moore, C.V., and Sangster, N. (1990). Distribution of *Legionella longbeachae* serogroup 1 and other *legionellae* in potting soils in Australia. Appl Environ Microbiol *56*, 2984-2988.
Steiner, B., Swart, A.L., Welin, A., Weber, S., Personnic, N., Kaech, A., Freyre, C., Ziegler, U., Klemm, R.W., and Hilbi, H. (2017). ER remodeling by the large GTPase atlastin promotes vacuolar growth of *Legionella pneumophila*. EMBO Rep *18*, 1817-1836.
Steiner, B., Weber, S., and Hilbi, H. (2018). Formation of the *Legionella*-containing vacuole: phosphoinositide conversion, GTPase modulation and ER dynamics. Int J Med Microbiol *308*, 49-57.
Steinert, M., and Heuner, K. (2005). *Dictyostelium* as host model for pathogenesis. Cell Microbiol *7*, 307-314.
Stern, A.M., and Zhu, J. (2014). An introduction to nitric oxide sensing and response in bacteria. Advances in applied microbiology *87*, 187-220.
Stewart, C.R., Muthye, V., and Cianciotto, N.P. (2012). *Legionella pneumophila* persists within biofilms formed by *Klebsiella pneumoniae*, *Flavobacterium* sp., and *Pseudomonas fluorescens* under dynamic flow conditions. PLoS One *7*, e50560.
Stone, B.J., and Kwaik, Y.A. (1998). Expression of multiple pili by *Legionella pneumophila*: identification and characterization of a type IV pilin gene and its role in adherence to mammalian and protozoan cells. Infection and immunity *66*, 1768-1775.
Striednig, B., and Hilbi, H. (2022). Bacterial quorum sensing and phenotypic heterogeneity: how the collective shapes the individual. Trends Microbiol *30*, 379-389.
Striednig, B., Lanner, U., Niggli, S., Katic, A., Vormittag, S., Brulisauer, S., Hochstrasser, R., Kaech, A., Welin, A., Flieger, A.*, et al.* (2021). Quorum sensing governs a transmissive *Legionella* subpopulation at the pathogen vacuole periphery. EMBO Rep *22*, e52972.
Swanson, M.S., and Isberg, R.R. (1995). Association of *Legionella pneumophila* with the macrophage endoplasmic reticulum. Infect Immun *63*, 3609-3620.
Swart, A.L., Gomez-Valero, L., Buchrieser, C., and Hilbi, H. (2020a). Evolution and function of bacterial RCC1 repeat effectors. Cellular Microbiology *22*, e13246.
Swart, A.L., Harrison, C.F., Eichinger, L., Steinert, M., and Hilbi, H. (2018). *Acanthamoeba* and *Dictyostelium* as cellular models for *Legionella* infection. Front Cell Infect Microbiol *8*, 61.
Swart, A.L., and Hilbi, H. (2020). Phosphoinositides and the fate of *Legionella* in phagocytes. Frontiers in immunology *11*, 25.
Swart, A.L., Steiner, B., Gomez-Valero, L., Schutz, S., Hannemann, M., Janning, P., Irminger, M., Rothmeier, E., Buchrieser, C., Itzen, A.*, et al.* (2020b). Divergent evolution of *Legionella* RCC1 repeat effectors defines the range of Ran GTPase cycle targets. mBio *11*, e00405-00420.
Tan, Y., and Luo, Z.Q. (2011). *Legionella pneumophila* SidD is a deAMPylase that modifies Rab1. Nature *475*, 506-509.
Tao, Y., Misko, T., Howlett, A., and Klein, C. (1997). Nitric oxide, an endogenous regulator of *Dictyostelium discoideum* differentiation. Development *124*, 3587-3595.
Taylor, M., Ross, K., and Bentham, R. (2009). *Legionella*, protozoa, and biofilms: interactions within complex microbial systems. Microb Ecol *58*, 538-547.
Thompson, C.M., Tischler, A.H., Tarnowski, D.A., Mandel, M.J., and Visick, K.L. (2019). Nitric oxide inhibits biofilm formation by *Vibrio fischeri* via the nitric oxide sensor HnoX. Molecular microbiology *111*, 187-203.
Tiaden, A., and Hilbi, H. (2012). α-Hydroxyketone synthesis and sensing by *Legionella* and *Vibrio*. Sensors *12*, 2899-2919.
Tiaden, A., Spirig, T., Carranza, P., Bruggemann, H., Riedel, K., Eberl, L., Buchrieser, C., and Hilbi, H. (2008). Synergistic contribution of the *Legionella pneumophila lqs* genes to pathogen-host interactions. J Bacteriol *190*, 7532-7547.
Tiaden, A., Spirig, T., and Hilbi, H. (2010a). Bacterial gene regulation by α-hydroxyketone signaling. Trends Microbiol *18*, 288-297.
Tiaden, A., Spirig, T., Sahr, T., Wälti, M.A., Boucke, K., Buchrieser, C., and Hilbi, H. (2010b). The autoinducer synthase LqsA and putative sensor kinase LqsS regulate phagocyte interactions, extracellular filaments and a genomic island of *Legionella pneumophila*. Environ Microbiol *12*, 1243-1259.
Tiaden, A., Spirig, T., Weber, S.S., Brüggemann, H., Bosshard, R., Buchrieser, C., and Hilbi, H. (2007). The *Legionella pneumophila* response regulator LqsR promotes host cell interactions as an element of the virulence regulatory network controlled by RpoS and LetA. Cell Microbiol *9*, 2903-2920.

Toyofuku, M., Morinaga, K., Hashimoto, Y., Uhl, J., Shimamura, H., Inaba, H., Schmitt-Kopplin, P., Eberl, L., and Nomura, N. (2017). Membrane vesicle-mediated bacterial communication. The ISME journal *11*, 1504-1509.
Toyofuku, M., Nomura, N., and Eberl, L. (2019). Types and origins of bacterial membrane vesicles. Nature Reviews Microbiology *17*, 13-24.
Toyofuku, M., Schild, S., Kaparakis-Liaskos, M., and Eberl, L. (2023). Composition and functions of bacterial membrane vesicles. Nature reviews Microbiology *21*, 415-430.
Tyson, J.Y., Pearce, M.M., Vargas, P., Bagchi, S., Mulhern, B.J., and Cianciotto, N.P. (2013). Multiple *Legionella pneumophila* Type II secretion substrates, including a novel protein, contribute to differential infection of the amoebae *Acanthamoeba castellanii*, *Hartmannella vermiformis*, and *Naegleria lovaniensis*. Infect Immun *81*, 1399-1410.
Ueno, T., Fischer, J.T., and Boon, E.M. (2019). Nitric oxide enters quorum sensing via the H-NOX signaling pathway in *Vibrio parahaemolyticus*. Frontiers in microbiology *10*, 2108.
Valentini, M., and Filloux, A. (2016). Biofilms and cyclic di-GMP (c-di-GMP) signaling: lessons from *Pseudomonas aeruginosa* and other bacteria. Journal of Biological Chemistry *291*, 12547-12555.
Valentini, M., and Filloux, A. (2019). Multiple Roles of c-di-GMP Signaling in Bacterial Pathogenesis. Annual review of microbiology *73*, 387-406.
Valster, R.M., Wullings, B.A., van den Berg, R., and van der Kooij, D. (2011). Relationships between free-living protozoa, cultivable *Legionella* spp., and water quality characteristics in three drinking water supplies in the Caribbean. Applied and environmental microbiology *77*, 7321-7328.
Vandersmissen, L., De Buck, E., Saels, V., Coil, D.A., and Anne, J. (2010). A *Legionella pneumophila* collagen-like protein encoded by a gene with a variable number of tandem repeats is involved in the adherence and invasion of host cells. FEMS Microbiol Lett *306*, 168-176.
Veening, J.W., Smits, W.K., and Kuipers, O.P. (2008). Bistability, epigenetics, and bet-hedging in bacteria. Annual review of microbiology *62*, 193-210.
Veltman, D.M. (2015). Drink or drive: competition between macropinocytosis and cell migration. Biochem Soc Trans *43*, 129-132.
Vergis, E.N., Akbas, E., and Victor, L.Y. (2000). Legionella as a cause of severe pneumonia. Paper presented at: Seminars in respiratory and critical care medicine *21*, 295-304.
Vormittag, S., Ende, R.J., Derre, I., and Hilbi, H. (2023a). Pathogen vacuole membrane contact sites - close encounters of the fifth kind. Microlife *4*, uqad018.
Vormittag, S., Husler, D., Haneburger, I., Kroniger, T., Anand, A., Prantl, M., Barisch, C., Maass, S., Becher, D., Letourneur, F*., et al.* (2023b). *Legionella*- and host-driven lipid flux at LCV-ER membrane contact sites promotes vacuole remodeling. EMBO Rep *24*, e56007.
Wadowsky, R.M., Wolford, R., McNamara, A., and Yee, R.B. (1985). Effect of temperature, pH, and oxygen level on the multiplication of naturally occurring *Legionella pneumophila* in potable water. Applied and environmental microbiology *49*, 1197-1205.
Wang, P.G., Xian, M., Tang, X., Wu, X., Wen, Z., Cai, T., and Janczuk, A.J. (2002). Nitric oxide donors: chemical activities and biological applications. Chemical reviews *102*, 1091-1134.
Wang, Y., Hoffmann, J.P., Chou, C.W., Honer Zu Bentrup, K., Fuselier, J.A., Bitoun, J.P., Wimley, W.C., and Morici, L.A. (2020). *Burkholderia thailandensis* outer membrane vesicles exert antimicrobial activity against drug-resistant and competitor microbial species. Journal of microbiology *58*, 550-562.
Wang, Y., and Ruby, E.G. (2011). The roles of NO in microbial symbioses. Cell Microbiol *13*, 518-526.
Weber, S., Steiner, B., Welin, A., and Hilbi, H. (2018). *Legionella*-containing vacuoles capture PtdIns (4) P-rich vesicles derived from the Golgi apparatus. MBio *9*, 02420-02418.
Weber, S.S., Joller, N., Kuntzel, A.B., Sporri, R., Tchang, V.S., Scandella, E., Rosli, C., Ludewig, B., Hilbi, H., and Oxenius, A. (2012). Identification of protective B cell antigens of *Legionella pneumophila*. Journal of immunology *189*, 841-849.
Weber, S.S., Ragaz, C., Reus, K., Nyfeler, Y., and Hilbi, H. (2006). *Legionella pneumophila* exploits PI(4)*P* to anchor secreted effector proteins to the replicative vacuole. PLoS Pathog *2*, e46.
Wei, Y., Perez, L.J., Ng, W.L., Semmelhack, M.F., and Bassler, B.L. (2011). Mechanism of *Vibrio cholerae* autoinducer-1 biosynthesis. ACS chemical biology *6*, 356-365.
West, S.A., and Cooper, G.A. (2016). Division of labour in microorganisms: an evolutionary perspective. Nature reviews Microbiology *14*, 716-723.
Whiley, H., and Bentham, R. (2011). *Legionella longbeachae* and legionellosis. Emerging infectious diseases *17*, 579-583.

Whiteley, M., Diggle, S.P., and Greenberg, E.P. (2017). Progress in and promise of bacterial quorum sensing research. Nature *551*, 313-320.
Williams, D.E., and Boon, E.M. (2019). Towards understanding the molecular basis of nitric oxide-regulated group behaviors in pathogenic bacteria. Journal of innate immunity *11*, 205-215.
Williams, D.E., Nisbett, L.M., Bacon, B., and Boon, E. (2018). Bacterial heme-based sensors of nitric oxide. Antioxid Redox Signal *29*, 1872-1887.
Winn, W.C. (1988). Legionnaires disease: historical perspective. Clinical Microbiology Reviews *1*, 60-81.
Wuthrich, D., Gautsch, S., Spieler-Denz, R., Dubuis, O., Gaia, V., Moran-Gilad, J., Hinic, V., Seth-Smith, H.M., Nickel, C.H., Tschudin-Sutter, S.*, et al.* (2019). Air-conditioner cooling towers as complex reservoirs and continuous source of *Legionella pneumophila* infection evidenced by a genomic analysis study in 2017, Switzerland. Eurosurveillance *24*. 1800192.
Wymann, M. (2023). The one health approach applied to surveillance and control of Legionnaires' disease in Switzerland. European Journal of Public Health *33*, ckad160. 084.
Yeo, J., Wang, X.C., and Hammond, M.C. (2017). Live flow cytometry analysis of c-di-GMP levels in single cell populations (Springer).
Yu, A.T., Kamali, A., and Vugia, D.J. (2019). Legionella Epidemiologic and Environmental Risks. Current Epidemiology Reports *6*, 310-320.
Yu, V.L., Plouffe, J.F., Pastoris, M.C., Stout, J.E., Schousboe, M., Widmer, A., Summersgill, J., File, T., Heath, C.M., Paterson, D.L.*, et al.* (2002). Distribution of *Legionella* species and serogroups isolated by culture in patients with sporadic community-acquired legionellosis: an international collaborative survey. J Infect Dis *186*, 127-128.

Acknowledgments

First, I would like to express my deep gratitude to my supervisor Prof. Dr. Hubert Hilbi. Thank you for giving me the opportunity to perform my doctoral studies in your research group on this exciting project; I certainly learned a lot on the way on a scientific and personal level. I very much appreciate that you were always available to provide scientific input and to be supportive during tough times. I also appreciate your open nature and your sense of humor, which makes early group meetings more fun and helps to find motivation in challenging times. Moreover, I would like to express my gratitude for all the great times we had outside of the institute, e.g., at the Rigi retreat, at rooftop BBQs, at Christmas dinners or at the Club Milano in Yokohama!

During my doctoral studies, I greatly benefited from the yearly meetings with my advisory committee, consisting of Hubert, Prof. Dr. Urs Jenal and Prof. Dr. Rolf Kümmerli. I am grateful that you took the time and effort to be present at the meetings as well as the Ph.D. defense itself. I would like to thank you for showing interest in my person and for providing inspiring scientific input, which pushed my PhD project further.

Furthermore, I would like to acknowledge my lab colleagues. Special thanks go to Ramon and Bianca for introducing me to the world of *Legionella* and showing me how much fun microscopy and flow cytometry can be. I would also like to thank Leoni for her great support over the past years - I highly appreciate you as a scientist and as a person and I am very happy to have you as a friend. I would also like to thank Dario for all the fun times we had together in and outside of work and for being my sports buddy. Special thanks go to my office colleagues: Pia, Tobi, Camille, Tong, Liz and Isa. I very much enjoyed the extended lunch breaks we had together and the great fun we had outside of the lab at the Züri Fäscht, birthday parties, BBQs, club nights and sledging days! A big thank you goes to my former master students Camille and Tong - it was a pleasure to work with you. I am very proud to see how you both have grown as scientists and how our strong teamwork has produced a very nice paper story. Moreover, I would like to thank Pia for her reflected opinions, her valuable suggestions, and the fun times we had together. A special thanks go to Liz, with whom I spent the longest time in this group. I cannot count how many good times we had together, at various MIM events, retreats, conferences, weekend trips and many more. Thank you for being so warm-hearted and for always having an open ear for me. I further thank the other members of the Institute of Medical Microbiology for their help, especially the kind people from the media kitchen. Also, many thanks to Judith, for creating a supportive and empathetic environment and for organizing fun MIM events.

I am incredibly grateful for the great friends from all over the world that I have made here in Switzerland and with whom I have spent some amazing years. Thank you for making me feel at home in this country! It was wonderful and inspiring to be surrounded by such an international environment and I am very much looking forward to spending lots of time with all of you in the future.

An enormous gratitude goes to my loved ones from Germany. Thank you to all my friends and relatives for helping me to take my mind of from work, for your endless support and for all coming to visit

me in Zurich. I would like to especially thank my parents, Martha and Uwe, for your loving support, your interest and continuous encouragement throughout the years. Furthermore, I would like to thank my siblings, Chrissi, Thomas, and Marie. I am incredibly grateful to have you by my side. Thank you for always having an open ear for me, for cheering me up and, above all, for the great fun we have together at home or on our many vacations.

Last but most importantly, I would like to thank the love of my life, Kenny, for your unconditional support and love. Together, we go through thick and thin, and I am incredibly grateful to have you at my side for so many years. We had an amazing time together here in Switzerland and I am very much looking forward to starting the next chapter of our lives in the UK soon.